ABSTRACT

The problems of optimal as well as suboptimal detection for CDMA transmissions over an additive white Gaussian noise (AWGN) channel, have been the focus of study in the recent past. However, CDMA transmissions are frequently made over channels which exhibit fading and/or dispersion; hence receivers need to be designed which take into account this behaviour.

In spite of the major research effort invested in multiuser demodulation techniques, several practical as well as theoretical open problems still exist. Some of them are considered in more detail in this thesis. The aim of the thesis is to develop multiuser demodulation algorithms for mobile communication systems in frequency-selective fading channels, and to analyze their implementation complexity. The emphasis is restricted to the uplink of an asynchronous DS-CDMA system where the users transmit in an uncoordinated manner and are received by one centralized receiver.

The original work that is undertaken for the MScEng study is the evaluation of a multiuser receiver structure for a frequency-selective fading channel, where there exists a steady specular path and two fading paths. Furthermore, the effect of using selection diversity is investigated by examining the bit error rate, asymptotic multiuser efficiency and near-far resistance of the proposed detector structure. These results are confirmed both analytically and by simulation in the thesis. An investigation is also conducted into the application of neural networks to the problem of multiuser detection in code division multiple access systems. The neural network will be used as a classifier in an adaptive receiver which incorporates an extended Kalman filter for joint amplitude and delay estimation. Finally, some open problems for future research will be pointed out in the thesis.

Keywords: AWGN channel, DS-CDMA system, frequency-selective, multiuser demodulation, asymptotic multiuser efficiency, near-far resistance, neural network, Kalman filter.

PREFACE

The research detailed in this thesis was carried out at the University of Natal in the School of Electrical and Electronic Engineering. I became involved with CDMA research while working at the RF and Microwave department at the previous company I was employed at, KENTRON. Returning to University on a part-time basis at the beginning of 1996, had given me the opportunity to concentrate more on academic research.

The first year of the research included mostly literature study. During this part of the studies, I have had the pleasure of working with Prof. F Takawira at the University of Natal on the subject of using a neural network and extended Kalman Filter based adaptive multiuser receiver for CDMA systems. The reader is referred to the original publication of [138] in this regard. The subsequent years consisted of writing simulation and analytical software, conducting extensive simulations that finally culminating in the compilation of this thesis. I have had the pleasure to be involved in the study of a subject matter that is very current, interesting and practical.

ACKNOWLEDGEMENTS

I wish to express my gratitude to my supervisor for his useful comments and guidance throughout the work. My warmest thanks also go to him for providing me with the opportunity to work on this interesting topic.

I am grateful to my mother and late father for the help, support and love they have provided me throughout my life. The positive attitude towards education in our home has been a motivating and driving force for my postgraduate studies.

Finally, I wish to express my deepest thanks to my dear friends (who are too many to mention) for the support and encouragement they have given me during my postgraduate studies.

Durban, December 24, 1999 Navin Runjit Singh

Contents

LIST OF FIGURES

LIST OF TABLES

List of symbols and abbreviations

A	diagonal matrix of transmitted complex amplitudes of all users at one symbol interval
A^{ij}	normalised specular, faded and specular-to-faded signal correlation matrix
$a_k(t)$	signature waveform of the kth user
$\underline{b}$	most likely sequence for b that was transmitted
b_i	initial bit estimate from the PIC detector
b_{dec}	data estimate from the decorrelator
b_{PE}	data estimate from the PE detector
b_{MMSE}	data estimate from the MMSE detector
B_d	doppler spread of the channel
D	ratio of specular to scattered power
$D_d(z)$	z-domain transfer function of the IIR filter
$E_k(x)$	specular energy of the kth user in the xth symbol interval
f_c	carrier frequency
F_{fad}	diagonal matrix of fading parameters
$h(\tau,t)$	channel impulse response
$H(f,t)$	time-variant transfer function
$I_0(.)$	modified Bessel function of order zero
J	order of diversity
Km	kilo meters
L	number of diversity branches
M	there are in total 2M+1 data bits
N	reference to the specific path
N	number of chips in the PN code sequence
N_s	number of stages of the PE detector
$n(t)$	additive white Gaussian noise
$O(K^2)$	of order K^2
Pe	probability of bit error
$p(t)$	a pulse waveform
p_k	bit error probability of the kth user
$q_f + q_f^*$	vector of sufficient statistics for the fading channel
Q	matrix which has the off-diagonal elements of R
$Q(d)$	Gaussian complementary error function
r	fading to additive noise variance ratio
$r(t)$	compound lowpass received signal

$r_k(t)$	received signal of the kth user
R	correlation matrix
R_c	chip rate
s(t)	composite transmitted signal for the k users
$s_k(t)$	equivalent lowpass transmitted waveform for the kth user
s_{lp}	equivalent lowpass transmitted signal
$S_{lp}(f)$	Fourier transform of $s_{lp}(t)$
$S_c(\lambda)$	Doppler power spectrum of the channel
T_c	a chip interval
T_m	delay spread of the channel
v(t)	received bandpass signal
w(x)	energy-bit vector in the xth symbol interval
w_i	polynomial coefficients for the PE detector
x	a specific symbol interval
y_k	output of the kth user's correlator for a particular bit interval
$y_{[MRC]K}$	output of the RAKE receiver for the kth user
$y_{[LIN]}$	output of a linear detector
z	variable used to indicate the z-transform
z_k	noise term obtained by correlation with the thermal noise
*	denotes the complex conjugate
$\delta(t)$	Dirac's delta function
$\theta_k(x)$	specular phase of the kth user's signal in the xth symbol interval
$\rho_{i,k}$	cross-correlation between the code waveforms of users i and k
ω_0	carrier frequency
β	the linear mapping function for the decorrelator
β_{MMSE}	the linear mapping function for the MMSE detector
β_{PE}	the linear mapping function for the PE detector
τ_k	transmission delay for the kth user
τ_{max}	maximum propagation time
$\tau_n(t)$	propagation delay for the nth path
η_k	AME in symbolic form
$\alpha_n(t)$	attenuation factor for the signal received on the nth path
$(\Delta f)_c$	coherence bandwidth of the channel
$(\Delta t)_c$	coherence time of the channel
ϕ_c	autocorrelation function of $h(\tau,t)$

$\phi_c(\tau)$	multipath intensity profile of the channel
λ	doppler frequency
$\lambda_{k,1}(x)$	Rayleigh distributed attenuation of the kth user in the xth symbol interval along the first faded signal path
$\lambda_{k,2}(x)$	Rayleigh distributed attenuation of the kth user in the xth symbol interval along the second faded signal path
$\phi_{k,1}(x)$	uniformly distributed phase shift of the kth user in the xth symbol interval along the first faded signal path
$\phi_{k,2}(x)$	uniformly distributed phase shift of the kth user in the xth symbol interval along the second faded signal path
σ^2	AWGN variance
(x.y)	equation x.y
[x]	reference x
AGISI	asynchronous Gaussian inter symbol interference
AME	asymptotic multiuser efficiency
AWGN	additive white Gaussian noise
BER	bit error rate
CDMA	code division multiple access
DS	direct sequence
EKF	extended Kalman filter
FDMA	frequency division multiple access
FH	frequency hopping
FIR	finite impulse response
HD-PIC	hard decision parallel interference cancellation
IC	interference cancellation
IIR	infinite impulse response
ISI	inter symbol interference
JD	joint detection
LPI	low probability of interception
MAI	multiple access interference
MC-CDMA	multicarrier CDMA
MF	matched filter
MHz	mega hertz
MLS	maximum likelihood sequence
MMSE	minimum mean squared error
MRC	maximal ratio combining
MSE	mean squared error
MUD	multiuser demodulation

NFR	near-far resistance
PDF	probability density function
PDMA	polarization-division multiple access
PE	polynomial expansion
PIC	parallel interference cancellation
PN	pseudo noise sequence
RLS	recursive least squares
SD	single user detection
SDMA	space division multiple access
SIC	successive interference cancellation
SNR	signal-to-noise ratio
SU	single user
TDMA	time division multiple access

Chapter 1: Introduction

The goal of wireless communications is to allow the user access to the capabilities of the global network at any time without restrictions imposed by location or mobility. Cellular systems are currently limited to voice and low-speed data communications within areas covered by base stations. Wider commercial applications are developing in terrestrial wireless voice telephony and interactive data transmission between personal computers and portable digital assistants. At present, there are over 30 million cellular subscribers worldwide most of which use analogue techniques.

1.1. Historical Background

Cellular systems were pioneered during the 70's by Bell Laboratories in the United States and the earliest systems were called Advanced Mobile Phone Service (AMPS). All of these "first generation" cellular systems used analogue frequency modulation for speech transmission and frequency shift keying for signaling. Users were separated in frequency and adjacent cells were allocated different parts of the spectrum. This resulted in a resource sharing mechanism known as frequency division multiple access. AMPS cellular service has been available to the public since 1983, and there are currently 20 million subscribers in the United States, Canada, Central and South America and Australia.

In Europe, several first-generation systems similar to AMPS were established. This included Total Access Communications Systems (TACS) in Britain, Spain, Austria and Italy; Nordic Mobile Telephone (NMT) in several countries, C-450 in Germany and Portugal. Similar to AMPS, these systems were based on FDMA for speech and FSK for signaling.

Apart from the TACS system, the European Community established a digital standard "Group Speciale Mobile" in 1982 based on time-division multiple access (TDMA). The work from this group became known as the Global System for Mobile Communications (GSM). The GSM system was deployed in 1993 and has experienced spectacular growth since then.

The UK Department of Trade and Industry started an initiative which led to assignment of 150MHz near 1.8GHz for personal communications networks (PCN) in Europe and the choice of GSM as a standard for that application. This system is known as DCS1800. In North America, second generation systems based on TDMA have been proposed in order to cope with the growing demand for mobile communications access and is known as IS-54. This system is able to offer triple the capacity (users per cell) of AMPS. A complication however is that the IS-54 standard must operate using the same spectrum as the existing AMPS systems, resulting in a "dual-mode" digital-analogue operation.

In Japan, a second generation TDMA based cellular system was established in 1991 called Personal Digital Cellular (PDC) which also offers advantages over analogue systems in terms of increased system capacity and reduced transmit power requirements.

From August 1995, CDMA based IS-95 has also been in operation in selected areas in the United States and other trial areas in non-US countries. The IS-95 CDMA system approach offers advantages over other digital standards in increased capacity, reduction of the need for planning frequency assignments to cells and the ability to accommodate different transmission rates. It is for this reason that CDMA has been chosen as the protocol for the 3rd generation systems [6].

1.2. Multiple-access techniques

Multiple-access refers to a technique to share a common communications channel between multiple users. When designing multiuser communication systems, one has the option of using space, time or frequency domain designs.

The oldest multiple-access technique is frequency-division multiple access (FDMA). Here, each user's signature waveform occupies its own frequency band and the receiver can separate the user's signals by simple bandpass filtering. FDMA is a simple scheme and is applicable to both analog and digital modulation. It is not, however, very flexible for providing variable

bit rates, which is an important requirement in future communication services.

The introduction of digital modulations enabled the appearance of time-division multiple-access (TDMA), in which each user's transmitted signal is limited to a predetermined time interval. TDMA is relatively simple to implement and it is very flexible for providing variable bit rates. Increasing the bit rate can be implemented by assigning to a user more transmission intervals. However, the transmissions of all the users must be exactly synchronized to each other.

The invention of spread-spectrum techniques for communication systems with anti-jamming and low probability of undesired interception capabilities lead to the idea of code-division multiple-access (CDMA). CDMA protocols do not achieve their multiple access property by a division of the transmissions of different users in either time or frequency. It instead assigns to each user a different code. This code is used to transform a user's signal into a wideband (spread-spectrum) signal. The CDMA protocol is classified according to the modulation method used to obtain the wideband signal. There are four protocol types: direct-sequence CDMA, frequency hopping CDMA, time hopping CDMA and hybrid CDMA. In direct-sequence CDMA, the original signal is modulated on a carrier and then further modulated by a binary code sequence with a bandwidth much larger than the original bandwidth. In the frequency hopping CDMA protocols, the wideband channel is divided into frequency bands. During the transmission of a user's signal, the carrier frequency is changed periodically resulting in a periodic change of the frequency band occupied by the user. In time hopping CDMA protocols, a user's signal is not transmitted continuously, but instead in short intervals. The start of each burst is decided by the code assigned to the user. The hybrid CDMA protocols use a combination of the modulation methods of direct sequence, frequency hopping or time hopping protocols to obtain the wideband signal. Combining the modulation methods uses the specific advantages that each modulation method offers.

1.3. CDMA System concepts

Section 1.3.1gives the theory on the transmission and generation of a direct-sequence CDMA signal. This is followed in Section 1.3.2 by a description of the reception of this CDMA signal.

1.3.1. DS-CDMA transmitter structure

In the DS-CDMA protocols the data signal is directly modulated by a digital code signal. The data signal can be either an analog signal or a digital one. In most cases, it will be a digital signal. In the case of a digital signal, the data signal is directly multiplied by the code signal and the resulting signal modulates the wideband carrier.

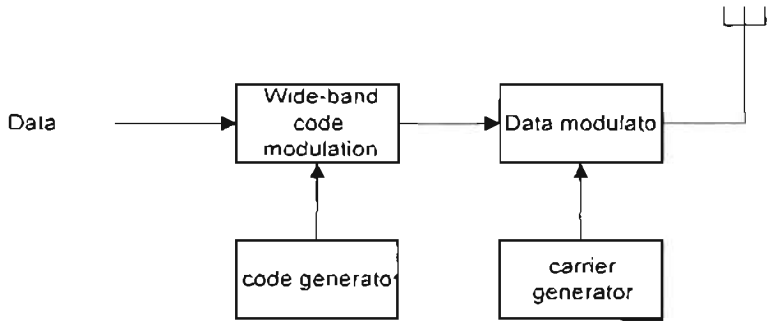

Figure 1.1
Transmitter block diagram

A block diagram of a DS-CDMA transmitter is shown in Figure 1.1. The binary data signal modulates a RF carrier. The modulated carrier is then modulated by the code signal. This code signal consists of a number of code bits or "chips" that can be either +1 or –1. To obtain the desired spreading of the signal, the chip rate of the code signal must be much higher than the data rate of the information signal. For the code modulation, various modulation techniques can be used but usually some form of phase shift keying (PSK) like binary phase shift keying (BPSK), differential binary phase shift keying (D-BPSK), quadrature phase shift keying (QPSK) or minimum shift keying (MSK) is employed.

1.3.2. CDMA receiver structure

After transmission of the signal, the receiver as shown in Figure 1.2, uses coherent demodulation to despread the spread spectrum signal, using a locally generated code sequence. To be able to perform the despreading operation, the receiver must not only know the code sequence used to spread the signal, but the codes of the received signal and the locally generated code must also be synchronized. This synchronization must be accomplished at the beginning of the reception and maintained until the whole signal has been received. The synchronization/tracking block performs this operation. After despreading, a data modulated signal results and after demodulation the original data can be recovered.

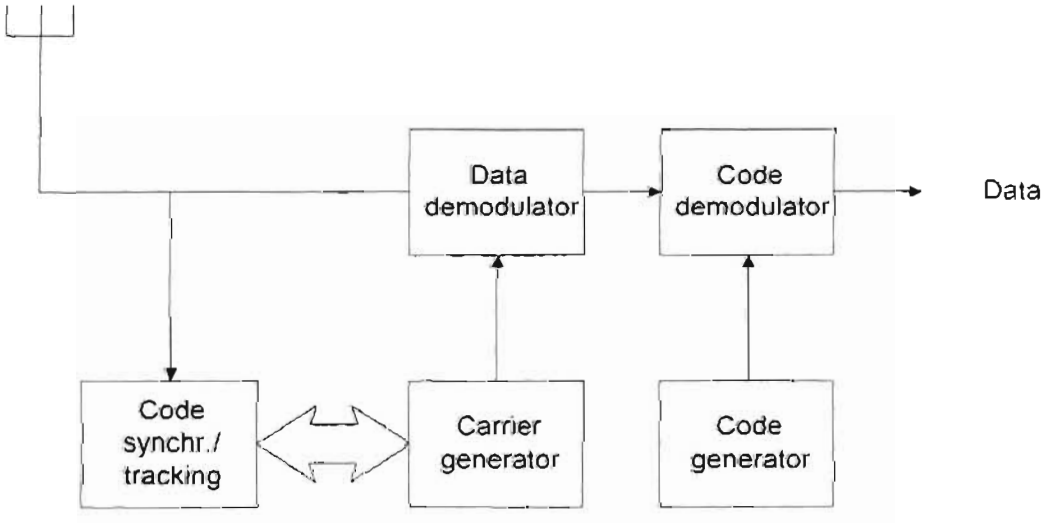

Figure 1.2
Receiver structure

The typical receiver consists of a bank of matched filters which are matched to the users spreading codes. The output of the matched filter bank goes into a detector. One of the distinguishing factors between CDMA receiver architectures is the way the output of the matched filter bank is processed. A number of structures have been proposed.

The first receiver structure is the simple matched filter receiver or conventional detector. For this receiver, the outputs of the matched filter bank are sampled at the symbol intervals and the data demodulation is accomplished by considering the sign of the output of the respective matched filter. This receiver will be discussed in detail in Chapter 2. At

this point, it will suffice to say that the conventional receiver is not optimal for demodulation. This receiver suffers from the near-far problem. Strong signals may completely bury the weak ones if the conventional receiver is applied. Therefore, the design of the conventional CDMA systems relies on accurate power control [5,7] to alleviate the near-far problem, and spreading sequence design [5,8,9, 10] to reduce the cross-correlations between the signature waveforms of the users. If the number of users is large, the performance of the conventional receiver is poor even in the absence of the near-far problem due to the large level of MAI. This conventional signal separation method was originally designed for synchronous transmission with orthogonal CDMA codes over ideal channels without multipath propagation. However, when this method is applied to the case of transmission over multipath channels, it is no longer optimum. This is due to the fact that the general principle is to detect the one user signal of interest and to treat all the other user signals as noise. This method of signal detection is termed single user detection. In the cellular mobile radio systems, the nature of the interfering signals which produce multiple-access interference (MAI) is not like noise because they are produced by other users with known CDMA codes. Information about the CDMA codes and channel impulse responses is available to both the desired and interfering users.

To overcome this suboptimality of the single user detection approach, the a priori knowledge about MAI has to be taken into account in the detection process. In this way, the decision of all the data symbols of all users becomes an interdependent process termed multi-user detection (MUD). An alternative to the conventional receiver is to apply a receiver designed to take the multiple-access interference into consideration, that is multiuser demodulation. The multiuser demodulation is related to co-channel interference rejection [11]. Co-channel interference is caused by signals of users transmitting in the same frequency band, and is usually rejected by adaptive filtering [12,13]. This can be seen as a special case of multiuser demodulation. A multiuser detector can also make a joint detection of the data of all users.

MUD utilises the MAI as redundant information which multiple access users are sharing in a common channel. MUD principles can be divided into interference cancellation (IC) and joint detection (JD) principles.
The idea of IC, which is closely related to decision feedback (DF) is:

- to detect part of the transmitted data symbols

- to reconstruct the contribution of these transmitted data symbols to the compound received signal and
- to subtract this contribution from the compound received signal

Hence, for signals not yet detected, interference is reduced and their signal-to-noise ratio is improved provided that most of the previously detected data symbols are detected correctly. Once the contribution of these data symbols is cancelled, the next part of the transmitted data symbols is detected and the contribution of this next part of the transmitted data symbols is cancelled from the compound received signal. By this principle, the effect of intracell interference is eliminated. However, the approach of IC is not optimum, as when detecting part of the transmitted data symbols, all the other contributions that have not yet been cancelled, are still treated as noise.

The idea of JD is to detect the data symbols of all users jointly in one step, using all the a priori knowledge about MAI. By JD, intracell interference is eliminated since no contribution of any user to the compound received signal is treated as noise. Hence, the principle of JD is optimum.

For two reasons, MUD is an obvious detection principle for the uplink. Firstly, it is the task of the base station receiver to detect the data symbols of all active users within the cell. Secondly, the knowledge required for MUD about all user-specific CDMA codes is available at the base station. Hence, intracell interference, which is a major component of the total interference, can be eliminated by applying MUD to the uplink. In the case of the downlink, at an individual mobile station receiver the spreading sequences used for transmission from the base station to other mobile stations are not known a priori. Furthermore, only the data symbols addressed to that individual mobile station have to be detected. Hence, the obvious data detection principle for the downlink is single user detection (SD). However, the application of MUD is also conceivable for the downlink. As in the uplink, also in the downlink MUD leads to a performance enhancement over SD due to the elimination of intracell interference. The application of MUD to the downlink requires that the spreading sequences of all active users are known at each mobile station. The applied spreading sequences of all presently active users can either be communicated from the base station to all mobile stations or can be estimated at the mobile stations.

The detector performance improves in the order SD, IC, JD. In the same order, the potential of interference elimination and therefore system capacity enhancement increases. JD has the potential to perfectly combat intracell interference, which is the main problem of CDMA. However, this substantial improvement has to be paid for by an increased receiver complexity.

The first publication on multiuser detection was presented by Schneider [14], who studied the zero-forcing decorrelating detector. Later, Kashihara [15] and Kohno et al. [16] studied multiple-access interference cancellation receivers. Both Schneider and Kohno also suggested the use of the Viterbi algorithm for optimal detection in asynchronous multiuser communications. The real trigger to the increasing interest in multiuser detection was Verdu's work on multiuser detection [17,18], where the application of the Viterbi algorithm for optimal maximum likelihood sequence (MLS) detection was developed, and its performance was analyzed. Verdu showed that the CDMA systems are neither interference nor near-far limited. However, these are the actual limitations of the conventional single-user receiver.

Since the optimal multiuser detection is prohibitively complex to implement for many practical applications, numerous suboptimal schemes have been investigated. A review of multiuser demodulation literature will be presented in Chapter 2. The work on multiuser receivers has demonstrated that even suboptimal detectors with a significantly lower implementation complexity than the optimal detector can greatly improve the detection performance and capacity of multiuser communication systems. Furthermore, robust detection in the presence near-far interference was shown to be possible.

1.4. Aim and outline of the thesis

In spite of the major research effort invested in multiuser demodulation techniques, several practical as well as theoretical open problems still exist in the field of multiuser receivers. Some of them are considered in more detail in this thesis. The aim of the thesis is to develop practical multiuser demodulation algorithms for mobile communication systems with frequency-selective fading channels, and to analyze their implimentation complexity. The emphasis is restricted to the uplink of asynchronous DS-

CDMA systems where users transmit in an uncoordinated manner and are received by one centralized receiver.

The work undertaken for this thesis is an extension of the work of [96,97] where a 2-path time dispersive fading channel was considered and a receiver structure was derived using maximal ratio combining. In this thesis, a 3-path time dispersive fading channel is considered. Furthermore, selection diversity is incorporated into the receiver structure.

The remainder of this chapter outlines the subsequent chapters in the thesis.

Chapter 2: The fundamentals of direct sequence spread spectrum are introduced in this chapter. The notations and mathematical model for the CDMA system to be utilized in the later chapters are introduced. The relevant literature on single-user fading channels as well as on multiuser demodulation is reviewed. Furthermore, this chapter deals with the discussion of detector structures for the additive-white Gaussian noise channel.

Chapter 3: This chapter deals with the theory behind fading. This background knowledge is required for the development of the system model for the channel for use in later chapters.

Chapter 4: This chapter deals with multiuser receiver structures for the fading channel, which is analogous to their counterparts for the Gaussian channel.

Chapter 5: This chapter is the original work that has been undertaken for the MSc study. This is the evaluation of a multiuser receiver structure for a frequency-selective fading channel, where there exists a steady specular path and two fading paths.

Chapter 6: This chapter is an extension of the work done in the Chapter 5. Here the effect of selection diversity is investigated by examining the bit error rate (BER) results. These results are confirmed both analytically and by simulation.

Chapter 7: This chapter is based on the research conducted in [138]. The application of neural networks to the demodulation of spread spectrum signals is examined. The proposed multiuser detector for CDMA systems

incorporates an extended Kalman filter and a neural network. The BER results for this receiver are obtained and compared with those in [60].

Chapter 8: This chapter concludes the thesis. The results and contributions of the previous chapters are summarized and discussed. Furthermore, some open problems for future research are pointed out.

1.5. Original contributions of this thesis

A number of original contributions in the theory of MUD have been made in this thesis. These are listed below.

- A MUD, incorporating maximal ratio combining (MRC), for a three path fading channel is derived. The BER and asymptotic multiuser efficiency (AME) of this detector are characterised. It is shown that the performance of this detector is good.

- A MUD for selection diversity is derived. The performance of this detector is characterised in terms of the BER and AME. It is shown that the results of the analytical and simulation models for this detector are in agreement with each other.

- An adaptive MUD based on the neural network is derived. The performance of this detector is studied via computer simulations showing that it performs favourably compared with others that have appeared in the literature.

Chapter 2: Detectors for the AWGN channel

2.1. Introduction

The emphasis in this chapter is on centralized multiuser detectors that process the matched filter output to provide statistics for both channel amplitude estimation and data detection in the AWGN channel.

Multiple access interference (MAI) is the factor which limits the capacity and performance of DS-CDMA systems. The conventional detector does not take into account the existence of MAI. It follows a single-user detection strategy in which each user is detected separately without regard for others. Because of the interference among users, it will be shown in Section 2.3. that the better detection strategy is one of multi-user detection. Here, information about multiple users is used jointly to better detect each individual user. It will be shown in this chapter that the utilization of multiuser detection algorithms has the potential to provide significant additional benefits for the DS-CDMA systems [6].

The organisation of this chapter is as follows: The CDMA system model is discussed in Section 2.2. Single user detectors are discussed in Section 2.3 while an investigation into multiuser detectors is conducted in Section 2.4.

2.2. CDMA system model

In Section 2.2.1. the CDMA signal model is first defined mathematically. In Section 2.2.2. the CDMA channel and receiver model are thereafter mathematically defined.

2.2.1. CDMA Signal model

One needs to consider a CDMA channel that is shared by K simultaneous users. Each user is assigned a signature waveform $a_k(t)$ of duration T, where T is the symbol interval. A signature waveform may be expressed as [6]:

$$a_k(t) = \sum_{n=0}^{N-1} a_k(n)\, p(t - nT_c), \quad 0 \le t \le T \qquad \text{.....(2.1)}$$

where:

- $a_k(n), 0 \le n \le N-1\}$ is a PN code sequence consisting of N chips that take values $\{\pm 1\}$
- p(t) is a pulse of duration T_c, where T_c is the chip interval
- T is defined as the symbol duration
- There are N chips per symbol and $T = N*T_c$

Assume that all K signature waveforms have unit energy per bit, hence

$$\int_0^T a_k^2(t)dt = 1 \qquad \text{.....(2.2)}$$

The cross-correlations between pairs of signature waveforms are defined as follows:

$$\rho_{i,k}(\tau) = \frac{1}{T}\int_0^T a_i(t)a_k(t-\tau)dt, \quad \textit{where } i \le k \qquad \text{.....(2.3)}$$

$$\rho_{k,i}(\tau) = \frac{1}{T}\int_0^T a_i(t)a_k(t+T-\tau)dt, \quad \textit{where } i \le k \qquad \text{.....(2.4)}$$

Note that i and k are the respective users.
Assuming that BPSK signaling is used, then the information sequence of the k th user is denoted by $\{b_k(x)\}$, where the value of each information bit may be ± 1 in the x^{th} symbol interval.

In purely asynchronous CDMA systems the data packet length are very large. Each user activates and deactivates its terminal independently from each other. Thus, it is not practical to assume that the whole received signal or the matched filter output vector would be processed in a receiver. The received signal can be processed in processing windows of length 2M+1 where M is a positive integer and the window length is measured in symbol durations T. The detection problem in an asynchronous channel is more complicated than in a synchronous channel. In a synchronous channel, the bits of each user are aligned in time. Detection can focus on one bit interval independent of the others. In most realistic applications, the channel is asynchronous and there is overlap between bits of different intervals. Any

decision made on a particular bit ideally needs to take into account the decisions on the two overlapping bits of each user; the decisions on these overlapping bits must then further take into account decisions on bits that overlap them and so on. Hence, the detection problem must optimally be framed over the whole message. More information on this model will be provided in Chapter 6 of this thesis.

Hence, consider the transmission of a block of bits of length 2M+1.
Then, the data block from the k^{th} user is:

$$b_k = [b_k(-M) \quad ..... \quad b_k(M)]^T \qquad (2.5)$$

The data symbols $b_k(x)$, x=-M...M, may be obtained after the steps of source and channel coding and interleaving.

The signal, before spreading, is given by [6]:

$$s_k(t) = \sqrt{E_k(t)}b_k(t)\cos(\omega_0 t + \theta_k) \qquad (2.6)$$

where:

- E_k is the energy of the signal of user k
- ω_0 is the carrier frequency
- θ_k is the phase of the signal of user k

Spreading is accomplished by the multiplying (2.6) by (2.1). Generation of the transmitted signal has been shown in Figure 1.1 and it is given by:

$$s_k(t) = \sqrt{E_k(t)}a_k(t)b_k(t)\cos(\omega_0 t + \theta_k) \qquad (2.7)$$

The bandwidth expansion factor or the processing gain, is defined as:

$$B_c = \frac{T}{T_c} = \frac{R_c}{R_b} \qquad (2.8)$$

where:

- R_b is the data rate
- R_c is the chip rate

The corresponding equivalent lowpass, transmitted waveform may be expressed as [6]

$$s_k(t) = \sqrt{E_k} \sum_{x=-M}^{M} b_k(x) a_k(t - xT) \cos\theta_k \quad \text{.....(2.9)}$$

where:

- E_k is the signal energy per bit.

The composite transmitted signal for the K users may be expressed as

$$s(t) = \sum_{k=1}^{K} s_k(t - \tau_k)$$

$$= \sum_{x=-M}^{M} \sum_{k=1}^{K} b_k(x) \sqrt{E_k} a_k(t - xT - \tau_k) \cos\theta_k \quad \text{.....(2.10)}$$

where:

- τ_k are the transmission delays, which satisfy the condition that $0 \le \tau_k < T$ for $1 \le k \le K$

This is the model for the multiuser transmitted signal in an asynchronous mode. In the case of synchronous transmission, $\tau_k = 0$ for $1 \le k \le K$

2.2.2. CDMA channel and receiver model

The signal $s_k(t)$ is transmitted over a time-variant linear radio channel with impulse response $h_k(\tau,t)$, where τ denotes the delay time, and t denotes the absolute time. This is shown in Figure 2.1.

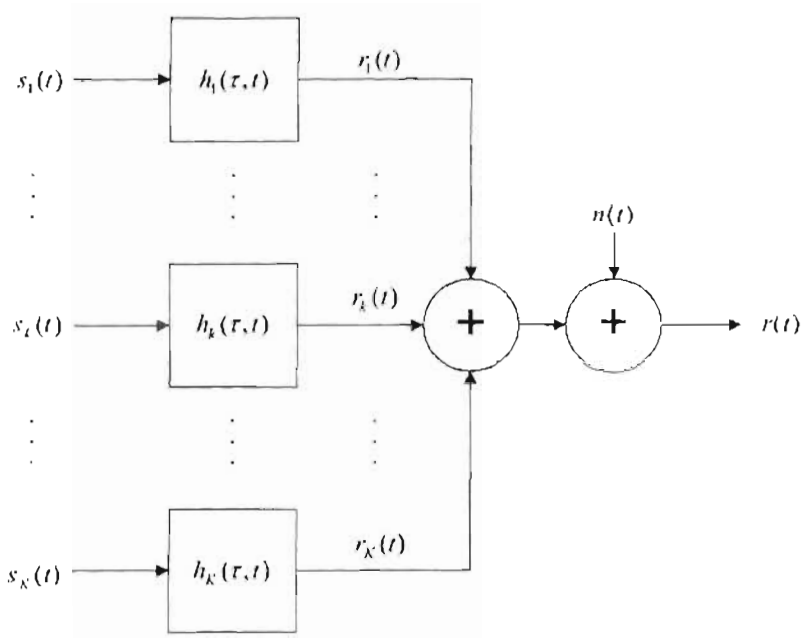

Figure 2.1.
Continuous-time transmission model for multiple access

- The index k in $h_k(\tau,t)$ designates the link between the mobile station transmitter k and the base station receiver.
- The delay time τ is the delay in excess of the minimum propagation time between transmitter k and receiver, and characterizes the time spread introduced by multipath propagation when a Dirac impulse is transmitted over the channel.
- The minimum delay time is zero.
- The maximum delay time resulting from multipath propagation is denoted by τ_{max}.

The signal contributions appearing at the receiver and resulting from the signal $s_k(t)$ transmitted by user k, is given by the convolution product

$$r_k(\tau) = \int_0^{\tau_{max}} s_k(t-\tau) h_k(\tau,t) d\tau \quad \text{.....(2.11)}$$

The compound received signal observed at the receiver is the superposition of the K contributions $r_k(t)$, k=1.....K of all K users and is disturbed by an additive noise signal n(t) .

$$r(t) = \sum_{k=1}^{K} r_k(t) + n(t) \quad \text{.....(2.12)}$$

Adjacent cell intracell interference and thermal noise contribute to n(t). In the case of CDMA, the K signals $r_k(t)$, k=1.....K, are neither disjoint in the frequency domain nor in the time domain, but are only separable by means of the different user-specific spreading sequences. It is assumed that the time duration of the signal $s_k(t)$ is so short, that the channel impulse response $h_k(\tau,t)$ may be considered time-invariant during the transmission of $s_k(t)$ ie. $h_k(\tau) = h_k(\tau,t)$.

2.3. Single user detection

The conventional detector is considered in Section 2.3.1 while methods of overcoming MAI are discussed in Section 2.3.2.

2.3.1. Conventional Detection

Herein a more detailed look is taken at the conventional detector and the effect of multiple access interference. In a synchronous channel, all bits of all users are aligned in time. To simplify the discussion, the assumption is made that the channel is synchronous and all carrier phases are equal to zero. This enables one to use baseband notation while working only with real signals. Further simplifications are that each transmitted signal arrives at the receiver over a single path (no multipath), and that the data modulation is binary phase-shift keying (BPSK). Using the results of (2.7) to (2.12), the received signal is given as (2.13).

$$r(t) = \sum_{k=1}^{K} \sqrt{E_k}(t) b_k(t) a_k(t) + n(t) \quad \text{.....(2.13)}$$

- As defined in Section 2.2.1, $\sqrt{E_k}$ (t), $a_k(t)$ and $b_k(t)$ are the amplitude, signature code waveform and modulation of the k^{th} user respectively.
- n(t) is additive white Gaussian noise, with a two-sided power spectral density of $N_0/2$ W/Hz.
- The power of the k^{th} user is assumed to be constant over a bit interval. As

explained in Section 2.2.1, a total of 2M+1 transmitted bits is assumed.

The conventional detector for the received signal described in (2.13) is a bank of K correlators as shown in Figure 2.2.

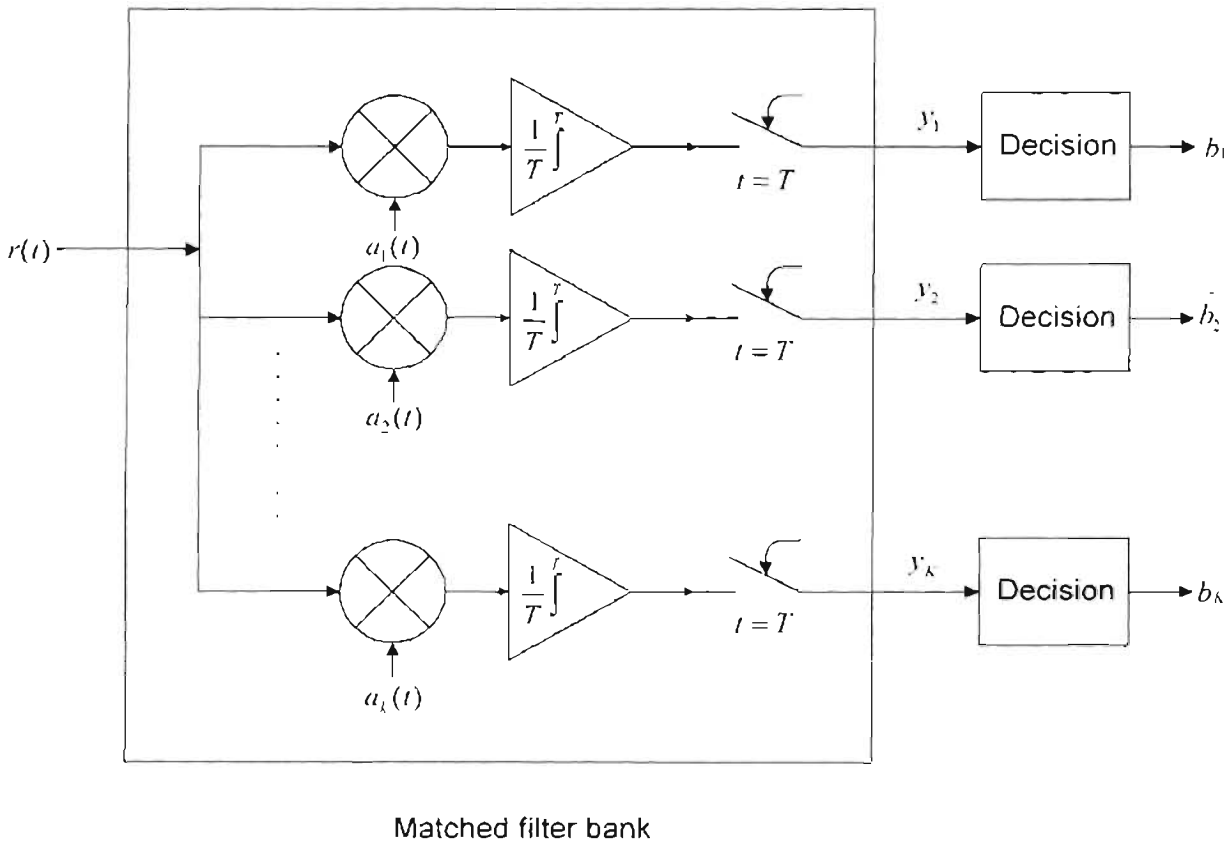

Figure 2.2.
The conventional detector

Each code waveform is regenerated and correlated with the received signal in a separate detector branch. The correlation detector can be equivalently implemented through what is known as simple matched filtering, hence the conventional detector is often referred to as the simple matched filter detector. The outputs of the correlators (or matched filters) are sampled at the bit times, which yields "soft" estimates of the transmitted data. The final ± 1 "hard" data decisions are made according to the signs of the soft estimates.

It is evident from Figure 2.2 that the conventional detector follows a single-user detector strategy, in that each branch detects one user without regard to the existence of the other users. Thus, there is no multi-user detection. The success of this detector depends on the properties of the correlations between codes. The requirement is that the correlations between the same code waveforms (autocorrelations) must be larger than the correlations between different codes (cross-correlations). The correlation value has been defined in (2.3) and is obtained by setting τ to 0 for the synchronous case, to yield:

$$\rho_{i,k} = \frac{1}{T}\int_0^T a_i(t)a_k(t)dt \qquad (2.14)$$

Note that if i=k, $\rho_{k,k}=1$, and if $i\neq k$, $0\leq\rho_{k,k}<1$. The output of the k^{th} user's correlator for a particular bit interval is [6]

$$\begin{aligned} y_k &= \frac{1}{T}\int_0^T r(t)a_k(t)dt \\ &= \sqrt{E_k}b_k + \sum_{i=1, i\neq k}^{K} \rho_{i,k}\sqrt{E_i}b_i + \frac{1}{T}\int_0^T n(t)a_k(t)dt \\ &= \sqrt{E_k}b_k + MAI_k + z_k \end{aligned} \qquad (2.15)$$

Correlation with the kth user itself gives rise to the recovered data term, correlation with all the other users gives rise to multiple access interference(MAI), and correlation with the thermal noise yields the noise term z_k.

The conventional detector has a complexity that grows linearly with the number of users and its vulnerability to the near-far problem requires some type of power control. One needs to consider other types of detectors that also have a linear computational complexity but does not suffer from the near-far problem.

2.3.2. Overcoming the effect of MAI

In this section, various methods are suggested on overcoming the detrimental effects of MAI. Some of these solutions entail optimal code waveform design, power control, FEC coding and sectored/adaptive antennas. Each of these solutions will be briefly discussed in this section.

a) code waveform design

This approach is aimed at the design of spreading codes with good cross-correlation properties. Ideally, if the codes were orthogonal, then $\rho_{i,k}=0$, and there would be no MAI term. However, since in practice most channels contain some degree of asynchronism, it is not possible to design codes that maintain orthogonality over all possible delays. So instead, one looks for codes that are nearly orthogonal, so that they have as low a cross-correlation as possible.

b) power control

The use of power control ensures that all users arrive at about the same power, and therefore no user is unfairly disadvantaged relative to the others. The mobiles adjust their power through two methods. One method is for the mobiles to adjust their transmitted power to be inversely proportional to the power level it receives from the base station (open loop power control). The other method is for the base station to send power control instructions to the mobiles based on the power level it receives from the mobiles (closed loop power control).

c) FEC Codes

The design of more powerful forward error correction (FEC) codes allows acceptable error rate performance at lower signal-to-interference ratio levels.

d) Sectored/Adaptive antennas

Directed antennas are used that focus reception over a narrow desired angle range. Hence, the desired signal and some fraction of the MAI are enhanced (through antenna gain), while the interfering signals that arrive from the remaining angles are attenuated. The direction of the antenna can be fixed, as is the case for sectored antennas, or adjusted dynamically. In the latter case, adaptive signal processing is used to focus the antenna in the direction corresponding to a particular desired user(s).

2.4. Multi-user detection

In multi-user detection, code and timing (and possibly amplitude and phase) information of multiple users are jointly used to better detect each individual user. The important assumption is that the codes of the multiple users are known to the receiver a priori.

Verdu's work [17, 18] , proposed and analyzed the optimal multiuser detector, or the maximum likelihood sequence detector. Unfortunately, this detector is too complex for practical DS-CDMA systems. Subsequently, most of the research has focused on finding suboptimal multiuser detector solutions which are more feasible to implement.

Most of the proposed detectors can be classified in one of two categories: linear multi-user detectors and subtractive interference cancellation detectors. In linear multi-user detection, a linear mapping is applied to the soft outputs of the conventional detector to produce a new set of outputs, which should ideally provide better performance. In subtractive interference cancellation detection, estimates of the interference are generated and subtracted out.

The organisation of this section is as follows: The matrix-vector notation is first introduced in Section 2.4.1. Some background information is given on the asynchronous channel in Section 2.4.2. A brief discussion on multiuser receiver performance is given in Section 2.4.3. In Section 2.4.4, MLS detection is considered while linear detectors are considered in Section 2.4.5. Subtractive interference detectors are considered in Section 2.4.6 while other detectors are considered in Section 2.4.7.

2.4.1. Matrix-Vector notation

In discussing multi-user detection, it is convenient to introduce a matrix-vector system model to describe the output of the conventional detector.

Consider a case with 3 users in a synchronous system. Let the amplitude of the signal for the kth user be given by $A_k = \sqrt{E_k}$. Using (2.15), the outputs of the matched filter banks for each of the 3 users for one bit are given as:

$$y_1 = A_1 b_1 + \sum_{i=1, i\neq k}^{3} \rho_{i,k} \sqrt{E_i} b_i + \frac{1}{T}\int_0^T n(t) a_1(t) dt \quad \text{.....(2.16)}$$
$$= A_1 b_1 + \rho_{2,1} A_2 b_2 + \rho_{3,1} A_3 b_3 + z_1$$

$$y_2 = A_2 b_2 + \sum_{i=1, i\neq k}^{3} \rho_{i,k} \sqrt{E_i} b_i + \frac{1}{T}\int_0^T n(t) a_2(t) dt \quad \text{.....(2.17)}$$
$$= A_2 b_2 + \rho_{1,2} A_1 b_1 + \rho_{3,2} A_3 b_3 + z_2$$

$$y_3 = A_3 b_3 + \sum_{i=1, i\neq k}^{3} \rho_{i,k} \sqrt{E_i} b_i + \frac{1}{T}\int_0^T n(t) a_3(t) dt \quad \text{.....(2.18)}$$
$$= A_3 b_3 + \rho_{1,3} A_1 b_1 + \rho_{2,3} A_2 b_2 + z_3$$

This can be written in the matrix-vector form as:

$$\begin{bmatrix} y_1 \\ y_2 \\ y_3 \end{bmatrix} = \begin{bmatrix} 1 & \rho_{2,1} & \rho_{3,1} \\ \rho_{1,2} & 1 & \rho_{3,2} \\ \rho_{1,3} & \rho_{2,3} & 1 \end{bmatrix} \begin{bmatrix} A_1 & 0 & 0 \\ 0 & A_2 & 0 \\ 0 & 0 & A_3 \end{bmatrix} \begin{bmatrix} b_1 \\ b_2 \\ b_3 \end{bmatrix} + \begin{bmatrix} z_1 \\ z_2 \\ z_3 \end{bmatrix} \quad \text{.....(2.19)}$$

or

$$y = RAb + z \quad \text{.....(2.20)}$$

- For a K user system, the vectors b,z and y are the K-vectors that hold the data, noise and matched filter outputs of all K users, respectively;
- the matrix A is a diagonal matrix containing the corresponding received amplitudes; the matrix R is KxK correlation matrix, whose entries contain the values of the correlations between every pair of codes.
- Note that since $\rho_{i,k} = \rho_{k,i}$, the matrix R is symmetric.

R can be split up into two matrices: one representing the autocorrelations, the other the crosscorrelations. Similar to (2.15), the conventional matched filter detector output can be expressed as three terms:

$$y = Ab + QAb + z \quad \text{.....(2.21)}$$

Q contains the off-diagonal elements (crosscorrelations) of R, ie. R=I + Q (I is the identity matrix). The first term Ab, is the decoupled data weighted by the received amplitudes. The second term, QAb, represents the MAI interference.

2.4.2. Asynchronous Channel

The continuous-time model expressed in (2.13) can easily be modified for asynchronous channels by including the relative time delays between signals, as explained in Section 2.2.1. The received signal is now written as

$$r(t) = \sum_{k=1}^{K} \sqrt{E_k}(t) b_k(t - \tau_k) a_k(t - \tau_k) + n(t) \quad \text{.....(2.22)}$$

where

- τ_k is the delay for user k.

The discrete-time matrix-vector model describing the asynchronous channel takes the same form as (2.20). However, now the equation must encompass the entire message, thus assuming there are 2M+1 bits per user, the size of the vectors and the order of the matrices are (2M+1)K. The vectors b, z and y hold the data, noise and matched filter outputs of all K users for all (2M+1) bit intervals , and the matrix A contains the corresponding received amplitudes. The matrix R now contains the partial correlations that exist between every pair of the 2M+1 code words and is of size [(2M+1) x (2M+1)]. Hence, (2.22) can now be rewritten as:

$$r(t) = \sum_{x=-M}^{M} \sum_{k=1}^{K} b_k(x) \sqrt{E_k} a_k(t - xT - \tau_k) + n(t) \quad \text{.....(2.23)}$$

2.4.3. Multi-user receiver performance

The performance of multiuser receivers can be measured by the bit error rate (BER), as well as by mean squared error (MSE) of the detector output or channel estimates. Furthermore, other performance criteria yielding simpler analysis than the bit error probability have also been considered. They include the asymptotic multiuser efficiency (AME) [17,18], and the near-far resistance (NFR) [21, 22]. The AME describes the asymptotic limit of the loss in the signal-to-noise ratio (SNR) as the power spectral density of the noise approaches zero. For coherent BPSK modulation in AWGN channels, AME is defined as

$$\eta_k = \sup_{\rho \in [0,1]} \lim_{\sigma^2 \to 0} \frac{P_k}{Q\left(\sqrt{\frac{\rho E_k}{\sigma^2}}\right)} < \infty \qquad (2.24)$$

where sup denotes the smallest upper bound and $\rho \in [0,1]$,

$$Q(d) = \frac{1}{\sqrt{2\pi}} \int_d^{\infty} e^{-t^2/2} dt \qquad (2.25)$$

is the normalized and scaled Gaussian complementary error function and P_k is the bit error probability of user k with the particular multiuser detector. The near-far resistance is the value of the AME for the worst possible interfering energy combination and is defined as

$$\bar{\eta}_k = \inf_{E_i \geq 0, i \neq k} \eta_k \qquad (2.26)$$

Note that inf denotes the infimum in (2.26).
The detector for user k is said to be near-far resistant if $\bar{\eta}_k > 0$. The optimal multi-user receiver is considered in Section 2.4.4 and suboptimal ones in the Sections 2.4.5, 2.4.6 and 2.4.7.

2.4.4. Maximum-likelihood sequence detection

The detector which yields the most likely transmitted sequence, $\bar{b}$, chooses $\bar{b}$ to maximize the probability that $\bar{b}$ was transmitted given that r(t) was received, where r(t) extends over the whole message. This probability is

referred to as the joint a posteriori probability. Under the assumption that all possible transmitted sequences are equally probable, this detector is known as the maximum-likelihood sequence (MLS) detector.

The derivation of the MLS detector can be found in [6] and will not be duplicated here. However, it will suffice to say that the optimum multiuser (MLS) detector selects the most likely hypothesis $\bar{b} = (\bar{b}_1, \ldots\ldots, \bar{b}_K)$ given the observations, which corresponds to selecting the noise realization with minimum energy (considering the synchronous case), that is:

$$\hat{b} \in \arg \min \int_0^T [r(t) - \sum_{k=1}^{K} \sqrt{E_k} b_k a_k(t)]^2 dt \qquad (2.27)$$

The problem with the MLS approach is that there are $2^{(2M+1)K}$ possible b vectors; an exhaustive search is impractical for typical message sizes and numbers of users. However, MLS detection can be implemented for DS-CDMA by following the matched filter bank with a Viterbi algorithm [6, 75-76]. However, the required Viterbi algorithm has a complexity that is still exponential in the number of users.

Another disadvantage of the MLS detector is that it requires knowledge of the received amplitudes and phases. These values, however, are not known a priori, and must be estimated. One would need to use some of the parameter estimation techniques as discussed in **Appendix 1**.

The asymptotic multiuser efficiency of the MLS detector has been analyzed in [18, 77-78]. MLS detector for trellis-coded modulated CDMA transmissions in AWGN channels has been studied in [79], and for convolutionally encoded transmissions in [80]. The effect of delay estimation errors of MLS detector has been considered in [45]. Joint maximum likelihood sequence detection and amplitude estimation in AWGN channels has been analyzed in [63]. In [20] a recursive, additive metric for complexity-constrained maximum likelihood detection using breadth-first detection algorithms was proposed. The metric required linear filtering of the matched-filtered received signal vector. However, for this method to work, perfect power control was required and the complexity of the receiver had not been substantially reduced. The performance of the MLS detector was analyzed in [17, 18]. It turned out to be impossible to derive a closed form bit error probability expression for the MLS detector.

Upper and lower bounds, most of which are complicated to calculate, were found. The simplest lower bound is the single-user bound (or matched filter bound) which is the performance of a communication system with one active user.

Despite the huge performance and capacity gains over conventional detection, the MLS detector is not practical. A realistic direct-sequence system has a relatively large number of active users; thus, the exponential complexity in the number of users makes the cost of this detector too high.

Various other suboptimal multiuser detectors are now examined in the following sections, which are simpler to implement. For the remainder of the chapter, an asynchronous channel is assumed unless otherwise stated.

2.4.5. Linear Detectors

It was shown that the conventional detector has a complexity that grows linearly with the number of users, but its vulnerability to the near-far problem requires some type of power control. In this section, detectors that also have a linear computational complexity but do not exhibit the vulnerability to other-user interference, are examined.

An important group of multi-user detectors are linear multi-user detectors. These detectors apply a linear mapping, β, to the soft output of the conventional detector to reduce the MAI seen by each user. The two most popular of the linear detectors are the decorrelating and minimum mean-squared error (MMSE) detectors. A polynomial expansion detector is considered in Section 2.4.5.3 , which can efficiently implement both the decorrelator and MMSE detectors.

The decorrelating and MMSE detectors are discussed in Sections 2.4.5.1 and 2.4.5.2, respectively. The polynomial expansion detector is discussed in Section 2.4.5.3.

2.4.5.1. Decorrelating Detector

The decorrelating detector applies the inverse of the correlation matrix

$$\beta = R^{-1} \quad \text{.....(2.28)}$$

to the conventional detector output of Figure 2.2, in order to decouple the data. From (2.20), the soft estimate of this detector is given by:

$$\begin{aligned} b_{dec} &= R^{-1}y = Ab + R^{-1}z \\ &= Ab + z_{dec} \end{aligned} \quad \text{.....(2.29)}$$

which is just the decoupled data plus a noise term. It is evident that the decorrelating detector completely eliminates the MAI. This detector is very similar to the zero-forcing equalizer [6] that is used to completely eliminate ISI.

The decorrelating detector was initially proposed in [23]. It was extensively analyzed by Lupas & Verdu in [21, 22] and is shown to have many attractive properties. Further justification for its study is provided by the fact that it is a solution to the maximum likelihood detector when the energies are not known by the receiver. The only requirement for the signal of a user to be detected reliably by the decorrelating detector regardless of the level of multiple-access interference, is that it does not belong to the subspace spanned by the other signals. Foremost among the advantages of the decorrelator are [21, 22, 24] that it:

a) provides substantial performance/capacity gains over the conventional detector under most conditions.

b) Does not need to estimate the received amplitudes. In contrast, detectors that require amplitude estimation are often quite sensitive to estimation error.

c) Has a computational complexity significantly lower than that of the maximum likelihood sequence detector – the per-bit complexity is linear in the number of users.

d) Corresponds to the maximum likelihood sequence detector when the energies of all users are not known at the receiver – it yields the joint maximum likelihood sequence estimation of the transmitted bits and their received amplitudes.

e) Has a probability of error independent of the signal energies – this simplifies the probability of error analysis, and makes the decorrelating detector resistant to the near-far problem.

f) Yields the optimal value of the near-far resistance performance metric

g) Can decorrelate one bit at a time – for bit l, one only needs to apply the lth row of R^{-1} to the matched filter bank outputs.

A disadvantage of this detector is that it causes noise enhancement which is similar to the zero-forcing equalizer [6]. The power associated with the noise term $R^{-1}z$ at the output of the decorrelating detector in (3.14) is always greater than or equal to the power associated with the noise term at the output of the conventional detector in (3.6) for each bit. This has been proven in [25]. Despite this drawback, the decorrelating detector generally provides significant improvements over the conventional detector. A more significant disadvantage of the decorrelating detector is that the computations needed to invert the matrix R are difficult to perform in real time. For synchronous systems, the problem is somewhat simplified: one bit at a time can be decorrelated. The inverse of a KxK correlation matrix can be applied. For asynchronous systems, R is of order (2M+1)K, which is quite large for a typical message length (2M+1).

There have been numerous suboptimal approaches to implementing the decorrelating detector [24, 26]. Many of them entail breaking up the detection problem into more manageable blocks [27-32] and possibly even to one transmission interval [24, 29]. The inverse matrix can then be exactly computed. A K-input K-output linear filter implementation is also possible as in [21], where the filter coefficients are a function of the cross-correlations.

Whichever suboptimal decorrelating detector technique is used, the computation required is substantial. The use of codes that repeat each bit is generally assumed so that the partial correlations between all signals are the same for each bit. This minimizes the need for recomputation of the matrix

inverse or the filter coefficients from one bit interval to the next. Where recomputation cannot be avoided, research has been directed at trying to simplify the cost of recomputation. The processing burden still appears to present implementation difficulties.

The estimate of the data given by (2.29), which is obtained by processing a block of 2M+1 bits, can also be computed sequentially. In [27], it has been demonstrated that the transmitted bits may be recovered sequentially from the received signal, by employing a form of decision-feedback equalizer with finite delay. Thus, there is a similarity between the detection of signals corrupted by ISI in a single-user communication system and the detection of signals in a multiuser system with asynchronous transmission [6].

Decorrelating detectors are ideally infinite memory-length detectors. This is because their memory length equals the number of users times the data packet length, which often can be assumed to approach infinity. To obtain practical detectors, which have low implementation complexity and are suitable for CDMA systems with time-variant system parameters (such as the number of users, delays of users and the signature waveforms), linear finite-memory length multiuser detectors have been studied in [37]. The infinite memory length also has been one motivation to introduce adaptive, decentralized, one-shot multiuser detectors [38-41]. The drawbacks of these detectors is that they may require long adaptation times, and the adaptation must be repeated frequently. The training sequences required in most adaptive detectors degrade the bandwidth efficiency, especially if the adaptation must occur frequently. Furthermore, the one-shot approach is inherently suboptimal, even in the class of linear detectors.

In [37], it was shown that the infinite-memory length decorrelating detector can be accurately approximated by detectors with finite and relatively short memory lengths. It is shown that the near-far resistance to a high degree can be obtained by moderate memory lengths. This result provides a mechanism to implement near-far resistant linear multiuser detectors in systems in which the number of users or their propagation delays change over time. This problem was detected in [27] and [42], but only the special case of the MMSE and noise-whitening detectors was considered.

The decorrelator can be characterized as the inverse of some form of correlation matrices. The correlation values depend on the number of users,

the signature waveforms and the delays of the users. A change in one of these parameters, results in a change in the correlations, and an update of the decorrelator is required. This is a computationally complex task due to the correlation matrix inversion. In [36], implementation algorithms for linear multiuser detectors were considered for systems where the detectors must be updated frequently. Iterative decorrelating and MMSE detectors were proposed. These iterative detectors used the steepest descent, conjugate gradient and preconditioned conjugate gradient algorithms. The implementation complexity of these detectors was alleviated as there was no need to invert or Cholesky factorize the matrix R. The performance of the iterative detectors was highly dependent on the number of iterations [36]. These iterative detectors provide a tradeoff between the implementation complexity and the performance. The simulation results in [36] showed that moderate numbers of iterations give the same performance as the ideal detectors.

Although the decorrelator presented in [21] did not require knowledge of signal amplitudes, the decorrelating method still required knowledge of the signature sequence arrival times. Similarly, the noncoherent differential phase shift keying (DPSK) decorrelator-based detector developed in [33], while not requiring knowledge of the received phase, still assumed known arrival times.

In [34], a linear decorrelator detector was proposed for a quasisynchronous code-division multiple-access (QS-CDMA) cellular system. The CDMA system is quasisynchronous if the delays are small compared to the symbol interval. It was assumed that each of the users had a global positioning system generated local clock and that they attempted to transmit synchronously with the other users in its cell. By using GPS, the mobiles could compensate for the path delays, thereby reducing the timing error. If the timing uncertainty occupied a sufficiently small region, it was possible to obtain excellent bit-error rate performance, without power control, using a relatively simple decorrelating detector. The decorrelator output could then be detected noncoherently, eliminating the need for phase estimation.

Optimum single-user decorrelating receivers, correlate the received signal with a sequence of (infinite precision) real numbers. In [35], designing optimum finite-precision decorrelators for CDMA networks was considered. When using these finite-precision decorrelators, multiplications can be performed with simple combinatorial logic circuits. From a practical view-

point, this problem is important because fixed-point implementations are cheaper, faster and more energy efficient than designs with floating point processing units. It was shown in [35] that the use of optimum finite-precision decorrelators in networks with rapidly time-varying multiuser interference is not feasible. However, in networks which allow for pre-computation of the decorrelator sequences, the proposed approach in [35] was feasible because of the low demodulation complexity of the resulting receivers. The results of [35] show that the optimum finite-precision receivers closely match the performance of infinite-precision decorrelators up to moderately high channel occupancies.

The principle of the decorrelating receiver has been extended to receivers utilizing antenna arrays [32, 82-83], multiple base stations [84-85] or multiple data rates [86-87]. Adaptive implementations of the decorrelating detector for synchronous CDMA systems have been considered in [74, 88]. The decorrelating receiver for convolutionally encoded CDMA transmissions in AWGN channels has been studied in [89]. Decorrelating receivers for quasi-synchronous CDMA systems in AWGN channels without precise delay estimation has been proposed in [29, 34, 90] and for code acquisition in quasi-synchronous CDMA in [91]. The effect of delay estimation errors to the decorrelating performance has been analyzed in [92-93].

2.4.5.2. Minimum Mean-squared error (MMSE) detector

The minimum mean-squared error (MMSE) detector [27] is a linear detector which takes into account the background noise and utilizes knowledge of the received signal powers. This detector implements the linear mapping which minimizes $E[|b - \beta y|^2]$, the mean-squared error between the actual data and the soft output of the conventional detector. This results in [27, 41]

$$\beta_{MMSE} = [R + (N_0/2)A^{-2}]^{-1} \quad \text{.....(2.30)}$$

The soft estimate of the MMSE detector is simply

$$b_{MMSE} = \beta_{MMSE} y \quad \text{.....(2.31)}$$

It is evident that the MMSE detector implements a partial or modified inverse of the correlation matrix. The amount of modification is directly proportional to the background noise; the higher the noise level, the less complete an inversion of R can be done without noise enhancement causing performance degradation. When the noise level is large compared with the signal level in the diagonal elements of R, β_{MMSE} approaches the identity matrix. In this low-SNR case, the detector basically ignores the interference from other users, because the additive noise is the dominant term. It should also be noted that the MMSE criterion produces a biased estimate of b_{MMSE}. As a result, there is some residual multiuser interference. The MMSE detector balances the function of decoupling the users (and completely eliminate MAI) with the function of not enhancing the background noise. This multi-user detector is exactly analogous to the MMSE linear equalizer used to combat ISI [6].

Because it takes the background noise into account, the MMSE detector generally provides better probability of error performance than the decorrelating detector. As the background noise goes to zero, the MMSE detector converges in performance to the decorrelating detector.

An important disadvantage of this detector is that, unlike the decorrelating detector, it requires estimation of the received amplitudes. Another disadvantage is that its performance depends on the powers of the interfering users [27].

Hence, there is some loss of resistance to the near-far problem as compared to the decorrelating detector. Like the decorrelating detector, the MMSE detector faces the task of implementing matrix inversion. Thus, most of the suboptimal techniques for implementing the decorrelating detector are applicable to this detector as well.

An adaptive multiuser detector based on a minimum mean-square error (MMSE) criterion was presented in [38]. Although this detector did not require parameter estimates, a training sequence was necessary to provide a data reference. Several interference suppression schemes based on the MMSE criterion were considered in [38]. Explicit knowledge of the interference parameters was not required. The scheme considered in [38] was a finite complexity approximation of the MMSE linear detector, and its

performance was not as good as the performance of the decorrelating detector.

[36] dealt with implementation algorithms for linear multiuser detectors for systems where the detectors must be updated frequently and iterative MMSE detectors were proposed. In [37], it was shown that the infinite-memory length detectors such as the MMSE detector could be accurately approximated by detectors with finite and relatively short memory lengths.

MMSE multiuser detection can be implemented by employing a tapped-delay-line filter with adjustable coefficients for each user and selecting the filter coefficients to minimize the mean square error for each user signal [6]. The received information bits are estimated sequentially with finite delay, instead of as a block.

2.4.5.3. Polynomial Expansion Detector

The polynomial expansion (PE) detector applies a polynomial expansion in R to the matched filter bank output, y. The linear mapping for the PE detector is

$$\beta_{PE} = \sum_{i=0}^{N_s} w_i R^i \quad \text{.....(2.32)}$$

and the soft estimates of the data are given by

$$b_{PE} = \beta_{PE} y \quad \text{.....(2.33)}$$

For a given R and N_s (no. of stages), the weights (polynomial coefficients) w_i, i=0,1,.....,N_s can be chosen to optimize some performance measure.

The structure which implements the matrix R is shown in Figure 2.3, and the full detector (with 2 stages) is shown in Figure 2.4. In Figure 2.3 the input is the matched filter bank output vector y, and the output is Ry. A diagram of the matched filter bank was shown in Figure 2.2. Each stage implements R by recreating the overall modulation (spreading), noiseless channel

(summing), and demodulation (matched filtering) process. From the expression for the noiseless conventional detector output, y = RAb, it is clear that R is implemented in the Figure 2.3. Cascading these stages produces higher-order terms of the polynomial. The detector in Figure 2.4 is a two-stage PE detector, while the detector corresponding to (2.32) requires N_s stages.

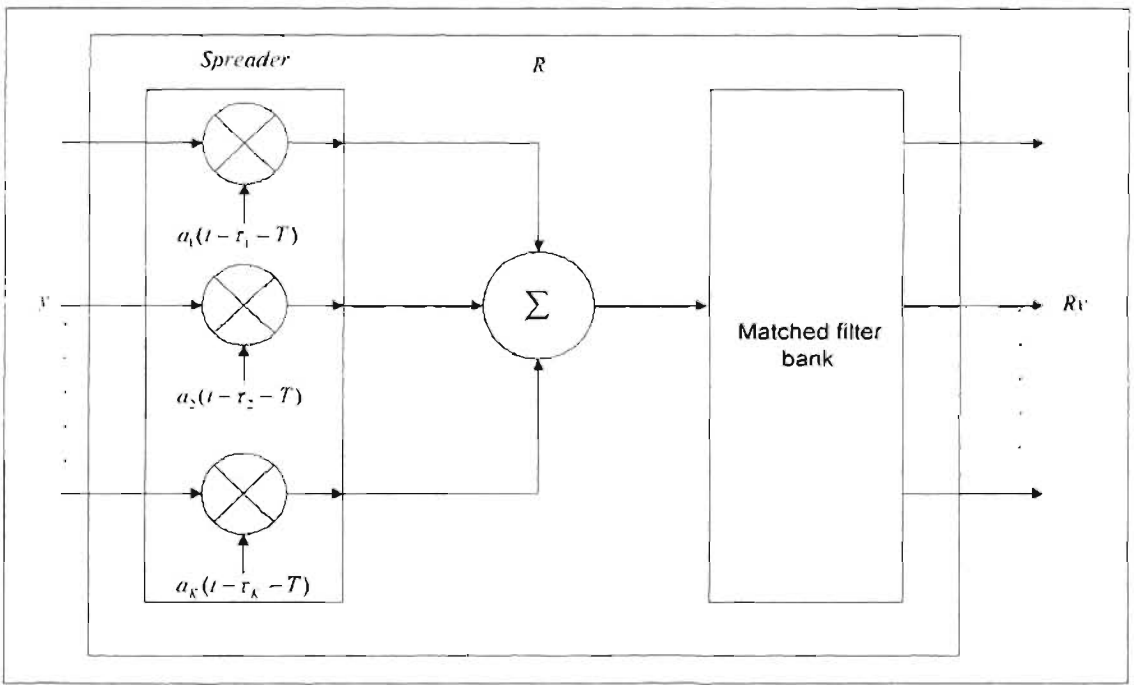

Figure 2.3.
One stage of the polynomial expansion detector

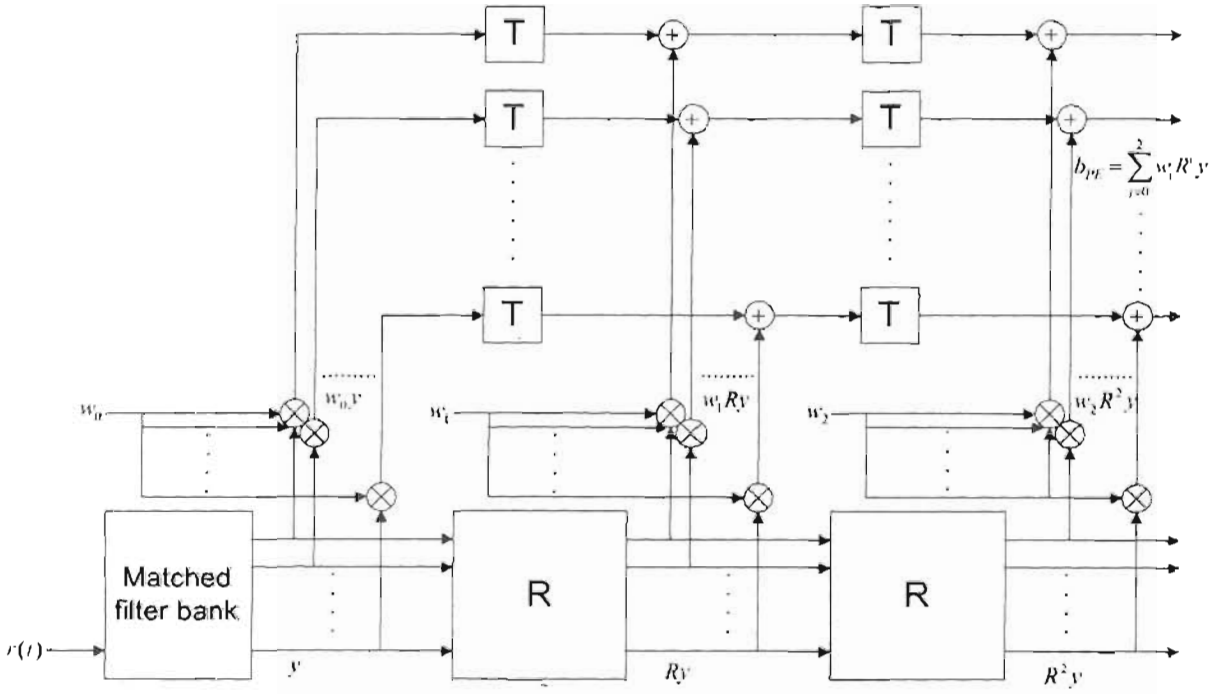

Figure 2.4.
DS-CDMA polynomial expansion detector with 2 stages

It can be shown (by the Cayley-Hamilton Theorem) that the PE detector structure can exactly implement the decorrelating detector for finite message length [43]. However, for a typical message length this would require a large number of stages, which is not feasible. As the message length approaches infinity, infinite stages would be needed, with one bit delay required per stage. However, good approximations can be obtained with a relatively small number of stages. Hence, one can choose the polynomial coefficients $w = [w_0 \; w_1 \; \ldots \; w_{N_s}]$ so that

$$p(R) = \sum_{i=0}^{N_s} w_i R^i \approx R^{-1} \qquad \text{.....(2.34)}$$

The resulting weights are used in the structure of Figure 2.4 to yield a K-input K-output finite memory-length detector, which approximates the decorrelating detector. The PE detector structure can also be used to approximate the MMSE detector, as described in [43].

The polynomial expansion detector has a number of attractive features [43], in that it:

a) Can approximate the decorrelating and MMSE detectors. As such, it has the desirable features of these two detectors, which has already been discussed in Sections 2.4.5.1. and 2.4.5.2.
b) Has a low computational complexity. In approximating the decorrelating (or MMSE) detector, there is no need to calculate the matrix R nor its inverse. Everything can be implimented on-line, using analog hardware or DSP chips.
c) Does not need to estimate the received amplitudes or phases. This important feature of the decorrelating detector, also holds for the PE detector in approximating the decorrelating detector. If the PE detector is approximating the MMSE detector, amplitude estimation will still be necessary.
d) Can be implimented just as easily using long codes as short codes
e) Can use weights that work well over a large variation of system parameters. As shown in [43], the use of additional stages in the PE detector allows more flexibility to use pre-computed weights that work well over a broad operating range. This eliminates the need to adapt the weights to changes in the operating environment.
f) Has a relatively simple structure. The types of system components used are the same as those of the conventional detector. The amount of system components increases linearly with the product of the number of users and the number of stages. The structure is very similar to that of the parallel interference cancellation detector (Section 2.4.6.2).

2.4.6. Subtractive interference cancellation

The basic operating principle for these detectors is the creation at the receiver of separate estimates of the MAI contributed by each user in order to subtract out some or all of the MAI seen by each user. Such detectors are often implemented with multiple stages, where the aim is that the decisions will improve at the output of successive stages.

These detectors are similar to feedback equalizers [6] used to combat ISI. In feedback equalization, decisions on previously detected symbols are fed

back in order to cancel part of the ISI. Thus, a number of these types of multiuser detectors are also referred to as decision-feedback detectors.
The bit decisions used to estimate MAI can be hard or soft. The soft-decision approach uses soft data estimates for the joint estimation of the data and amplitudes, and is easier to implement. The hard-decision approach feeds back a bit decision and is nonlinear; it requires reliable estimates of the received amplitudes in order to generate estimates of the MAI. If reliable amplitude estimation is possible, hard-decision subtractive interference cancellation detectors generally outperform their soft-decision counterparts. Studies such as [44, 45] indicate that the need for amplitude estimation is a significant liability of the hard-decision techniques as imperfect amplitude estimation may significantly reduce or even reverse the performance gains available.

A major disadvantage of nonlinear detectors is their dependence on reliable estimates of the received amplitudes. Studies such as [44, 45] indicate that imperfect amplitude estimation may significantly reduce or even reverse the gains to be had from using these detectors.

In Section 2.4.6.1, successive interference cancellation is discussed while parallel interference cancellation is discussed in Section 2.4.6.2. The zero-forcing decision-feedback (ZF-DF) detector is discussed in Section 2.4.6.3.

2.4.6.1. Successive interference cancellation (SIC)

The successive interference cancellation (SIC) detector [46, 47] uses a serial approach to canceling interference. Each stage of this detector forms decisions, regenerates and cancels out one additional direct-sequence user from the received signal, so that the remaining users see less MAI in the next stage. A simplified diagram of the first stage of this detector is shown in Figure 2.5 where a hard-decision approach is assumed.

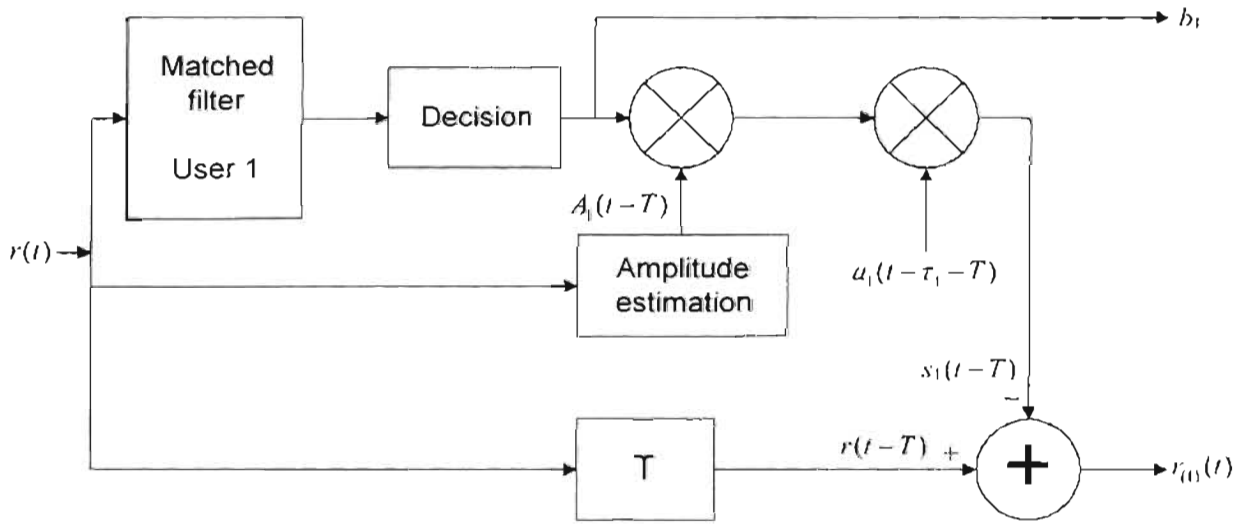

Figure 2.5.
First stage of the SIC detector

Prior to the first stage is an operation which ranks the signals in descending order of received powers. The first stage is responsible for implementing the following steps:

1) To detect with the conventional detector the strongest signal, q_1.
2) Make a hard data decision on q_1
A) Regenerate an estimate of the received signal for user one, $\bar{q}_1(t)$, using:
   - Data decision from step 2
   - Knowledge of its PN sequence
   - Estimates of its timing, amplitude and phase
3) Subtract out $\bar{q}_1(t)$ from the total received signal, r(t), yielding a partially cleaned version of the received signal, $r_{(1)}(t)$.

Assuming that the estimation of $\bar{q}_1(t)$ in step 3 above was accurate, the outputs of the first stage are:

a) A data decision on the strongest user
b) A modified received signal without the MAI caused by the strongest user

This process can be repeated in a multistage structure where stage Ns takes as its input the partially cleaned received signal output of the previous stage, $r_{(Ns-1)}(t)$, and outputs one additional data decision and a cleaner received signal $r_{(Ns)}(t)$.

The reasons for canceling the signals in descending order of signal strength is outlined in [26, 47]. Firstly, it is easiest to achieve acquisition and demodulation on the strongest users that offer the best chance for a correct data decision. Secondly, the removal of the strongest users gives the most benefit for the remaining users. The result of this algorithm is that the strongest user will not benefit from any MAI reduction but the weakest users will see a huge reduction in their MAI.

The SIC detector requires little additional hardware to the conventional detector, and it has the potential to provide significant improvement over the conventional detector.

Some of the implementation problems posed by the SIC detector are now listed. First, one additional bit delay is required per stage of cancellation [48]. Hence a trade-off needs to be made between the number of users that are cancelled and the amount of delay that can be tolerated. Secondly, there is a need to reorder the signals whenever the power profile changes. A trade-off must be made between the precision of the power ordering and the acceptable processing complexity.

A potential problem with the SIC detector occurs if the initial data estimates are not reliable. In this case, even if the timing, amplitude and phase estimates are perfect, if the bit estimate is wrong, the interfering effect of that bit on the signal-to-noise ratio is quadrupled in power. This is because if the amplitude doubles, the power quadruples. Hence, a certain minimum performance level of the conventional detector is required for the SIC detector to yield improvements. It is crucial that the data estimates of at least the strong users that are cancelled first be reliable.

By using a simple successive IC scheme, one can effectively estimate and cancel a CDMA signal and thus substantially reduce near/far effects from a CDMA system and increase the system capacity [48].

2.4.6.2. Parallel interference cancellation

In contrast to the SIC detector, the parallel interference (PIC) detector estimates and subtracts out all of the MAI for each user in parallel. The multistage PIC structure was introduced in [49]. A basic one stage PIC structure was assumed in [47, 50].

The first stage of this detector is shown in Figure 2.6 where a hard-decision approach is assumed. The initial bit estimates, $\bar{b}_i(0)$, are derived from the matched filter detector, which is referred to as stage 0 of this detector. These bits are then scaled by the amplitude estimates and respread by the codes, which produces a delayed estimate of the received signal for each user, $\bar{q}_k(t-T)$. The partial summer sums up all but one input signal at each of the outputs, which creates the complete MAI estimate for each user.

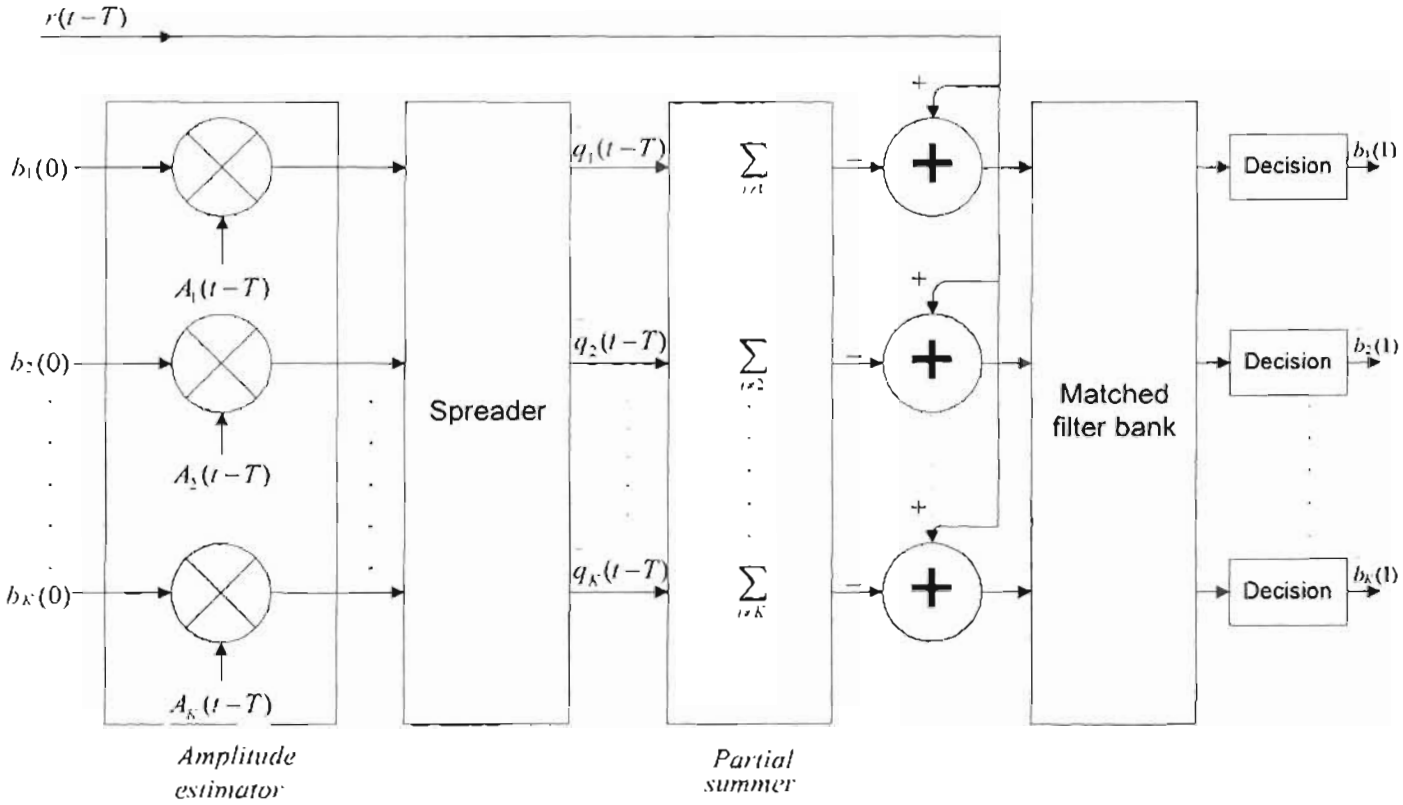

Figure 2.6.
One stage of the PIC detector

Assuming perfect amplitude and delay estimation, the result after subtracting the MAI estimate for user k is

$$r(t-T)-\sum_{i\neq k}^{K}\bar{q}_i(t-T)=b_k(t-\tau_k-T)A_k(t-\tau_k-T)a_k(t-\tau_k-T)+n(t-T)$$
$$+\sum_{i\neq k}^{K}\left(b_i(t-\tau_i-T)-\bar{b}_i(t-\tau_i-T)\right)A_i(t-\tau_i-T)a_i(t-\tau_i-T) \quad \text{.....(2.35)}$$

As can be seen in Figure 2.6, the result of (2.35), for k=1....K, is passed on to a second bank of matched filters to produce a new and better set of data estimates.

This process can be repeated for multiple stages. Each stage takes as its input the data estimates of the previous stage and produces a new set of estimates at its output. A matrix-vector formulation can be used to describe the soft output of stage Ns+1 of the PIC detector for all (2M+1) bits of all K users as [51]

$$\bar{b}(Ns+1)=y-QA\bar{b}(Ns)$$
$$=Ab+QA(b-\bar{b}(Ns))+z \quad \text{.....(2.36)}$$

The term QA $\bar{b}$ (Ns) represents an estimate of the MAI [52]. For BPSK, the hard data decisions are obtained by taking the signs of the soft data outputs, $\bar{b}$(Ns). Perfect data estimates, together with the assumption of perfect amplitude and delay estimation, result in the total elimination of MAI.

A number of studies have investigated PIC detection which utilizes soft decisions, such as [53, 54, 55]. In [53] soft-decision PIC and SIC detectors were compared and since soft-decision SIC exploits power variation by canceling in order of the signal strength, it is found to be superior in a fading channel. On the other hand, soft-decision PIC is found to be superior in a well-power-controlled channel. The PIC detector requires more hardware than the SIC which faces the problems of power reordering and large delays [53].

A number of variations on the PIC detector have been proposed for improved performance. Some of these variations are listed and explained below.

a) The decorrelating detector can be used as the first stage [51]. The performance of the PIC detector depends heavily on the initial data estimates [49]. As was pointed out for the SIC detector, the subtraction of an interfering bit based on an incorrect bit estimate causes a quadrupling in the interfering power for that bit. Hence, too many incorrect initial data estimates may cause performance to degrade relative to the conventional detector. Therefore, using the decorrelating detector as the first stage significantly improves performance of the PIC detector.

   It was shown in [51] that the multistage detector based on a decorrelating first stage, performed significantly better than the decorrelating and optimum linear detectors, in a number of situations of practical interest such as in high bandwidth utility and in near-far situations. Note however, that the detectors of [49, 51] had been developed for the case of known user energies.

   The decorrelator is an excellent choice for the first stage due to its performance invariance to interfering signal energies. However, its implementation in asynchronous systems may involve large storage and long decoding delays. While the conventional first stage is inferior to the decorrelator, its use in the multistage detector in an asynchronous system results in an easily implementable detector with a small storage requirement and a short decoding delay.

b) One may use the already detected bits at the output of the current stage to improve detection of the remaining bits in the same stage [56]. As a result of this, the most up-to-date bit decisions available are always used. This contrasts with the standard PIC detector, which only uses the previous stage's decisions. This detector is referred to as a multistage decision feedback detector [56]. Proposals for the initial stage of this detector include a decision-feedback detector [56], the conventional detector [27], and the decorrelating detector [31].

c) One may also linearly combine the soft-decision outputs of different stages of the PIC detector [43] – This simple modification yields very large gains in performance over the standard soft-decision PIC detector.

The reason for this has to do with the extensive noise correlations that exist between outputs of different stages. The linear combination is made in a way as to capitalize on the noise correlations and cause cancellation among noise terms.

d) One can also do a partial MAI cancellation at each stage, with the amount of cancellation increasing for each succesive stage [54]. Similar to [49, 51], the basic idea is that at each stage of the iteration, an attempt is made for each user to completely cancel the interference caused by all the other users. It was shown in [54] that this is not necessarily the best philosophy. When the interference estimate is poor (as in the early stages of interference cancellation), it is preferable not to cancel the entire amount of estimated multiuser interference. As the interference cancellation operation progresses, the estimates of the multiuser interference improve. The MAI estimate is first scaled by a fraction before cancellation and the value of the fraction increases for successive stages. This takes into account the fact that the decisions of the earlier stages are less reliable than those of the later stages. Huge gains in performance and capacity are reported over the standard PIC detector.

2.4.6.3. Zero-forcing decision-feedback (ZF-DF) detector

The zero-forcing decision-feedback detector [31- 32, 57- 58] performs two operations: linear preprocessing followed by a form of SIC detection. The linear operation partially decorrelates the users (without enhancing the noise), and the SIC operation provides decisions and subtracts out the interference from one additional user at a time, in descending order of signal strength. The initial partial decorrelation enables the SIC operation to be much more powerful.

The ZF-DF detector is based on a white noise channel model. A noise-whitening filter is obtained by factoring R by the Cholesky decomposition [59], $R=F^{T}F$, where F is a lower triangular matrix. Applying $(F^{T})^{-1}$ to the matched filter bank outputs in (2.20) yields the white noise model [57]

$$y_w = FAb + z_w \quad \text{.....(2.37)}$$

The covariance matrix of the noise term, z_w is $(N_0/2)I$. (This is similar to the white noise model that is derived for ISI channels [6].)

In the white noise model of (2.37), the data bits are partially decorrelated. This can be shown to arise from the fact that the matrix F is lower triangular [57]. The output for bit one of the first user contains no MAI, the output for bit one of the second user contains MAI only from bit one of the first user, and is completely decorrelated from all other users; similarly, the output for user k at bit interval i is completely decorrelated from users k + 1, k + 2,...K, at time i, and from all bits at future time intervals.

The ZF-DF detector uses SIC detection to exploit the partial decorrelation of the bits in the white noise model. The soft output of bit one of the first user, which is completely free of MAI, is used to regenerate and cancel out the MAI it causes, thereby leaving the soft output of bit one of the second user also free of MAI. This process continues: for each iteration, the MAI contributed by one additional bit (the previously decorrelated bit) is regenerated and canceled, thereby yielding one additional decorrelated bit.

Prior to forming and applying $(F^T)^{-1}$ to create the white noise model, the users are ordered according to their signal strength, thus ensuring that interference cancellation takes place in descending order of signal strength. This maximises the gains to be had from SIC detection, as discussed earlier. The ZF-DF detector is shown in Figure 2.7, where a synchronous channel is shown for clarity.

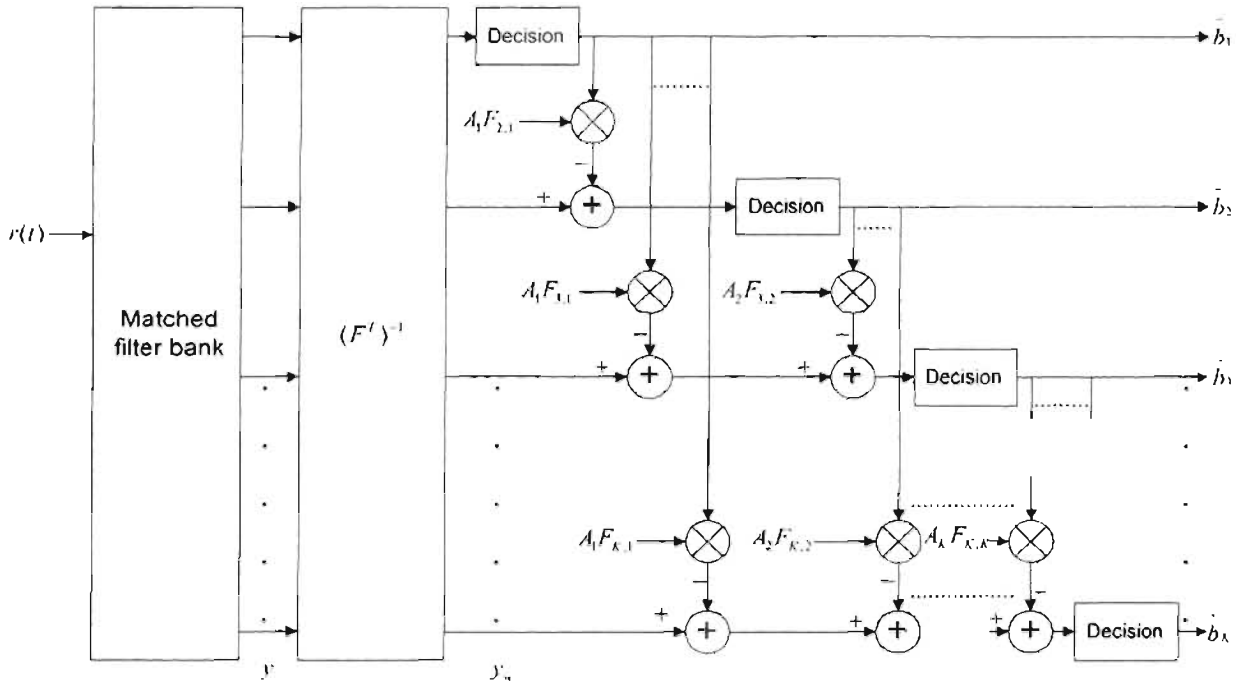

Figure 2.7.
The ZF-DF detector

For the zero-forcing decision-feedback detector, the forward and feedback filters of this detector are chosen to eliminate multiuser interference at the inputs to the decision devices. In addition, the objective of the detector is to maximize the ideal signal-to-noise ratio at the input to each decision device.

Assuming perfect estimates of F and the received amplitudes, the soft output for the kth user is [57]

$$\bar{b}_k = y'_{w,k} - \sum_{i=0}^{k-1} F_{k,i} A_i b_i \qquad \text{.....(2.38)}$$

Where b_i= sign [$\bar{b}_i$] are the previously detected bits (of the stronger users), A_i is the received amplitude of this bit, and $F_{k,i}$ is the (k,i)th element of F.

Under the assumption that all past decisions are correct, the ZF-DF detector eliminates all MAI and maximizes the signal-to-noise ratio [31]. It is analogous to the ZF-DF equalizer used to combat ISI [6].

An important measure of the performance for a decision-feedback detector is the signal-to-noise ratio at the input to the decision device under the assumption of correct previous decisions. The signal-to-noise ratio for the decision feedback detector is [57]

$$SNR_k = \frac{F_{k,k}^2 A_k}{\sigma^2} \quad \text{.....(2.39)}$$

Given the same order of making decisions, this SNR is the largest achievable by any decision-feedback detector which attempts to cancel all multi-user interference.

An important difficulty with the ZF-DF detector is the need to compute the Cholesky decomposition and the whitening filter $(F^T)^{-1}$. Attempts to simplify its implementation are similar to those of the decorrelating detector. The ZF-DF detector, like the other nonlinear detectors, has the disadvantage of needing to estimate the received signal amplitudes. If the soft outputs of the decorrelating detector are used to estimate the amplitudes, the ZF-DF detector is equivalent to the decorrelating detector [31]. If the amplitude estimates are more reliable than those produced by the decorrelating detector, the ZF-DF detector performs better than the decorrelating detector; and if less reliable, the ZF-DF detector performs worse than the decorrelating detector.

2.4.7. Other detector types

Finally, in this section, some of the detector structures for CDMA reception which have not been considered in the previous sections, will be discussed here.

Application of the expectation maximization (EM) based algorithms to the problem of data detection in the Gaussian multiple-access channel leads to a variety of convergent receiver structures that incorporated soft-decision feedback for interference cancellation and sequential updating of iterative bit

estimates. In [62] new iterative multiuser receivers based on the EM algorithm were considered. The EM algorithm provided an iterative approach to the likelihood-based parameter estimation when direct maximization of the likelihood function was not feasible. Although convergence of the algorithm to the maximum-likelihood estimator was not always guaranteed, EM did produce estimates that monotonically increased in likelihood. The resulting receivers had multi-stage-like structures that used sequential bit-estimate updates and intermediate soft-decisions for interference cancellation.

In [29], a receiver-based synchronous CDMA system with a linear multiuser interference canceller had been proposed, and its performance in a microcellular environment was investigated theoretically. The multiuser interference was removed on a symbol-by-symbol basis by a deterministic matrix operation. The receiver structure of the receiver based synchronous CDMA system was composed of a bank of matched-filters corresponding to all the mobile users in the cell, a correlation peak position detector and a matrix calculator. The linear canceller of [29] did not require knowledge of the received power levels of active users, and hence resulted in a high capacity and near-far resistance.

An adaptive receiver was considered for use in combating the near-far problem in direct-sequence CDMA in [39]. The receiver used a chip matched filter followed by an adaptive equalizer structure to perform the despreading operation. This adaptive structure allowed the receiver to adjust to the prevailing interference and noise environment. The receiver was shown to be immune to the near-far problem in the sense that the performance without any power control was nearly identical to the performance with perfect power control. The receiver was also shown to offer a two-fold increase in capacity relative to a conventional receiver with perfect power control. With the adaptive receiver, no information about the interference was needed, only a known data preamble was needed for the equalizer to converge on the form of the optimum receiver filter. The equalizer did not even need to know the desired code sequence in order to converge. As a result, after the equalizer had converged close to a steady state value, the value of the tap weights could be used to extract timing information and thus provide code acquisition and tracking. In [39] it was also shown that this receiver had the ability to overcome multipath and narrowband interference. A practical limitation of the receiver is that the number of taps must be equal to the number of chips per bit. Hence, this

receiver cannot be used in a direct sequence system with a large processing gain. Also the adaptive equalizers have a difficult time in channels that are rapidly changing. This will present a problem in situations where the fading rate of the channel is substantial.

Optimal decentralized multiuser detectors for AWGN channels have been considered in [81], where the multiple-access interference was modeled as non-Gaussian noise. The optimal decentralized multiuser detectors can also allow for the utilization of the knowledge of a subset of the K-1 interfering signature waveforms. However, the optimal decentralized multiuser detector also has a computational complexity which depends exponentially on the number of users.

The highly structured nature of MAI suggests that a neural network should be able to learn how to remove the MAI effectively. A multi-user receiver is essentially a decision making device, hence a neural network is a natural architecture for implementing this device. Due to their highly parallel structure and adaptability to system parameters, receivers employing neural networks prove to be a desirable alternative to the optimum and conventional receivers for multiple-access communications. Neural network detectors will be examined in more detail in Chapter 7.

2.5. Conclusion

The emphasis of this chapter has been on centralized multiuser detectors that process the matched filter output to provide the statistics for both the estimation of the signal amplitudes as well as for data detection in the AWGN channel.

The models for the transmitter, receiver and CDMA channel have been derived in this chapter. The performance of multiuser receivers can be measured by the bit error rate, asymptotic multiuser efficiency and near-far resistance.

The conventional detector follows a single user detection strategy, has a computational complexity that grows linearly with the number of users and is vulnerable to the near far problem. Maximum likelihood sequence

detection can be implemented for DS-CDMA by following the matched filter bank with a Viterbi algorithm. However, the required Viterbi algorithm has a complexity that is still exponential in the number of users.

Detectors which have a linear computational complexity but do not exhibit the vulnerability to other-user interference, were also examined. The two most popular of the linear detectors are the decorrelating and minimum mean-squared error detectors. A polynomial expansion detector can efficiently implement both the decorrelating and MMSE detectors.

The basic operating principle for successive interference cancellation detectors is the creation at the receiver of separate estimates of the MAI contributed by each user in order to subtract out some or all of the MAI seen by each user. Such detectors are often implemented with multiple stages, where the aim is that the decisions will improve at the output of successive stages. Three categories of subtractive interference cancellation detectors can be identified, and these are the SIC, PIC and ZF-DF detectors.

Neural network and other detectors were also considered. Since MAI has a highly structured nature, a neural network should be able to learn how to remove the MAI effectively.

The detectors presented in this chapter serve as a basis for more advanced detectors which are used in fading channels. In particular, the decorrelator, discussed in Section 2.4.5.1, will form the basis of the discussions in Chapters 5 and 6.

Chapter 3: Fading models

3.1. Introduction

CDMA transmissions are frequently made over channels which exhibit fading and dispersion, hence it is important to design receivers which take this behaviour of the channels into account. Section 3.2. will discuss some of the propagation problems experienced in CDMA transmissions. In Section 3.3, the fading multipath channel will be characterized, while the selection of the channel model will be discussed in Section 3.4. Diversity techniques for fading multipath channels are considered in Section 3.5, while combining technology will be considered in Section 3.6. Finally, in Section 3.7, the model of a frequency selective fading channel will be provided.

3.2. Propagation Problems

Some of the different propagation problems experienced are:

a) propagation loss
b) scattering
c) doppler shift
d) time dispersion
e) loss due to rain and fog
f) noise
g) fading

A brief explanation of each of the above phenomena follows:

a) Propagation loss

The amount of energy received by an antenna is inversely proportional to the fourth power of the distance from the transmitter. These electro-magnetic waves are susceptible to absorption, reflection, diffraction and scattering by the earth's surface as well as obstacles in their path. However, accommodation can be made for the propagation loss by using some form of power control at the receiver.

b) Scattering

This is caused by obstacles along the propagation path such as buildings, and trees, etc. They produce reflected waves of the same frequency, but at an attenuated amplitude and a phase which is dependant on the angle of incidence. Figure 3.1. illustrates the principle of reflection.

c) Doppler shift

The doppler shift effect is only applicable to a receiver in motion. The time variations of the channel are evidenced as a Doppler spread in the frequency domain, which is determined as the width of the spectrum when a single sinusoid is transmitted.

d) Time dispersion

Many reflected waves are received at the receiver, each with a different path length, and hence a different propagation time delay. For example, if a short pulse was to be transmitted, it may be received as a train of pulses at the receiver, and this effect is called time dispersion. This distortion causes inter-symbol interference.

e) Loss due to rain and fog

The droplets in clouds and fog cause attenuation of the transmitted signal due to absorption and scattering

f) Noise

The received signal is affected by thermal noise, man-made noise and interference noise

g) Fading

The mobile receives many reflected waves, and one direct wave. They either interact constructively or destructively, producing variations in the received signal amplitude. This effect is termed multipath fading and is illustrated in Figure 3.2.

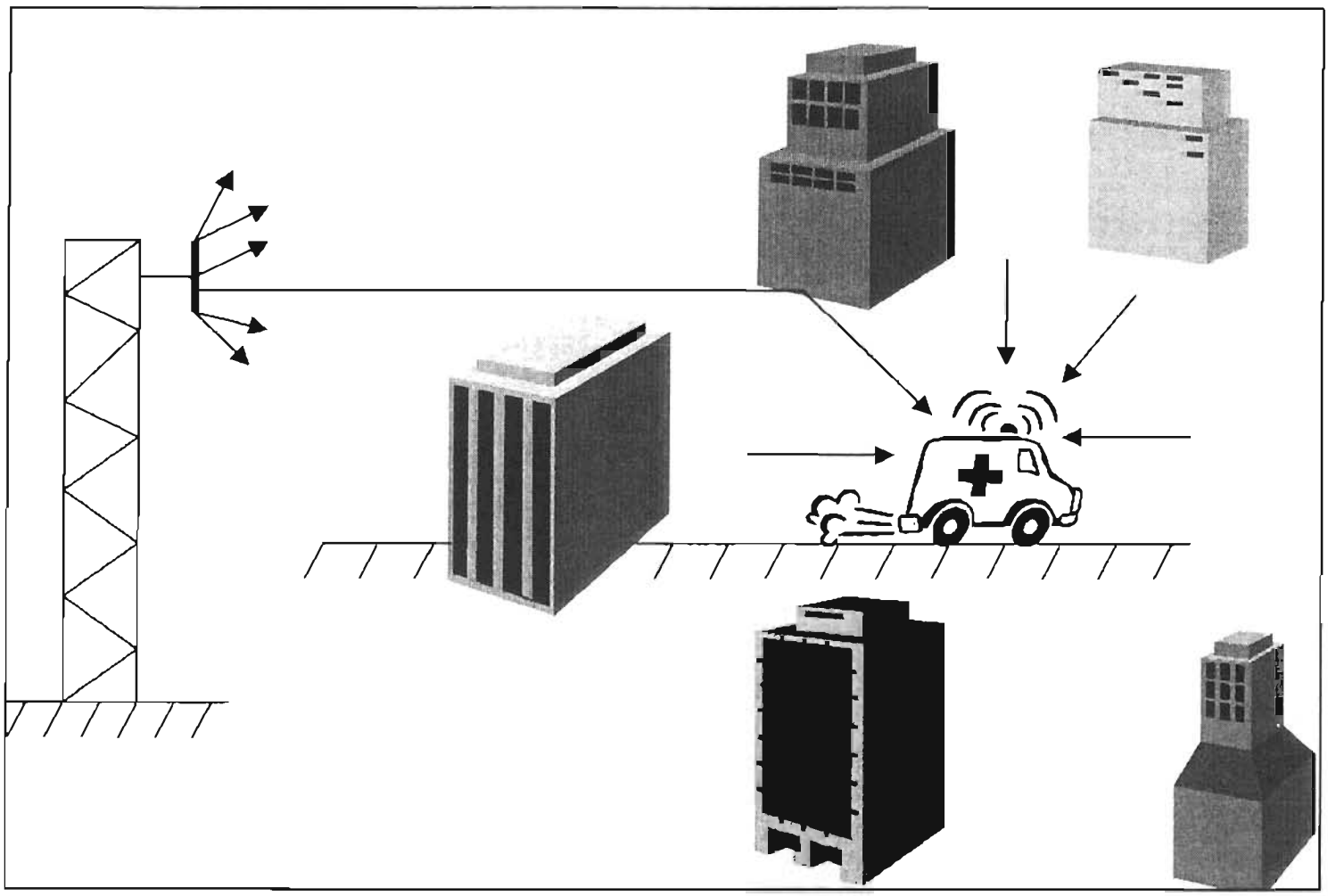

Figure 3.1
Illustration of the principle of reflection

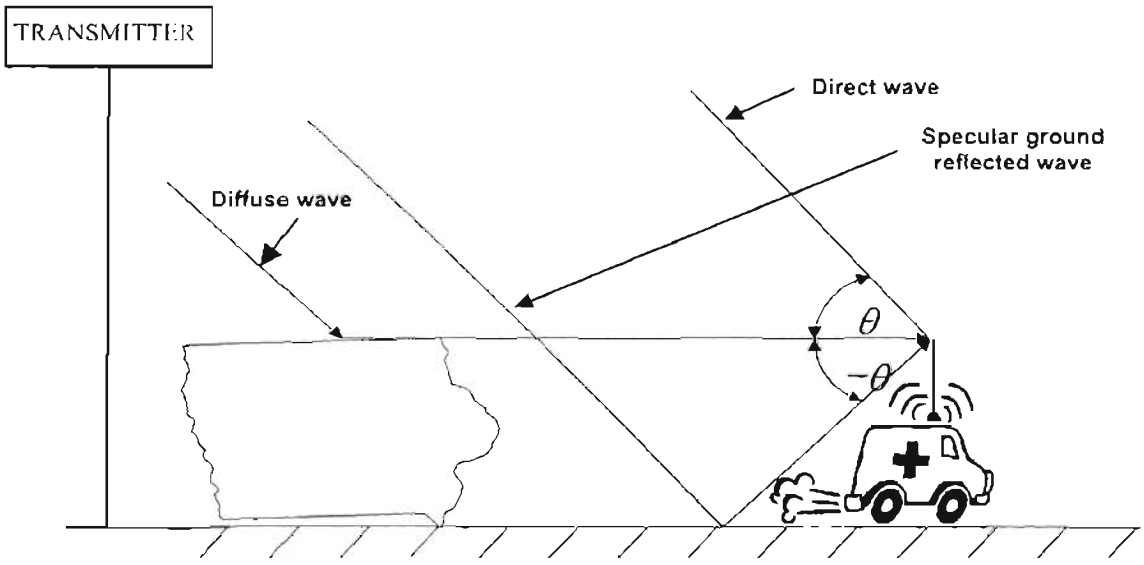

Figure 3.2
The concept of multipath fading

With reference to Figures 3.1 and 3.2, in open areas most of the energy is in the direct wave. The remaining power is received by the ground reflected wave and the other scattered waves.

It is possible to distinguish two fading components in the signal. They are referred to as short term fading and long term fading. Short term fading is also known as fast fading, and it manifests itself as fast fluctuations of the signal. Short term fading is caused by reflected signals when the receiver moves. Long-term fading is caused by attenuation of the direct wave due to obstructions like buildings, trees or poles along the road.

3.3. Characterization of fading multipath channels

The characteristics of a fading channel are introduced in Section 3.3.1. In Section 3.3.2, a number of useful correlation functions and power spectral density functions that define the characteristics of a fading multipath channel, are introduced. In Section 3.3.3, several probability distributions are considered in an attempt to model the statistical characteristics of the fading channel. The description that follows is very similar to that covered in [6].

3.3.1. Characteristics of fading channels

If an extremely short pulse, ideally an impulse, is transmitted over a time-varying multipath channel, the received signal might appear as a train of pulses [6].

One characteristic of a multipath medium is the time spread introduced in the signal that is transmitted through the channel. A second characteristic is due to the time variations in the structure of the medium. As a result of such time variations, the nature of the multipath varies with time. These time variations also appear to be unpredictable to the user of the channel. Hence, it is reasonable to characterize the time-variant multipath channel statistically.

One needs to examine the effects of the channel on a transmitted signal that is represented in general as:

$$s(t) = \mathrm{Re}[s_{lp}(t)\exp(j2\pi f_0 t)] \quad \text{.....(3.1)}$$

where:

- $s_{lp}(t)$ is the equivalent lowpass transmitted signal.

One needs to assume that there are multiple propagation paths. Associated with each path is a propagation delay and an attenuation factor. Both the propagation delays and the attenuation factors are time-variant as a result of changes in the structure of the medium. Thus, the received bandpass signal may be expressed in the form

$$v(t) = \sum_n \lambda^n(t) s(t - \tau^n(t)) \quad \text{.....(3.2)}$$

where:

- $\lambda^n(t)$ is the attenuation factor for the signal received on the n^{th} path
- $\tau^n(t)$ is the propagation delay for the n^{th} path.

Substitution for s(t) from (3.1) into (3.2) yields the result:

$$v(t) = \mathrm{Re}\{\sum_n \lambda^n(t) \exp(-j2\pi f_c \tau^n(t)) s_l(t - \tau^n(t))] \exp(j2\pi f_c t)\} \quad \text{.....(3.3)}$$

It will be observed from (3.3) that the equivalent lowpass received signal is:

$$r(t) = \sum_n \lambda^n(t) \exp(-j2\pi f_c \tau^n(t)) s_{lp}(t - \tau^n(t)) \quad \text{..... .... (3.4)}$$

Since r(t) is the response of an equivalent lowpass channel to the equivalent lowpass signal $s_{lp}(t)$, it follows that the equivalent lowpass channel is described by the time-variant impulse response

$$h(\tau, t) = \sum_n \lambda^n(t) \exp(-j2\pi f_c \tau^n(t)) \delta(t - \tau^n(t)). \quad \text{.....(3.5)}$$

Referring to (3.4), considering the case of an unmodulated carrier at frequency f_c, then $s_l(t)=1$ for all t, and hence the received signal for the case of discrete multipath, given in (3.4) reduces to

$$r(t) = \sum_n \lambda^n(t) \exp(-j2\pi f_c \tau^n(t)) \quad \text{.....(3.6)}$$

Defining $\theta^n(t)=2\pi f_c\tau^n(t)$, then the received signal consists of the sum of a number of time-variant vectors having amplitudes $\lambda^n(t)$ and phases $\theta^n(t)$. One can expect the delays $\tau^n(t)$ associated with the different signal paths to change at different rates and in a random manner. This implies that the received signal r(t) can be modeled as a random process. When there are a large number of paths, the central limit theorem can be applied. In that case, r(t) may be modeled as a complex-valued gaussian random process. This also means that the time-variant impulse response $h(\tau,t)$ is a complex-valued gaussian random process in the t variable.

The multipath propagation model for the channel embodied in the received signal r(t), given in (3.6) results in signal fading. The fading phenomena is primarily as a result of the time variations in the phases $\theta^n(t)$. The amplitude variations in the received signal are due to the time-variant multipath characteristics of the channel.

When the impulse response $h(\tau,t)$ is modeled as a zero-mean complex valued gaussian process, the envelope $|h(\tau,t)|$ at any instant t is Rayleigh distributed. In this case, the channel is said to be a Rayleigh fading channel. If there are fixed scatterers in the medium, in addition to randomly moving scatterers, $h(\tau,t)$ can no longer be modeled as having zero mean. In that case, the envelope $|h(\tau,t)|$ has a Rice distribution and the channel is said to be a Ricean fading channel. Common alternatives to these two fading distributions are the Nakagami and Lognormal distributions which will be discussed further in Section 3.3.3.

3.3.2. Channel Correlation Functions and Power Spectra

The equivalent low-pass impulse response $h(\tau,t)$ is characterized as a complex-valued random process in the t variable. It is assumed that $h(\tau,t)$ is wide-sense stationary. The autocorrelation function of $h(\tau,t)$ is defined as [6]:

$$\phi_c(\tau_1,\tau_2;\Delta t)=\frac{1}{2}E[h^*(\tau_1;t)h(\tau_2;t+\Delta t)] \quad \text{.....(3.7)}$$

In most radio transmission media, the attenuation and phase shift of the channel associated with path delay τ_1 is uncorrelated with the attenuation and phase shift associated with path delay τ_2. This is called uncorrelated scattering. The assumption is made that the scattering at two different delays is uncorrelated and is incorporated into (3.7) to obtain:

$$\frac{1}{2}E[h^*(\tau_1;t)h(\tau_2;t+\Delta t)] = \phi_c(\tau_1;\Delta t)\delta(\tau_1-\tau_2) \quad \text{.....(3.8)}$$

If Δt is set to 0, the resulting autocorrelation function $\phi_c(\tau;0) \equiv \phi_c(\tau)$ is the average power output of the channel as a function of the time delay τ. $\phi_c(\tau)$ is called the multipath intensity profile of the channel.

In practice, the function $\phi_c(\tau;\Delta t)$ is measured by transmitting very narrow pulses and cross-correlating the received signal with a delayed version of itself. Typically, the measured function $\phi_c(\tau)$ may appear as shown in Figure 3.3.

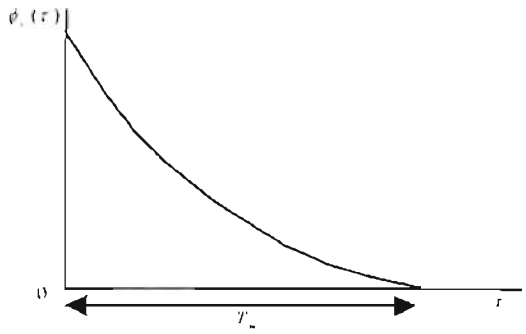

Figure 3.3
A typical multipath intensity profile

The range of values of τ over which $\phi_c(\tau)$ is nonzero is called the multipath spread of the channel and is denoted by T_m.

An analogous characterization of the time-variant multipath channels can also be done in the frequency domain. By taking the Fourier transform of $h(\tau;t)$, one obtains the time-variant transfer function $H(f;t)$ where f is the frequency variable.

$H(f;t)$ has the same statistics as $h(\tau;t)$, which has been modeled as a complex-valued zero-mean gaussian random process in the t variable. Under the assumption that the channel is wide-sense stationary, the autocorrelation function is defined as:

$$\Phi_c(f_1, f_2;\Delta t) = \frac{1}{2}E[H^*(f_1;t)H(f_2;t+\Delta t)] \quad \text{.....(3.9)}$$

$\Phi_c(f_1,f_2;\Delta t)$ is related to $\phi_c(\tau;\Delta t)$ by the Fourier transform;

$$\Phi_c(f_1,f_2;\Delta t) = \int_{-\infty}^{\infty} \phi_c(\tau_1;\Delta t)\exp(-j2\pi\Delta f\tau_1)\ d\tau_1 \equiv \phi_c(\Delta f;\Delta t) \quad \text{.....(3.10)}$$

where:

- $\Delta f = f_2 - f_1$

$\Phi_c(\Delta f;\ \Delta t)$ is the spaced-frequency, spaced-time correlation function of the channel. In practice, it can be measured by transmitting a pair of sinusoids separated by Δf and cross-correlating the two separately received signals with a relative delay Δt.

If in (3.10) Δt is set to zero, then with $\Phi_c(\Delta f;0) \equiv \Phi_c(\Delta f)$ and $\phi_c(\tau;0) \equiv \phi_c(\tau)$, the transform relationship simply is:

$$\Phi_c(\Delta f) = \int_{-\infty}^{\infty} \phi_c(\tau)\exp(-j2\pi\Delta f\tau)\ d\tau \quad \text{.....(3.11)}$$

This relationship is depicted graphically in Figure 3.4.

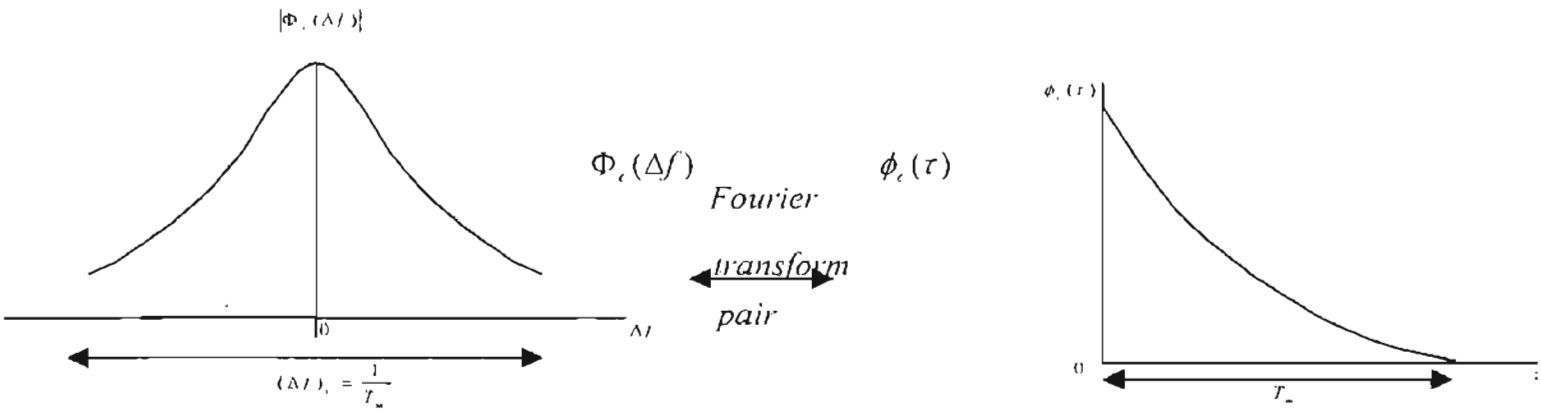

Spaced – frequency correlation function

Multipath int *ensity profile*

Figure 3.4
Relationship between $\Phi_c(\Delta f)$ and $\phi_c(\tau)$

As a result of the Fourier transform relationship between $\Phi_c(\Delta f)$ and $\phi_c(\tau)$, the reciprocal of the multipath spread is a measure of the coherence bandwidth of the channel. This relationship is given by:

$$(\Delta f)_c \approx \frac{1}{T_m} \quad \text{.....(3.12)}$$

$(\Delta f)_c$ denotes the coherence bandwidth. Two sinusoids with a frequency separation greater than $(\Delta f)_c$ are affected independently by the channel. When an information-bearing signal is transmitted through the channel, if $(\Delta f)_c$ is small in comparison to the bandwidth of the transmitted signal, the channel is said to be frequency-selective. In this case, the signal is severely distorted by the channel. However, if $(\Delta f)_c$ is large in comparison with the bandwidth of the transmitted signal, the channel is said to be frequency-nonselective.

The time variations in the channel are evidenced as a Doppler broadening. In order to relate the Doppler effects to the time variations of the channel, the Fourier transform of $\phi_c(\Delta f;\Delta t)$ with respect to the variable Δt is defined to be the function $S_c(\Delta f;\alpha)$.

With Δf set to zero and $S_c(0;\alpha) \equiv S_c(\alpha)$, the equation is

$$S_c(\alpha) = \int_{-\infty}^{\infty} \phi_c(\Delta t) \exp(-j2\pi\alpha\Delta t)\, d\Delta t \quad \text{.....(3.13)}$$

The function $S_c(\alpha)$ is called the Doppler power spectrum of the channel, and it gives the signal intensity as a function of the Doppler frequency α. From (3.13), it is noted that if the channel is time-variant, then $\phi_c(\Delta t)=1$ and $S_c(\alpha)$ becomes equal to the delta function $\delta(\alpha)$. Hence, when there are no time variations in the channel, there is no spectral broadening observed in the transmission of a pure frequency tone.

The range of values of α over which $S_c(\alpha)$ is nonzero is called the Doppler spread B_d of the channel. Since $S_c(\alpha)$ is related to $\phi_c(\Delta t)$ by the Fourier transform, the reciprocal of B_d is a measure of the coherence time of the channel and the relationship is given by:

$$(\Delta t)_c \approx \frac{1}{B_d} \quad \text{.....(3.14)}$$

$(\Delta t)_c$ denotes the coherence time. From (3.14), it can be seen that a slowly changing channel has a large coherence time, or equivalently, a small Doppler spread. Figure 3.4 illustrates the relationship between $\phi_c(\Delta t)$ and $S_c(\alpha)$.

3.3.3. Statistical Models for Fading Channels

Several probability distributions can be considered in attempting to model the statistical characteristics of the fading channel. When there are a large number of scatterers in the channel that contribute to the signal at the receiver, as is the case in ionospheric or tropospheric signal propagation, application of the central limit theorem leads to a gaussian process model for the channel impulse response. The probability density function (PDF) of the Gaussian distribution is defined by [6]:

$$p(x) = \frac{1}{\sigma\sqrt{2\pi}} e^{\frac{(x-\eta)^2}{2\sigma^2}} \quad \text{.....(3.15)}$$

where:

- η is the mean and σ is the standard deviation

The PDF for the Gaussian distribution with zero mean and unit variance is shown in Figure 3.5.

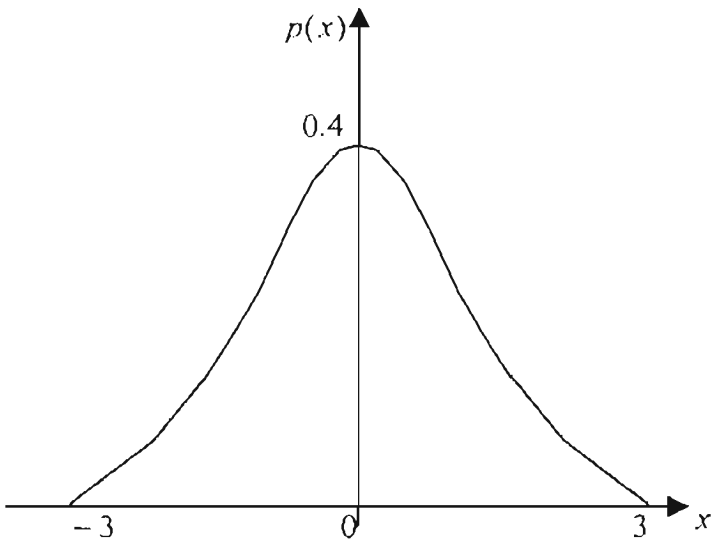

Figure 3.5.
PDF for a Gaussian distribution

The amplitude distribution for a complex valued Gaussian process is described by a Rayleigh random variable. If the process is zero-mean, then the envelope of the channel response at any time instant has a Rayleigh probability distribution and the phase is uniformly distributed in the interval $(0,2\pi)$. In urban areas, due to the congestion of buildings, etc. most of the received energy is in the scattered components, with the specular component having the least energy. This fading scenario is best described by a Rayleigh distribution function, where the probability density function (PDF) is given by:

$$p(x) = \frac{x}{\sigma_s^2} e^{(-x^2/2\sigma_s^2)} \quad for\ x \geq 0,\ and\ 0\ otherwise \qquad \text{.....(3.16)}$$

where:

- σ_s is the Rayleigh parameter

The mean and variance of the distribution are related to those of the complex Gaussian distribution by:

$$m_1 = \sqrt{\pi}\, 2\sigma_s \qquad \text{.....(3.17)}$$

$$\sigma^2 = 2\sigma_s^2 - \frac{\pi\sigma_s^2}{2} = \sigma_s^2\left(2 - \frac{\pi}{2}\right) \qquad \text{.....(3.18)}$$

The mean square or the mean power is equal to

$$m_2 = 2\sigma_s^2 \qquad \text{.....(3.19)}$$

The PDF for a Rayleigh distribution is shown in Figure 3.6 for σ_s=0.5.

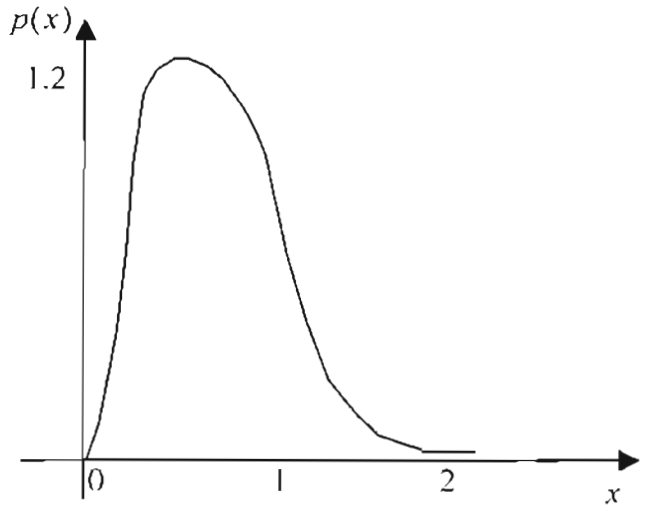

Figure 3.6
PDF for a Rayleigh distribution

If the unresolved paths are partially correlated, then the resultant amplitudes may be defined by a Nakagami distribution. The Nakagami distribution is given by:

$$p(x) = \frac{2m^m x^{2m-1} e^{-\frac{m}{\Omega}x^2}}{\Gamma(m)\Omega^m} \quad \text{.....(3.20)}$$

where:

- x denotes the received signal strength in volts
- $\Omega = E(X^2)$
- m is the mean value, and it is the parameter that determines the fading characteristics of the signals

The mean value is defined as:

$$m = \frac{\Omega^2}{x^2 - \Omega} \quad \text{.....(3.21)}$$

The gamma function, $\Gamma(m)$, is defined as:

$$\Gamma(m) = \int_0^\infty z^{m-1} e^{-z} dz \quad \text{.....(3.22)}$$

In contrast to the Rayleigh distribution, which has a single parameter that can be used to match the fading channel statistics, the Nakagami distribution is a two-parameter distribution. As a consequence, this distribution provides more flexibility and accuracy in matching the observed signal statistics. The Nakagami distribution can be used to model fading channel conditions that are either more or less severe than the Rayleigh distribution, and it includes the Rayleigh distribution as a special case for m=1.

One of the main advantages of the Nakagami distribution is its wide applicability. In addition to its attractive mathematical properties, it has also been shown in [6] that the Nakagami model can be used to accurately describe the fading behaviour of multipath signals. Specifically it was shown that the Nakagami distribution can be used to describe varying physical scattering processes.

For satellite reception in open-fields such as in rural areas where there is line of sight communications, most of the energy is in the specular received component rather than in the scattered components. This fading has a Rician distribution which has a power spectral density given by:

$$p(x) = \begin{cases} \frac{x}{\sigma_s^2} e^{-\frac{x^2+D^2}{2\sigma_s^2}} I_0\left(\frac{xD}{\sigma_s^2}\right) & x \geq 0 \\ 0 & x < 0 \end{cases} \quad \text{.....(3.23)}$$

where:

- $I_0(.)$ is the Bessel function of order zero
- σ_s is as before
- D^2 is the power of the signal of the fixed path

The Rician factor for the branch is given by:

$$K_b = \frac{D^2}{2\sigma_s^2} \quad \text{.....(3.24)}$$

The mean of this distribution is given by:

$$m_1 = \frac{1}{2}\sqrt{\frac{\pi}{1+K}} e^{\frac{K_b}{2}} \left[(1+K_b) I_0\left(\frac{K_b}{2}\right) + K_b I_1\left(\frac{K_b}{2}\right)\right] \quad \text{.....(3.25)}$$

where:

- $I_1(.)$ is the first order modified Bessel function

The variance is given by:

$$\sigma^2 = 1 - m_1^2 \quad \text{.....(3.26)}$$

The PDF for a Rician distribution is shown in Figure 3.7.

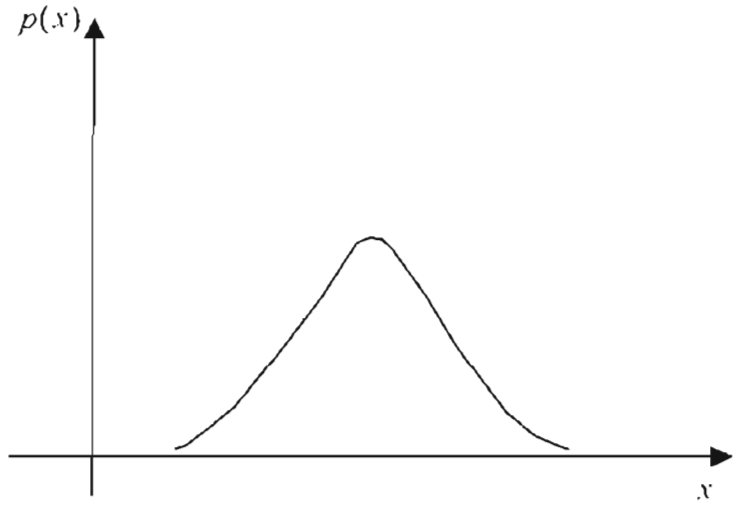

Figure 3.7
PDF of a Rician distribution

If the line-of-sight component in the first branch, or the fixed path in later branches, is affected by shadowing or intermittent short-term fading due to moving obstructions, then the simple path loss exponent model is not adequate and a log-normal distribution is used for that branch. The log-normal distribution is defined by:

$$p(x) = \frac{1}{\sigma_n (2\pi)^{\frac{1}{2}}} \exp\left\{\frac{-[\ln x - \eta_n]^2}{2\sigma_n^2}\right\} \quad for\ x \geq 0, \quad and\ 0\ otherwise \qquad \text{.....(3.27)}$$

The distribution of $\ln x$ is normal with mean η_n and variance σ_n^2. The mean and variance of the log-normal distribution are given by:

$$m_1 = e^{\eta_n + \frac{\sigma_n^2}{2}} \qquad \text{.....(3.28)}$$

$$\sigma^2 = e^{2\eta_n + \sigma_n^2}(e^{\sigma_n^2} - 1) \qquad \text{.....(3.29)}$$

The PDF of the Lognormal distribution is shown in Figure 3.8, for η_n set to 0, and σ_n set to 1.

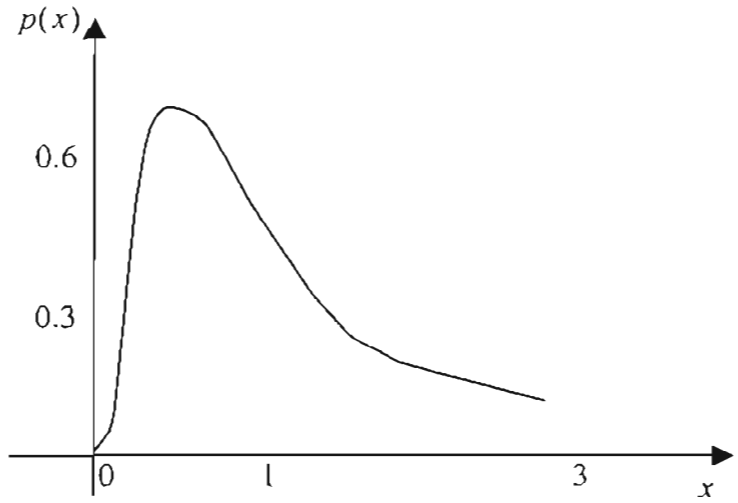

Figure 3.8.
PDF of a Lognormal Distribution

3.4. Selection of the channel model

When the transmitted signal $s_{lp}(f)$ has a bandwidth B greater than the coherence bandwidth $(\Delta f)_c$ of the channel, $s_{lp}(f)$ is subjected to different gains and phase shifts across the band. In such a case, the channel is said to be frequency selective. Additional distortion is caused by the time variations in the channel impulse response H(f;t). This type of distortion shows itself as a variation in the received signal strength, and is termed fading. It should be noted that frequency selectivity and fading are viewed as two different types of distortion. The former depends on the multipath spread or, equivalently, on the coherence bandwidth of the channel relative to the transmitted signal bandwidth. The latter depends on the time variations of the channel, which are characterized by the coherence time $((\Delta t)_c$ or, equivalently, by the Doppler spread B_d.

The effect of the channel on the transmitted signal $s_{lp}(t)$ is a function of the choice of signal bandwidth and signal duration. When the signal bandwidth B is much smaller than the coherence bandwidth $(\Delta f)_c$ of the channel, the received signal is simply the transmitted signal multiplied by a complex-valued random process C(0;t), which represents the time-variant characteristics of the channel. In this case, the multipath components in the received signal are not resolvable because $B<<(\Delta f)_c$.

Suppose it is possible to select a signal bandwidth B to satisfy the condition $B<<(\Delta f)_c$ and the signaling interval T to satisfy the condition $T<<(\Delta t)_c$. Since T is smaller than the coherence time of the channel, the channel attenuation and phase shift are essentially fixed for the duration of at least one signaling interval. When this condition holds, this channel is called a slowly fading channel. Furthermore, when $B\approx 1/T$, the conditions that the channel be frequency-nonselective and slowly fading imply that the product of T_m and B_d must satisfy the condition $T_m B_d<1$. The product $T_m B_d$ is called the spread factor of the channel. If $T_m B_d<1$, the channel is said to be underspread; otherwise, it is overspread.

The multipath spread, Doppler spread , and the spread factor are listed in Table 1 [6].

Type of channel	**Multipath Duration [sec]**	**Doppler Spread [sec^{-1}]**	**Spread factor**
Shortwave ionospheric propagation (HF)	10^{-3}-10^{-2}	10^{-1}-1	10^{-4}-10^{-2}
Ionospheric propagation conditions (HF)	10^{-3}-10^{-2}	10-100	10^{-2}-1
Ionospheric forward scatter (VHF)	10^{-4}	10	10^{-3}
Mobile comms	10^{-4}-10^{-6}	10	10^{-3}-10^{-4}
Tropospheric scatter (SHF)	10^{-6}	10	10^{-5}
Orbital scatter (X band)	10^{-4}	10^{3}	10^{-1}
Moon at max. libration (f_0 = 0.4kmc)	10^{-2}	10	10^{-1}

Table 1
Listing of the multipath spread, doppler spread and spread factor for several time-variant multipath channels

3.5. Model of a frequency selective fading channel

The model of a frequency selective fading channel is derived in **Appendix 2**. The form for the received signal in (A2.6) implies that the time-variant frequency-selective channel can be modeled as a tapped delay line with tap spacing 1/B and tap weight coefficients $h^n(t)$.

The truncated tapped delay line model of the frequency selective fading channel is depicted in Figure 3.9. The time-variant tap weights $h^n(t)$ are complex-valued stationary random processes. In the special case of Rayleigh fading, the magnitudes $|h^n(t)| \equiv \lambda^n(t)$ are Rayleigh distributed and the phases $\phi^n(t)$ are uniformly distributed. In urban areas, the tap coefficients are modeled as independent Rayleigh random variables with individual Doppler shifts [6].

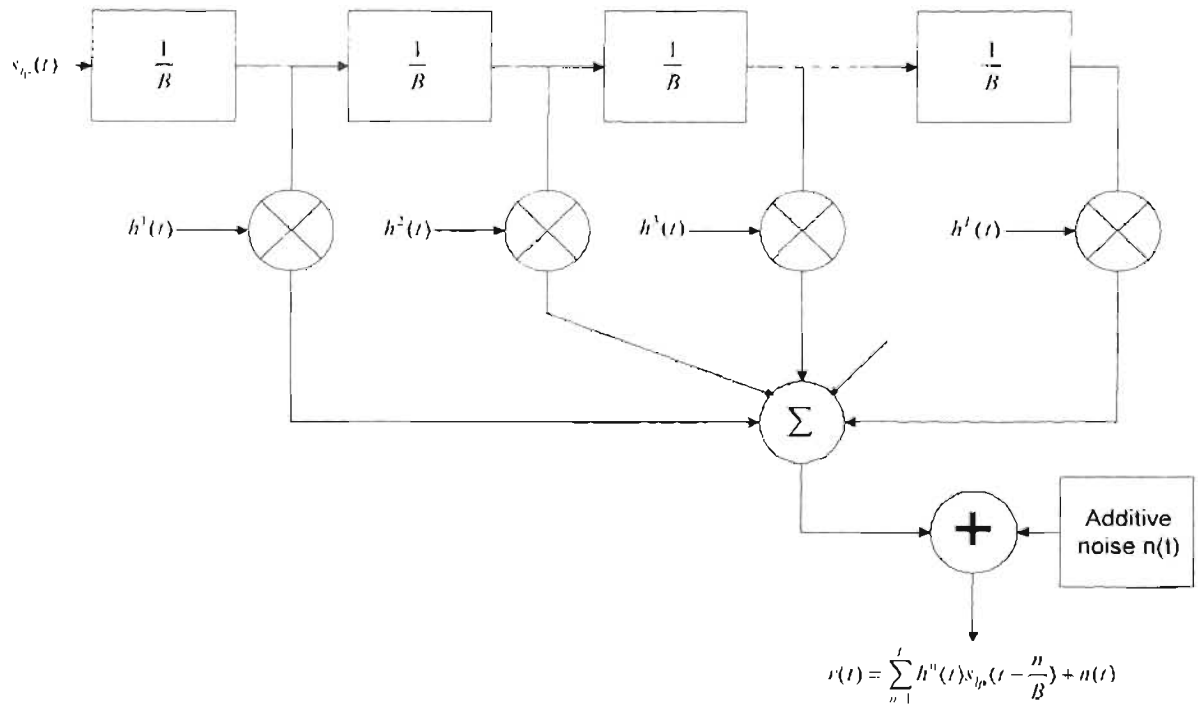

Figure 3.9
Tapped delay line model of a frequency selective channel

3.6. Diversity techniques for fading multipath channels

Diversity techniques are based on the conception that errors occur in reception when the channel attenuation is large, such as when the channel is in a deep fade [6]. If the receiver can be supplied with several replicas of the same information signal transmitted over independently fading channels, the probability that all the signal components will fade simultaneously is reduced considerably. The effect of fading caused by terrain obstructions can be reduced by diversity techniques. These techniques can be applied either at the base station or the mobile. This technique requires that a number of independent signals, carrying the same information are available. The underlying idea is that the probability of a number of independent signals being below a given level is much less than the probability of any individual sample being below that level. There are several ways in which diversity can be achieved, and these are now discussed:

a) Frequency diversity

In this method, a number of different frequencies can be used to transmit the same message, where the separation between successive frequencies equals or exceeds the coherence bandwidth $(\Delta f)_c$ of the channel. The frequencies need to be separated enough to ensure independent fading associated with each frequency. A frequency separation of the order of several times the coherence bandwidth will guarantee that the fading statistics for different frequencies will be essentially uncorrelated.

b) Time diversity

A second method for achieving a number of independently fading versions of the same information-bearing signal is to transmit the signal in different time slots, where the separation between successive time slots equals or exceeds the coherence time $(\Delta t)_c$ of the channel. This results in uncorrelated fading signals at the receiver.

c) Space diversity

Another commonly used method for achieving diversity employs multiple antennas. One may employ a single transmitting antenna and multiple receiving antennas. The receiving antennas must be spaced sufficiently far apart that the multipath components in the signal have different propagation delays at the antennas. Usually a separation of at least 10

wavelengths is required between two antennas in order to obtain signals that fade independently.

d) Angle diversity

If the received signal arrives at the antenna via several paths, each with a different angle of arrival, the signal components can be isolated by means of directive antennas. Each directive antenna will isolate a different angular component. Directive mobile antennas pointing in different directions can receive scattered waves at the mobile site from all directions and can provide a less severe fading signal. If directional antennas are mounted on the mobile unit, the signals received from different directive antennas pointing at different angles are uncorrelated.

e) Other diversity methods

A more sophisticated method for obtaining diversity is based on the use of a signal having a bandwidth much greater than the coherence bandwidth $(\Delta f)_c$ of the channel [6]. Such a signal with bandwidth B will resolve the multipath components and , hence, provide the receiver with several independently fading signal paths. The time resolution is 1/B. The use of a wideband signal may be viewed as another method for obtaining frequency diversity of order $L \approx B/(\Delta f)_c$.

3.7. Combining technology

Signal performance that is degraded by severe fading can be improved by increasing transmitter power, antenna size and height but these solutions are costly in mobile-radio communications and sometimes impractical. In this section, combining techniques for macroscopic and microscopic diversity are analyzed. Note that macroscopic diversity deals with long-term fading, while microscopic diversity deals with short-term fading. The macroscopic diversity scheme is used for combining two or more long-term lognormal signals, which are obtained via independently fading paths received from two or more different antennas at different base-station sites. The microscopic diversity scheme is used for combining two or more short-term Rayleigh signals, which are obtained via independently fading paths received from two or more different antennas but at the same base-station site.

Combining techniques for macroscopic diversity will be addressed in Section 3.7.1, while combining techniques for microscopic diversity will be discussed in Section 3.7.2.

3.7.1. Combining techniques for macroscopic diversity

Selective diversity combining is chosen primarily to reduce long-term fading. Reducing the effects of long-term fading by combining two signals received from two different transmitting antennas is possible because the local means of the two signals at any given time interval are seldom the same. To effectively reduce fading requires the combining of two fading signals that have equal mean strengths. If two differently located base-station transmitters are not very stable, the phase jittering generated in each of the transmitters will degrade the combined signal. Hence, the technique of selective diversity combining can be used effectively, as it is only a selection between two signals, rather than a combination of two signals.

3.7.2. Combining techniques for microscopic diversity

In microscopic diversity, the principle is to obtain a number of signals with equal mean power through the use of diversity schemes. If the individual mean powers of the various signals are unequal, a degree of degradation that is proportional to the differences in mean power will result.

a) Selection diversity

Selection diversity is based on selecting the strongest of a group of signals carrying the same information. With respect to a DS-CDMA system, the multiple resolvable paths can be used to accomplish selection diversity by selecting the path with the largest autocorrelation peak (output of the matched filter). This implies that the highest order of diversity that can be achieved with one antenna is equal to the number of resolvable paths. If the order of diversity that can be achieved with one antenna is too low because there are too few resolvable paths, multiple antennas can be used to increase the maximum order of diversity. The process of selection diversity is depicted in Figure 3.9.

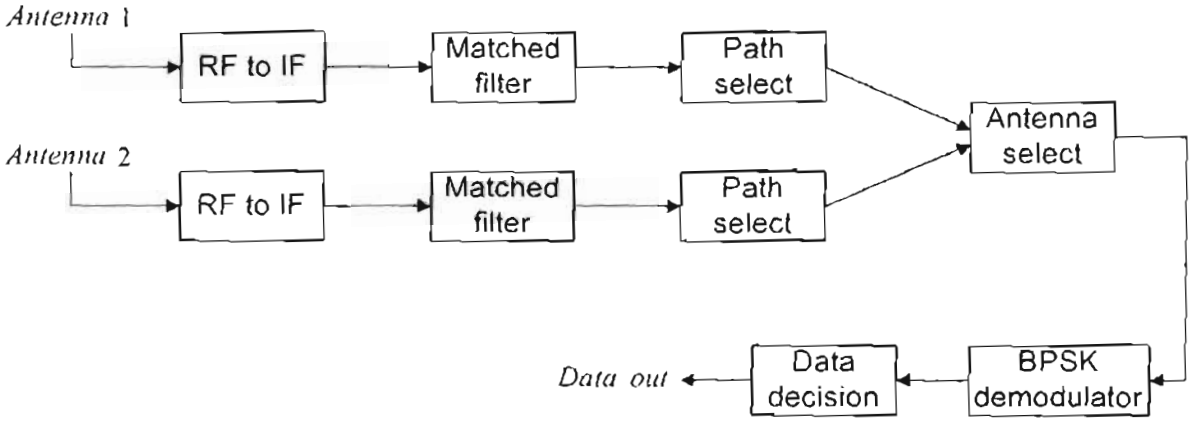

Figure 3.10
The process of selection diversity

The traditional analysis of a selection diversity system specifies that of L diversity branches j=1,2,.....,L, the one providing the largest signal-to-noise power ratio (SNR) must be selected for data recovery, and it assumes that the noise power is constant across all the branches. For practical implementations, however, the measurement of SNR may be difficult or expensive, especially for high signaling rates. For this reason, many practical selection systems choose the branch based on the largest signal-plus-noise (S+N) selection sample of a filter output [19]. Historical justification for the extensive use of an SNR analysis to describe the performance of S + N selection systems stems from the idea that any branch which has the largest SNR must also have the largest sum of signal power and noise power if the noise power is taken to be a constant on all branches. When physically realizing S + N selection, though, by sampling the output of a matched filter, the noise is a random variable. Thus, it is inexact to specify the performance of S + N selection systems using a constant noise analysis.

b) Maximal ratio combining (MRC)

Maximal ratio combining is a linear diversity combining technique and is accomplished by summing the demodulation results of a group of signals carrying the same information and using this result as a decision variable. In MRC/BPSK of order J, the decision variable is the weighted sum of the demodulation results of J copies of the signal. The weights are taken equal to the corresponding channel gain. The effect of this multiplication is to compensate for the phase shift in the channel and to weight the signal by a factor that is proportional to the signal strength. Hence, a strong signal carries a larger weight than a weak signal.

c) Equal gain combining

This is another linear combining technique that uses a simple phase-locked summing circuit to sum all of the individual signal branches. The equal-gain combining technique still provides incoherent summing of the various noise elements, but it also provides the required coherent summing of all the individual signal branches.

3.8. Conclusion

Because CDMA transmissions are frequently made over channels which exhibit fading and/or dispersion, it is important to design receivers which take this behaviour of the channels into account. Various propagation problems are experienced in a CDMA channel, and these have been listed and discussed in this chapter.

One characteristic of a multipath medium is the time spread introduced in a signal that is transmitted through the channel. A second characteristic is due to time variations in the structure of the medium, where as a result of such time variations, the nature of the multipath varies with time. The multipath propagation model for the channel which results in signal fading, has been derived in this chapter. Several probability distributions can be considered in attempting to model the statistical characteristics of the fading channel. The distributions that have been discussed in this chapter are the Rayleigh, Nakagami, Rician and Lognormal distributions. The fading phenomena is primarily as a result of time variations in the phases, and the amplitude variations in the received signal are due to the time-variant multipath characteristics of the channel.

By supplying the receiver with several replicas of the same information signal transmitted over independently fading channels, the probability that all the signal components will fade simultaneously is considerably reduced. This is the principle used for diversity techniques, which can be used to reduce the effect of fading caused by terrain obstructions. The different forms of diversity include frequency, time, space, and angle.

Combining techniques for macroscopic and microscopic diversity were analyzed in this chapter. The macroscopic diversity scheme is used for combining two or more long-term lognormal signals, which are obtained via independently fading paths received from two or more different antennas at different base-station sites. On the other hand, the

microscopic diversity scheme is used for combining two or more short-term Rayleigh signals. The combining techniques for microscopic diversity include selection diversity, maximal ratio combining and equal gain combining.

Chapter 4: Multiuser detectors for the fading channel

4.1. Introduction

Multipath fading often presents a major limitation on CDMA system performance, as discussed in Chapter 3. A concise treatment was given to the characteristics of fading in Chapter 3. In Chapter 2, extensive information was given of detectors for the AWGN channel. In this chapter, an investigation is conducted to check if the detectors for the AWGN channel can also be used in the fading channel, and if not, whether modifications to them will facilitate their use in the fading channel. The main emphasis in this chapter is on multi-user demodulation techniques for DS-CDMA fading systems in fading channels, which are most important either from a practical or theoretical point of view.

This chapter is organised as follows: In Section 4.2, the signal model for the fading channel communications is introduced, while in Section 4.3, a system overview is given. In Section 4.4, a discussion is given of receivers for the fading channel communications. Finally, in Section 4.5, concluding remarks are provided for this chapter.

4.2. Signal model

Note that (3.5) can be rewritten for a specific user for a specific time interval x as:

$$h_{k,x}(t) = \sum_{n=1}^{L} \lambda_k^{n}(x)\exp(j\theta_k^{n}(x))\delta(t-\tau_k^{n}) \quad \text{.....(4.1)}$$

where:

- L is the number of multipath components for the channel
- τ_k^n is the delay of the nth multipath component of user k during symbol interval x
- $\delta(t)$ is the Dirac's Delta function
- The term $\lambda_k^n(x)\exp(-j2\pi f_c\tau_k^n)$ is the complex coefficient of the nth multipath component of the kth user during symbol interval x.
- $\theta_k^n(x)$ is the time varying phase of the kth user for the nth path during the xth symbol interval

The transmitted signal has already been described by (2.7). The time-variant impulse response of the channel was described by (3.5). The

received signal at the receiver was described by (2.11), (2.12) and (2.23). With the aid of the above equations, the received signal through a fading channel can be expressed as:

$$r(t) = \sum_{x=-M}^{M} \sum_{k=1}^{K} \sum_{n=1}^{L} b_k(x)\lambda_k^{n}(x)\sqrt{E_k(x)}a_k(t - xT - \tau_k^{n})e^{j\theta_k^{n}(x)} + n(t) \quad \text{.....(4.2)}$$

This model will be used for the derivation of the detectors for the fading channel in the subsequent sections.

As defined earlier, let A be the diagonal matrix of the amplitudes of the user's signals. In addition, define λ as the diagonal matrix of the channel coefficient vectors $\lambda_k^{n}(x)$. Similar to (2.20), the matched filter output vector can be written as:

$$y = R\lambda Ab + z \quad \text{.....(4.3)}$$

The elements of (4.3) have already been defined in Chapter 2 and will not be repeated here.

4.3. System overview

Most centralized multi-user receivers, which make a joint detection of the symbols of the different users, can be illustrated as in Figures 4.1 and 4.2.

Note that the same notation used for detectors for the AWGN channel, are used here as well. The matched filter output of the k^{th} user for the L^{th} multipath component in the x^{th} symbol interval is denoted by $y_k^{L}(x)$. For the purposes of clarity, the output of multiuser detector for the k^{th} user for the L^{th} multipath component in the x^{th} symbol interval is denoted by $y_{[MUD]k}^{L}(x)$. Similarly, the maximal ratio combined matched filter bank output vector for the k^{th} user in the x^{th} symbol interval is denoted by $y_{[MRC]k}(x)$.

As can be seen from Figures 4.1 and 4.2, the multiuser signal processing can be performed either before multipath combining, by processing the matched filter bank output vector, y, or after multipath combining by processing the maximal ratio combined matched filter bank output vector $y_{[MRC]}$. It should however be noted that the block diagrams in Figures 4.1. and 4.2 are simplified and cannot fit all multi-user receivers into their framework. Most multi-user receivers can also be implemented before matched filtering, that is, by processing the received spread-spectrum signal samples r.

The AME for multiuser detectors for the AWGN channel have already been discussed in Section 2.4.3. Note that the AME for multiuser detectors in Rayleigh fading channels has been defined in [94, 95]. The Rician fading case has been considered in [96, 97].

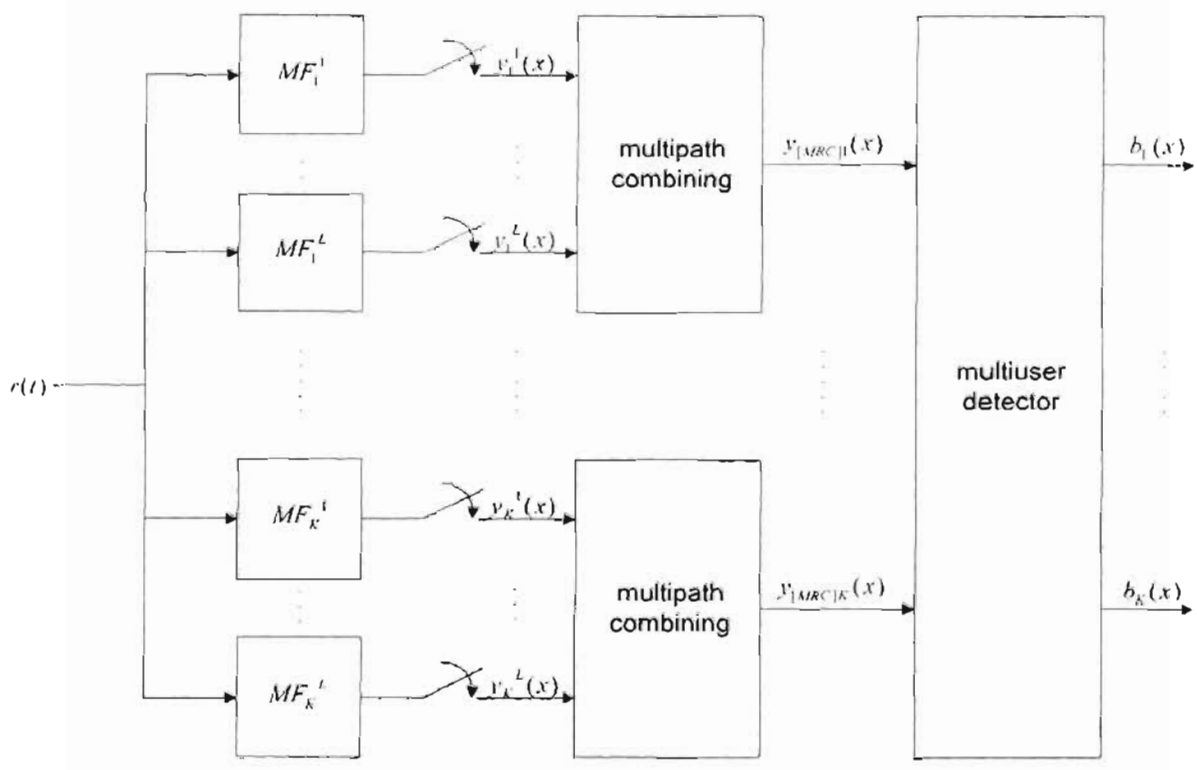

Figure 4.1.
Multiuser signal processing after multipath combining

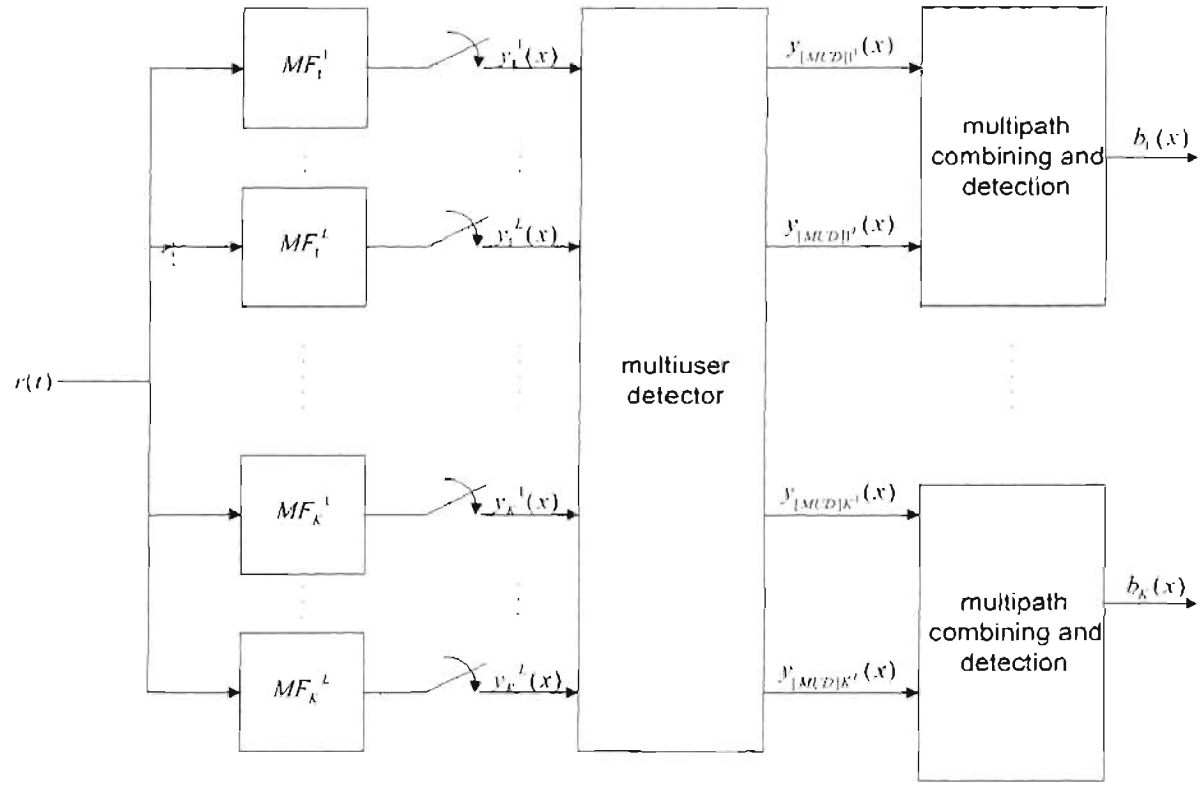

Figure 4.2
Multiuser signal processing before multipath combining

4.4. Receivers for fading channel communications

In this section a brief discussion will given of multiuser receivers for the fading channel. In Section 4.4.1, an overview of the receivers for the fading channel will be given, while the optimal multiuser demodulator for the fading channel will be discussed in Section 4.4.2. In Section 4.4.3, a discussion will be given on suboptimal multiuser demodulation schemes for the fading channel.

4.4.1. Overview

For slowly fading channels the channel impulse response can be estimated precisely and can be assumed to be known. In that case the optimal receiver which yields the lowest probability of symbol error for the single user k includes a filter matched to the convolution of the signature waveform $a_{k,x}(t)$ and the channel impulse response $h_{k,x}(t)$ for the

kth user in the xth symbol interval. In multipath channels such a matched filter is called a coherent RAKE receiver. The conventional approach to data detection is to employ an independent, single-user RAKE receiver for each user, which is optimal in the absence of MAI. However, the RAKE receiver suffers from the near-far effect in the presence of interfering signals received over independent fading channels. The RAKE receiver is discussed in **Appendix 3**. The output of the coherent RAKE receiver for user k in the x^{th} symbol interval is obtained by maximal ratio combining (MRC) the matched filter outputs for different propagation paths and is given by:

$$y_{[MRC]k}(x) = \sum_{n=1}^{L} h_k^{'n}(x) y_k^{''}(x) \quad \text{.....(4.4)}$$

If the delay spread is significantly smaller than the symbol interval ($T_m << T$), the intersymbol interference (ISI) can be assumed to be negligible and a hard decision on the RAKE output $y_{[MRC]k}(x)$ yields the optimal decision. If the channel introduces ISI, the receiver minimizing the error probability is significantly more complicated to implement. Thus, another optimization criterion, namely the minimum symbol sequence error probability, is selected. The optimum receiver then performs maximum likelihood sequence detection [6] in the presence of ISI. Suboptimal receivers, which are simpler than MLS detectors and do not require separate channel estimators for ISI channels include linear and decision-feedback equalizers (DFE) [6]. These DFE's can be applied in frequency-selective channels [98]. Their overall impulse response should be such that the equalizer implicitly performs both maximal ratio combining and ISI reduction. The equalizers can be made adaptive so that they automatically tune their impulse response to approximate the desired one [6] or the impulse response can be computed by utilizing a channel impulse response estimate [99].

In fast or relatively fast fading channels, the channel impulse response can not be assumed to be known. Thus, the optimal receiver is somewhat different from that in the slowly fading channels. The receiver minimizing the symbol error probability is again complex to implement and difficult to analyze [100]. Therefore, the MLS detector is usually selected to be the optimal reference receiver. However, as discussed in Section 2.4.4, the MLS detector is not feasible in most practical applications. Like in the AWGN channel, suboptimal receivers for the fading channel will also need to be investigated.

4.4.2. Optimal multiuser demodulation

The maximum likelihood detector incorporates the structure of the receiver in Figure 4.1. The theory for the MLS detector has already been presented in Section 2.4.4 for the AWGN and will not be repeated here.

However, it is sufficient to state that the MLS detector minimises the probability of an erroneous decision on the bit vector b including the data symbols of all users in all symbol intervals. If the channel is known, then using the results of (2.27) and [17, 94], the data decision can be expressed as:

$$\hat{b} = \arg \min_{b \in \{-1,1\}} \Omega(b) \quad \text{.....(4.5)}$$

Where the log-likelihood function Ω(b) is:

$$\Omega(b) = 2\,\mathrm{Re}\,(b'^{T} A'^{T} \lambda'^{T} y) - b'^{T} A'^{T} \lambda'^{T} R \lambda A b \quad \text{.....(4.6)}$$

Note that in (4.6), T represents the transpose.

MLS detectors for flat Rician fading channels with synchronous CDMA have been considered in [96] and two path Rician fading channels with asynchronous CDMA in [97]. MLS detectors in unknown slowly fading channels has been considered in [101].

The maximum likelihood sequence detection for relatively fast fading channels has also been analyzed. MLS detectors for synchronous CDMA in Rayleigh fading channels has been presented in [95, 102]. The resulting MLS receiver consists of the received noiseless signal estimator for all possible data sequences and a correlator, which multiplies the received signal with the estimated received noiseless signal (estimator-correlator receiver). The MLS detector allows for the structure of the receiver in Figure 4.1 to be used.

The optimal MLS receiver for channels with unknown user and multipath delays τ_k and $\tau_{k,l}$ is significantly more difficult to derive. The reason for this is the fact that the received signal depends nonlinearly on the delays, and the MLS receiver does not allow for a simple estimator-correlator interpretation. One way to approximate the MLS detector for the reception of a signal with unknown delays is to perform joint maximum likelihood estimation on the data, the received complex amplitude and the delays [103]. The joint ML estimation has an extremely high

computational complexity, which is exponential in the product of the number of users K, the number of propagation paths L and the number of samples per symbol interval.

4.4.3. Suboptimal multiuser demodulation

As discussed in Section 2.4.4, due to the optimal MLS detector being computationally complex to implement, suboptimal solutions have been studied extensively. These suboptimal receivers approximate the optimal MLS detector. Most receivers can process either the matched filter bank output (Figure 4.2) or its maximal ratio combined version (Figure 4.1). The latter receivers do not eliminate the effect of MAI on channel estimation. Therefore, the multiuser detectors processing the MF bank output are often more desirable in practice. Section 4.3.3.1 concentrates on linear equalizer type receivers, whereas interference cancellation receivers are considered in Section 4.3.3.2.

4.4.3.1. Linear equalizer type multiuser demodulation

The linear equalizer type multiuser receivers process the matched filter output vector y (or the maximal ratio combined vector $y_{[MRC]}$) by a linear operation. In other words, the output $y_{[LIN]}$ of a linear multiuser detector is given by:

$$y_{[LIN]} = \beta^T y \quad \text{.....(4.7)}$$

Different choices of the matrix β yield different multiuser receivers. If β is equal to the identity matrix, then this receiver is equivalent to the conventional single-user receiver. The linear equalizer type receivers apply the principles of linear equalization, which has been used in ISI reduction [6].

4.4.3.1.1. The Decorrelator

The decorrelator or zero-forcing receiver, which completely removes the MAI, has been described by (2.28) where it was given that $\beta=R^{-1}$. The decorrelator that was used in the AWGN channel can also be utilized in the fading channel. The performance of the decorrelator in known,

slowly fading channels has been analyzed in [104, 94, 105, 106] and the differentially coherent case has been considered in [107]. The corresponding analysis for estimated, relatively fast fading channels has been presented in [95, 96, 97, 108, 109]. The performance of the decorrelator utilizing the matched filter bank output y or the maximal ratio combined MF bank output $y_{[MRC]}$ has been compared in [110]. The principle of the decorrelating receiver has been extended to receivers utilizing antenna arrays [32, 82, 83], multiple base stations [84, 85], or multiple data rates [86, 87]. Adaptive implementations of the decorrelating receiver for synchronous CDMA systems have been considered in [74, 88] and for asynchronous CDMA systems in [111].

4.4.3.1.2. The LMMSE Detector

If the information symbols are independent and the channel is known, the linear receiver which minimises the mean squared errors at the detector output is called the LMMSE detector [112] and is described by:

$$\beta = [R + \sigma^2(\lambda A A^{*T} \lambda^{*T})^{-1}]^{-1} \quad \text{.....(4.8)}$$

where, as previously defined:

- R is a matrix of cross correlations of signature waveforms for all multipath components of all users over all symbol intervals
- σ^2 is the two-sided power spectral density of the noise
- λ is the matrix of the channel coefficient vectors of all users over all symbol intervals
- A is the diagonal matrix of transmitted complex amplitudes of all users over all symbol intervals

The LMMSE receiver is equal to the linear receiver maximizing the signal-to-interference-plus-noise ratio (SINR) [38]. Centralized LMMSE receivers have been proposed for fading channels in [58, 113] and for antenna array receivers [32, 114, 115]. The LMMSE receivers have attracted most interest due to their applicability to decentralized adaptive implementation. Decentralized LMMSE multiuser receivers for slowly

fading channels suitable for adaptive implementation based on training has been considered in [38, 116, 117, 118].

The convergence of the adaptive algorithms for the LMMSE multiuser receivers has been considered in [119, 120, 121]. A modified multiuser receiver applicable to relatively fast fading frequency selective channels with channel state information has been proposed in [122].

4.4.3.1.3. Finite and infinite impulse response filters

The linear multiuser receivers process the complete received data block, the length of which approaches infinity in asynchronous CDMA systems. In other words, the memory-length of the linear equalizer type receivers is infinite. In [21] it was shown that as the number of symbols in the data packet approaches infinity, the decorrelating detector approaches a time-invariant, stable digital multichannel infinite impulse response (IIR) filter with z-domain transfer function

$$D(z) = [R(2)z^{-2} + R(1)z^{-1} + R(0) + R(-1)z + R(-2)z^{-2}]^{-1} \quad \text{.....(4.9)}$$

The input of D(z) is the matched filter bank output vector sequence y. Since the matrix algebraic structure of the LMMSE detector is similar to that of the decorrelating detector, (4.9) can be generalized for it. The detectors can be presented in the form of (4.9) in systems with time-invariant signature waveforms only. The implementation of the multichannel IIR filter of the form (4.9) is not straightforward due to the symbolic computation of the inverse. Any multichannel IIR filter of the form of (4.9) can also be represented in the form

$$D(z) = \sum_{p=-\infty}^{\infty} D(p)z^{-p} \quad \text{.....(4.10)}$$

Note that D(p) are the matrix coefficients of the expansion which are functions of the auto and cross-correlations of the user's spreading sequences.

Truncation of (4.10) to obtain the finite impulse response (FIR) filters has been suggested in [21] for the decorrelating detector. However, the effect of such a truncation on the detector performance was not analyzed.

Several other ways to obtain finite memory-length multiuser detectors have been proposed. The most natural way is to leave symbol intervals regularly without transmission. This will result in finite blocks of transmitted symbols and the detectors would then have finite memory-length [30, 43]. In [30], such an approach was called "isolation bit insertion". This, however, degrades the bandwidth efficiency and requires some form of the synchronism between users. Other approaches to obtaining finite memory-length multi-user detectors have already been outlined in Section 2.4.5.1.

4.4.3.2. Interference cancellation

For the fading channel, the aim of interference cancellation receivers is to estimate the multiple-access and multipath induced interference and then subtract the interference estimate from the MF bank (or MRC) output. The interference cancellation can be derived as an approximation of the MLS detector with the assumption that the data, amplitude and delays of the interfering users are known[47].

As discussed in Section 2.4.6, there are several principles of estimating the interference leading to different IC techniques. The interference can be canceled simultaneously from all users leading to parallel interference cancellation, or on a user by user basis leading to successive interference cancellation. Also parallel interference cancellation is possible. The interference estimation can utilize tentative data decisions. The scheme is called hard decision (HD) interference cancellation. If tentative data decisions are not used, the scheme is called soft decision (SD) interference cancellation. The interference cancellation can also iteratively improve the interference estimates. Such a technique is utilized in multistage receivers.

Similar to the discussion in Section 2.4.6.2 and (2.36), the multistage hard-decision parallel interference (HD-PIC) output at the Ns+1 stage can be presented as:

$$b_{[HD-PIC](Ns+1)} = y - Q\lambda(Ns)A\dot{b}(Ns) \quad \text{.....(4.11)}$$

where:

- $\bar{\lambda}$ (Ns) denotes the channel estimates provided by stage Ns of the multistage HD-PIC receiver.
- $\bar{b}$(Ns) denotes the data estimates provided by the stage Ns of the multistage HD-PIC receiver.
- Q $\bar{\lambda}$A $\bar{b}$(Ns) represents an estimate of the MAI [52]

The multistage PIC can be initialized by any linear equalizer type receiver. In the soft-decision parallel interference cancellation (SD-PIC) the amplitude-data product is estimated linearly without making any explicit data decision, or a tentative data decision with a soft nonlinearity is made. The tentative estimates and decisions may be replaced by final ones at those symbol intervals for which they are available. The result is decision-feedback HD-PIC receiver.

The multistage HD-PIC receiver for slowly fading channels has been studied in [47, 123, 124, 125, 126, 127, 128] and for relatively fast fading channels in [129, 130, 131]. The application of the HD-PIC to multiuser delay estimation in relatively fast fading channels has been considered in [132, 133, 134]. The SD-PIC receivers with linear data-amplitude product estimation for slowly fading channels have been considered in [135, 136] and for multicellular systems in [137].

The successive interference cancellation is performed on a user by user basis as discussed in Section 2.4.6. In the SIC case, the amplitude and data of user 1 are estimated first. Using the obtained estimates the MAI estimate of user 1 is subtracted from the matched filter outputs of the rest of the users. Then the amplitude and data of user 2 are estimated and the MAI estimate of user 2 is subtracted from the matched filter outputs of the users k=3,4, ...,K etc. The cancellation should start with the user with the largest average power, the second powerful user should be canceled next, etc. For the SIC receiver, ordering of the users in order of their power is a problem in relatively fast fading channels, since it must be updated frequently.

4.5. Conclusion

An investigation was done in this chapter to check if the detectors for the AWGN channel can also be used in the fading channel, and whether any modifications to them were required.

Multiuser signal processing can be performed either before multipath combining, by processing the matched filter bank output vector, or after multipath combining by processing the maximal ratio combined matched filter bank output vector. Most multiuser receivers can also be implemented before matched filtering, by processing the received spread-spectrum signal.

The optimal receiver for the multipath channel is the coherent RAKE receiver. The conventional approach to data detection is to employ an independent, single-user RAKE receiver for each user, which is optimal in the absence of MAI. However, the RAKE receiver suffers from the near-far effect in the presence of interfering signals received over independent fading channels. MLS detectors for synchronous CDMA in Rayleigh fading channels have been presented in [95, 102]. The joint ML estimation has an extremely high computational complexity, which is exponential in the product of the number of users, the number of propagation paths and the number of samples per symbol interval.

The linear equalizer type multiuser receivers process the matched filter output vector using a linear operation. The linear operations that were considered were for the decorrelator and the LMMSE detector. The LMMSE detector minimises the mean squared errors at the detector output. These detectors have attracted most attention due to their applicability to decentralised adaptive implementation. It was shown in [21] that as the number of symbols in the data packet approaches infinity, the decorrelating detector approaches a time-invariant, stable digital multichannel infinite impulse response (IIR) filter. The purpose of interference cancellation receivers is to estimate the multiple-access and multipath induced interference and then subtract the interference estimate from the matched filter bank output. The interference can be cancelled simultaneously from all users as parallel interference cancelation, or on a user by user basis as successive interference cancellation.

Chapter 5: Multiuser demodulation in Rayleigh fading channels

5.1. Introduction

As stated in Chapter 2, the problem of optimal as well as sub-optimal detection for CDMA transmission over an additive white Gaussian noise (AWGN) channel has been the focus of study in [17, 18, 22, 27, 33, 51]. However, as discussed in Chapters 3 and 4, CDMA transmissions are frequently made over channels that exhibit fading. Hence, an attempt will be made in this chapter to obtain receivers which take into account this behavior of the channels.

The work in this chapter is an extension of the Chapter 4 and the research undertaken in [96, 97]. In this Chapter, a three-path Rician fading CDMA channel will be considered instead of the two path model as in [96, 97]. With the aid of the information presented in the preceding chapters, multiuser receivers will be derived for the three-path time-dispersive Rician fading CDMA.

The problem will be formulated in Section 5.2 and the relevant notation to be used for the derivation of the receivers, will be introduced in Section 5.3. In Section 5.4, under the assumption that the fading parameters are uncorrelated, this fading CDMA channel will be shown to be equivalent to a Gaussian CDMA channel over which a modified signal set is employed. This equivalence result is necessary in order to facilitate the use of some of the detectors for the Gaussian channel in Chapter 2, for this Rician fading channel. In Section 5.5, a discussion will be given of the detectors for this fading channel. These detectors include the conventional detector, the optimum detector, and discussion will be provided on suboptimal multiuser demodulation. In particular, the decorrelating detector for both the finite and infinite message length will be derived and their operation discussed. In Section 5.6, a brief discussion will be given on mismatched detectors over this fading channel. An attempt will be made in this section to quantify the loss in performance incurred by these mismatched detectors. Finally, in Section 5.7, concluding remarks will be provided for the work covered in this chapter

5.2. Problem formulation

In this Chapter, the investigation of multiuser detection for asynchronous CDMA communication over the time-dispersive Rician fading channel will be undertaken. For each user there exists a steady specular path and Rayleigh faded paths, all of them appearing asynchronously at the receiver.

A detailed model is given of the three-path Rician fading CDMA channel and the underlying assumptions are specified in Section 5.2.1. Performance measures for the detection strategies over the three path Rician fading channel are discussed in Section 5.2.2.

5.2.1. Received signal model

The signal model that is assumed for the CDMA transmissions through this fading channel is given by:

$$r(t) = \sum_{x=-M}^{M} \sum_{k=1}^{K} b_k(x) s_k(t) + \sum_{x=-M}^{M} \sum_{k=1}^{K} \sum_{n=1}^{2} b_k(x) f_k^{n}(t) + n(t) \quad \text{.....(5.1)}$$

In (5.1), the first term corresponds to the signal received along the spectral path. The second term corresponds to the signal received along the two fading paths. The third term corresponds to the additive-white Gaussian noise.
Note that (5.1) is very similar to (4.2), with the addition of the unfaded spectral signal path.

The terms $s_k(t)$ and $f_k^{n}(t)$ are given by the expressions:

$$s_k(t) = \sqrt{E_k(x)}\, a_k(t - xT - \tau_k^{0}) e^{j\phi_k(x)} \quad \text{.....(5.2)}$$

$$f_k^{n}(t) = \lambda_k^{n}(x) a_k(t - xT - \tau_k^{n}) e^{j\phi_k^{n}(x)} \quad \text{.....(5.3)}$$

Substitution of (5.2) and (5.3) into (5.1), results in the following definition of the received signal model for the CDMA transmission through the three-path Rician fading channel as:

$$r(t) = \sum_{x=-M}^{M} \sum_{k=1}^{K} b_k(x)\left(\sqrt{E_k(x)}a_k(t - xT - \tau_i^{\,0})e^{j\theta_k(x)} + \lambda_k^{\,1}(x)a_k(t - xT - \tau_k^{\,1})e^{j\phi_k^{\,1}(x)}\right.$$

$$\left. + \lambda_k^{\,2}(x)a_k(t - xT - \tau_k^{\,2})e^{j\phi_k^{\,2}(x)}\right) + n(t) \quad \text{.....(5.4)}$$

where:

- The receiver observes the sum of the specular and fading transmissions of each of the K users corrupted by the complex zero mean, additive white Gaussian noise process n(t) .

- The noise variance is σ^2 and there are 2M+1 signaling intervals, each of duration T, in accordance with the stipulations of Section 2.4.2

- The signals of the K users are indexed in the order in which their specular components arrive at the receiver. Hence, $\tau_k^{\,0} \geq \tau_i^{\,0}$ for $k \geq i$. Note that $\tau_k^{\,0}$ is the delay of the kth user for the spectral path. Similarly, $\tau_k^{\,1}$ is the delay of the kth user for the first fading path and $\tau_k^{\,2}$ is the delay of the kth user for the second fading path.

- BPSK signaling is assumed, where the data symbol $b_k(x)$ represents the bit transmitted by the kth user in the xth bit interval and is chosen from the set $\{1,-1\}$.

- The signal $a_k(t)$ which is time-limited to [0,T], is the normalized low-pass signature signal of the kth user.

- $E_k(x)$ and $\theta_k(x)$ denote the energy and phase of the direct component of the signature signal of the (k,x)th user at the receiver – the kth user in the xth symbol interval.

- The (k,x)th fading parameters $\lambda_k^{\,1}(x)$ and $\phi_k^{\,1}(x)$ are the Rayleigh distributed attenuation and uniformly distributed phase shift that the (k,x)th user's signal undergoes along the first fading path. The (k,x)th fading parameters $\lambda_k^{\,2}(x)$

and $\phi_k^2(x)$ are the Rayleigh distributed attenuation and uniformly distributed phase shift that the (k,x)th user's signal undergoes along the second fading path.

The specular component is associated with a clear path between the transmitter and receiver, while alternate paths along which the signal may be considerably weakened in strength give rise to the fading components. The assumption is made that the fading parameters affecting the various users are independent of each other, justified by the fact that the paths traveled by the signals of the users are most likely different. If the fading parameters over successive bit intervals are assumed independent, then all possible realizations of the transmitted vectors of data bits are considered equally likely a priori.

The approach taken is similar to the one in [97] where the discrete-time fading amplitude process of each user is assumed to be memoryless, and these processes for different users and the additive Gaussian noise n(t) are statistically independent of one another. The assumption of the fading being memoryless is an idealization, but it does allow for an indepth mathematical analysis of the problem. This assumption of the absence of fading memory is valid as the fading parameters such as the random attenuation and phase shifts, are likely to change relatively frequently. These changes could even occur over successive bit intervals, and this would make it unfeasible to estimate them. This lack of memory does not need the estimation of fading amplitudes and so the availability of only the fading variances is assumed, that statistically characterize the random variations of the faded signal amplitudes. Detectors designed for this model would be expected to be robust to such variations.

5.2.2. Performance measures

The asymptotic performance criteria for the detection strategies over the three-path Rician fading channel, are described in this section. An attempt will be made in this chapter to obtain detectors which are computationally feasible and which achieve performance levels that are as close as possible to those attained by the optimal detectors discussed in Chapter 2, under the AME criteria. The AME has already been defined in (2.24) for detectors for the AWGN channel in Chapter 2. This result is extended to the received signal model in (5.4).

Extending the result of (2.24), the AME for the (k,x)th user is defined as:

$$\eta_k(x) = \sup_{\{(r,\sigma^2)\}} \lim_{\sigma^2 \to 0} \frac{P_k}{Q\left(\sqrt{\frac{2rE_k(x)}{\sigma^2}}\right)} < \infty \quad \text{.....(5.5)}$$

where:

- r is equal to the fading to additive noise variance ratio for a particular user in a particular symbol interval.
- The Q-function has already been defined in (2.25).
- Note that the other variables in (5.5) have already been defined in Chapter 2 for (2.24).

In the definition of the AME in (5.5), the fading to additive noise variance ratios are held constant, and the fading variances are assumed to be independent of the specular component energies. Since the AME is parameterized by both specular energy and fading to additive noise variance ratios, it quantifies the effects of both the specular energies and the fading on the detector performance.

The AME defined in (5.5) compares the multiuser error probability to that of the corresponding single user in the AWGN. Furthermore, it captures the loss in performance due to the presence of the other users at fixed variance ratio levels in the high SNR and high signal to fading noise ratio (SFNR) regions. Examining the definition of the AME in (5.5), it can be stated that $\eta_k(x)E_k(x)$ is the transmitted energy required by the kth user in a single-user AWGN environment so that the logarithm of the resulting bit error probability decays at the same rate as that for the user in the xth bit interval in a multiuser environment in which the same transmission is made with energy $E_k(x)$.

The near-far resistance of a detector used in the AWGN channel has been defined in (2.26). The near-far resistance is a measure of the robustness of a detection scheme to variations in the specular energies of the users under the assumptions of constant fading to additive noise variance ratios. Furthermore, the fading variances must be independent of the specular energies. As explained in Section 2.4.3, a detector with a nonzero near-far resistance is called near-far resistant. A near-far resistant detector achieves an exponential rate of decay in error probability as all the noise in the system vanishes irrespective of the interfering specular energies. This behaviour is similar to that of the

optimum detectors over single-user channels and is desired in the multiuser environment as well.

5.3. Overview of notation used

The notation required for the derivation of detectors for this fading channel are introduced in this section. Additionally, a vector and matrix notation is introduced to facilitate an easy description of the results for the subsequent sections. For a concise treatment of the detection strategies, the system parameters need to be organised in (2M+1)K dimensional vectors and matrices.

The presentation of this section is as follows: In Section 5.3.1, the equations for the matched filter output vectors are derived while the notation for the specular and fading diagonal matrices is discussed in Section 5.3.2. Finally, in Section 5.3.3, the notation for the signal correlation matrices is introduced.

5.3.1. Matched filter bank output vectors

Similar to Chapter 2, the output of the filter banks matched to the signals of the users over the various paths is given by:

$$y_p^{\,j} = \int_{T+\tau_p^{\,j}}^{(T+1)+\tau_p^{\,j}} a_p(t-T-\tau_p^{\,j})r^*(t)dt \quad \text{.....(5.6)}$$

where:

- p represents the relevant user and p∈(1....K)

- The asterix (*) denotes the complex conjugate

- The vector y^j is composed of the matched filter bank outputs in (5.6) for all K users over the (2M+1) signaling intervals and is of dimension [(2M+1)K x 1].

- j∈(0,1,2) represents the specular, fading path 1 and fading path 2 signal components, respectively. The output of the filter banks matched to the specular signal of the users over the transmission interval, is defined by y^0

while y^1 contains outputs of the filter banks matched to the signal from the first fading path. The outputs of the filter banks matched to the signal of the users from the second fading path over that transmission interval, is described by y^2.

5.3.2. Specular and fading diagonal matrices

The diagonal matrices for the user's specular energies and phases are given by (5.7) and (5.8), respectively. E and Θ are of dimension [(2M+1)K x (2M+1)K].

$$E_{pq} = E * \delta_{p-q} \quad \text{.....(5.7)}$$

$$\Theta_{pq} = e^{j\theta} * \delta_{p-q} \quad \text{.....(5.8)}$$

Σ^2 is the diagonal matrix of the fading-to-additive noise variance ratios and is of dimension [(2M+1)K x (2M+1)K]. It is defined as:

$$\Sigma^2_{pq} = r * \delta_{p-q} \quad \text{.....(5.9)}$$
$$= \frac{\sigma^2_{fading}}{\sigma^2_{noise}} * \delta_{p-q}$$

The diagonal matrix of the fading parameters for the first fading path is given by F_{fad}^1 and is of dimension [(2M+1)K x (2M+1)K] and is described as:

$$F_{fad}^1 = f^1 * \delta_{p-q} \quad \text{.....(5.10)}$$
$$= \lambda_p^1(x) e^{j\phi_p^1(x)} \delta_{p-q}$$

where:

- $\lambda_p^1(x)$ is the Rayleigh distributed attenuation that the p^{th} user undergoes in the x^{th} bit interval along the first faded path.

- $\phi_p^1(x)$ is the uniformly distributed phase shift that the p^{th} user undergoes in the x^{th} bit interval along the first faded path.

The diagonal matrix of the fading parameters for the second fading path is given by $F_{fad}^{\ 2}$ and is of dimension [(2M+1)K x (2M+1)K] and is described as:

$$F_{fad}^{\ 2} = f^2 * \delta_{p-q} \quad \text{.....(5.11)}$$
$$= \lambda_p^{\ 2}(x) e^{j\phi_p^{\ 2}(x)} \delta_{p-q}$$

where:

- $\lambda_p^{\ 2}(x)$ is the Rayleigh distributed attenuation that the p^{th} user undergoes in the x^{th} bit interval along the second faded path.

- $\phi_p^{\ 2}(x)$ is the uniformly distributed phase shift that the p^{th} user undergoes in the x^{th} bit interval along the second faded path.

5.3.3. Signal correlation matrices

The normalised specular, faded and specular-to-faded signal correlation matrices are given by A^{ij} which is of dimension [(2M+1)K x (2M+1)K]. The definition of A^{ij} is given as:

$$A_{pq}^{ij} = \int_{p,q=0}^{K} a_p(t - xT - \tau_p^{\ i}) a_q^{*}(t - xT - \tau_q^{\ j}) dt \quad \text{.....(5.12)}$$

where:

- p,q are the respective users and p,q $\in$ (0....K)
- i,j are the respective paths and i,j $\in$ (0,1,2)

From (5.12), the following signal correlation matrices can be obtained:

A^{00} is the normalized specular correlation matrix
A^{11} is the normalized faded correlation matrix for fading path 1
A^{22} is the normalized faded correlation matrix for fading path 2
A^{01} is the normalized specular-to-fading path 1 signal correlation matrix
A^{02} is the normalized specular-to-fading path 2 signal correlation matrix
A^{12} is the normalized fading path 1-to-fading path 2 correlation matrix

5.4. Equivalence between fading and AGISI channel

It would be preferable to be able to specify multiuser detectors for the fading channel for each multiuser detector that is known for the Gaussian channel. In order to facilitate this, an equivalence will now be shown between the fading channel and the Gaussian channel, where the method followed will be similar to that presented in [96, 97]. It will be shown that the time-dispersive Rician fading asynchronous CDMA channel bears an equivalence to an asynchronous Gaussian intersymbol interference (AGISI) channel.

The detection problem formulation for the Gaussian channel is obtained using (2.27), (4.5) and (4.6) and is given by:

$$\hat{b} = \arg_{b\in\{-1,1\}^K} \max \quad 2b^T(q_g + q_g^*) - b^T(H_g + H_g^*)b \qquad (5.13)$$

where:

$$q_g + q_g^* = (H_g + H_g^*)b + n_g + n_g^* \qquad (5.14)$$

$$n_g + n_g^* = [0, \sigma^2(H_g + H_g^*)] \qquad (5.15)$$

and:

$$H_g = E^{\frac{1}{2}}\Theta A \Theta^T E^{\frac{1}{2}} \qquad (5.16)$$

$$q_g = E^{\frac{1}{2}}\Theta y \qquad (5.17)$$

Note that y is now the vector of normalised matched filter outputs obtained when fading is absent. The vector $q_g+q_g^*$ is denoted as the vector of sufficient statistics for the Gaussian channel, while A and E are the normalised signal cross-correlation and energy matrices, respectively. One needs to now find the exact relationship between the faded and Gaussian channel.

Proposition

The time-dispersive Rician fading asynchronous CDMA channel bears an equivalence to an asynchronous Gaussian intersymbol interference (AGISI) channel over which the users transmit data using signals whose cross-correlation matrix is A^{eq} with energies specified by the diagonal elements of the matrix E^{eq}.

The equations for the equivalent signal cross-correlation matrix and the equivalent diagonal energy matrix are given as:

$$A^{eq} = \bar{E}^{-\frac{1}{2}}\{A^{00} - [(A^{01} + A^{21})(\Sigma^{-2} + A^{11})^{-1}(A^{10} + A^{12})] - [(A^{02} + A^{12})(\Sigma^{-2} + A^{22})^{-1}(A^{20} + A^{21})]\}E^{-\frac{1}{2}} \quad \text{.....(5.18)}$$

$$E^{eq} = E\,E \quad \text{.....(5.19)}$$

where:

- The elements of $\bar{E}$ are chosen such that $A_{xx}^{eq} = 1$ for $-MK+1 \le x \le (M+1)K$.
- There are 2M+1 signaling intervals and K users

Illustration of the equivalence result

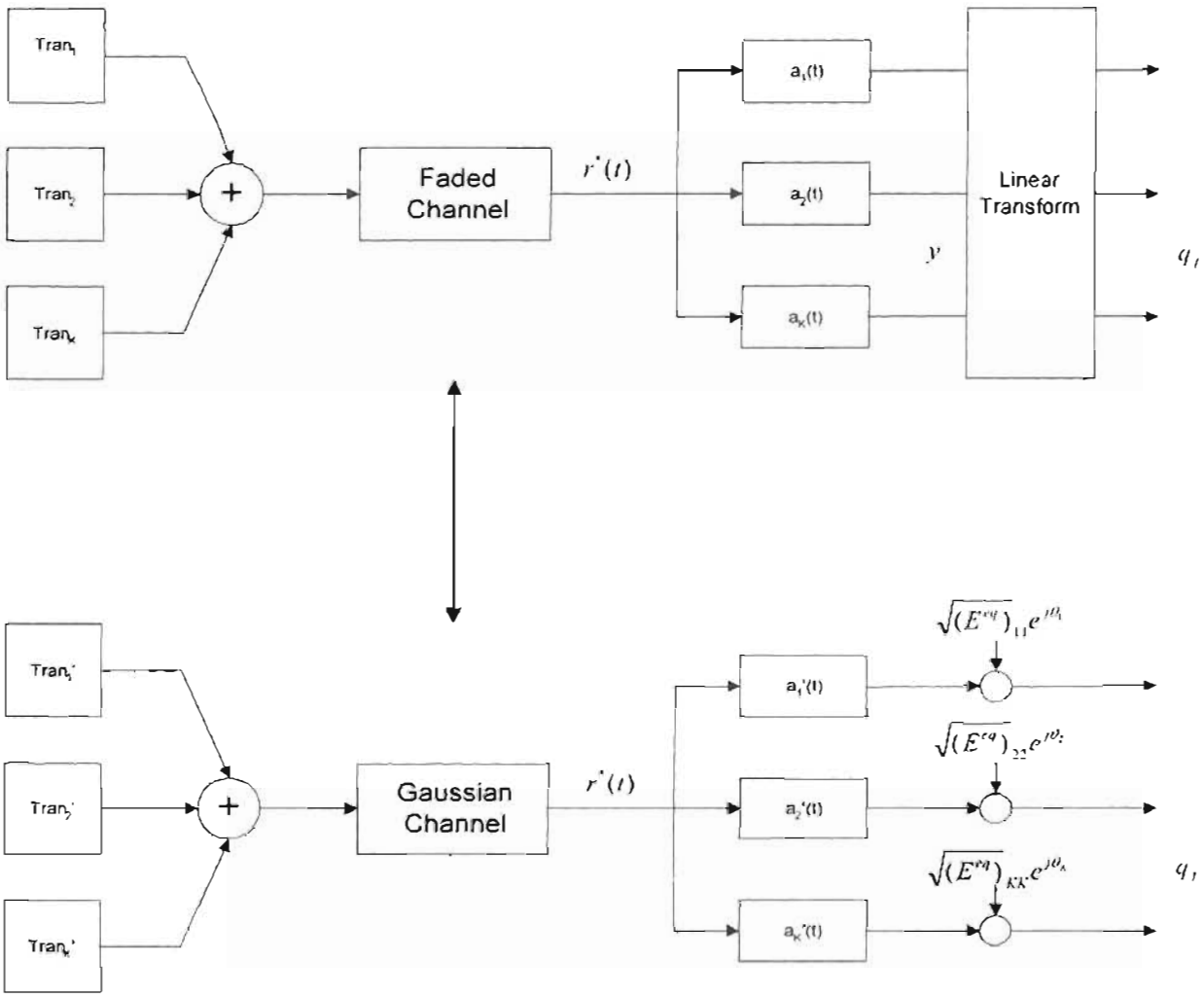

Figure 5.1: Equivalence of faded and Gaussian CDMA channels

Figure 5.1 illustrates the equivalence result stated in (5.18) and (5.19). The cross-correlation matrix of the signals $\{a_1(t), \ldots\ldots, a_k(t)\}$ used by the transmitters $\{ Tran_1, \ldots.., Tran_K \}$ in the equivalent Gaussian channel is A^{eq} and the transmissions are made with energies E^{eq}. The complex conjugate of the channel output is $r^*(t)$ and it is correlated with the signals shown in Figure 5.1. The decision statistics q_f are obtained after the appropriate operations.

Proof

One needs to first obtain the equations relating vector $q_f+q_f^*$ to the data vector, making use of the fact that the fading parameters are uncorrelated with each other, and with the noise components produced at the receiver end by the additive white Gaussian noise processes.

Using the definition of the matched filter bank output vector in (5.6) and substituting the expression for r(t) in (5.4) into the definition of the normalised filter bank outputs y^0, y^1 and y^2, it can be shown that:

$$y^0 = A^{00}\Theta^* E^{\frac{1}{2}} b + (A^{01} F_{fad}^{*1} + A^{02} F_{fad}^{*2}) b + n^0 \quad \text{.....(5.20)}$$

$$y^1 = (A^{10} + A^{12})\Theta^* E^{\frac{1}{2}} b + A^{11} F_{fad}^{*1} b + n^1 \quad \text{.....(5.21)}$$

$$y^2 = (A^{20} + A^{21})\Theta^* E^{\frac{1}{2}} b + A^{22} F_{fad}^{*2} b + n^2 \quad \text{.....(5.22)}$$

In (5.20), (5.21) and (5.22), the additive noise components are described for each path $j \in (0,1,2)$ for users p=1 to K by:

$$n_p^{\,j} = \int_{T+\tau_p^{\,j}}^{(T+1)+\tau_p^{\,j}} a_p(t - T - \tau_p^{\,j}) n^*(t) dt \quad \text{.....(5.23)}$$

Combining the fading and additive noise components in (5.20), (5.21) and (5.22), the following expressions are obtained:

$$n^{s0} = (A^{01} F_{fad}^{*1} + A^{02} F_{fad}^{*2}) b + n^0 \quad \text{.....(5.24)}$$

$$n^{s1} = A^{11} F_{fad}^{*1} b + n^1 \quad \text{.....(5.25)}$$

$$n^{s2} = A^{22} F_{fad}^{*2} b + n^2 \quad \text{.....(5.26)}$$

Substituting (5.20), (5.21) and (5.22) for y^0, y^1 and y^2 into (5.17) one obtains:

$$q_f = H_f b + n \quad \text{.....(5.27)}$$
$$= H_f b + E^{\frac{1}{2}}\Theta n^{s0} - E^{\frac{1}{2}}\Theta(A^{01} + A^{21})(\Sigma^{-2} + A^{11})^{-1} n^{s1} - E^{\frac{1}{2}}\Theta(A^{02} + A^{12})(\Sigma^{-2} + A^{22})^{-1} n^{s2}$$

Finally, the real part of q_f is related to the data vector and the associated noise vector is characterised as:

$$q_f + q_f^{'} = (H_f + H_f^{'})b + n + n^{'} \quad \text{.....(5.28)}$$

$$n + n^{'} : [0, \sigma^2 (H_f + H_f^{'})] \quad \text{.....(5.29)}$$

Comparison of (5.28), (5.13), (5.14), (5.15) and (5.29), one sees that from the point of view of optimal detection, the fading channel may be seen as an AGISI channel over which the users transmit data using signals whose cross-correlation matrix is A^{eq} with energies specified by the diagonal elements of the matrix E^{eq}.

This concludes the proof. This equivalence result allows for the specification of a multiuser detector for the fading channel for each multiuser detector that is known for the Gaussian CDMA channel. The suboptimal detectors such as the decorrelating and multistage detectors when specified for the equivalent Gaussian channel, give rise to the corresponding fading multiuser detectors for the Rician fading channel. Furthermore, the bit-error probabilities of the fading detectors can be obtained by using the corresponding results for the equivalent Gaussian channel.

5.5. Detectors for the fading channel

The organisation of this section is as follows:

The conventional detector for the fading channel will be discussed in Section 5.5.1 while the optimum detector will be discussed in Section 5.5.2. In Section 5.5.3, the vector of sufficient statistics for the channel will be obtained, which will be used for the derivation of the detectors for suboptimal multiuser demodulation in Section 5.5.4.

5.5.1. The Conventional detector

As discussed in Section 2.3.1, the optimum detection strategy for the single-user environment, when employed in the multiuser channel, has been defined as the conventional detector. This resulted in the matched-filter detector of Figure 2.2, which had very little computational complexity.

However, for the time-dispersive fading channel, the conventional detector definition leads to a sequence detector of the Viterbi type since it recognises and takes into account the dispersion of the user's signal. This detector is also near/far limited when used over the corresponding multiuser channel because the presence of the interfering users is not taken into account [96].

The strategy followed here is the same as in [97] where an alternative single-user strategy of less complexity was considered. This resulted from assuming not only the absence of the interfering users, but also that the desired user transmission was single-shot. The optimum detector under this assumption is a diversity combiner that accounts for the multipath resulting from the single transmission but unlike the Viterbi detector ignores self-ISI.

Similar to the method followed in [97], the data estimate from the conventional detector is derived in this section.

The single user decision rule applied in the multiuser system constitutes the conventional detector. The conventional decision rule for each user is thus obtained by assuming the absence of other users and is derived in the multiuser environment to be [97]:

$$\tilde{b}_k(x) = \operatorname{sgn} \Re\{E_k^{\frac{1}{2}}(x)\Theta(x,x)_{k,k}(y^0(x)_k - \frac{r_k^{\,1}(x)}{r_k^{\,1}(x)+1} A^{01}(x,x)_{k,k} y^1(x)_k$$

$$- \frac{r_k^{\,2}(x)}{r_k^{\,2}(x)+1} A^{02}(x,x)_{k,k} y^2(x)_k)\} \quad \text{.....(5.30)}$$

where:

- $r_k^{\,1}(x)$ is the fading path 1 to additive noise variance ratio for user k in symbol interval x
- $r_k^{\,2}(x)$ is the fading path 2 to additive noise variance ratio for user k in symbol interval x

The definitions of y^0 , y^1 and y^2 are obtained by expanding out (5.6) for the first user and are given by:

$$y^0 = \int_{T+\tau_1^{\,0}}^{(T+1)+\tau_1^{\,0}} a_1(t - T - \tau_1^{\,0}) r^*(t) dt \quad \text{.....(5.31)}$$

$$y^1 = \int_{T+\tau_1^{\,1}}^{(T+1)+\tau_1^{\,1}} a_1(t - T - \tau_1^{\,1}) r^*(t) dt \quad \text{.....(5.32)}$$

$$y^2 = \int_{T+\tau_1^{\,2}}^{(T+1)+\tau_1^{\,2}} a_1(t - T - \tau_1^{\,2}) r^*(t) dt \quad \text{.....(5.33)}$$

Note that in (5.31), (5.32) and (5.33), r(t) represents the received signal over the single-user faded channel. The existence of a faded signal component does not change the form of the conventional detector in the single user fading environment from that in the Gaussian channel. However, there is an increase in the associated probability of error.

To simplify the equations that follow, define the variables $w_k^{\,1}(x)$ and $w_k^{\,2}(x)$ for use in (5.30) as follows:

$$w_k^{\,1}(x) = \frac{r_k^{\,1}(x)}{r_k^{\,1}(x)+1} A^{01}(x,x)_{k,k} \quad \text{.....(5.34)}$$

$$w_k^{\,2}(x) = \frac{r_k^{\,2}(x)}{r_k^{\,2}(x)+1} A^{02}(x,x)_{k,k} \quad \text{.....(5.35)}$$

In the definitions of (5.34) and (5.35), $r_k^{\,1}(x)$ is the fading path 1 to additive noise variance ratio for user k in symbol interval x. $r_k^{\,2}(x)$ is the fading path 2 to additive noise variance ratio for user k in symbol interval x

The next step is to obtain the conventional detector's bit error rate (BER). The terms in the BER to be evaluated are of the form $P(\overline{b}_k(x)=1 \,/\, b_k(x)=-1)$. Note that the notation implies that the estimated data bit is +1 when −1 was transmitted.

Using the method outlined in [97], the following result is obtained:

$$P(b_k(x)=1/b_k(x)=-1)=Q\left(\frac{-\sqrt{E_k(x)}}{\sigma}\cdot\frac{(\Gamma(x,.)_k+\Gamma^{*}(x,.)_k)b}{\sqrt{\Pi(x,x)_{k,k}+\Pi^{*}(x,x)_{k,k}}}\right) \quad \text{.....(5.36)}$$

where:

- $(x,.)_k$ denotes the (k,x)th row of the matrix it indexes
- The definition of Γ is as follows:

$$\Gamma = E^{n\frac{1}{2}}\Theta(A^{00}-w_k^{\,1}(x)A^{10}-w_k^{\,2}(x)A^{20})\Theta^{*}E^{n\frac{1}{2}} \quad \text{.....(5.37)}$$

where:

$$E^{n\frac{1}{2}} = \frac{E^{\frac{1}{2}}}{\sqrt{E_k(x)}} \quad \text{.....(5.38)}$$

In (5.36), the definition of $\Pi(x,x)_{k,k}$ is as follows:

$$\Pi(x,x)_{k,k} = \begin{bmatrix}1 & -w_k^{\,1}(x) & -w_k^{\,2}(x)\end{bmatrix} \times \begin{bmatrix}X1,1 & X1,2 & X1,3\\ X2,1 & X2,2 & X2,3\\ X3,1 & X3,2 & X3,3\end{bmatrix}\begin{bmatrix}1\\ -w_k^{\,1}(x)\\ -w_k^{\,2}(x)\end{bmatrix} \quad \text{.....(5.39)}$$

In (5.39), the elements of the matrix X are defined as follows:

$$X1,1 = (A^{00} + A^{01}\Sigma^2 A^{10} + A^{02}\Sigma^2 A^{20})(x,x)_{k,k}$$
$$X1,2 = (A^{01} + A^{01}\Sigma^2 A^{11} + A^{02}\Sigma^2 A^{22})(x,x)_{k,k}$$
$$X1,3 = (A^{02} + A^{01}\Sigma^2 A^{11} + A^{02}\Sigma^2 A^{22})(x,x)_{k,k}$$
$$X2,1 = (A^{10} + A^{11}\Sigma^2 A^{10} + A^{22}\Sigma^2 A^{20})(x,x)_{k,k}$$
$$X2,2 = (A^{11} + A^{11}\Sigma^2 A^{11} + A^{22}\Sigma^2 A^{22})(x,x)_{k,k}$$
$$X2,3 = (A^{12} + A^{12}\Sigma^2 A^{21} + A^{22}\Sigma^2 A^{21})(x,x)_{k,k}$$
$$X3,1 = (A^{20} + A^{21}\Sigma^2 A^{12} + A^{22}\Sigma^2 A^{22})(x,x)_{k,k}$$
$$X3,2 = (A^{21} + A^{12}\Sigma^2 A^{21} + A^{21}\Sigma^2 A^{12})(x,x)_{k,k}$$
$$X3,3 = (A^{22} + A^{12}\Sigma^2 A^{11} + A^{22}\Sigma^2 A^{21})(x,x)_{k,k}$$

The asymptotic efficiency of the kth user of the conventional detector may now be obtained by using the bit error probability expression (5.36) and the definition in (5.5). The expression for the detector asymptotic efficiency follows by considering the worst-case error probability, and is given as:

$$\eta_k(x) = \max^2\left\{0, \frac{1}{\sqrt{2}} \frac{\Gamma(x,x)_{k,k} + \Gamma^*(x,x)_{k,k} - \sum_{s=-M}^{M}\sum_{r=1}^{K}(1-\delta_{s-r}\delta_{k-l})\left|\Gamma(x,s)_{kr} + \Gamma^*(x,s)_{kr}\right|}{\sqrt{\Pi(x,x)_{k,k} + \Pi^*(x,x)_{k,k}}}\right\} \quad .....(5.40)$$

With the aid of (5.30 – 5.35), the data estimate from the conventional detector can be simplified and written as:

$$\hat{b}_k(x) = \operatorname{sgn}\Re\{E_k^{\frac{1}{2}}(x)\Theta(x,x)_{k,k}(y^0(x)_k - w_k^{\,1}(x)y^1(x)_k - w_k^{\,2}(x)y^2(x)_k)\} \quad ....(5.41)$$

With reference to (5.34), (5.35) and (5.41), it will be observed that when the fading components are absent or when the spectral and faded signal components are coincident, ie. $A^{01}(x,x)_{kk} = A^{02}(x,x)_{kk} = 1$, or when they do not overlap at all, ie. $A^{01}(x,x)_{kk} = A^{02}(x,x)_{kk} = 0$, then the faded signal component is useless and the rule becomes the matched-filter detector.

The performance analysis of this single-user, single-shot, diversity-combining detector over the CDMA channel is obtained by accounting for the presence of interfering users and data sequence transmissions in computing the relevant matched filter outputs in (5.41). The expression for the BER and AME for the conventional detector has been given in (5.36) and (5.40), respectively. In the expression for the AME in (5.40), only those interferers may contribute that are correlated with either the (k,x)th user specular or faded components. For an appropriate choice of specular energies for these users, the asymptotic efficiency may be set to zero. Hence, this conventional detector is near/far limited.

Given the functional dependence of the AME on the interfering specular energy ratios, the near-far resistance of this conventional detector is zero, except when the signal of the user in question is orthogonal to the subspace spanned by the signals of the K-1 users.

5.5.2. The Optimum detector for the channel

In this section, the problem of optimally detecting the 2M+1 length sequences transmitted by each of the K users is considered. In Section 2.4.4, under the assumption that all the possible transmissions by each user over the interval under consideration are equally likely, the MLS detection rule was shown to be optimal.

The MLS detection rule for detection of asynchronous CDMA transmissions was discussed in Section 2.4.4 for the Gaussian channel and in Section 4.4.2 for the fading channel. The results of (2.27), (4.5) and (4.6) will be extended in this section and using the method followed in [97], and the MLS detection rule for the fading channel will be determined.

In this derivation, the problem of optimally detecting the 2M+1 length sequences transmitted by each of the K users is considered. Under the assumption that all the possible transmissions by each user over the interval under consideration are equally likely, the maximum likelihood sequence detection rule is optimal. The following proposition states the MLS rule for the three-path fading channel.

Proposition

The MLS rule for the detection of asynchronous CDMA transmissions over a three-path Rician fading channel with uncorrelated fading is given by:

$$b = \arg_{b\in\{-1,1\}} \max \quad 2\Re\{b^T q_f\} - b^T H_f b \qquad (5.42)$$

where:

$$q_f = E^{\frac{1}{2}}\Theta[y^0 - (A^{01} + A^{21})(\Sigma^{-2} + A^{11})^{-1} y^1 - (A^{02} + A^{12})(\Sigma^{-2} + A^{22})^{-1} y^2] \qquad (5.43)$$

and:

$$H_f = E^{\frac{1}{2}}\Theta\{A^{00} - [(A^{01} + A^{21})(\Sigma^{-2} + A^{11})^{-1}(A^{10} + A^{12})] - [(A^{02} + A^{12})(\Sigma^{-2} + A^{22})^{-1}(A^{20} + A^{21})]\}\Theta^* E^{\frac{1}{2}} \qquad (5.44)$$

Proof

The method followed for the proof is similar to the method used in [97]. To obtain the maximum likelihood rule, the characterization of the vectors of normalized filter outputs are used, which are sufficient statistics for b.

$$\begin{bmatrix} y^0 \\ y^1 \\ y^2 \end{bmatrix} = \begin{bmatrix} A^{00}\Theta^* E^{\frac{1}{2}} \\ A^{10}\Theta^* E^{\frac{1}{2}} \\ A^{10}\Theta^* E^{\frac{1}{2}} \end{bmatrix} [b] + \sigma^2 \begin{bmatrix} A^{00} + A^{01}\Sigma^2 A^{10} + A^{02}\Sigma^2 A^{20} & A^{01} + A^{01}\Sigma^2 A^{11} + A^{02}\Sigma^2 A^{22} & A^{02} + A^{02}\Sigma^2 A^{22} + A^{01}\Sigma^2 A^{11} \\ A^{10} + A^{11}\Sigma^2 A^{10} + A^{22}\Sigma^2 A^{20} & A^{11} + A^{11}\Sigma^2 A^{11} + A^{22}\Sigma^2 A^{22} & A^{12} + A^{12}\Sigma^2 A^{12} + A^{22}\Sigma^2 A^{22} \\ A^{20} + A^{22}\Sigma^2 A^{20} + A^{11}\Sigma^2 A^{11} & A^{21} + A^{21}\Sigma^2 A^{21} + A^{22}\Sigma^2 A^{22} & A^{22} + A^{22}\Sigma^2 A^{22} + A^{12}\Sigma^2 A^{12} \end{bmatrix} \qquad (5.45)$$

Note in (5.45) that $A^{10}=(A^{01})^{*T}$, $A^{20}=(A^{02})^{*T}$ and $A^{12}=(A^{21})^{*T}$

Proof of the validity of (5.45) has already been covered in Section 5.4. Similar to [97], the maximum likelihood rule, obtained from (5.45) after some simplification is given by:

$$b = \arg \max_{b} 2\Re\{b^T E^{\frac{1}{2}}\Theta(y^0 - (A^{01} + A^{21})((A^{11})^{-1} - (A^{11} + A^{11}\Sigma^2 A^{11})^{-1} y^1)$$
$$-(A^{02} + A^{12})((A^{22})^{-1} - (A^{22} + A^{22}\Sigma^2 A^{22})^{-1} y^2)\}$$
$$-b^T E^{\frac{1}{2}}\Theta\{(A^{00} + (A^{01} + A^{21})((A^{11})^{-1} - (A^{11} + A^{11}\Sigma^2 A^{11})^{-1} A^{10})$$
$$+(A^{02} + A^{12})((A^{22})^{-1} - (A^{22} + A^{22}\Sigma^2 A^{22})^{-1} A^{20})\}\Theta^* E^{\frac{1}{2}} b \quad \text{.....(5.46)}$$

In (5.46), the elements in the diagonal matrix of variance ratios Σ^2 that correspond to nonfaded users are set to zero. When all the users are faded, (5.46) may be simplified using Woodbury's Identity to obtain the likelihood rule given in (5.42).

The Woodbury's Identity can be explained mathematically as follows:

$$(A + BCD)^{-1} = A^{-1} - A^{-1}B(DA^{-1}B + C^{-1})^{-1}DA^{-1} \quad \text{.....(5.47)}$$

Where:

- A and C are nonsingular

This concludes the proof for the MLS detection rule for the fading channel.

The structure of the optimum detector is illustrated in Figure 5.2. With reference to Figure 5.2, the entire system model has been depicted for clarity. The carrier signal is first modulated by the data steam and then spread by the code sequence. This CDMA signal is then passed through a fading channel, and is further corrupted by the AWGN process.

For the reception of the signal, carrier demodulation is first performed. The resulting lowpass input signal is called r(t). The complex conjugate of this lowpass input signal is passed through the filter bank with impulse responses $\{a_k(T-t)\}$, and the outputs are sampled at t=T to yield the normalized output

vector y. The vectors $q_f+q_f^*$, defined by (5.43) are obtained by means of linear transformations on the real and imaginary parts of y, and then passed to the decision algorithm of (5.42), to produce estimates of the transmitted data vector.

The combinatorial maximization in (5.42) is NP hard and requires an exhaustive search through all 2^K possible choices for the data vector [96, 97]. This follows from the fact that the functional form of the likelihood is the same as in [22]. Hence, the optimum multiuser detector described in this section is unimplementable.

Despite its unimplementability, the near-far resistance performance of the MLS detector needs to be considered. These results will serve as a benchmark against which the suboptimal strategies for the fading channel will be considered. The equivalence of the fading channel to the AGISI channel discussed in Section 5.4 allows for a straightforward specification of the near-far resistance of the optimal detection strategy. Using the results of (5.5) and (2.26), the near-far resistance for this detector can be derived, which is the highest achievable over this channel. This near-far resistance may be shown to be [96, 97]:

$$\eta_k(x) = \frac{1}{2((R_f + R_f^*)^{-1})(x,x)_{kk}} \qquad \text{.....(5.48)}$$

where:

$$R_f = E^{-\frac{1}{2}} H_f E^{-\frac{1}{2}} \qquad \text{.....(5.49)}$$

The discussion in this section points to the fact that the optimum detector is unimplimentable. Hence, suboptimal detectors will be considered in Section 5.5.4, which are feasible to implement. Their near-far resistance will be obtained and compared against (5.48).

Figure 5.2.
The Optimum Detector

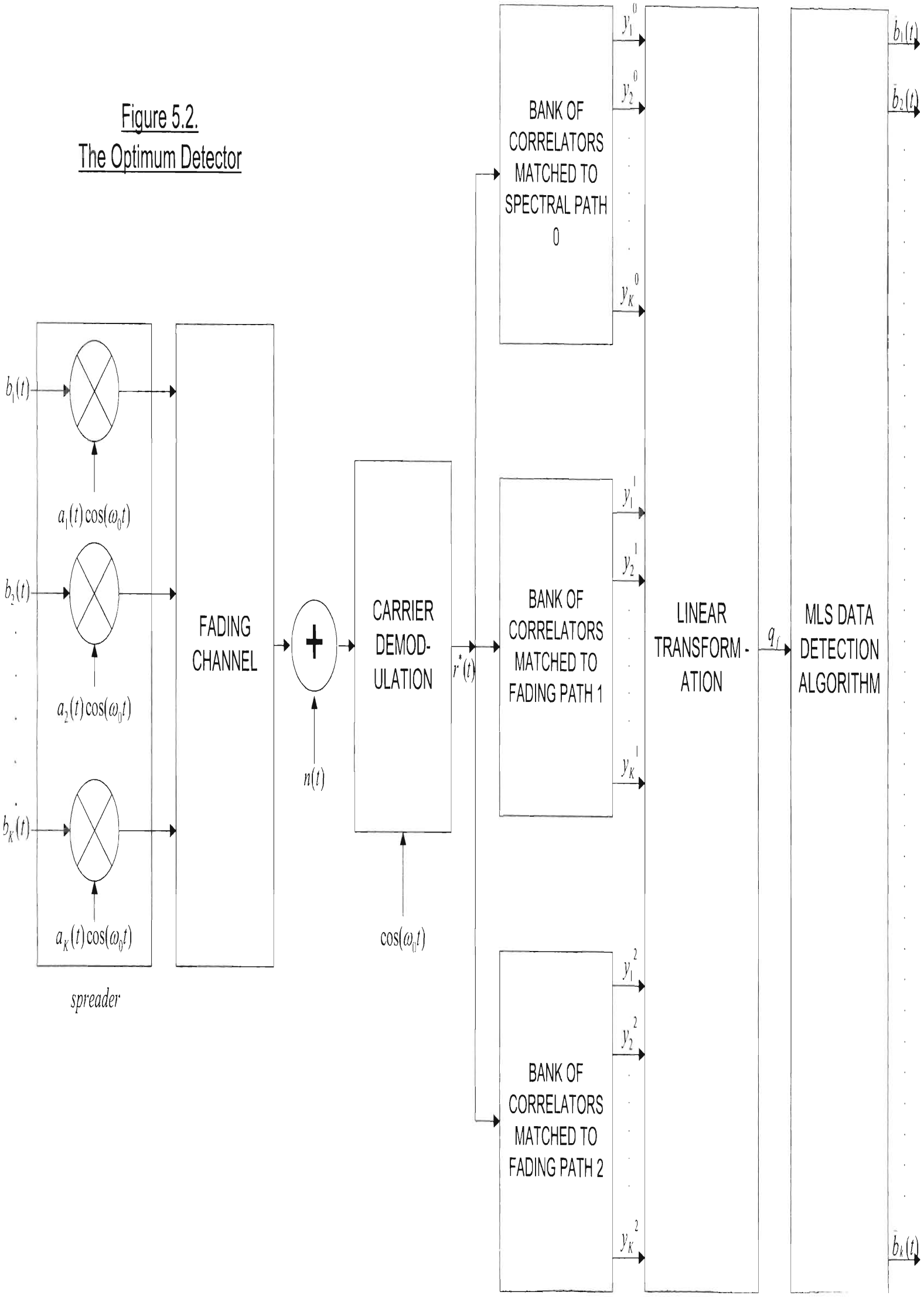

5.5.3. Vector of sufficient statistics for the channel

In this section, the derivation of the vector of sufficient statistics for the channel is undertaken. The vector $2\Re\{q_f\}$ in (5.42) may be referred to as the vector of sufficient statistics for the three-path fading channel. The derivation of the vector of sufficient statistics for the channel is important at this point, as this result will be used for the derivation of suboptimal detectors for the channel in Section 5.5.4. The vector of sufficient statistics may also be written as $(q_f+q_f^*)$.

It was shown in Section 5.4 that by using the definition of the matched filter bank output vector in (5.6) and substituting the expression for r(t) in (5.4) into this definition, the normalised filter bank outputs y^0, y^1 and y^2 could be written as (5.20), (5.21) and (5.22).

Additionally, in (5.20), (5.21) and (5.22), the additive noise components could be described for each path $j\in(0,1,2)$ for users p=1 to K by (5.23) as:

$$n_p^{\,j} = \int_{T+\tau_p^{\,j}}^{(T+1)+\tau_p^{\,j}} a_p(t-T-\tau_p^{\,j})n^*(t)dt$$

where:

- n_p^j is the noise for user p for path j.
- n^j can be defined as a matrix of all the users' noise for path j and its elements are n_p^j.
- n^j is of dimension [(2M+1)Kx1].

Combining the fading and additive noise components in (5.20), (5.21) and (5.22), the following expressions are obtained:

$$n^{s0} = (A^{01}F_{iad}^{*1} + A^{02}F_{jad}^{*2})b + n^0 \quad \text{.....(5.50)}$$

$$n^{s1} = A^{11}F_{iad}^{*1}b + n^1 \quad \text{.....(5.51)}$$

$$n^{s2} = A^{22} F_{fad}^{*2} b + n^2 \quad \text{.....(5.52)}$$

Substituting (5.20), (5.21) and (5.22) for y^0, y^1 and y^2 into (5.43) one obtains:

$$q_f = H_f b + n \quad \text{.....(5.53)}$$
$$= H_f b + E^{\frac{1}{2}} \Theta n^{s0} - E^{\frac{1}{2}} \Theta (A^{01} + A^{21})(\Sigma^{-2} + A^{11})^{-1} n^{s1} - E^{\frac{1}{2}} \Theta (A^{02} + A^{12})(\Sigma^{-2} + A^{22})^{-1} n^{s2}$$

It may be shown that n in (5.31) is a zero-mean Gaussian random vector with covariance matrix H_f. This is because n^{s0}, n^{s1} and n^{s2} are zero-mean Gaussian random vectors with the respective covariance matrices given by (5.54), (5.55) and (5.56).

$$\sigma^2 (A^{11} + A^{11} \Sigma^2 A^{11}) \quad for \ n^{s1} \quad \text{.....(5.54)}$$

$$\sigma^2 (A^{00} + A^{01} \Sigma^2 A^{10} + A^{02} \Sigma^2 A^{20}) \quad for \ n^{s0} \quad \text{.....(5.55)}$$

$$\sigma^2 (A^{22} + A^{22} \Sigma^2 A^{22}) \quad for \ n^{s2} \quad \text{.....(5.56)}$$

By relating the real part of q_f in (5.53) to the data vector b, the following expression is obtained:

$$2\Re(q_f) = q_f + q_f^*$$
$$= H_f b + n + H_f^* b + n^*$$
$$= (H_f + H_f^*) b + n + n^* \quad \text{.....(5.57)}$$

Furthermore, the noise vector in (5.57) can be characterised as follows:

$$n + n^* : [0, \sigma^2 (H_f + H_f^*)] \quad \text{.....(5.58)}$$

Hence, the vector of sufficient statistics for the channel is given by (5.57), with all the variables of the equation having been defined in this section.

5.5.4. Suboptimal multiuser demodulation

It was shown in Section 5.5.1 that the conventional detector for this channel is near-far limited. It was also shown in Section 5.5.2 that the optimum detector is difficult to implement in practice. In this section, a linear detection strategy will be considered for the Rician channel that is computationally less expensive than the MLS detector yet achieves the same near-far resistance as given by (5.48). The specification of this detector is induced from the equivalence shown between the faded and Gaussian CDMA channel in Section 5.4.
Since the vector of sufficient statistics for the channel in (5.57) can be seen as having been produced by a Gaussian ISI channel, the decorrelation strategy is the best choice for linear detector for the fading channel. This is because the previous results of Section 2.4.5.1 showed the decorrelator to be a good choice for the Gaussian channel.

The organisation of this section is as follows:

In Section 5.5.4.1, the decorrelating detector for a finite message length will be derived, while the decorrelator for an infinite message length will be derived in Section 5.5.4.2. The operation of the decorrelator in this fading channel will be discussed in Section 5.5.4.3.

5.5.4.1. The Decorrelating Detector for a finite sequence length

The decorrelating strategy was discussed in Sections 2.4.5.1 and 4.4.3.1.1 where it was also shown that this detector is independent of the specular energies. By rearranging (5.57), making the data the subject of the formula, neglecting the noise contribution and taking the sign of this estimate then the decorrelating strategy can be defined as:

$$b = Sgn(H_l + H_l^{*})^{-1}(q_l + q_l^{*}) \quad \text{.....(5.59)}$$

Defining the variable $\bar{q}$ and $\bar{b}$ as:

$$q = E^{-\frac{1}{2}} q_f \quad \text{.....(5.60)}$$

$$\bar{b} = E^{-\frac{1}{2}} b \quad \text{.....(5.61)}$$

Making use of the definition of R_f in (5.49), $\bar{q}$ in (5.60) and $\bar{b}$ in (5.61), then (5.59) can be re-written as:

$$\dot{b} = Sgn(R_f + R_f^*)^{-1}(\dot{q} + \dot{q}^*) \quad \text{.....(5.62)}$$

For the matrix $R_f+R_f^*$ in (5.62) to be invertible, the requirement is that [97]:

$$\begin{bmatrix} A^{00} & A^{01} & A^{02} \\ A^{10} & A^{11} & A^{12} \\ A^{20} & A^{21} & A^{22} \end{bmatrix} > 0 \quad \text{.....(5.63)}$$

The proof for the invertibility of $R_f+R_f^*$ will not be undertaken here as it was proven in [96,97] that the requirement in (5.63) is met and that the matrix $R_f+R_f^*$ is invertible.

Using the method followed in Section 5.5.1 where the bit error rate of the conventional detector was derived, the probability of an error in detecting the (k,x)th user's bit by the decorrelator is derived to be:

$$P_k(x) = Q\left(\frac{1}{\sigma \sqrt{((H_f + H_f^*)^{-1})(x,x)_{kk}}} \right) \quad \text{.....(5.64)}$$

The asymptotic efficiency and near-far resistance of this decorrelating detector in the finite horizon case is given in (5.65), which is obtained using the results of (5.5), (2.26) and (5.40).

$$\bar{\eta}_k(x) = \eta_k(x) = \frac{1}{2((R_f + R_f^*)^{-1})(x,x)_{kk}} \quad \text{.....(5.65)}$$

It can be seen in (5.65) that the asymptotic efficiency and near-far resistance is independent of the specular energy. This is the highest achievable near-far resistance, since it is equal to the near-far resistance of the MLS detector that had been derived in (5.48). Hence, the decorrelator is near-far resistant and is suitable for use in the fading channel as the optimal linear detector.
The implementation of the decorrelator in (5.62) involves the computation of q_f given in (5.43) and the computation of the matrix inverse $(R_f+R_f^*)^{-1}$ defined in (5.49). The size of the matrix R_f is (2M+1)K, hence the size of the matrix $(R_f+R_f^*)$ to be inverted is also (2M+1)K. This is computationally impractical for large values of K and M.

5.5.4.2. Decorrelating detector for an infinite sequence length

In this section, the implementation of the decorrelator described by (5.62) will be considered as the sequence length $M \rightarrow \infty$. The discussion of the decorrelating detector in the infinite horizon case is almost identical to that for the finite horizon case, except that the z-transform notation is now required. Recall that some mathematical preliminaries were introduced with regards to the z-transform in (4.10), where the characterization of an infinite-dimensional block-toeplitz matrix in terms of its z-transform representation was considered.

The infinite horizon case is now assumed, with the further assumption that the specular component phases and fading variances of the users do not change over successive bit intervals. In accordance with the discussion in Section 4.4.3.1.3, the decorrelating detector of (5.62) can now be expressed as:

$$\bar{b}(z) = Sgn(R_f(z) + R_f^*(z^*))^{-1}(\bar{q}(z) + \bar{q}^*(z^*)) \quad \text{.....(5.66)}$$

where:

- $\bar{q}(z)$ is the vector z-transform of the sequence $\bar{q}(x)$

- $R_f(z)$ is the matrix z-transform representation of the infinite dimensional block toeplitz matrix R_f.

Using the definitions of R_f and $\bar{q}$ in (5.49) and (5.60) respectively, then (5.43) and (5.44) where q_f and H_f were related to the system parameters, can now be re-written in terms of the z-transform as:

$$\bar{q}(z) = \Theta(0)[y^0(z) - (A^{01}(z) + A^{21}(z))(\Sigma^{-2}(0) + A^{11}(z))^{-1} y^1(z) - (A^{02}(z) + A^{12}(z))(\Sigma^{-2}(0) + A^{22}(z))^{-1} y^2(z)] \quad \text{.....(5.67)}$$

$$R_f(z) = \Theta(0)\{A^{00}(z) - [(A^{01}(z) + A^{21}(z))(\Sigma^{-2}(0) + A^{11}(z))^{-1}(A^{10}(z) + A^{12}(z))] - [(A^{02}(z) + A^{12}(z))(\Sigma^{-2}(0) + A^{22}(z))^{-1}(A^{20}(z) + A^{21}(z))]\}\Theta^*(0) \quad \text{.....(5.68)}$$

Recall that in Section 3.7 combining technology was discussed where the microscopic diversity scheme was used for combining two or more Rayleigh signals which were received via independent fading paths received from two or more different antennas at the same base-station site. Hence, (5.67) represents the optimum multiuser diversity combiner as it combines the signals from the different paths in an optimal manner . This is a linear time invariant (LTI) filter for which a graphical representation is given in Figure 5.3. With reference to Figure 5.3, it can be seen that this LTI filter linearly combines the matched filter output sequences $y^0(x)$, $y^1(x)$ and $y^2(x)$ to produce $\bar{q}(x)$. It then retains only the real part of the output sequence to yield the vector sequence $\{\bar{q}(x) + \bar{q}^*(x)\}$, which has a z-transform representation of $\{\bar{q}(z) + \bar{q}^*(z^*)\}$.

The output of the diversity combiner of Figure 5.3 forms the input to the K input/ K output decorrelating filter for this fading channel. With reference to (5.66), it will be observed that the transfer function of this decorrelating filter is given by:

$$G(z) = (R_f(z) + R_f^*(z^*))^{-1} \quad \text{.....(5.69)}$$

By using the definition of R_f in (5.68), the decorrelating filter described by G(z) can be represented in a graphical format as shown in Figure 5.4. It will now be

proven that the output of the decorrelating filter is the sequence of estimates of the transmitted energy-bit vector.

The vector of sufficient statistics for the channel given by (5.57) is reproduced here for clarity, and is written in the z-domain as:

$$\begin{aligned} 2\Re(q_f) &= q_f(z) + q_f^*(z^*) \\ &= H_f(z)b(z) + n(z) + H_f^*(z^*)b(z) + n^*(z^*) \\ &= (H_f(z) + H_f^*(z^*))b(z) + n(z) + n^*(z^*) \end{aligned} \quad \text{.....(5.70)}$$

The definition of (5.49) states that:

$$R_f(z) = E^{-\frac{1}{2}} H_f(z) E^{-\frac{1}{2}} \quad \text{.....(5.71)}$$

From (5.71), the expression for $H_f(z)$ can be written as:

$$H_f(z) = E^{\frac{1}{2}} R_f(z) E^{\frac{1}{2}} \quad \text{.....(5.72)}$$

From (5.60), the expression for $\bar{q}$ is given by:

$$q(z) = E^{-\frac{1}{2}} q_f(z) \quad \text{.....(5.73)}$$

Rearranging the subject of (5.73), the following expression is obtained for $q_f(z)$:

$$q_f(z) = E^{\frac{1}{2}} q(z) \quad \text{.....(5.74)}$$

Solving for (5.70) results in:

$$q_f(z) + q_f^*(z^*) = H_f(z)b(z) + n(z) + H_f^*(z^*)b(z) + n^*(z^*)$$
$$= (H_f(z) + H_f^*(z^*))b(z) + n(z) + n^*(z^*) \quad \text{.....(5.75)}$$

(5.75) can be expanded by substituting (5.74) and (5.72) and can be expressed as:

$$E^{\frac{1}{2}} q(z) + E^{\frac{1}{2}} q^*(z^*) = (E^{\frac{1}{2}} R_f(z) E^{\frac{1}{2}} + E^{\frac{1}{2}} R_f^*(z^*) E^{\frac{1}{2}})b + n(z) + n^*(z^*) \quad \text{.....(5.76)}$$

By multiplying on both sides of the equality sign in (5.76) by $E^{-1/2}$, (5.76) can be simplified and rewritten as:

$$q(z) + q^*(z^*) = (R_f(z)E^{\frac{1}{2}} + R_f^*(z^*)E^{\frac{1}{2}})b + E^{-\frac{1}{2}} n(z) + E^{-\frac{1}{2}} n^*(z^*) \quad \text{.....(5.77)}$$

(5.77) can still be simplified further as:

$$q(z) + q^*(z^*) = (R_f(z) + R_f^*(z^*))E^{\frac{1}{2}} b + E^{-\frac{1}{2}} n(z) + E^{-\frac{1}{2}} n^*(z^*) \quad \text{.....(5.78)}$$

Defining the following:

$$w(x) = E^{\frac{1}{2}}(x, x)b(x) \quad \text{.....(5.79)}$$

$$w(z) = \sum_{x=-\infty}^{\infty} w(x) z^{-1} \quad \text{.....(5.80)}$$

$$n^{d^*}(z^*) = \sum_{x=-\infty}^{\infty} E^{-\frac{1}{2}}(x, x) n(x) z^{x-1} \quad \text{.....(5.81)}$$

$$n^d(z) = \sum_{x=-\infty}^{\infty} E^{-\frac{1}{2}}(x, x) n(x) z^{-1} \quad \text{.....(5.82)}$$

Substitution of (5.79)-(5.82) into (5.78) results in:

$$q(z) + \dot{q}^{*}(z^{*}) = (R_f(z) + R_f^{*}(z^{*}))w(z) + n^{d}(z) + n^{d^{*}}(z^{*}) \quad \text{.....(5.83)}$$

By rearranging (5.83), making the energy-data vector the subject of the formula, neglecting the noise contribution and taking the sign of this estimate, then the output of the decorrelator can be written as:

$$\dot{w}(z) = Sgn(R_f(z) + R_f^{*}(z^{*}))^{-1}(\bar{q}(z) + \bar{q}^{*}(z^{*}) \quad \text{.....(5.84)}$$

where:

- $\bar{w}(z)$ is an estimate of the transmitted energy-bit vector, w(z)

The data detection in (5.62) can be seen as a process that involves polarity detection at the output of the cascade of the optimum diversity combiner and the decorrelating filter of Figures 5.3 and 5.4, respectively.

The bit error-performance of the decorrelating detector in the infinite horizon case will now be described. Assuming that the specular phases are time invariant, the expression for the bit error probability of the (k,x)th user in the infinite horizon case is the limiting form of (5.64) and is given by:

$$P_k(x) = Q\left(\frac{\sqrt{E(x,x)_{kk}}}{\sigma \sqrt{\frac{1}{2\pi j} \oint ((R_f(z) + R_f^{*}(z^{*}))^{-1})_{kk} \frac{dz}{z}}} \right) \quad \text{.....(5.85)}$$

In contrast to (5.65), in the infinite horizon case, the near-far resistance of the decorrelator loses its bit-interval dependence and is specified by:

$$\dot{\eta}_k = \eta_k = \frac{1}{\frac{1}{\pi j}\oint((R_f(z) + R_f^{\dagger}(z^*))^{-1})_{kk}\frac{dz}{z}} \qquad \text{.....(5.86)}$$

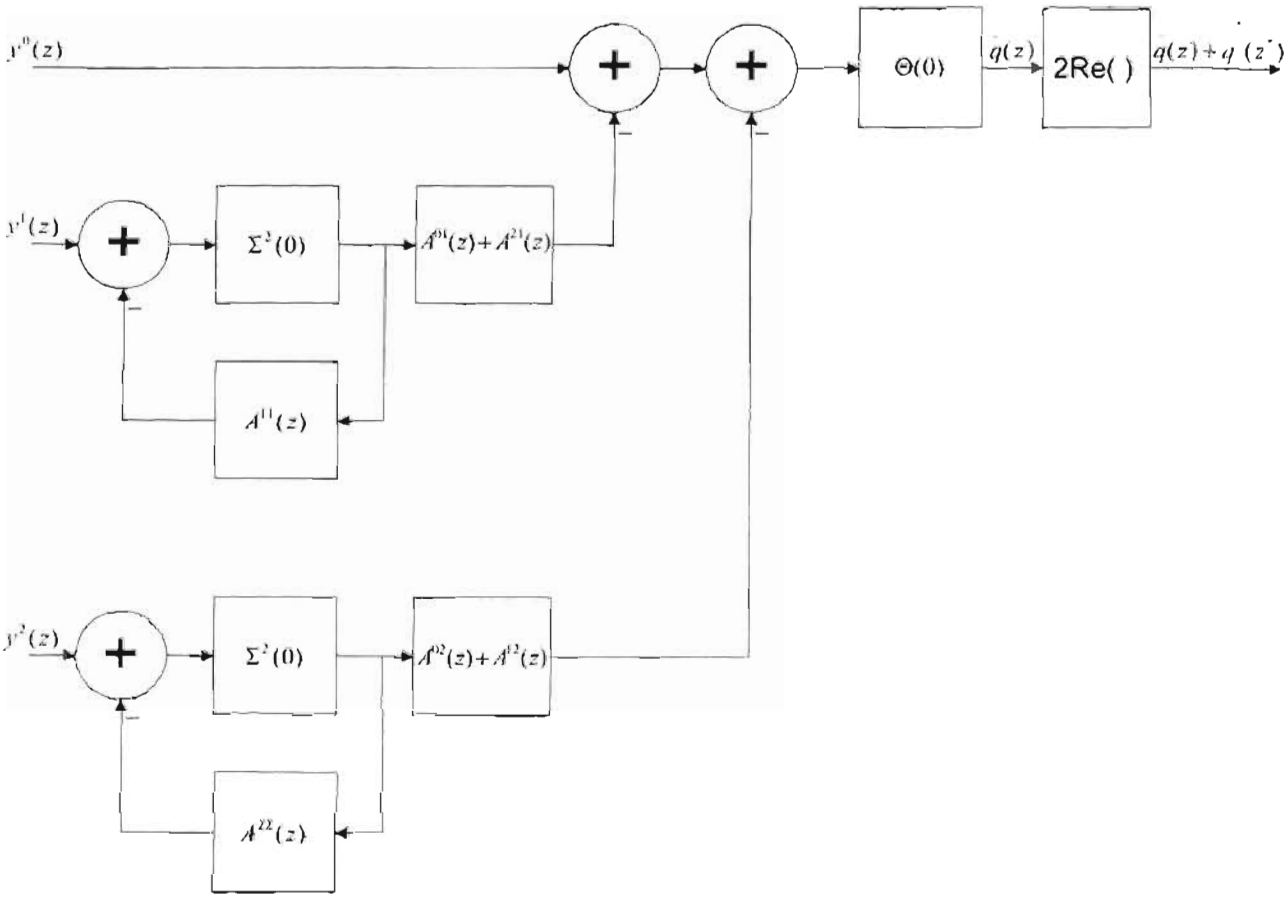

Figure 5.3.
The optimum multiuser diversity combiner

Figure 5.4.
The decorrelating filter

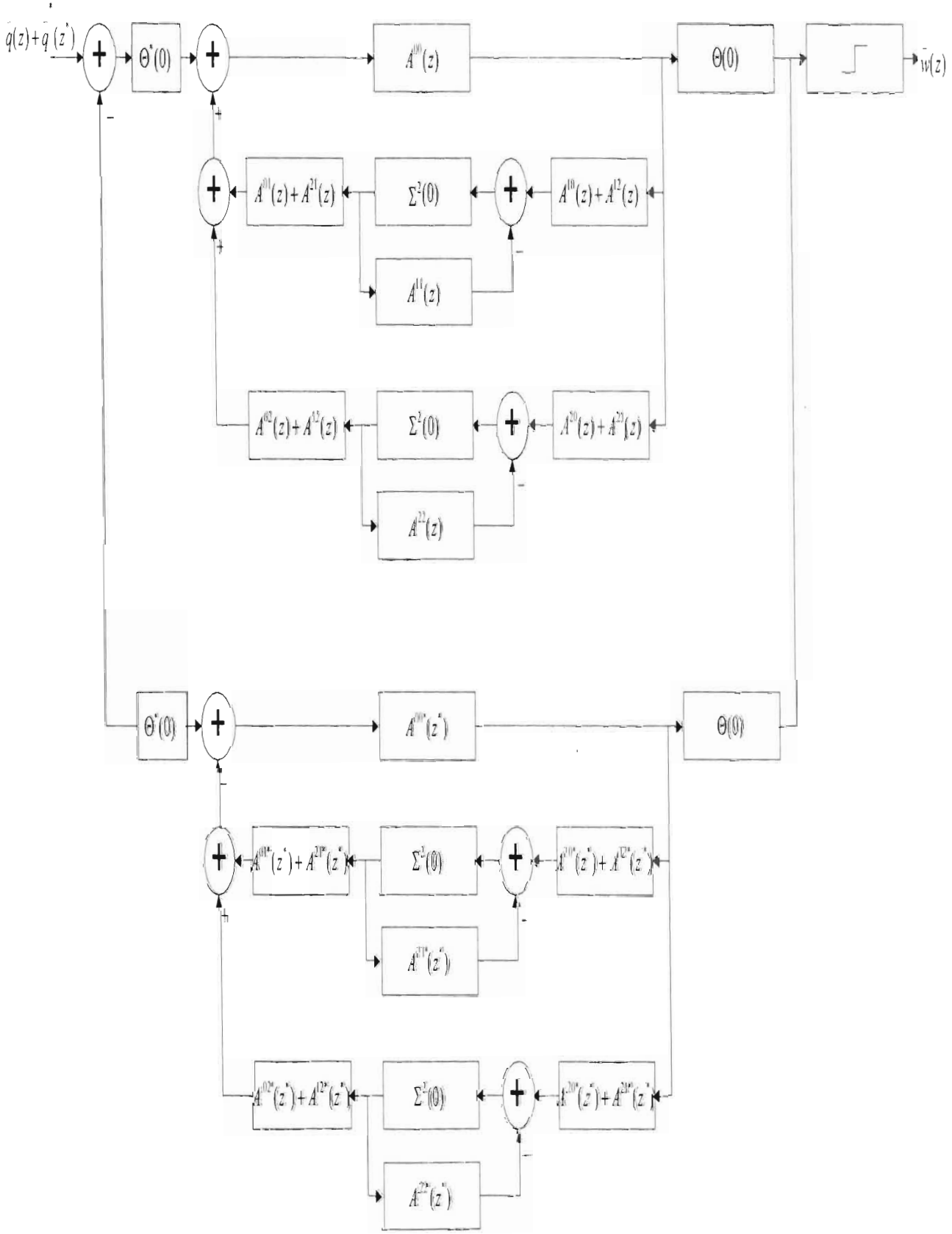

5.5.4.3. Operation of the diversity combiner and decorrelator

A discussion will be undertaken of the operation of the multiuser diversity combiner and decorrelating filter of Figures 5.3 and 5.4, respectively.

The inputs to the multiuser diversity combiner are the matched filter bank output vectors $y^0(z)$, $y^1(z)$ and $y^2(z)$. The multiuser diversity combiner has to be designed such that noise variance at the output of the decorrelating filter is minimized. With reference to Figure 5.3, it will be seen that the multiuser diversity combiner subtracts only as much of the fading as is beneficial to the overall detection process. When some of the users are heavily faded while the others are not, the diversity combiner subtracts mainly the fading associated with the former users. This is because the benefits of removing the light fading interference are outweighed by the loss incurred due to the increased noise variance at the output of the decorrelator. However, when all the users are heavily faded, the fading is subtracted off almost entirely. On the other hand, when none of the users are faded, the outputs $y^1(z)$ and $y^2(z)$ are blocked out by the diversity combiner, and only $y^0(z)$ is passed through. In that case, the output from the diversity combiner can be obtained from (5.67) by ignoring the contributions of the matched filter bank outputs $y^1(z)$ and $y^2(z)$. The result is:

$$q(z) = \Theta(0) y^0(z) \quad \text{.....(5.87)}$$

The vector of sufficient statistics for the channel can then be written as:

$$q(z) + q(z^*) = \Theta(0) y^0(z) + \Theta^*(0) y^{0*}(z^*) \quad \text{.....(5.88)}$$

In this scenario the decorrelating filter of Figure 5.4 will coincide with the decorrelator for the Gaussian channel as discussed in Section 2.4.5.1.

With regards to the decorrelating filter in Figure 5.4, it will be noticed that this decorrelator is built around the decorrelator for the Gaussian channel. Removing the feedback arms associated with the upper and lower main branches of Figure 5.3 results in the decorrelator for the Gaussian channel. The input to the decorrelator for the Gaussian channel is then given by (5.88), which is the vector of sufficient statistics for the Gaussian channel. (5.68) is then edited to remove the fading contributions and can be re-written as:

$$R_f(z) = \Theta(0)A^{00}(z)\Theta^{*}(0) \quad \text{.....(5.89)}$$

The estimated energy bit vector from the decorrelator for the Gaussian channel is obtained by substituting (5.88) and (5.89) into the definition of (5.84). Igoring the z-transforms, the result is:

$$\begin{aligned} \hat{w}(z) &= Sgn(R_f + R_f^{*})^{-1}(\hat{q} + \hat{q}^{*}) \\ &= Sgn(\Theta A^{00}\Theta^{*} + \Theta^{*}A^{00^{*}}\Theta)^{-1}(\Theta y^{0} + \Theta^{*}y^{0^{*}}) \end{aligned} \quad \text{.....(5.90)}$$

With reference to Figure 5.4, as the fading dominates the additive white Gaussian noise, the decorrelator approaches a limiting form where no use is made of the fading statistics. This situation corresponds to the scenario where the diversity combiner in Figure 5.3 will subtract off all the fading interference in $q^{0}(z)$.

It has been shown in Section 4.4.3.1.3 that in the infinite horizon case, the diversity combiner and decorrelating filter can be implemented as linear time invariant filters. The pictorial forms of Figures 5.3 and 5.4 are only given to illustrate the mechanism of diversity combining and decorrelation and not the actual implementation. This is because the impulse responses that specify these filters are noncausal [97]. The actual implementation is obtained by first computing the causal FIR approximations to the IIR diversity combining and decorrelating filters, which are parameterized by the phases, correlations and variance ratios. In practice, a single computation of the required filter coefficients is done using the phases, correlations and variance ratios in a single acquisition.

5.6. Conclusion

The purpose of this chapter was to derive multiuser receiver structures for the time-dispersive, three-path Rician fading CDMA channel. For each user, there exists a steady specular path and Rayleigh faded paths, all of them appearing asynchronously at the receiver. The received signal model is given in (5.4) for CDMA transmission through the three-path Rician fading channel.

The AME for the detectors for this fading channel was given in (5.5), where the fading and additive noise variance ratios are held constant, and the fading variances are assumed to be independent of the specular component energies. This definition of AME quantifies the effects of both the specular energies and the fading on the detector performance. The near-far resistance of the detectors in this fading channel is defined as a measure of the robustness of the detection scheme to variations in the specular energies of the users under the assumptions of constant fading to additive noise variance ratios.

It was shown that the time-dispersive Rician fading asynchronous CDMA channel bears an equivalence to an asynchronous Gaussian intersymbol interference (AGISI) channel. This equivalence result allows for the specification of a multiuser detector for the fading channel for each multiuser detector that is known for the Gaussian CDMA channel.

For the time-dispersive fading channel, the conventional detector definition leads to a sequence detector of the Viterbi type since it recognises and takes into account the dispersion of the user's signals. This detector is near-far limited when used over the multiuser channel because the presence of the interfering users is not taken into account. The MLS detector for the channel was obtained and it could not be practically implemented. Despite its complexity, the near-far resistance performance of the MLS detector was considered. This result served as a benchmark against which the suboptimal strategies for the fading channel were considered.

The decorrelating strategy was considered for the Rician channel that was computationally less expensive than the MLS detector yet achieves the same near-far resistance. The specification of this detector was induced from the equivalence between the fading and Gaussian CDMA channels. The decorrelators for both the finite and infinite sequence lengths were derived and their operation was explained. It was found that the asymptotic efficiency and near-far resistance of the decorrelator is independent of the specular energy, which made it suitable for use in the fading channel as the optimal linear detector.

Chapter 6: Decorrelating detection employing selection diversity

6.1. Introduction

A discussion was given on suboptimal multiuser demodulation in Section 5.5.4, where the decorrelator was found to be the best choice for linear detection over the fading channel. Furthermore, the optimum multiuser diversity combiner for the channel was discussed in Section 5.5.4.2, where the signals from the different paths were first combined in an optimal manner. The output of this multiuser diversity combiner then served as an input to the decorrelating detector.

In this chapter, selection diversity will be used by a path selector to first select the strongest path for the channel, which would then serve as the input to the decorrelating detector. Recall that an extensive discussion was given of diversity and combining techniques for fading channels in Sections 3.5 and 3.7, respectively.

The method to be followed here is in accordance with the theory of Section 3.7 where multiple resolvable paths can be used to accomplish selection diversity by selecting the path with the largest autocorrelation peak at the output of matched filters. For example, assume that for user k, the corresponding outputs of the matched filters $y_k^{(0)}$, $y_k^{(1)}$ and $y_k^{(2)}$ are such that:
$|y_k^{(0)}| > |y_k^{(1)}|$ and $|y_k^{(0)}| > |y_k^{(2)}|$, then in that case, selection diversity chooses the specular path as the strongest path for that user in that symbol interval.

To facilitate an easy explanation and derivation, the assumption made in this section will be that the sequence length is not too large. This assumption will then facilitate the use of the results for the decorrelators for finite and infinite sequence lengths of Sections 5.5.4.1 and 5.5.4.2, but without the requirement of the z-transform notation.

The organisation of this chapter is as follows:

The problem will be formulated in Section 6.2 where the system model will be described both pictorially and mathematically. The operation of the path selector and decorrelator will also be discussed in this section. A discussion will be given of the software algorithms used to obtain numerical results for the performance of the decorrelator, in Section 6.3. Both the analytical and simulation models will be discussed in this section. A numerical performance

evaluation will be undertaken in Section 6.4, with the aid of the results obtained using both the analytical and simulation software models of Section 6.3. Finally, a conclusion to this chapter will be provided in Section 6.5.

6.2. Problem formulation

In contrast to the method followed in Section 5.5.4, where MRC was used for the suboptimal multiuser detectors that were derived, the aim here is to use selection diversity instead. A description will be given of the selection diversity system in Section 6.2.1 and the selection diversity system will be mathematically described in Section 6.2.2. The operation of the path selector and decorrelator will be discussed in Section 6.2.3.

6.2.1. Selection diversity system description

Selection diversity can be incorporated into the receiver structure that has already been given for the optimum detector in Figure 5.2, but the data detection strategy is no longer the MLS detection rule, but corresponds to that for the decorrelating detector. With the incorporation of selection diversity into the receiver structure depicted in Figure 5.2, the resulting selection diversity system is obtained as shown in Figure 6.1.

The discussion of this selection diversity system is very similar to that given for the discussion of Figure 5.2, where the entire system model had been depicted for clarity. For the reception of the signal in Figure 6.2, carrier demodulation is first performed and the resulting lowpass input signal is r(t). The complex conjugate of this lowpass input signal is passed through the filter bank and the outputs are sampled at t=T to yield the normalised matched filter output vector q. For each user k, the outputs of the matched filter bank is q_k^0, q_k^1 and q_k^2. q_k^0 corresponds to the output of the filter bank for user k matched to the specular signal path. q_k^1 and q_k^2 correspond to the output of the filter banks for user k matched to the first and second fading paths, respectively. Selection diversity is next performed where the path with the largest autocorrelation peak is chosen at the output of the matched filter bank for each user.

Once the path selection has been accomplished for each user, linear transformations are then taken of these outputs to yield the vector q_s. The vector of sufficient statistics for the channel is now defined as $(q_s + q_s^*)$, which

is then passed to the decorrelating data detection algorithm to produce estimates of the transmitted data vector.

Figure 6.1.
System model with selection diversity

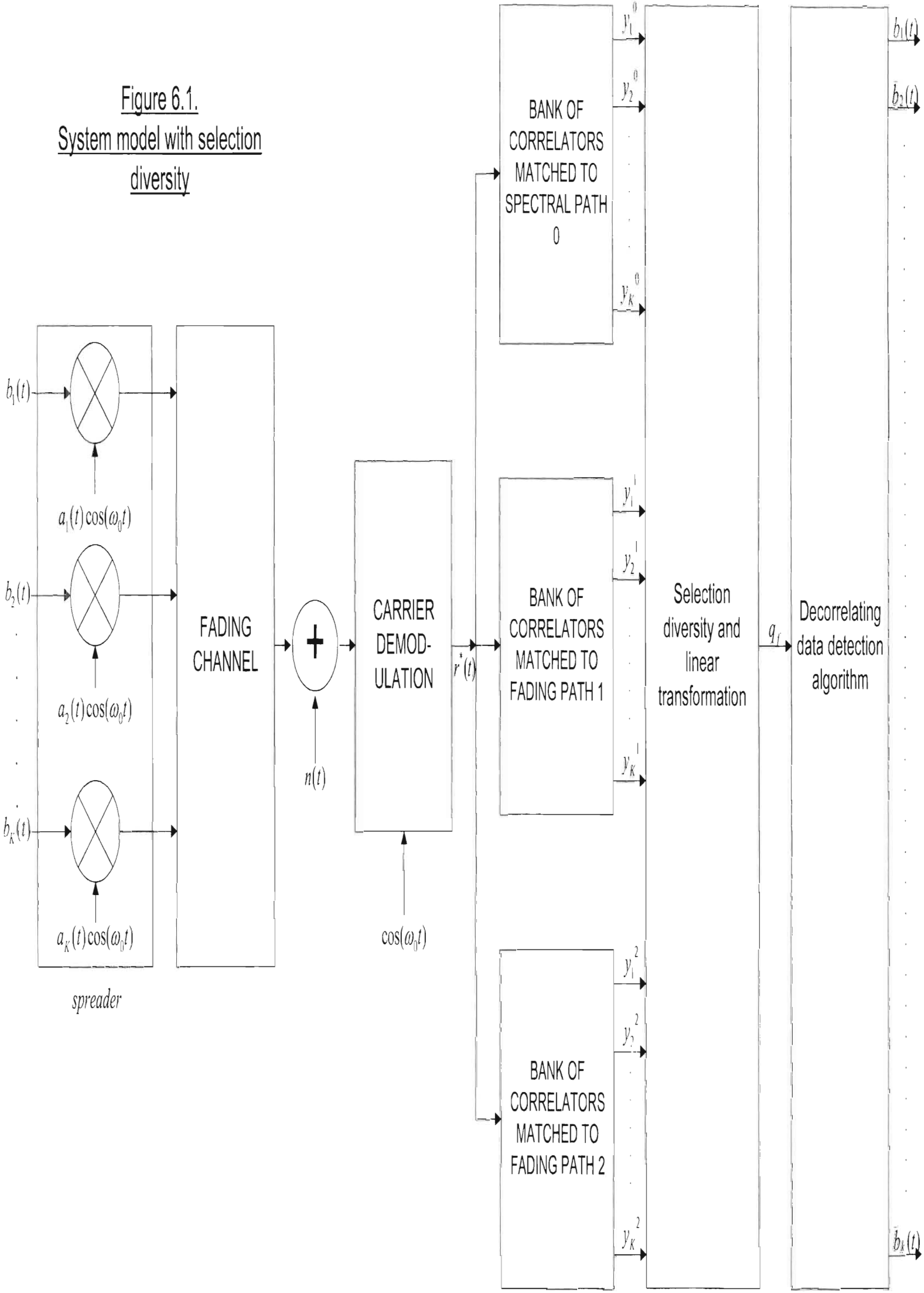

6.2.2. Mathematical Preliminaries

In order to incorporate selection diversity into the system model, as depicted in Figure 6.1, and to make use of the equations that have been derived in Chapter 5, it is useful to introduce the diagonal matrices C, D and G. The dimension of these matrices is [(2M+1)K x (2M+1)K]. These matrices will aid in the path selection process, where the C matrix will help in the selection of the specular path and the elimination of the other paths. The D matrix will aid in the selection of the first fading path and the elimination of the other paths. Similarly, the G matrix will help in the selection of the second fading path and the elimination of the other paths.

Assume for example that for a particular symbol interval, the output from the filter bank matched to the specular path of the first user is stronger than the corresponding outputs from the filter banks matched to the first and second fading paths of the same user. In that case, the correct operation of the path selection function would be to select the specular path while eliminating the other two paths. In order to meet this end, the first element in the C matrix corresponding to the first user, $C_{1,1}$, is set to 1. Furthermore, the first elements in the D and G matrices corresponding to the first user, $D_{1,1}$ and $G_{1,1}$, are each set to 0. This will ensure that when the output of the path selector is passed to the decorrelator, the contributions of the two fading paths have been removed. The same principle applies to all the other users in that particular symbol interval for the determination of their corresponding elements in the C, D and G matrices.

With the incorporation of selection diversity into the system model as depicted in Figure 6.1 and in accordance with the discussion given above, (5.43) and (5.44) can be modified accordingly. These equations can be modified and re-written as:

$$q_s = E^{\frac{1}{2}}\Theta[Cy^0 - D(A^{01} + A^{21})(\Sigma^{-2} + A^{11})^{-1}y^1 - G(A^{02} + A^{12})(\Sigma^{-2} + A^{22})^{-1}y^2 \quad \text{.....(6.1)}$$

$$H_s = E^{\frac{1}{2}}\Theta\{CA^{00} - D[(A^{01} + A^{21})(\Sigma^{-2} + A^{11})^{-1}(A^{10} + A^{12})] - G[(A^{02} + A^{12})(\Sigma^{-2} + A^{22})^{-1}(A^{20} + A^{21})]\}\Theta^* E^{\frac{1}{2}} \quad \text{.....(6.2)}$$

Note that all the equations with the subscript "f" in Chapter 5 where MRC was used, are now given the subscript "s" since selection diversity is being employed.

Depending on the elements of the C, D and G matrices in (6.1) and (6.2), these equations are only left with either the contributions of the specular path, fading path 1 or fading path 2. Hence, selection diversity has been successfully realised for the channel with the aid of the matrices C, D and G.

Note that the definition of $\bar{q}$ in (5.60) needs to be re-written as follows:

$$q_s = E^{-\frac{1}{2}} q_s \quad \text{.....(6.3)}$$

With the aid of (6.3), the definition of $\bar{q}$ in (5.67) can be modified and rewritten for the selection diversity receiver as:

$$q_s = \Theta\{Cv^0 - D(A^{01} + A^{21})(\Sigma^{-2} + A^{11})^{-1}v^1 - G(A^{02} + A^{12})(\Sigma^{-2} + A^{22})^{-1}v^2 \quad \text{.....(6.4)}$$

Also the definition of R_f in (5.49) has to now be re-written as:

$$R_s = E^{-\frac{1}{2}} H_s E^{-\frac{1}{2}} \quad \text{.....(6.5)}$$

With the aid of (6.5) the definition of R_f in (5.68) can be modified for the selection diversity receiver and re-written as follows:

$$R_s = \Theta\{CA^{00} - D[(A^{01} + A^{21})(\Sigma^{-2} + A^{11})^{-1}(A^{10} + A^{12})] - G[(A^{02} + A^{12})(\Sigma^{-2} + A^{22})^{-1}(A^{20} + A^{21})]\}\Theta' \quad \text{.....(6.6)}$$

Since (6.4) now represents selection diversity instead of MRC, its structure now represents that of the path selector. With the aid of (6.4), the graphical form of the path selector is obtained and depicted in Figure 6.2. The output of this path selector now serves as the input to the decorrelating detector, which is depicted in Figure 6.3.

Similar to the method followed in Section 5.5.4.2, it can be seen in (6.7) that the output of the decorrelating filter is the sequence of estimates $\bar{w}(x)$ of the transmitted energy-bit vector which is given by:

$$w = Sgn(R_{s} + R_{c}^{*})^{-1}(q_{c} + q_{s}^{*}) \quad \text{.....(6.7)}$$

The data detection in (6.7) can be seen as a process that involves polarity detection at the output of the cascade of the multiuser path selector of Figure 6.2 and the decorrelating filter of Figure 6.3.

The near-far resistance of this modified decorrelator is almost identical to (5.65). The asymptotic efficiency and near-far resistance of this decorrelating detector is independent of the specular energies and can be expressed as:

$$\bar{\eta}_{k}(x) = \eta_{k}(x) = \frac{1}{2((R_{c} + R_{c}^{*})^{-1})(x,x)_{k,k}} \quad \text{.....(6.8)}$$

The discussion and derivation of the bit error performance of this decorrelating detector will be postponed until Section 6.2.4.

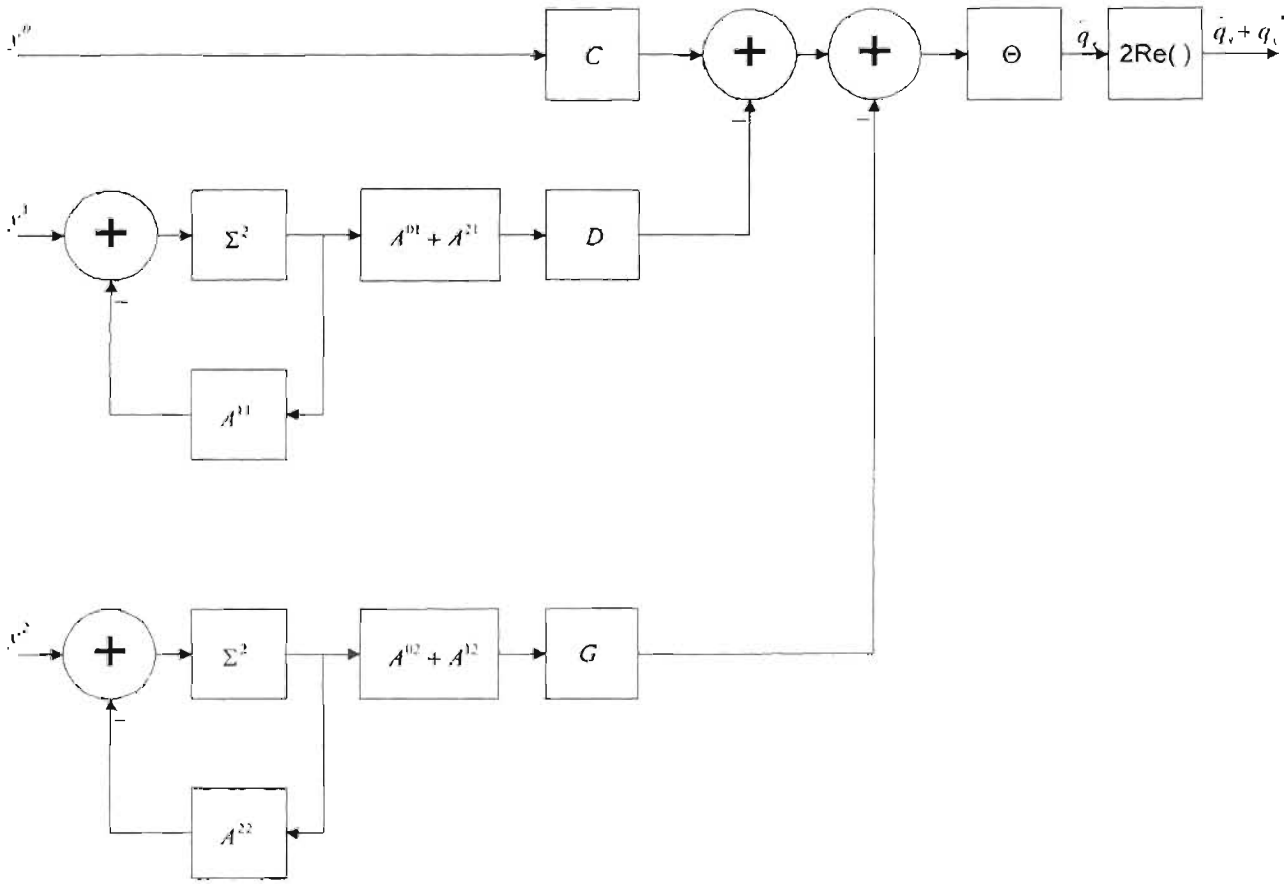

Figure 6.2
The multiuser path selector

Figure 6.3.
The Decorrelator

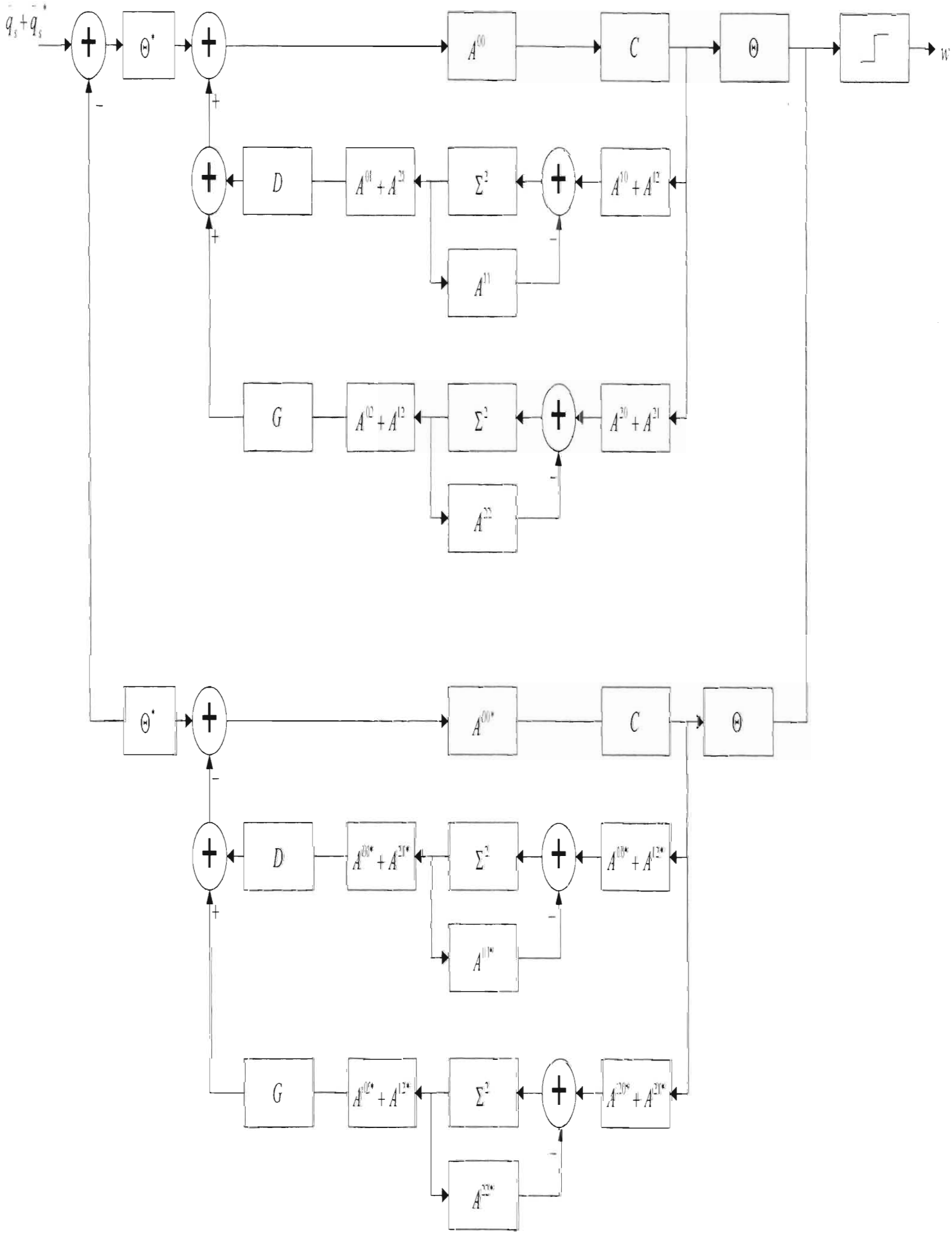

6.2.3. Operation of the multiuser path selector and decorrelator

Unlike the operation of the optimum multiuser diversity combiner of Figure 5.2, rather than combining the signals from the different paths, the multiuser path selector of Figure 6.2 selects only the strongest matched filter output for a user for that particular symbol interval. With reference to Figure 6.2, it can be seen that this multiuser path selector simply selects the matched filter output sequences $y^0(x)$, $y^1(x)$ or $y^2(x)$, to produce $\bar{q}_s(x)$. It then retains only the real part of this output sequence to yield the vector sequence $\{ \bar{q}_s(x) + \bar{q}_s^*(x)\}$. It is evident from Figure 6.2 that with the proper choice of the matrices C, D and G, when y^0 is the strongest output of the bank of matched filters, then the contributions of y^1 and y^2 are blocked out. In that case, the decorrelator of Figure 6.3 will coincide with the decorrelator for the Gaussian channel.

The matrices C, D and G can also be incorporated into the decorrelating structure of Figure 5.4, for the purposes of selection diversity, to result in the modified decorrelator of Figure 6.3, the inputs to which are the output of the path selector of Figure 6.2. It is evident from Figure 6.3 that in the case where y^0 is the strongest output of the bank of matched filters, then the feedback arms associated with the upper and lower branches of the decorrelator of Figure 6.3 are removed due to the respective elements of the D and G matrices being set to zero. This results in the decorrelator for the Gaussian channel, as discussed in Section 5.5.4.3.

6.2.4. Bit error rate computation

For each symbol interval, there are a number of combinations of the strongest paths for each of the k users. From this point forth, for the discussion that follows, a specific user, assumed to be user 1, is taken as the reference user and the bit error rate computation is carried out for this reference user.

But first, some definitions will need to be given in order to facilitate the computation of the bit error rate. Let $v_l^{(m)}$ be a vector which refers to the

different combinations of the strongest paths of all the users, excluding the reference user. Let the variable Σ_m refer to the number of combinations of these strongest signal paths of all the users, with the reference user being excluded. Let the variable m index that specific combination of signal paths of all the users, with the reference user excluded, for that specific symbol interval. Let the variable *l* refer to the strongest signal path of the reference user in that symbol interval, where the specular signal path is denoted as path 0, the first faded signal path as path 1 and the second faded signal path as path 2. Hence, *l* can take on values of 0, 1 and 2, corresponding to each of the three signal paths.

For example, for a specific symbol interval, assume that the strongest signal path for the reference user is its specular signal path, hence *l* is assigned the value of 0. For the purposes of the discussion, assume that there are three other users. Let the indexed value of m be 4, where for this value of m, the combinations of the other three user's signal paths are as follows:

The strongest signal path for user 2 is its path 1, while user 3's strongest signal path is its path 1 as well. However, for user 4, its strongest signal path is its path 0. Accordingly, the vector $v_l^{(m)}$ takes on the values of [1 1 0] where the first element in $v_l^{(m)}$ denotes the fact that the user 2's strongest signal path is its path 1, the second element denotes the fact that user 3's strongest signal path is its path 1 and the third element denotes the fact that user 4's strongest signal path is its path 0. The variable Σ_m equates to 3 as the number of combinations of $v_l^{(m)}$ is 3 ie. $v_l^{(m)}$ can either be [1 1 0], [1 0 1] or [0 1 1].

The bit error rate of this detector is conditioned on the vector $v_l^{(m)}$ and can be denoted as $P_e| v_l^{(m)}$. This conditional bit error performance of the decorrelator is almost identical to (5.64) and can be written as:

$$P_e\left|v_l^{(m)}(x) = Q\left(\frac{1}{\sigma\sqrt{((H_s + H_s^{\cdot})^{-1})(x,x)_{k,k}}}\right)\right. \quad \text{.....(6.9)}$$

Note that (6.9) can be simplified and written as follows:

$$P_e\left|v_l^{(m)}(x) = Q\left(\sqrt{\frac{2\Re(H_s)}{\sigma^2}}\right)\right. \quad \text{.....(6.10)}$$

From [96, 97], the bit error rate for the reference user has been defined as:

$$\text{Probability\_of\_error} = \sum_{l=0}^{2}\sum_{k=1}^{K} P_e\left|v_l^{(k)} p(v_l^{(k)})\right. \quad \text{.....(6.11)}$$

where:

- there are a total of K users
- *l* represents the strongest signal path for the reference user

In accordance with the discussion given thusfar, (6.11) can be simplified and re-written as:

$$\text{Probability\_of\_error} = \frac{\sum_{l=0}^{2}\sum_{m=1}^{m_{max}} P_e\left|v_l^{(m)} * \Sigma_m\right.}{3^K} \quad \text{.....(6.12)}$$

where:

- K is the total number of users
- M indexes the different $v_l^{(m)}$ vectors and can range from 1 to m_{max}

Substitution of (6.10) into (6.12) for the definition of $P_e|\, v_l^{(m)}$ results in:

$$Probability\_of\_error = \frac{\sum_{l=0}^{2}\sum_{m=1}^{m_{max}} Q\left(\frac{2\Re(H_s)}{\sigma^2}\right) * \Sigma_m}{3^K} \qquad \text{.....(6.13)}$$

6.3. Numerical and simulation models

The aim of the numerical exercise is to analytically determine the bit-error rate for a particular user. This analytical value of bit-error rate is to be compared against that produced by the actual simulation model, which will be developed for the users under different fading conditions, specular energies and delays. Ideally, the bit-error rate value returned by the simulation model software should be the same as that produced by the analytical model.

The organisation of this section is as follows:

In Section 6.3.1, some preliminary information will be given together with the assumptions that have been made in developing both the analytical and simulation models. The analytical model will be discussed in Section 6.3.2 while the simulation model will be discussed in Section 6.3.3.

6.3.1. Preliminaries

User 1 is taken as the reference user and all the other delays are with respect to the delay of the specular path signal of this user. It is further assumed that there are four users so that the matrices to be used in the software algorithms will not be too large and can be computed relatively easily. However the same qualitative result would be achieved by using only four users, as opposed to considering more users.

BPSK signaling is used, where the data bits for the users take on values of ±1. Gold sequences of length 31 are chosen for the code waveforms of the four users. The following codes are assigned to the respective user:

a_1=[-1,-1,1,-1,-1,-1,-1,1,1,1,1,1,-1,1,-1,1,-1,-1,-1,1,1,-1,1,-1,-1,1,-1,-1,1,1,1,1]
a_2=[-1,-1,-1,-1,1,1,-1,-1,-1,1,1,1,-1,1,1,-1,1,1,-1,-1,1,-1,1,1,1,1,-1,-1,1,1,-1,1,1,-1]
a_3=[1,-1,-1,1,1,1,1,-1,1,1,1,-1,-1,-1,-1,-1,1,1,-1,1,-1,1,-1,-1,1,-1,-1,1,-1,1,1,1,-1]
a_4=[-1,-1,-1,-1,-1,-1,1,1,1,1,-1,1,-1,-1,1,-1,-1,-1,-1,1,-1,-1,1,1,1,1,1,1,1,1,1,-1,1,-1]

Furthermore, it is assumed that the specular energies, phases and variance ratios are time invariant over that particular symbol interval, denoted as the x^{th} symbol interval. The assumption is also made that the phases of the users is zero, so there is no requirement for the complex operation in the 6.2. At all times it is assumed that the noise is Gaussian with zero-mean and variance σ^2.

Similar to (5.53), the vectors of sufficient statistics for the selection diversity case, given in (6.1) can be written as:

$$q_s = H_s b + n \quad \text{.....(6.14)}$$

Substitution of H_s defined in (6.2) into (6.14), the system model in accordance with the assumptions made above, can be given for the synchronous case as (6.15). The output data estimates from the decorrelating detector is then obtained using (6.7).

$$
\begin{bmatrix} q_{1,x} \\ q_{2,x} \\ q_{3,x} \\ q_{4,x} \end{bmatrix} = \begin{bmatrix} E_{1,x} & 0 & 0 & 0 \\ 0 & E_{2,x} & 0 & 0 \\ 0 & 0 & E_{3,x} & 0 \\ 0 & 0 & 0 & E_{4,x} \end{bmatrix}^{\frac{1}{2}} \begin{bmatrix} \Theta_{1,x} & 0 & 0 & 0 \\ 0 & \Theta_{2,x} & 0 & 0 \\ 0 & 0 & \Theta_{3,x} & 0 \\ 0 & 0 & 0 & \Theta_{4,x} \end{bmatrix} \left\{ \left\{ \begin{bmatrix} C_{1,x} & 0 & 0 & 0 \\ 0 & C_{2,x} & 0 & 0 \\ 0 & 0 & C_{3,x} & 0 \\ 0 & 0 & 0 & C_{4,x} \end{bmatrix} \begin{bmatrix} A_{1,1,x}^{00} & A_{1,2,x}^{00} & A_{1,3,x}^{00} & A_{1,4,x}^{00} \\ A_{2,1,x}^{00} & A_{2,2,x}^{00} & A_{2,3,x}^{00} & A_{2,4,x}^{00} \\ A_{3,1,x}^{00} & A_{3,2,x}^{00} & A_{3,3,x}^{00} & A_{3,4,x}^{00} \\ A_{4,1,x}^{00} & A_{4,2,x}^{00} & A_{4,3,x}^{00} & A_{4,4,x}^{00} \end{bmatrix} - \left\{ \begin{bmatrix} D_{1,x} & 0 & 0 & 0 \\ 0 & D_{2,x} & 0 & 0 \\ 0 & 0 & D_{3,x} & 0 \\ 0 & 0 & 0 & D_{4,x} \end{bmatrix} \begin{bmatrix} A_{1,1,x}^{01} & A_{1,2,x}^{01} & A_{1,3,x}^{01} & A_{1,4,x}^{01} \\ A_{2,1,x}^{01} & A_{2,2,x}^{01} & A_{2,3,x}^{01} & A_{2,4,x}^{01} \\ A_{3,1,x}^{01} & A_{3,2,x}^{01} & A_{3,3,x}^{01} & A_{3,4,x}^{01} \\ A_{4,1,x}^{01} & A_{4,2,x}^{01} & A_{4,3,x}^{01} & A_{4,4,x}^{01} \end{bmatrix} \right. \right.
$$

$$
\left. \left. + \begin{bmatrix} A_{1,1,x}^{21} & A_{1,2,x}^{21} & A_{1,3,x}^{21} & A_{1,4,x}^{21} \\ A_{2,1,x}^{21} & A_{2,2,x}^{21} & A_{2,3,x}^{21} & A_{2,4,x}^{21} \\ A_{3,1,x}^{21} & A_{3,2,x}^{21} & A_{3,3,x}^{21} & A_{3,4,x}^{21} \\ A_{4,1,x}^{21} & A_{4,2,x}^{21} & A_{4,3,x}^{21} & A_{4,4,x}^{21} \end{bmatrix} \right\} \left\{ \begin{bmatrix} \Sigma_{1,x} & 0 & 0 & 0 \\ 0 & \Sigma_{2,x} & 0 & 0 \\ 0 & 0 & \Sigma_{3,x} & 0 \\ 0 & 0 & 0 & \Sigma_{4,x} \end{bmatrix}^{-2} + \begin{bmatrix} A_{1,1,x}^{11} & A_{1,2,x}^{11} & A_{1,3,x}^{11} & A_{1,4,x}^{11} \\ A_{2,1,x}^{11} & A_{2,2,x}^{11} & A_{2,3,x}^{11} & A_{2,4,x}^{11} \\ A_{3,1,x}^{11} & A_{3,2,x}^{11} & A_{3,3,x}^{11} & A_{3,4,x}^{11} \\ A_{4,1,x}^{11} & A_{4,2,x}^{11} & A_{4,3,x}^{11} & A_{4,4,x}^{11} \end{bmatrix}^{-1} \left\{ \begin{bmatrix} A_{1,1,x}^{10} & A_{1,2,x}^{10} & A_{1,3,x}^{10} & A_{1,4,x}^{10} \\ A_{2,1,x}^{10} & A_{2,2,x}^{10} & A_{2,3,x}^{10} & A_{2,4,x}^{10} \\ A_{3,1,x}^{10} & A_{3,2,x}^{10} & A_{3,3,x}^{10} & A_{3,4,x}^{10} \\ A_{4,1,x}^{10} & A_{4,2,x}^{10} & A_{4,3,x}^{10} & A_{4,4,x}^{10} \end{bmatrix} + \begin{bmatrix} A_{1,1,x}^{12} & A_{1,2,x}^{12} & A_{1,3,x}^{12} & A_{1,4,x}^{12} \\ A_{2,1,x}^{12} & A_{2,2,x}^{12} & A_{2,3,x}^{12} & A_{2,4,x}^{12} \\ A_{3,1,x}^{12} & A_{3,2,x}^{12} & A_{3,3,x}^{12} & A_{3,4,x}^{12} \\ A_{4,1,x}^{12} & A_{4,2,x}^{12} & A_{4,3,x}^{12} & A_{4,4,x}^{12} \end{bmatrix} \right\} \right\}
$$

$$
- \left\{ \begin{bmatrix} G_{1,x} & 0 & 0 & 0 \\ 0 & G_{2,x} & 0 & 0 \\ 0 & 0 & G_{3,x} & 0 \\ 0 & 0 & 0 & G_{4,x} \end{bmatrix} \left\{ \begin{bmatrix} A_{1,1,x}^{02} & A_{1,2,x}^{02} & A_{1,3,x}^{02} & A_{1,4,x}^{02} \\ A_{2,1,x}^{02} & A_{2,2,x}^{02} & A_{2,3,x}^{02} & A_{2,4,x}^{02} \\ A_{3,1,x}^{02} & A_{3,2,x}^{02} & A_{3,3,x}^{02} & A_{3,4,x}^{02} \\ A_{4,1,x}^{02} & A_{4,2,x}^{02} & A_{4,3,x}^{02} & A_{4,4,x}^{02} \end{bmatrix} + \begin{bmatrix} A_{1,1,x}^{12} & A_{1,2,x}^{12} & A_{1,3,x}^{12} & A_{1,4,x}^{12} \\ A_{2,1,x}^{12} & A_{2,2,x}^{12} & A_{2,3,x}^{12} & A_{2,4,x}^{12} \\ A_{3,1,x}^{12} & A_{3,2,x}^{12} & A_{3,3,x}^{12} & A_{3,4,x}^{12} \\ A_{4,1,x}^{12} & A_{4,2,x}^{12} & A_{4,3,x}^{12} & A_{4,4,x}^{12} \end{bmatrix} \left\{ \begin{bmatrix} \Sigma_{1,x} & 0 & 0 & 0 \\ 0 & \Sigma_{2,x} & 0 & 0 \\ 0 & 0 & \Sigma_{3,x} & 0 \\ 0 & 0 & 0 & \Sigma_{4,x} \end{bmatrix}^{-2} + \begin{bmatrix} A_{1,1,x}^{22} & A_{1,2,x}^{22} & A_{1,3,x}^{22} & A_{1,4,x}^{22} \\ A_{2,1,x}^{22} & A_{2,2,x}^{22} & A_{2,3,x}^{22} & A_{2,4,x}^{22} \\ A_{3,1,x}^{22} & A_{3,2,x}^{22} & A_{3,3,x}^{22} & A_{3,4,x}^{22} \\ A_{4,1,x}^{22} & A_{4,2,x}^{22} & A_{4,3,x}^{22} & A_{4,4,x}^{22} \end{bmatrix}^{-1} \right\} \right.
$$

$$
\left. \left\{ \begin{bmatrix} A_{1,1,x}^{20} & A_{1,2,x}^{20} & A_{1,3,x}^{20} & A_{1,4,x}^{20} \\ A_{2,1,x}^{20} & A_{2,2,x}^{20} & A_{2,3,x}^{20} & A_{2,4,x}^{20} \\ A_{3,1,x}^{20} & A_{3,2,x}^{20} & A_{3,3,x}^{20} & A_{3,4,x}^{20} \\ A_{4,1,x}^{20} & A_{4,2,x}^{20} & A_{4,3,x}^{20} & A_{4,4,x}^{20} \end{bmatrix} + \begin{bmatrix} A_{1,1,x}^{21} & A_{1,2,x}^{21} & A_{1,3,x}^{21} & A_{1,4,x}^{21} \\ A_{2,1,x}^{21} & A_{2,2,x}^{21} & A_{2,3,x}^{21} & A_{2,4,x}^{21} \\ A_{3,1,x}^{21} & A_{3,2,x}^{21} & A_{3,3,x}^{21} & A_{3,4,x}^{21} \\ A_{4,1,x}^{21} & A_{4,2,x}^{21} & A_{4,3,x}^{21} & A_{4,4,x}^{21} \end{bmatrix} \right\} \begin{bmatrix} \Theta_{1,x} & 0 & 0 & 0 \\ 0 & \Theta_{2,x} & 0 & 0 \\ 0 & 0 & \Theta_{3,x} & 0 \\ 0 & 0 & 0 & \Theta_{4,x} \end{bmatrix}^{*} \begin{bmatrix} E_{1,x} & 0 & 0 & 0 \\ 0 & E_{2,x} & 0 & 0 \\ 0 & 0 & E_{3,x} & 0 \\ 0 & 0 & 0 & E_{4,x} \end{bmatrix}^{\frac{1}{2}} \right) \begin{bmatrix} b_{1,x} \\ b_{2,x} \\ b_{3,x} \\ b_{4,x} \end{bmatrix} + \begin{bmatrix} n_{1,x} \\ n_{2,x} \\ n_{3,x} \\ n_{4,x} \end{bmatrix} \quad \text{.....(6.15)}
$$

6.3.2. The analytical model

The aim of the analytical model is to analytically obtain the bit error rate of the reference user 1, using (6.13). An attempt will be made in this section to simplify the expression in (6.13) and to obtain all the terms in this equation so that it can be solved analytically using mathematical software routines.

As discussed in Section 6.2.1, for each symbol interval, there are a number of combinations of the strongest paths for each of the four users. Recalling the discussion in Sections 6.2.2 and 6.2.4, the combinations of strongest paths for the four users can be tabulated as in Table 2.

		$v_l^{(m)}$			
Strongest path for user 1 where ($l \in 0,1,2$)	**Indexed value of m**	strongest path for user 2	strongest path for user 3	strongest path for user 4	PATH_VARIETY_VALUE *(no of combinations of $v_l^{(m)}$)*
1	1	0	0	0	1
1	2	1	0	0	3
1	3	2	0	0	3
1	4	1	1	0	3
1	5	2	1	0	6
1	6	2	2	0	3
1	7	1	1	1	1
1	8	2	1	1	3
1	9	2	2	1	3
1	10	2	2	2	1
					TOTAL = 27

Table 2
Combinations of the strongest paths for the different users for a particular symbol interval

As can be seen from Table 2, for a specific value of l for the reference user 1, the total number of combinations of the other users' strongest paths for that symbol interval is 27. For all the three values that l can assume, in total the number of combinations of signal paths for any symbol interval is obtained by multiplying 27 by 3, with the result being 81.

The probability of bit error for any single user was given by (6.13). From the information from Table 2, the value of m_{max} in (6.13) is 10. As there are 4 users in total, the total number of strongest path combinations from the previous discussion is 81. Using this information, the solution in (6.13) can be simplified and rewritten as:

$$Probability\_of\_error = \frac{\sum_{l=0}^{2}\sum_{m=1}^{10} Q\left(\frac{2\Re(H_s)}{\sigma^2}\right) * \Sigma_m}{81} \qquad \text{.....(6.16)}$$

From (6.16), it can be seen that the probability of error is found for the reference user for all the 81 combinations of the strongest signal paths.

Corresponding to the combination of the user's strongest paths during that symbol interval, in accordance with the discussion in Section 6.2.2, the elements of the C, D and G matrices are chosen accordingly. For example, assume that the specular signal path is the strongest for users 1 and 4 during that symbol interval. Assume also that the second fading path signal is the strongest for user 2 and first fading path signal is the strongest for user 3. Hence, l=0 and $v_l^{(m)}$ = [2 1 0] which corresponds to the case of m=5 in Table 2.

Hence, $C_{l,m} = C_{0.5}$ and its elements are given by:

$$C_{0.5} = \begin{bmatrix} 1 & 0 & 0 & 0 \\ 0 & 0 & 0 & 0 \\ 0 & 0 & 0 & 0 \\ 0 & 0 & 0 & 1 \end{bmatrix}$$

Likewise, $D_{l,m} = D_{0.5}$ and its elements are given by:

$$D_{0.5} = \begin{bmatrix} 0 & 0 & 0 & 0 \\ 0 & 0 & 0 & 0 \\ 0 & 0 & 1 & 0 \\ 0 & 0 & 0 & 0 \end{bmatrix}$$

Finally, $G_{l,m} = G_{0.5}$ and its elements are given by:

$$G_{0.5} = \begin{bmatrix} 0 & 0 & 0 & 0 \\ 0 & 1 & 0 & 0 \\ 0 & 0 & 0 & 0 \\ 0 & 0 & 0 & 0 \end{bmatrix}$$

From the definition in (5.9), the variable r was defined as the ratio of fading to additive noise variances. Note that for even, light fading, the value of r is taken to be 1. Hence, the $\sum$ matrix in (6.15) evaluates to be a unit matrix.

The signal-to-noise ratio (SNR) is given by the ratio of the user's energy to additive noise variance. For unit variance Gaussian noise, the SNR is simply the user's energy in decibels (dB's).

Assume for example that the noise has unit variance and that the SNR of the reference user 1 is 6 dB's. In that case, the energy of user 1 in the x^{th} bit interval is solved from:

$$10\log_{10} E_{1,x} = 6$$

$$Hence,\ E_{1,x} = 10^{\frac{6}{10}} = 4\ watts$$

Hence, the first element of the E matrix in (6.15) is set to 4. The energies of the other three users are obtained in a similar manner, and these values are inserted into the respective elements of the E matrix in (6.15).

All delays are with respect to the delay of the specular signal path of the first user, which is taken to be zero. With the assumption that the phase difference is zero between all the other signals relative to the specular path signal of the first user, from (5.8) the Θ matrix evaluates to be a unity matrix in (6.15).

It is now possible to solve for H_s that had been defined in (6.2), from the system model in (6.15). The value of the H_s matrix can then be substituted into the expression for the bit error rate, given in (6.16).

Note that the standard definition of the Q function was given in (2.25), in terms of the complementary error function. For completeness, the Q function definition of (2.25) can be rewritten as:

$$Q(d) = \frac{1}{2} erfc\left\{\frac{d}{\sqrt{2}}\right\} \qquad \text{.....(6.17)}$$

where :

- erfc is the complementary error function

Substitution of (6.17) into (6.16), allows the expression for the bit error rate to be rewritten as:

$$Probability\_of\_error = \frac{\sum_{l=0}^{2}\sum_{m=1}^{10}(\frac{1}{2}erfc(\sqrt{H_x}))*\Sigma_m}{81} \quad \text{.....(6.18)}$$

The analytical model flowchart is given in **Appendix 4**, as Figure A4.1, along with all the main software subroutines. The aim of the analytical model is to calculate the bit error rate using the definition in (6.18).

The software for the analytical model was written in the C^{++} programming language and the routines for vector and matrix definitions, complementary error function, matrix inversion, etc. are not discussed here and may be found in any books on numerical recipes for mathematical functions.

To test that the analytical model software routines were operational, it was necessary to set the contributions of the fading paths to zero in order to check if similar results were obtained as for the ideal BPSK case. For the ideal BPSK case, the probability of bit error for the kth user in the xth symbol interval is obtained from [6]:

$$P_e(BPSK) = \frac{1}{2}erfc\left\{\sqrt{\frac{E_k}{2\sigma^2}}\right\} \quad \text{.....(6.19)}$$

where:

- As before, E_k is the energy of kth user's signal
- σ^2 is the noise variance

In the analytical model, in order to negate the contributions from the fading paths in the determination of H_s, the fading variance is set to zero. In so doing, the Σ matrix in (6.2) and (6.15) evaluates to be a zero matrix. For

identical SNR's, the probability of bit error for both the ideal BPSK case and from the analytical model were obtained and compared. The results of the comparison are shown in Table 3.

SNR (dB's)	P_e (BPSK)	P_e (analytical model)
0	0.1535	0.158655
3	0.0785	0.078650
6	0.02385	0.022750
7,5	0.00865	0.007153
9	0.00219	0.002339
10	0.00063	0.000783
11	0.00023	0.000266

Table 3
Probability of error for BPSK in AWGN, and the analytical model

As can be seen from Table 3, the results produced by the analytical model when the effect of fading is removed, produces bit error rate results similar to that of the ideal BPSK case. Hence, this confirms that the analytical model was working correctly.

6.3.3. The simulation model

The aim of the simulation model is to transmit a known data sequence through the channel, and then to try and demodulate it. The composite transmitted signal for each user is generated by the software, and the detector of Figure 6.3 is tested in software to see if it can demodulate the transmitted data bits correctly. The demodulation of the data sequence is obtained by using the system model of (6.15) and the result of (6.7).

For a specific value of SNR, a total of 1 million simulations were performed. The data bits were randomly generated by a random number generator with values of ±1 for BPSK signaling. The entire flowchart for the simulation model is depicted in **Appendix 4**, as Figure A4.2. The routines for the generation of Rayleigh and Gaussian generated variables are not given and can be found in any books with mathematical software subroutines.

Assumptions made in the simulation model are that the noise is zero mean with variance σ^2, and there are four users with their spreading codes given in Section 6.3.2. A further assumption is that the phase difference is zero between all the other signals relative to the specular signal path of the first user. This alleviates the need for any complex conjugate calculations in the system model of (6.15). As stated previously, all delays are with respect to the delay of the specular signal of the first user, which is taken to be zero. Furthermore, the assumption is that the specular energies, phases and variance ratios are time invariant over a bit interval.

In the simulation model, for each bit that is incorrectly demodulated, an error counter is incremented. Once 1 million simulations have been done for that particular value of SNR, the value of the error counter is divided by a million to determine the bit error rate corresponding to that SNR. A total of twenty-four different SNR cases are considered in the simulation software. Once all twenty-four SNR cases have been completed, the execution of the software is complete. It must be noted that the simulations are conducted for various values of fading to additive noise variance ratios and user delays.

6.4. Performance Evaluation Results

User 1 was chosen as the reference user, and its bit error rate was determined via simulation. These values of bit error rate were then plotted graphically. Similar conditions were set in the analytical model as in the simulation model in respect of delays, SNR's and fading parameters to check if both models produced similar if not identical results. An attempt was also made to check if the decorrelator for the fading channel was near far resistant and thereafter to determine its asymptotic efficiency.

In the first instance, an attempt had been made to obtain bit error rate results similar to that for the BPSK case, from the simulation model. In order to achieve this, the synchronous case was used by setting all delays to zero, and the fading variances were also set to zero so that the $\sum$ matrix would evaluate to a zero matrix. This was to get rid of the contributions of the two fading paths and only to use the contribution of the specular path.

In Table 4 and Figure 6.4, the results of the bit error rate for the simulation model are shown first in a tabular form and then graphically, based on the above information. These results were compared to those of the ideal BPSK case in [6] and other references, and they were found to be very similar. The bit error rate results of Figure 6.4 will serve as a benchmark for all the other simulation results in this section.

SNR (dB's)	P_e
0	0.1535
3	0.07865
3.5	0.06724
4	0.05656
4.5	0.04655
5	0.03773
5.5	0.02977
6	0.02385
6.5	0.01725
7	0.01267
7.5	0.00865
8	0.006
8.5	0.0039
9	0.00219
9.5	0.00142
10	0.00063
10.5	0.00041
11	0.00023
11.5	0.000085
12	0.000034
12.5	0.000012
13	0.000004
13.5	0.000003
14	0.000002

Table 4
Tabulated results for bit error rate for the BPSK in AWGN case

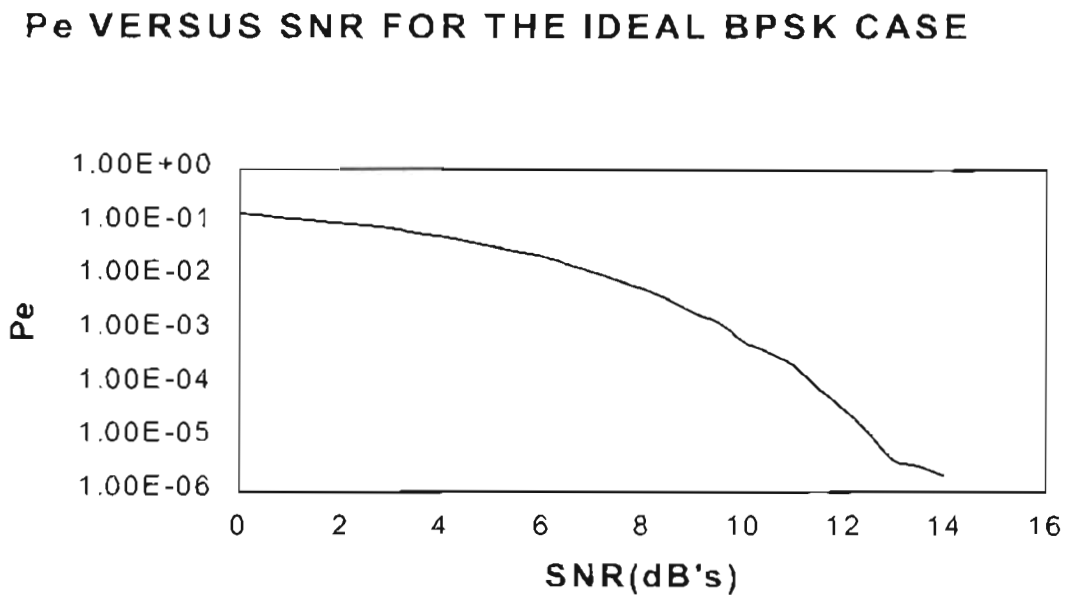

Figure 6.4
Simulation results for bit error rate for the BPSK in AWGN case

The performance measure of asymptotic efficiency will be considered for the selection diversity decorrelator of Figure 6.3. Its bit error rate will also be illustrated which will make it possible to assess its relative performance over a large set of operating conditions.

In the following simulation results, various conditions were set in the simulation software in order to determine their effect on the bit error rate result. As a benchmark for all the results, the bit error rate for the ideal BPSK case of Figure 6.4 is shown.

For the following simulation results shown, Cases 1 to 6 are considered, corresponding to different simulation scenarios. These different cases are as follows:

Case 1:

A bandwidth efficient, finite horizon case is considered for the four users where their spreading waveforms have been defined in Section 6.3.1. An even and light fading scenario is considered, where the value for r in (5.9) for each of the four users, evaluates as r1=r2=r3=r4=1.

The bit error rates for the ideal BPSK case of Figure 6.4, the single-user diversity combiner, discussed in Section 5.5.1, and for the MRC decorrelator discussed in Section 5.5.4.3 are displayed for the purposes of comparison. The bit error rate of the selection diversity decorrelator discussed in this chapter is obtained both analytically and by simulation and is considered over the range of realistic channel conditions with moderate SNR values. The bit error rates are plotted against the first user's SNR, which is increased by holding the additive noise variance fixed and increasing its specular energy. The specular energies of the other users are all set to 4.

The relative delays are arbitrarily chosen in multiples of the chip duration T_c, and are tabulated in Table 5. The results are shown in Figure 6.5 and a discussion of the results is given shortly thereafter.

	Specular path delay	Fading path 1 delay	Fading path 2 delay
User 1	0	$9T_c$	$11T_c$
User 2	$2T_c$	$11T_c$	$15T_c$
User 3	$5T_c$	$7T_c$	$6T_c$
User 4	$3T_c$	$14T_c$	$9T_c$

Table 5
Tabulation of the user's delays for Case 1

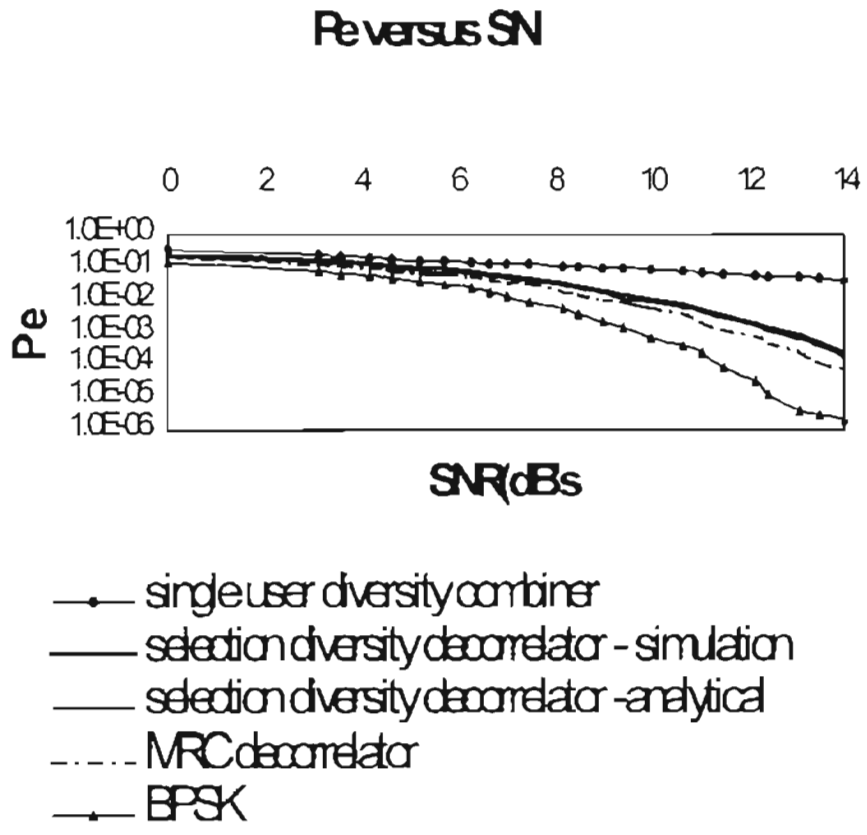

Figure 6.5
Bit error rate results for even and light fading conditions of Case 1

With reference to Figure 6.5, it will be observed that the ideal BPSK case still has the best bit error rate results. The detector with the worst bit error rate performance is the single-user diversity combiner and the selection diversity decorrelator performed far better than this detector. Furthermore, the simulation and analytical bit error rate results for the selection diversity decorrelator were very similar. However, the bit error rate results for the selection diversity decorrelator were not as good as those for the MRC decorrelator.

Case 2:

In this simulation run, the same parameters are used as for Case 1, but it is conducted for various sets of delays for the asynchronous case as the main aim of the simulation is to verify the analytical performance. The relative delays are arbitrarily chosen in multiples of the chip duration T_c, and are tabulated in Table 6. Figure 6.6 consists of several plots of Pe versus SNR for the selection diversity decorrelator for different delay sets. Once again, the bit error rate plot for the ideal BPSK case serves as a benchmark for all the results. A discussion of the results of Figure 6.6 is given shortly thereafter. The analytical results were found to be very similar to the simulation results, and are not shown in Figure 6.6 in order to prevent the plots in this figure from becoming too cluttered.

	First delay set			Second delay set			Third delay set		
	Specular path delay	Fading path 1 delay	Fading path 2 delay	Specular path delay	Fading path 1 delay	Fading path 2 delay	Specular path delay	Fading path 1 delay	Fading path 2 delay
User 1	0	$9T_c$	$11T_c$	0	$3T_c$	$6T_c$	0	$1T_c$	$5T_c$
User 2	$2T_c$	$11T_c$	$15T_c$	$7T_c$	$6T_c$	$6T_c$	$1T_c$	$2T_c$	$6T_c$
User 3	$2T_c$	$7T_c$	$6T_c$	$3T_c$	$5T_c$	$4T_c$	$2T_c$	$3T_c$	$7T_c$
User 4	$3T_c$	$14T_c$	$9T_c$	$10T_c$	$11T_c$	$1T_c$	$4T_c$	$8T_c$	$8T_c$

Table 6
Tabulation of the user's delays for Case 2

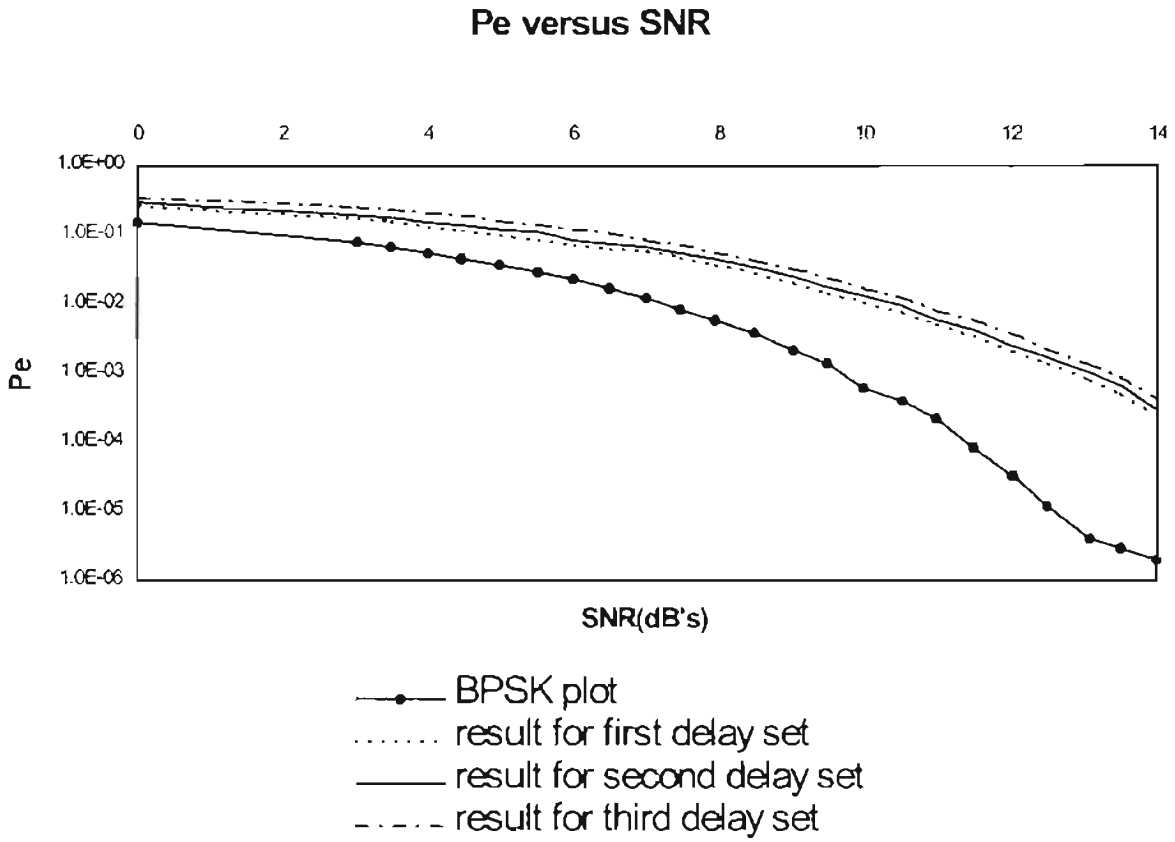

Figure 6.6
Bit error rate for the selection diversity decorrelator for different sets of delays

With reference to Figure 6.6, it will be observed that the delays do not substantially affect the bit error rate of the selection diversity decorrelator, and that all the bit error rate plots are very similar. Hence, it can be stated that the bit error rate of the decorrelator is fairly independent of the asynchronous path delays of the users for the delay set chosen in Table 6.

Case 3:

The parameters used for this simulation are the same as for Case 1, but instead of increasing the SNR by increasing the specular energy and keeping the noise variance fixed, the SNR is increasing by fixing the specular energy of the desired user and correspondingly decreasing the noise variance.

User 1's energy is set to 1 and the other users energy are set to 4. The fading to additive noise variance ratio is still held fixed at r1=r2=r3=r4=1. The effect of this is that as the SNR is increased, the fading variances are correspondingly reduced because the noise variance has to be reduced to provide the higher SNR. The bit error rate results are shown in Figure 6.7 and a brief discussion of the result is given thereafter.

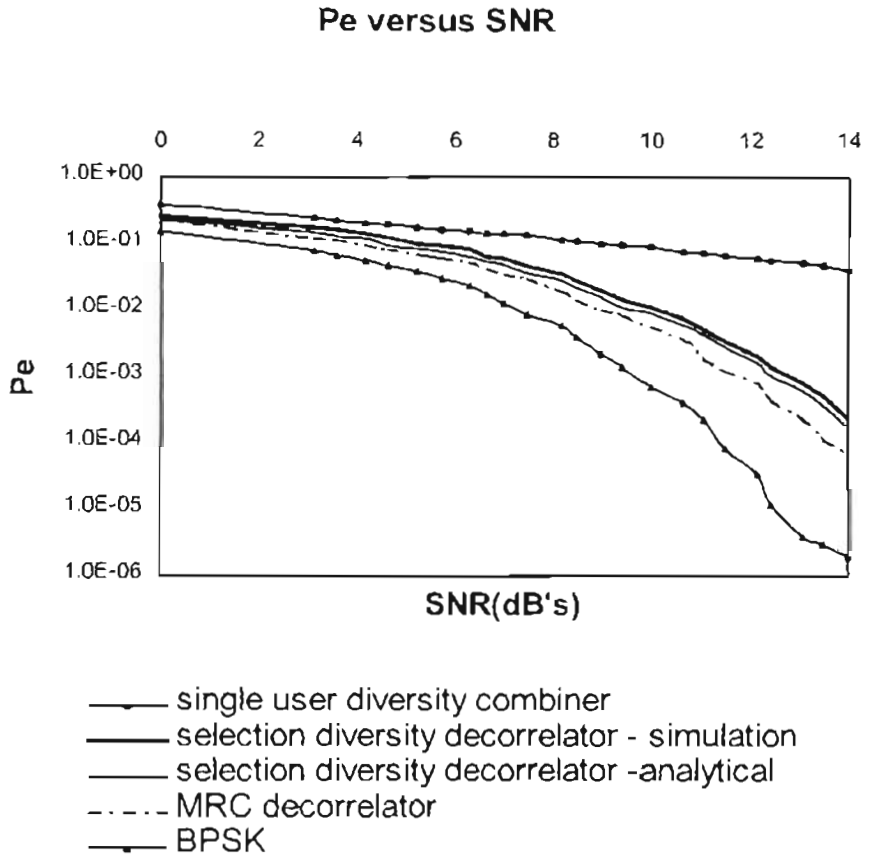

Figure 6.7
Results for the even and light fading conditions of Case 3

With reference to Figure 6.7, it can be seen that the bit error rate plot of both the selection diversity and MRC decorrelators decay much more rapidly than that of the single user diversity combiner, even for medium SNR values. These plots are indicative of how the near-far problem associated with the single-user diversity combiner manifests itself under this fading channel condition. Note that the simulation and analytical results of bit error rate for the selection diversity decorrelator are very similar. From Figure 6.7, one notices that as one approaches the high-SNR end, performance loss is mainly due to the interferer specular energy and is not due to the effects of the additive and fading noises which are very low for these high SNR. The bit error rate results for the ideal BPSK case have been given as reference and are the lowest achievable for the CDMA case. It is clear that the results of Figures 6.5 and 6.7 are very similar, where irrespective of whether the user's SNR was increased by increasing the specular energy and fixing the noise variance, or fixing the specular energy and reducing the noise variance, the bit error rate is almost the same for the corresponding value of SNR.

Case 4:

An attempt is made here to show the near-far resistance of the MLS detector of Section 5.5.2, selection diversity and MRC decorrelators for the fading channel. Furthermore, the severe near-far limitations of the single user diversity combiner of Section 5.5.1 will also be shown.

Case 4.1.

The delays of the signals from the different paths are as shown in Table 7.

	Specular path delay	**Fading path 1 delay**	**Fading path 2 delay**
User 1	0	$9T_c$	$11T_c$
User 2	$2T_c$	$11T_c$	$15T_c$
User 3	$2T_c$	$6T_c$	$7T_c$
User 4	$3T_c$	$9T_c$	$14T_c$

Table 7
Tabulation of the user's delays for Case 4.1

The energy of the first user is set to 2. Even and light fading conditions are used with the variance ratios r1=r2=r3=r4=1. Of the three interfering users, it is assumed that user 2 is the dominant interferer. The noise variance is kept fixed. The energy of users' 3 and 4 are both set to 1. However, the energy of user 2 is varied. This is done to check whether an increase in the SNR of the interferer has a major impact on the bit error rate performance of the desired user (user 1). This would in turn reflect the near-far resistance of the decorrelator. The bit error rate of user 1 for the selection diversity decorrelator is shown in Figure 6.8 for a fixed SNR, in response to the variation in the interferer's SNR. Figure 6.8 depicts the bit error rate for user 1 as the ratio of the square root of user 2's energy to user 1's energy is varied.

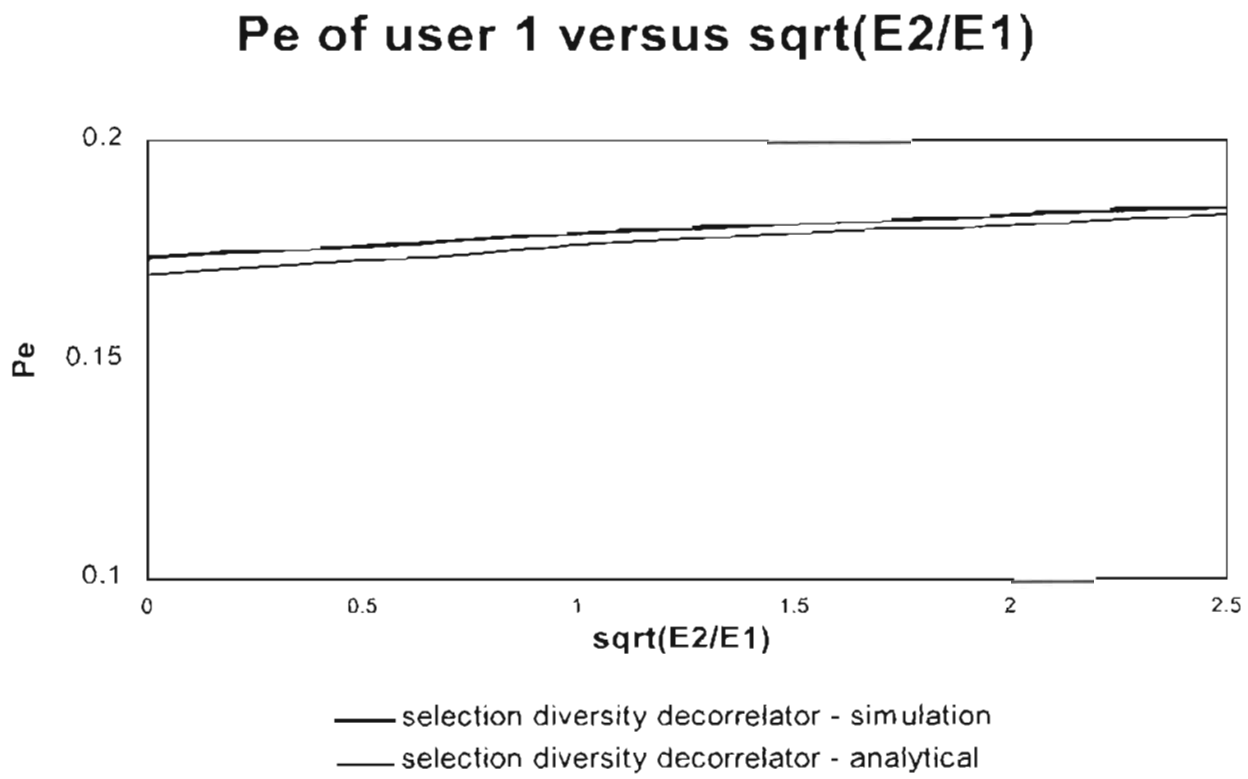

Figure 6.8.
Pe of user 1 for a fixed SNR, as the SNR of user 2 is varied

With reference to Figure 6.8, it can be seen that an increase in the SNR of the interferer has very little effect on the bit error rate results of the desired user. This indicates that the selection diversity decorrelator is near-far

resistant. It will also be observed that the simulation and analytical results for the selection diversity decorrelator are very similar.

Case 4.2:

To verify the near-far resistance of the selection diversity decorrelator that the results of Case 4.1 seem to point to, an attempt is made to determine its asymptotic efficiency via simulation. Figure 6.9 illustrates the asymptotic efficiency of the first user over the xth symbol interval of the MLSD, selection diversity and MRC decorrelators and the single-user diversity combiner as a function of the energy of the second user relative to the desired user, which was varied as in Case 4.1. The performance of these detectors is considered as the interfering specular energy of user 2 increases with respect to that of the desired user 1, while the noise variance is kept fixed. Furthermore, even and light fading conditions are assumed, and the fading to additive noise variance ratios are accordingly set as r1=r2=r3=r4=1.

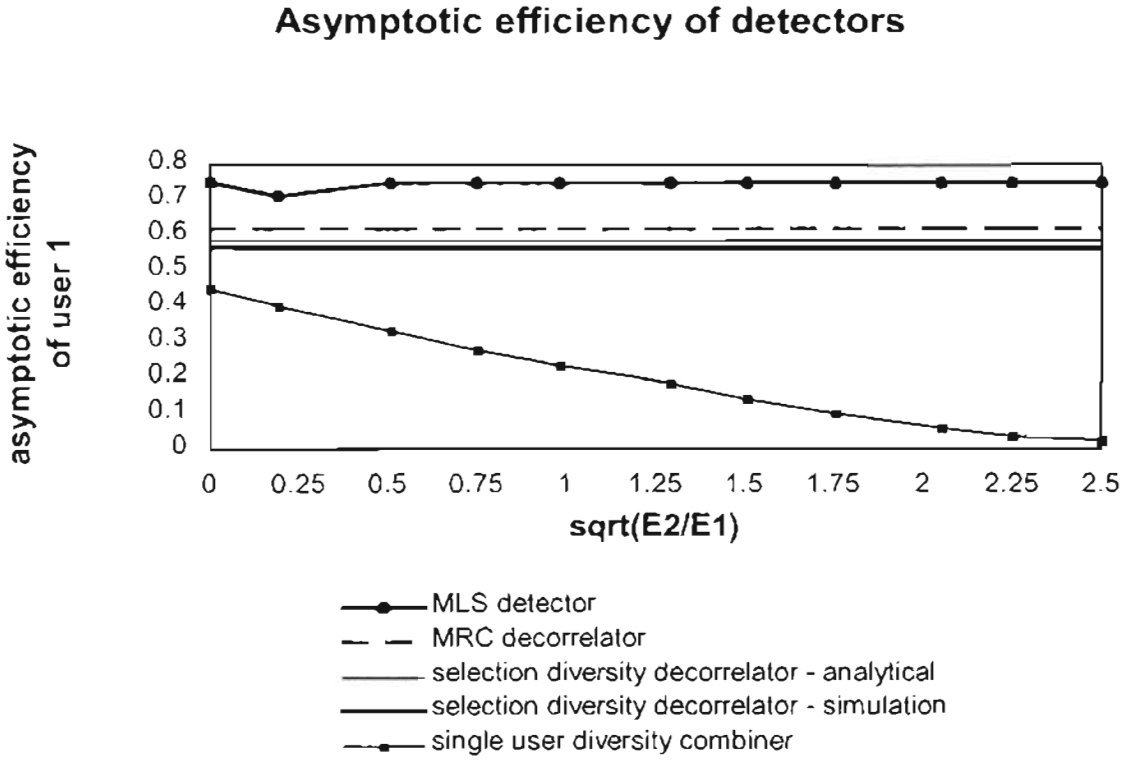

Figure 6.9
Asymptotic efficiencies of detectors for Case 4.2

The results of Figure 6.9 indicate that the MLS detector performs best with the MRC and selection diversity decorrelators performing almost as well. It is observed that the MRC decorrelator performs better than the selection diversity decorrelator. Both the simulation and analytical results for the selection diversity decorrelator are very similar. However, the selection diversity decorrelator performs significantly better than the single-user diversity combiner. It is observed that the asymptotic efficiency of the single user diversity combiner alone decays to zero with increasing values of the interfering energy. This is an illustration of the near-far problem of single user detectors as it applies to the fading channel.

Case 5:

For the previous four cases, simulation results were obtained for even and light fading conditions. For this case, an attempt will be made to obtain simulation results for uneven fading conditions.

Case 5.1:

The simulation parameters are set the same as for Case 4.1, with the exception that the fading levels which are now set for user 2 as r2=5 and for the other users as r1=r3=r4=1. The bit error rate of the first user is shown in Figure 6.10 for the selection diversity decorrelator, as a function of the square root of the ratio of user 2's energy to its own energy.

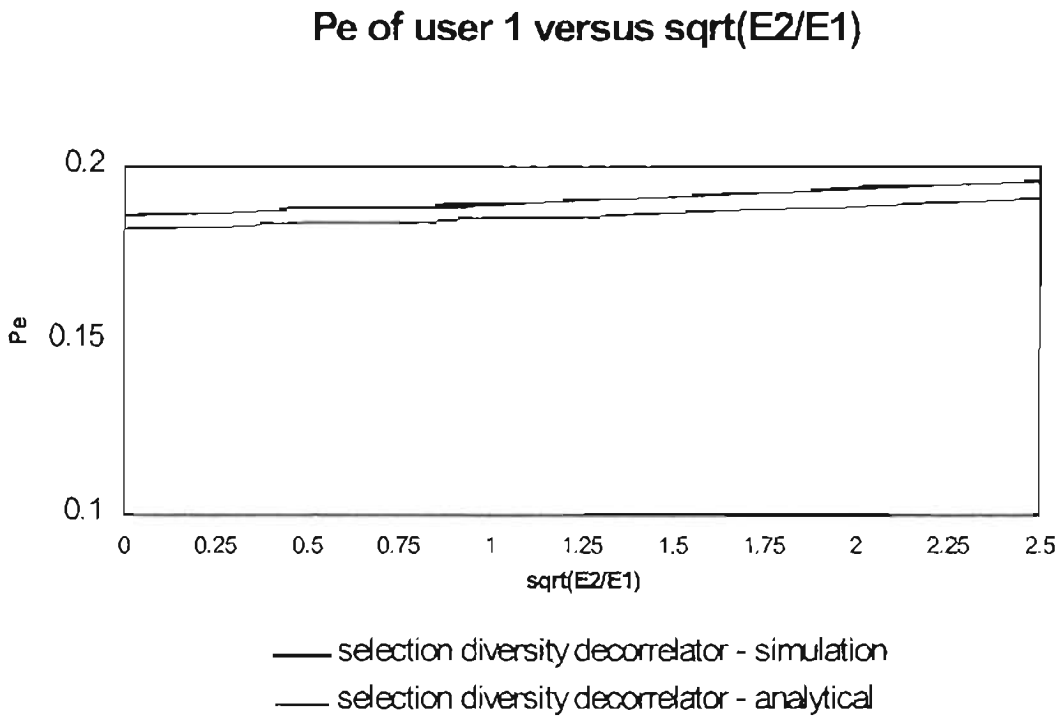

Figure 6.10
Pe of user 1 for a fixed SNR as the SNR of user 2 is varied

In the result of Figure 6.10, there is now a higher interferer fading relative to the additive noise. Comparing the results of Figures 6.10 and 6.8, it will be observed that for the uneven fading case, the near-far resistance of the selection diversity decorrelator is reduced, but not substantially. Once again, the simulation and analytical results for the selection diversity decorrelator are almost identical.

Case 5.2:

The parameters are set the same as for Case 3, except for the fading levels which are now set for the interferer as r2=5 while for the other users it is set as r1=r3=r4=1. User 1's energy is set to 1 and the other users' energy are set to 4. To increase the SNR of user 1, the noise variance is reduced. The bit error rate performance for the uneven fading condition is shown in Figure 6.11.

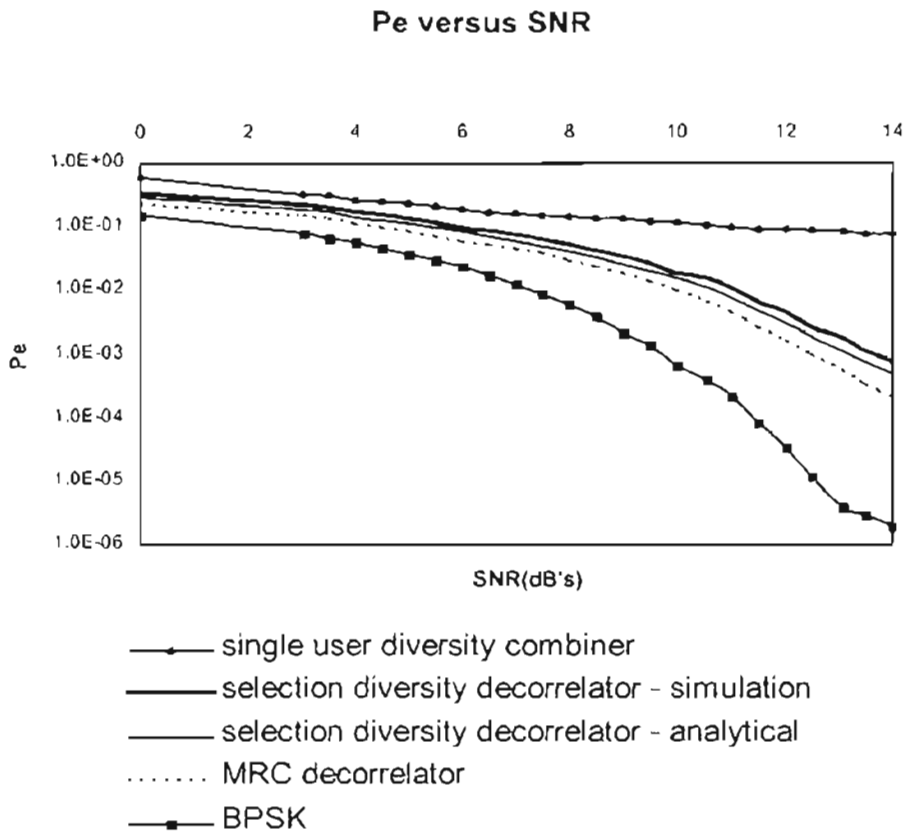

Figure 6.11
Bit error performance for uneven fading conditions

From Figure 6.11 it is observed the bit error rate of the MRC and selection diversity decorrelators increase relative to the results for the light and even fading case, but not substantially. The single-user diversity combiner suffers further relative to its already poor performance in Figure 6.7. The bit error rate of both the MRC and selection diversity decorrelators has increased relative to the results of Figure 6.7 due to the interferer fading level being so high. As the fading of the interferer increases further, the bit error rates of all these detectors will correspondingly increase. Also note that both the simulation and analytical bit error rate results for the selection diversity decorrelator are very similar.

Case 5.3:

The parameters are the same as for Case 1, except for the fading levels which are now set for the interferer as r2=5 while for the other users it is set as r1=r3=r4=1. To increase the SNR of user 1, its specular energy is increased while the noise variance is held fixed. The asymptotic efficiency performance of the various detectors under this condition is shown in Figure 6.12.

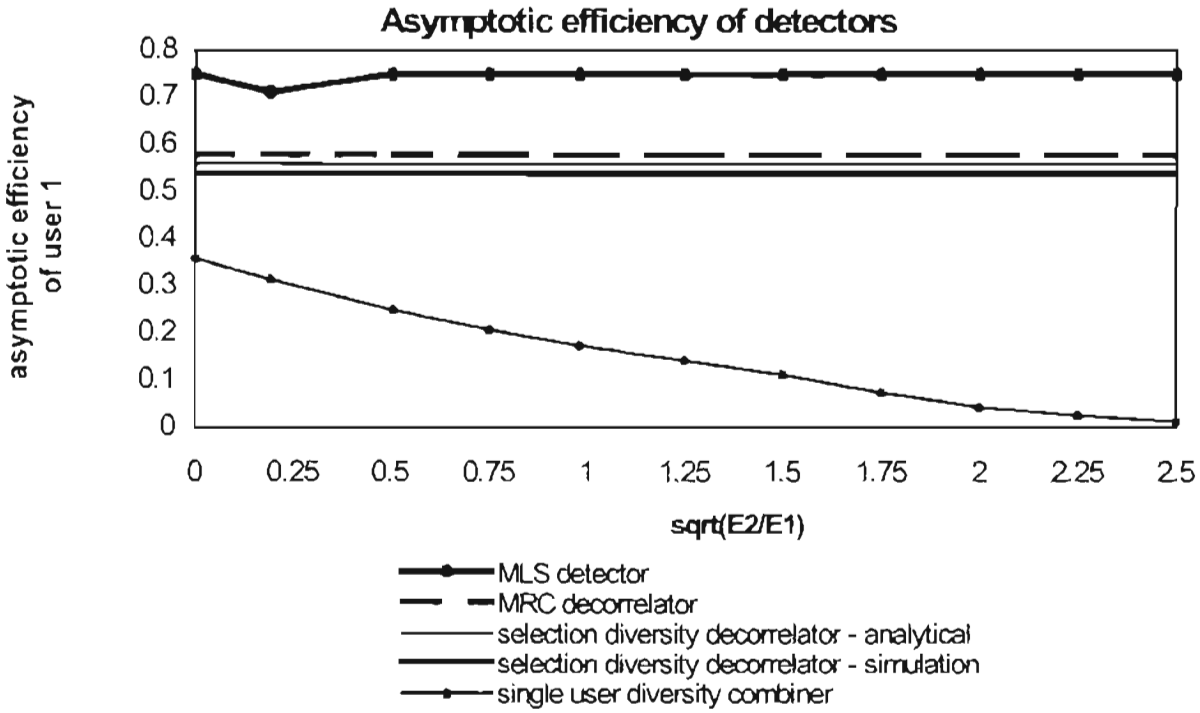

Figure 6.12
Asymptotic efficiency for uneven fading conditions

In the results of Figure 6.12, the uneven fading case was considered in order to determine its effect on the asymptotic efficiency of the detectors already determined in Figure 6.9. The asymptotic efficiency of both the selection diversity and MRC decorrelators decreases relative to the results in Figure 6.9 due to the interferer fading level being so high, as shown in Figure 6.12. As the fading of the interferer increases, the performance of all these detectors will correspondingly reduce. Once again, it is evident that the simulation and analytical results for the selection diversity decorrelator are very similar.

Case 6:

The four users are assigned gold signature sequences as before. The delays for the signals from the various paths are assigned as shown in Table 7.

The fading variance ratios are set with r1=1 and the rest being equal to 2. All the interfering specular energies are equal to that of the desired user, which is set to 2. Figure 6.13 is a plot of the bit error probability of the desired user using the MRC and selection diversity decorrelators and the single-user diversity combiner with the ideal BPSK case shown for the purposes of comparison.

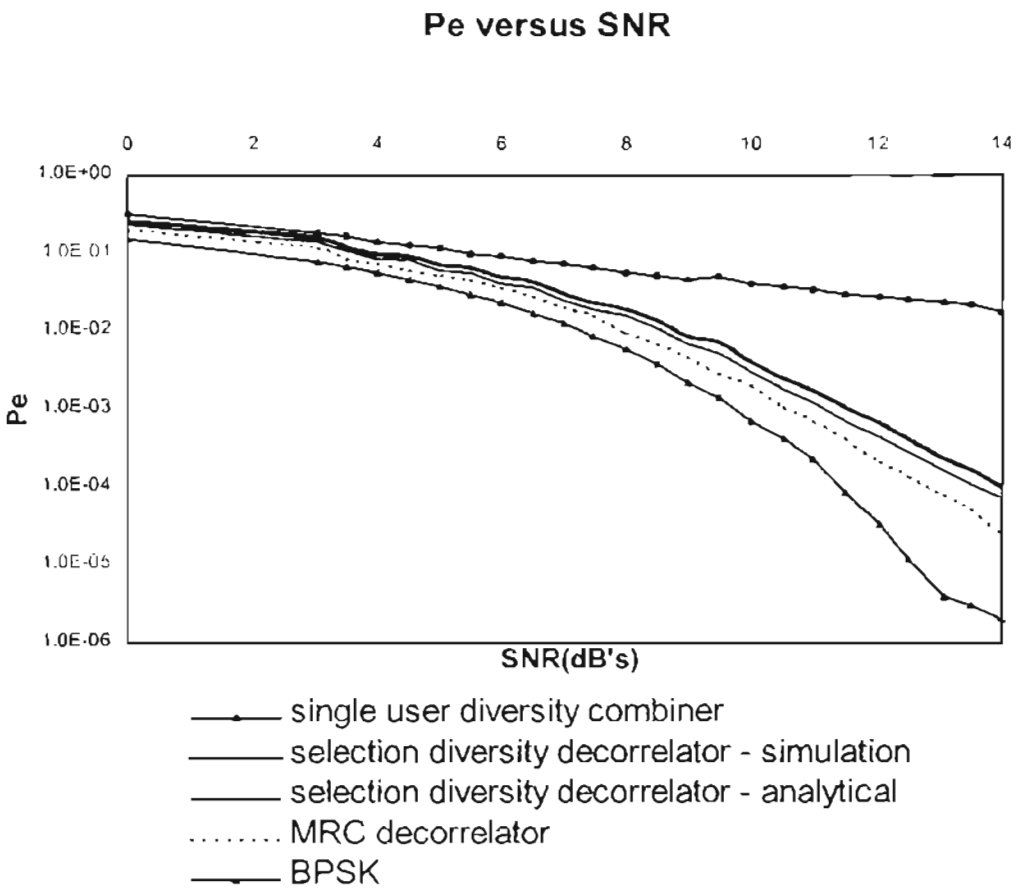

Figure 6.13.
Bit error performance for equal specular energies and even fading

For the results shown in Figure 6.13, the fading to additive noise variance ratio for the first user is set to 1 and it is set to 2 for the other users. All the interfering specular energies are equal to that of the desired user which is set to 2. This is traditionally considered an ideal power-controlled, nonnear-far situation and is regarded as the most favorable condition for single-user detectors such as the single user diversity combiner. In the results of Figure 6.13, it is observed that there is still an improvement in performance given by both the MRC and selection diversity decorrelators, over the single-user detector even in this ideal nonnear-far situation. Once again, the simulation and analytical results for the selection diversity decorrelator are very similar. It is clear that the single-user receivers suffer from more than just the near-far problem. The single-user receivers can support only bandwidth-inefficient CDMA communications. On the other hand, multiuser detection solves more than just the near-far problem. It supports CDMA communications for much higher bandwidth efficiencies than does single-user detection, irrespective of the near-far conditions.

6.5. Conclusion

Selection diversity was used by a path selector to first select the strongest path for the channel, which then served as the input to the selection diversity decorrelating detector. Multiple resolvable paths can be used to accomplish selection diversity by selecting the path with the largest autocorrelation peak at the output of the matched filters. The multiuser path selector selects only the strongest matched filter output for a user for a particular symbol interval. When the specular signal path is the strongest at the output of the bank of correlators, then the selection diversity decorrelator for the fading channel is transformed into the decorrelator for the Gaussian channel.

The aim of the software exercise was to analytically determine the bit-error rate for a particular user using the selection diversity decorrelator. This analytical value of bit-error rate is to be compared against that produced by the actual simulation model. The assumption that had to be made was that the specular energies, phases and variance ratios are time invariant over a particular symbol interval. Furthermore, it was assumed that there were four users.

From the numerical results, it was evident that the BPSK in AWGN gave the best bit error rate results. The detector with the worst bit error rate performance was the single-user diversity combiner, and the selection diversity decorrelator performed much better than this detector. However, the MRC decorrelator still gave better performance than the selection diversity decorrelator. The MLS detector has the best asymptotic efficiency with the selection diversity and MRC decorrelators performing almost as well. However, both these decorrelators perform significantly better than the single-user detector. The asymptotic efficiency of the single user diversity combiner alone decays to zero with increasing values of the interfering energy. For the case of uneven fading, the near-far resistance of both the decorrelators is reduced, and their bit error rate increases, but not substantially. Even in the ideal nonnear-far situation, these decorrelators still give better performance than the single-user diversity combiner. This points to the fact that single-user receivers suffer from more than just the near-far problem, and that they can support only bandwidth-inefficient CDMA communications. For all the results in this chapter, both the simulation and analytical results for the selection diversity decorrelator were very similar, thereby confirming the correctness of the software model used.

Chapter 7: Neural Network based multiuser detector

7.1. Introduction

In this chapter a receiver is proposed which is an extension of that considered in [60]. The Kalman filter based multiuser detector of Iltis and Mailaender [66] is combined with the neural network approach in [60]. The input set to the neural network is expanded to include estimates of the signal amplitudes. The signal amplitudes and user delays are estimated using an extended Kalman filter (EKF).

The organisation of this chapter is as follows:

Section 7.2 will give an overview of the research work conducted on multiuser receivers using neural networks. The system model for the receiver proposed in this chapter will be given in Section 7.3. Amplitude and delay estimation will be discussed in Section 7.4, while the neural network classifier will be discussed in Section 7.5. The performance evaluation results will be provided in Section 7.6 while a conclusion to the chapter will be provided in Section 7.7.

7.2. Overview of neural network receivers

In this section, a brief discussion is given of neural network and their incorporation into detector structures for CDMA.

The highly structured nature of MAI suggests that a neural network should be able to learn how to remove the MAI effectively. A multi-user receiver is essentially a decision making device, hence a neural network is a natural architecture for this problem. Artificial neural networks are highly interconnected networks of processing units (referred to as nodes or perceptrons) which operate in parallel. A perceptron is a non-linear decision device comprised of layers of non-linear nodes. Each non-linear node in a layer operates on a linear combination of the outputs of the previous layer. It is possible to have multi-layered and single layer perceptrons. The multilayer perceptron is capable of approximating arbitrary decision regions in the input space for most classification problems. Due to their highly parallel structure and adaptability to system parameters, receivers employing neural networks prove to be a desirable alternative to the optimum and conventional receivers for multiple-access communications.

The most intriguing aspect of neural net design is the structure modification rule employed for learning. The learning problem can be formulated as an algorithm to modify the internal structure of the network to minimize an external criterion function that is relevant to the task. The multilayer perceptron is trained to demodulate spread spectrum signals. The training is an iterative process of modifying weights and thresholds to minimize the error function. The back-propagation algorithm is a typical example of training algorithms that have been successfully applied to many classification problems. It is successful in training the neural net receiver for the single-user and multiuser detection problems in multiple-access channels.

Unlike the optimum detector, most computational needs of the neural network receiver come during the training period and prior to actual data transmission. For demodulation of information bits, the neural net receiver relies on parallel computation in each layer, which implies constant demodulation time complexity and exponential hardware complexity in the number of users.

In [60], an artificial neural network was employed for the demodulation of spread-spectrum signals in a multiple-access environment. The neural networks were trained for the demodulation of signals via back-propagation type algorithms. A modified back-propagation algorithm was introduced for single user and multiuser detection with near-optimum performance. Even with the standard back-propagation algorithm, the multilayer perceptron was very successful in classifying signals in the presence of interfering users. In all the examples considered in [60], the proposed neural net receiver significantly outperformed the conventional receiver. The performance of the neural net receivers, with reasonable training periods, closely tracks that of the optimum receiver. The multi-layered network was found in [60] to perform no better than a single layer one.

The receiver in [60] required knowledge of the other user's bits, and the number of neurons in this receiver grew exponentially in the number of users. The work in [60] did not prove that the neural network will converge to an optimum set of weights. The neural network was not trained in the presence of noise beyond MAI, hence this is an unrealistic communication environment. Nevertheless, the work is valuable and achieves its goal in showing that the neural network can perform as a multi-user communications receiver.

In [61], a multi-user receiver was developed, which exploits knowledge of the desired user's spreading code while initially being ignorant of the codes of the interferers. These receivers are based on the use of both linear and non-linear adaptive algorithms.

In [61], the work of [60] was extended by providing comparisons of the perceptron's performance to that of a linear adaptive receiver as well as providing convergence analysis of the neural network in the multi-user context. Both analysis scenarios were considered, the multiuser signal in the absence of ambient channel noise and in the presence of ambient noise.

Classical Lyapunov techniques were used to show that the single layer perceptron converges to optimal weights for the noiseless multi-user case [61]. The adaptive algorithms that were studied in [61] are appropriate for multi-user communication scenario where it is expected that the spreading codes of the interfering users are unknown to the receiver.

All of the multi-user detectors examined in [61] outperform the conventional matched filter detector. It was also observed in [61] that the neural network algorithm performance improves as the communication scenario becomes more hostile for the desired user.

7.3. System model

The received signal is the sum of K simultaneous CDMA transmissions plus additive Gaussian noise. To obtain the baseband equivalent of the signal, the incoming signal is first down converted to baseband, then low-pass filtered and sampled at the Nyquist rate. Thus the baseband equivalent of the signal transmitted by the k-th user represents a sequence of binary valued rectangular pulses of width T_c

$$a_k(t) = \sum_{n=0}^{N-1} a_k(n)\, p(t - nT_c), \quad 0 \le t \le T \qquad \text{.....(7.1)}$$

where:

- $a_k(n), 0 \le n \le N-1\}$ is a PN code sequence consisting of N chips that take values $\{\pm 1\}$
- p(t) is a pulse of duration T_c, where T_c is the chip interval

- T is defined as the symbol duration
- There are N chips per symbol and $T = N*T_c$

Ideal low-pass filtering to a bandwidth of $1/T_c$ yields

$$a_k'(t) = a_k(t) * h(t) \quad \text{.....(7.2)}$$

where as before, h(t) is the impulse response of the ideal filter. It is easy to show that for

$$h(t) = \frac{\sin\left(2\pi \frac{t}{T_c}\right)}{\pi t} \quad \text{.....(7.3)}$$

$$a_k'(t) = \sum_{n=0}^{N-1} \frac{a_k(n)}{\pi}\left[G\left(\frac{2\pi(t - nT_c)}{T_c}\right) - G\left(\frac{2\pi(t - nT_c - T_c)}{T_c}\right)\right] \quad \text{.....(7.4)}$$

where:

$$G(u) = \int_0^u \frac{\sin x}{x}\, dx \quad \text{.....(7.5)}$$

The composite CDMA signal which is received during the x-th symbol interval is

$$r(xN_s + m) = \sum_{l=0}^{1}\sum_{k=1}^{K} b_k(x - l).A_k.a_k'(mT_s + lT - \tau_k) + n(m) \quad \text{.....(7.6)}$$

and m=1,2----N_s

In (7.4) and (7.6), τ_k is the delay that accounts for the asynchronous nature of the system. T is the symbol duration and $T_s = T_c/2$ is the corresponding Nyquist sampling interval. Thus $N_s = T/T_s$ is the number of samples per bit. $b_k(x)$ is the x-th message bit of user k and A_k the

amplitude of user k's signal. Thus $A_k = \sqrt{2E_b^{(k)}}/T$ where $E_b^{(k)}$ is the received energy per bit for user k. The additive noise n(m) is assumed circular Gaussian with correlation function

$$E\{n(m)n(j) = \frac{2N_0}{T_s}\delta(mj) \quad \text{.....(7.7)}$$

The receiver, a block diagram of which is given in Figure 7.1 consists of a bank of correlators, a Kalman filter and a neural network classifier. The bank of correlators produce the sufficient statistics $\{y_k\}$ from which decisions are made. In this case

$$y_k = \sum_{m=0}^{N_s} r(xN_s + m).a_k(mT_s - \tau_k) \quad \text{.....(7.8)}$$

The delays $\{\tau_k\}$ needed in (7.8) are estimated through the Kalman filter. The Kalman filter also produces an estimate of the amplitudes $\{A_k\}$. The neural network classifier uses the K outputs $\{y_k\}$ of the correlator bank and the K amplitudes $\{A_k\}$ as input.

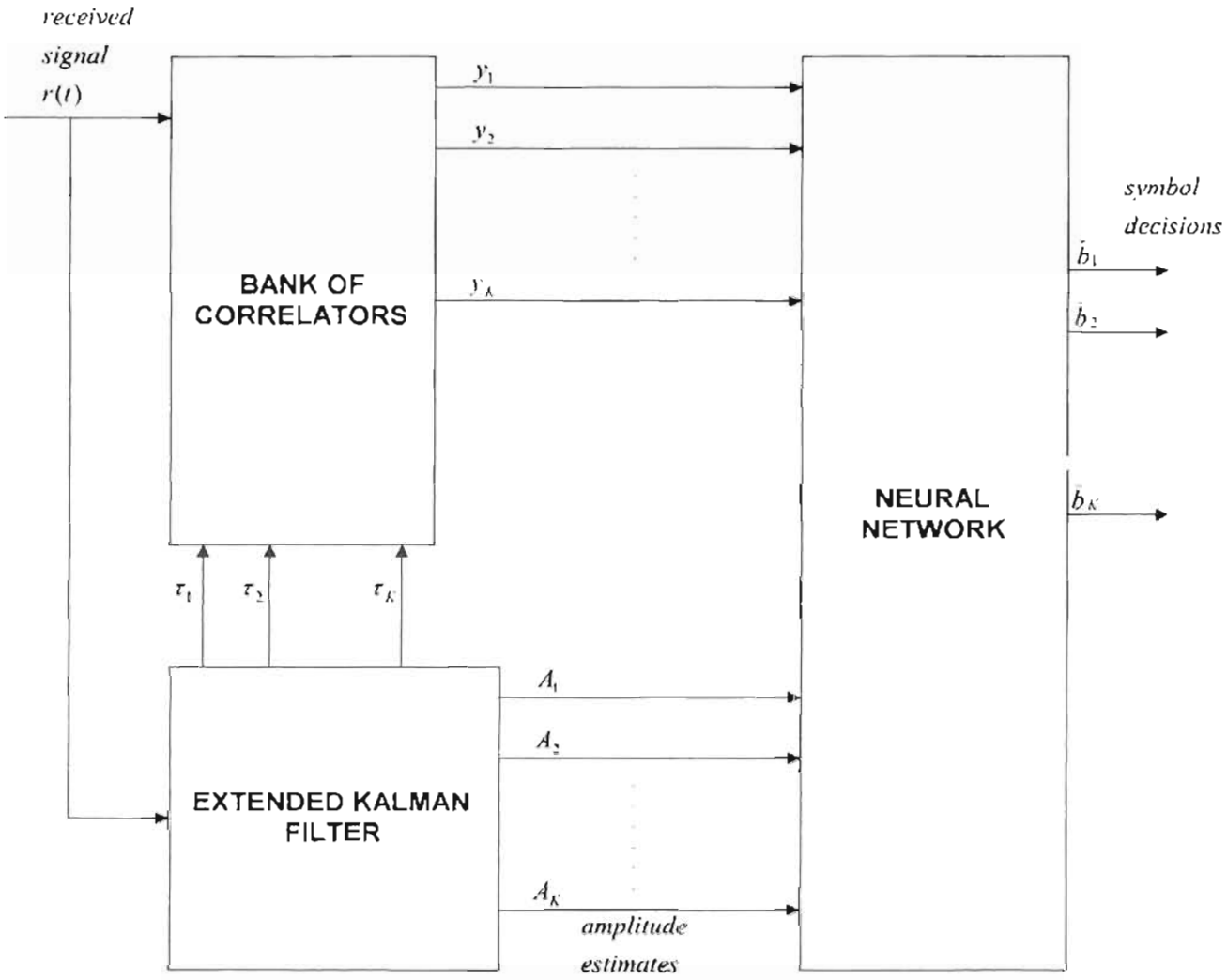

Figure 7.1.
The adaptive multiuser receiver

7.4. Amplitude and Delay Estimation

If one examines the form of $r(xN_s + m)$, it is evident that it is linear in the amplitude $\{A_k\}$ but highly nonlinear in the delays $\{\tau_k\}$. If one assumes that the parameters comprise a first order Gauss-Markov process then it is well known that the Kalman filter provides the minimum variance estimate of the state vector [139]. In this case, because the measurement sequence is nonlinear in the state, the extended Kalman filter is used. The state vector is defined as:

$$x(m) = [A_1(m), A_2(m), \ldots A_K(m), \tau_1(m), \ldots \tau_K(m)] \quad \ldots\ldots(7.9)$$

Then the process model is [66, 139]

$$x(m+1) = Fx(m) + w(m) \quad \ldots\ldots(7.10)$$

where:

- F is the transition matrix
- w(m) is a circular white Gaussian sequence with covariance matrix

$$E\{w(x)w^T(m)\} = Q \quad \ldots\ldots(7.11)$$

The measurement model is [139]

$$r(m) = H(x(m)) + n(m) \quad \ldots\ldots(7.12)$$

In the EKF, r(m) is linearised around its one step prediction $\bar{x}(m|m-1)$ [139]. The Kalman filter measurement update is then given by:

$$\begin{bmatrix} A_1(m|m) \\ \ldots\ldots \\ A_K(m|m) \\ \tau_1(m|m) \\ \ldots\ldots \\ \tau_K(m|m) \end{bmatrix} = \begin{bmatrix} A_1(m|m-1) \\ \ldots\ldots \\ A_K(m|m-1) \\ \tau_1(m|m-1) \\ \ldots\ldots \\ \tau_K(m|m-1) \end{bmatrix} + \frac{P(m|m-1)}{\sigma(m|m-1)} \begin{bmatrix} \frac{\partial g(m)}{\partial A_1} \\ \ldots\ldots \\ \frac{\partial g(m)}{\partial A_K} \\ \frac{\partial g(m)}{\partial \tau_1} \\ \ldots\ldots \\ \frac{\partial g(m)}{\partial \tau_K} \end{bmatrix} [r(m) - g(m)] \quad \ldots\ldots(7.13)$$

In (7.13), g(m) is the estimated signal based on the one step predictions $\{\bar{A}_k(m|m-1)\}$ and $\{\bar{\tau}_k(m|m-1)\}$, and is given by:

$$g(m) = \sum_{k=1}^{K} \bar{A}_k(m|m-1).a_k(mT_s - \bar{\tau}_k(m|m-1)) \quad \ldots\ldots(7.14)$$

Note that in (7.13), the correction term that is normally added [66, 139] has been ignored.

The error covariance matrix {P(m|m-1)} and the innovations variance {σ(m|m-1)} are defined as follows [139]:

$$P(m|m-1) = FP(m-1|m-1)F^T + Q \quad \text{.....(7.15)}$$

$$P(m|m) = \left[1 - \frac{P(m|m-1)}{\sigma(m|m-1)} H'(m).H'^T(m)\right].P(m|m-1) \quad \text{.....(7.16)}$$

$$\sigma(m|m-1) = H'^T(m)P(m|m-1)H'(m) + \frac{2N_0}{T_s} \quad \text{.....(7.17)}$$

In (7.16) and (7.17), H'(m) represents the gradient of the estimated signal g(m), and is given by:

$$H'(m) = \left[\frac{\partial g(m)}{\partial A_1} \cdots \frac{\partial g(m)}{\partial A_K}, \frac{\partial g(m)}{\partial \tau_1} \cdots \frac{\partial g(m)}{\partial \tau_K}\right] \quad \text{.....(7.18)}$$

7.5. Neural Network Classifier

The neural network receiver proposed in this chapter is based on the Aazhang et al [60] design. The input set to the neural network is expanded by including the amplitude estimates of the system users as shown in Figure 7.1. This effectively makes the receiver robust to the near-far problem. The Neural Works Professional 11+ development environment was used. The training was done using the standard back-propagation algorithm. The sine transfer function was used since the desired output is bipolar. Using the more common sigmoid function necessitates scaling the output values.

To account for the asynchronous nature of the model, the training set takes into account all possible permutations of previous bit, current bit and future bit. This provides the network with information concerning dependencies on past and future bits. The training sets are produced

ignoring channel noise, as it was observed from experimentation that the network produces better results when trained without noise.

7.6. Performance evaluation results

The multiuser detector was simulated for the case of three users. From experimentation, it was observed that a single hidden layer comprising six nodes was optimal for convergence. Fewer neurons took far longer to converge, whereas more neurons proved to be redundant. A 7 chip length Gold sequence was used as the spreading sequence. The delays of the three users were chosen as 0, $3T_c$ and $5T_c$. The powers of the users were chosen such that $E_b^{(3)}/ E_b^{(1)} = E_b^{(2)}/ E_b^{(1)} = 6$dB.

The Kalman filter parameters were chosen as follows:

$$F = diag\left\{\sqrt{E_b^{(1)}}, \sqrt{E_b^{(2)}}, \sqrt{E_b^{(3)}}\right\}$$

$$Q = diag\left\{\frac{\sqrt{E_b^{(1)}}}{100}, \frac{\sqrt{E_b^{(2)}}}{100}, \frac{\sqrt{E_b^{(3)}}}{100}\right\}$$

Figure 7.2 shows the performance of the receiver as the signal to noise ratio of user 1 was varied. This receiver was compared to the receiver of Aazhang et al in [60] showing that the expansion of the input set into the neural network improves performance. In Figure 7.3, the ratio E_b/N_0 for user 1 was fixed at 8dB and then the ratio of the received powers of users 2 and 3 was varied relative to that of user one. The results of Figure 7.3 indicates that this receiver is robust to the near far problem.

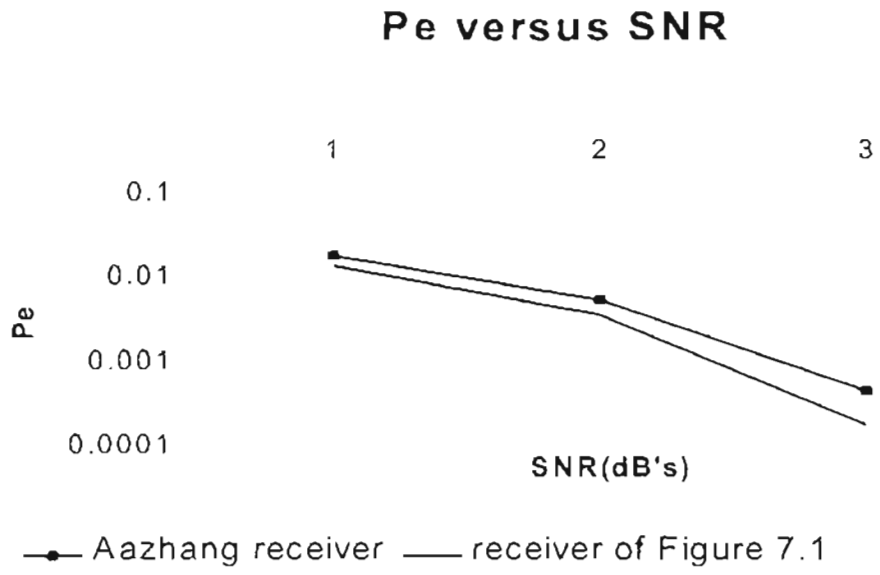

Figure 7.2
Probability of error for user 1

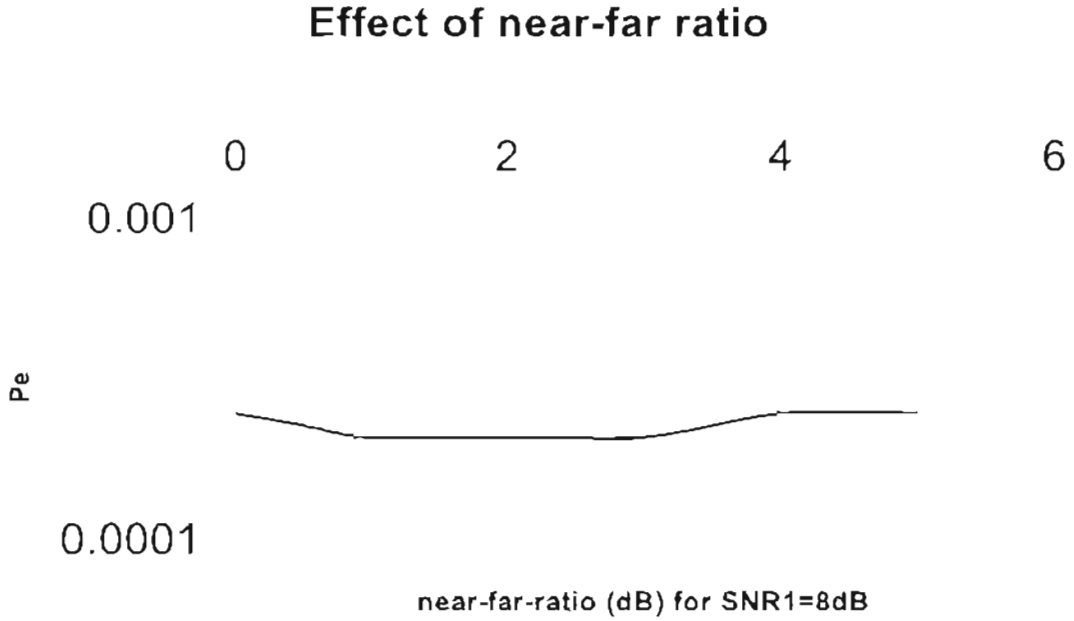

Figure 7.3.
Effect of near-far ratio

7.7. Conclusion

In this chapter, an investigation was done into the application of multilayer perceptrons to the problem of multiuser detection in code division multiple access systems.

The neural network was used as a classifier in an adaptive receiver which incorporates an extended Kalman filter for joint amplitude and delay estimation. The performance was studied via computer simulations showing that the receiver performs favourably compared with others that have appeared in the literature.

Chapter 8: Conclusions

8.1. Conclusion

The aim of this thesis was to develop multiuser demodulation algorithms for mobile communication systems in frequency-selective fading channels, as well as to analyze their implementation complexity. The emphasis was restricted to the uplink of an asynchronous DS-CDMA system where the users transmit in an uncoordinated manner and are received by one centralized receiver.

This thesis has attempted to fulfill this by investigating different receiver structures in an attempt to select one with moderate computational complexity and acceptable performance. Other areas have been dedicated to improving the accuracy of modelling CDMA systems, principally through modeling the wide-band channels and interference structures, which enable the performance of more accurate and more realistic system evaluation simulations.

Multiuser detection was considered for asynchronous CDMA communication over a time-dispersive Rician fading channel, where for each user there exists a steady specular path and two Rayleigh faded paths, all of them appearing asynchronously at the receiver. The conventional detector for the fading channel evaluates to be a diversity combiner that accounts for the multipath resulting from a single transmission. Like the conventional detector for the Gaussian channel, it too was found to be near-far limited. The multiuser maximum likelihood sequence detector was next derived. It estimates the received noiseless signal and correlates the received signal with the estimate. The estimation-correlation must be performed for all possible received data sequences. Due to the prohibitive complexity of the optimal receiver, suboptimal demodulators were considered.

In order to aid in this, an equivalence of the fading channel to an asynchronous Gaussian intersymbol interference CDMA channel was established. This equivalence result allowed for the specification of a multiuser detector for the fading channel for each multiuser detector that was known for the Gaussian channel. Since the decorrelator performed very well over the Gaussian channel, it was chosen as the detector to be utilised and investigated over the fading channel. This decorrelator was to be used

in conjunction with the multiuser diversity combiner, which linearly combines the matched filter output sequence. This decorrelator was referred to as the MRC decorrelator. The data detection can be seen as a process that involves polarity detection at the output of the cascade of the diversity combiner and MRC decorrelator. An attempt was then made to incorporate selection diversity instead of MRC into the decorrelator structure. The decorrelator was then used in conjunction with a path selector, which selects the strongest signal path out of the bank of matched filters. This decorrelator was referred to as the selection diversity decorrelator. Once again, the data detection could be seen as a process that involves polarity detection at the output of the cascade of the path selector and selection diversity decorrelator.

Both the MRC and selection diversity decorrelators investigated in this Thesis

- are near-far resistant, and their near-far resistance is the same as for the MLS detector
- their asymptotic efficiencies and near-far resistances are independent of the specular energies
- offer very high capacity compared to the conventional receiver
- offer much better performance than the conventional receiver
- have complexity of the same order as the conventional, single user receiver

The final detector to be derived was a neural network based multiuser detector. It incorporated an extended Kalman filter and a neural network.

The neural network multiuser detector presented in this thesis

- showed a remarkable insensitivity to the near far problem
- required a training time that was exponentially proportional to the number of users

The decorrelator for the fading channel of course has limitations, and where possible improvements have been suggested and alternatives or effects investigated. Furthermore, the advantages and disadvantages of the neural network based multiuser detector has been investigated and highlighted. The remainder of this chapter summarises the contributions of each section of this thesis.

Chapter 2 – Detectors for the AWGN channel

The emphasis of this chapter has been on centralized multiuser detectors that process the matched filter output to provide the statistics for both the estimation of the signal amplitudes as well as for data detection in the AWGN channel.

The models for the transmitter, receiver and CDMA channel have been derived in this chapter and it was stated that the performance of multiuser receivers can be measured by the bit error rate, asymptotic multiuser efficiency and near-far resistance.

The conventional detector which follows a single user detection strategy, has a computational complexity that grows linearly with the number of users and is vulnerable to the near-far problem. Next, maximum likelihood sequence detection was considered and implemented for DS-CDMA by following the matched filter bank with a Viterbi algorithm. However, the required Viterbi algorithm had a complexity that is still exponential in the

number of users. It was pointed out that another drawback of the MLS detector is that it requires knowledge of the received amplitudes and phases.

Due to the prohibitive complexity of the optimal receiver and the near-far effects that the conventional detector is prone to, suboptimal detectors had to be considered. They decouple the data detection and complex channel coefficient estimation from each other, and estimate the channel coefficients and detect the data for all users separately. An examination was conducted of detectors that have a linear computational complexity but do not exhibit the vulnerability to other-user interference. The two most popular of the linear detectors are the decorrelating and minimum mean-squared error detectors which could be efficiently implemented using the polynomial expansion detector.

Successive interference cancellation detectors were also considered where the basic operating principle was the creation at the receiver of separate estimates of the MAI contributed by each user in order to subtract out some or all of the MAI seen by each user. Such detectors are often implemented with multiple stages, where the aim is that the decisions will improve at the output of successive stages. Finally, since MAI has a highly structured nature, it was stated that a neural network should be able to learn how to remove the MAI effectively.

This chapter served to highlight the advantages and disadvantages of conventional, optimal and suboptimal detectors for CDMA reception in an AWGN channel.

Chapter 3 – Fading models

Because CDMA transmissions are frequently made over channels which exhibit fading and/or dispersion, it is important to design receivers which take this behaviour of the channels into account. Various propagation problems are experienced in a CDMA channel, and these have been highlighted and discussed in this chapter.

It was explained that the fading phenomena is primarily as a result of time variations in the phases, and the amplitude variations in the received signal are due to the time-variant multipath characteristics of the channel. A discussion had been given of the channel correlation, autocorrelation and

power spectra functions. The coherence bandwidth was also defined and a discussion had been given of both frequency selective and non-selective channels in this regard.

Several probability distributions can be considered in attempting to model the statistical characteristics of the fading channel. The distributions that have been discussed in this chapter are the Rayleigh, Nakagami, Rician and Lognormal distributions. The use of diversity techniques such as frequency, time, space and angle were discussed in trying to reduce the effect of fading caused by terrain obstructions. Finally, combining techniques for macroscopic and microscopic diversity were discussed, which include selection diversity, maximal ratio and equal gain combining.

Chapter 4 – Multiuser detectors for the fading channel

An investigation was done in this chapter to check if the detectors for the AWGN channel can also be used in the fading channel, and whether any modifications to them were required. It was shown that multiuser signal processing can be performed either before multipath combining, by processing the matched filter bank output vector, or after multipath combining by processing the maximal ratio combined matched filter bank output vector.

The optimal receiver for the multipath channel is the coherent RAKE receiver. The conventional approach to data detection is to employ an independent, single-user RAKE receiver for each user, which is optimal in the absence of MAI. However, the RAKE receiver suffers from the near-far effect in the presence of interfering signals received over independent fading channels. MLS detectors for synchronous CDMA in Rayleigh fading channels have been presented in [95, 102]. The resulting MLS receiver consists of the received noiseless signal estimator for all possible data sequences and a correlator, which multiplies the received signal with the estimated received noiseless signal. The joint ML estimation has an extremely high computational complexity, which is exponential in the product of the number of users, the number of propagation paths and the number of samples per symbol interval.

The linear detectors that were considered were the decorrelator and the LMMSE detector. The LMMSE detector minimises the mean squared errors at the detector output. It was shown in [21] that as the number of symbols in

the data packet approaches infinity, the decorrelating detector approaches a time-invariant, stable digital multichannel infinite impulse response (IIR) filter. The operation of the interference cancellation receivers was to estimate the multiple-access and multipath induced interference and then subtract the interference estimate from the matched filter bank output

Chapter 5 – Multiuser demodulation in Rayleigh fading channels

The purpose of this chapter was to derive multiuser receiver structures for the time-dispersive, three-path Rician fading CDMA channel, where for each user, there exists a steady specular path and two Rayleigh faded paths, all of them appearing asynchronously at the receiver.

The AME and near-far resistance for the detectors for this fading channel were derived. It was shown that the time-dispersive Rician fading asynchronous CDMA channel bears an equivalence to an asynchronous Gaussian intersymbol interference (AGISI) channel. This equivalence result allows for the specification of a multiuser detector for the fading channel for each multiuser detector that is known for the Gaussian CDMA channel.

For the time-dispersive fading channel, the conventional detector definition leads to a sequence detector of the Viterbi type since it recognises and takes into account the dispersion of the user's signals. This detector is near-far limited when used over the multiuser channel because the presence of the interfering users is not taken into account. The MLS detector for the channel was obtained and it could not be practically implemented. Despite its complexity, the near-far resistance performance of the MLS detector was considered. This result served as a benchmark against which the suboptimal strategies for the fading channel was considered.

The decorrelating strategy was considered for the Rician channel, in conjunction with the multiuser diversity combiner, that was computationally less expensive than the MLS detector yet achieves the same near-far resistance. It was found that the asymptotic efficiency and near-far resistance of this MRC decorrelator is independent of the specular energy, which made it suitable for use in the fading channel.

Chapter 6 – Decorrelating detection employing selection diversity

The receiver in the previous chapter consisted of the cascade of a multiuser divesity combiner and the MRC decorrelator. In this chapter, instead of using MRC, selection diversity is utilised. Selection diversity is used by a path selector to first select the strongest path for the channel, which then served as the input to the selection diversity decorrelator.

The aim of the software exercise was to analytically determine the bit-error rate for a particular user for the selection diversity decorrelator. This analytical value of bit-error rate is to be compared against that produced by the actual simulation model. The assumption that had to be made was that the specular energies, phases and variance ratios are time invariant over a particular symbol interval. Furthermore, it was assumed that there were four users.

From the numerical results, it was evident that the BPSK in AWGN gave the best bit error rate results. The detector with the worst bit error rate performance was the single-user diversity combiner, and both the selection diversity and MRC decorrelators performed much better than this detector. The analytical and simulation results for the selection diversity decorrelator were almost identical. It was also noted that the delays of the signals from the various paths do not substantially affect the bit error rate of the selection diversity decorrelator. The MLS detector has the best asymptotic efficiency with both the MRC and selection diversity decorrelators performing almost as well. It was observed that both the MRC and selection diversity decorrelators performed significantly better than the single-user detector. The asymptotic efficiency of the single user diversity combiner alone decays to zero with increasing values of the interfering energy. For the case of uneven fading, the near-far resistance of both the MRC and selection diversity decorrelators was reduced, and their bit error rate increased, but not substantially. Even in the ideal nonnear-far situation, both these decorrelators still gave better performance than the single-user diversity combiner. This points to the fact that single-user receivers suffer from more than just the near-far problem, and that they can support only bandwidth-inefficient CDMA communications. In all the simulation results, the MRC decorrelator gave better performance than the selection diversity decorrelator. This indicates that for the time-dispersive, three-path Rician fading channel, MRC should be chosen instead of selection diversity.

Chapter 7 – Neural network based multiuser detector

A receiver was proposed in this chapter which was an extension of that considered in [60].

The highly structured nature of MAI suggested that a neural network could be able to learn how to remove the MAI effectively. Due to their highly parallel structure and adaptability to system parameters, receivers employing neural networks prove to be a desirable alternative to the optimum and conventional receivers for multiple-access communications.

The neural network receiver proposed in this chapter was based on the work of [60]. The input set to the neural network was expanded by including the amplitude estimates of the system users. This effectively made the receiver robust to the near-far problem. The neural network was used as a classifier in the adaptive receiver which incorporated an extended Kalman filter for joint amplitude and delay estimation.

The performance evaluation results for this detector showed that it performed well compared to existing designs and it showed a remarkable insensitivity to the near far problem. However, the disadvantage of this detector was that it required a training time that was exponentially proportional to the number of users.

8.2. Summary

This thesis has set out to investigate various aspects of CDMA systems in order to improve the total system efficiency. The work has focussed in six main areas; detectors for the AWGN channel, fading channel modeling, detectors for the fading channel, decorrelators employing MRC and selection diversity and a neural network based multiuser detector. This Thesis has successfully addressed relevant and interesting issues related to CDMA systems.

This thesis has been successful in developing multiuser detectors for the fading channel, in particular, the decorrelator. An investigation was done on the feasibility of applying both MRC and selection diversity to the decorrelating structure, to see which gave superior performance. Aditionally, an investigation was done into the feasibility of using a neural

network based multiuser detector to the problem of multiuser detection in code division multiple access systems. Finally, the Thesis has shed light on the importance of being aware of the presence of fading, when designing receivers for these channels, as the characteristics of the fading channel is much different from that of the Gaussian channel.

8.3. Suggestions for further work

Centralized multiuser receivers have been considered in this Thesis. There are, however, several applications (eg. the downlink receiver of a mobile communication system), where decentralized receivers need to be applied. Recently, there has been a considerable amount of interest in decentralized adaptive receivers. However, several open problems still exist.

More work on the performance of different adaptive algorithms is required. In general, the impact of various practical nonidealities (eg. delay estimation errors and quantization in DSP hardware) to the performance of the receivers should be considered. The performance of the multiuser receivers with more realistic channel models and system parameters should be studied. The analysis of all real-life nonidealities is impossible, and computer simulation of nonidealities are intractable due to long simulation times and incomplete models for nonidealities. Hence, it will be necessary to carry out hardware simulations and construct testbeds and trial systems to determine the practical feasibility of multiuser demodulation for future communication systems.

References

[1] Lee WCY (1991) Overview of cellular CDMA, IEEE Transactions on Vehicular Technology 40(2): p 291-302.

[2] Bingham JAC (1990) Multicarrier modulation for data transmission: An idea whose time has come. IEEE Communications Magazine 28(5): p5-14.

[3] Prasad R & Hara S (1996) An overview of multi-carrier CDMA. Proc. IEEE International Symposium on Spread Spectrum Techniques and Applications (ISSSTA), Mainz, Germany, p107-114.

[4] Cover TM & Thomas JA (1991) Elements of Information Theory. John Wiley and Sons, New York City, New York, USA.

[5] Viterbi AJ (1995) CDMA: Principles of Spread Spectrum Communications. Addison-Wesley, Reading, Massachusetts, USA.

[6] Proakis JG (1995) Digital Communications. McGraw-Hill, New York City, New York, USA, 3r^{d} edition.

[7] Pichna R & Wang Q (1996) Power Control. In: Gibson JD. The Mobile Communications Handbook, CRC Press, chap 23, p370-380.

[8] Simon MK, Omura JK, Scholtz RA & Levitt BK (1994) Spread Spectrum Communications Handbook. McGraw-Hill, New York City, New York, USA.

[9] Dixon RC (1994) Spread Spectrum Systems with Commercial Applications. John Wiley and Sons, New York City, New York, USA.

[10] Peterson RL, Ziemer RE & Borth DE (1995) Introduction to Spread Spectrum Systems. Prentice-Hall, Englewood Cliffs, New Jersey, USA.

[11] Batra A & Barry JR (1995) Blind cancellation of co-channel interference. Proc. IEEE Global Telecommunication Conference (GLOBECOM), Singapore, p157-162.

[12] Haykin S (1991) Adaptive Filter Theory. Prentice Hall, Englewood Cliffs, New Jersey, USA, 2nd edition.

[13] Widrow B & Stearns SD (1985) Adaptive Signal Processing. Prentice Hall, Englewood Cliffs, New Jersey, USA.

[14] Schneider KS (1979) Optimum detection of code division multiplexed signals. IEEE Transactions on Aerospace and Electronic Systems, p181-185.

[15] Kashihara TK (1980) Adaptive cancellation of mutual interference in spread spectrum multiple access. Proc. IEEE International Conference on Communications, p44.4.1-44.4.5.

[16] Kohno R, Imai H & Hatori M (1983) Cancellation technique of co-channel interference in asynchronous spread-spectrum multiple-access systems. EIECE Transactions on Communications, p416-423.

[17] Verdu S (1986) Minimum probability of error for asynchronous Gaussian multiple-access channels. IEEE Transactions on Information Theory, p85-96.

[18] Verdu S (1986) Optimum multiuser asymptotic efficieny. IEEE Transactions on Communications, p890-897.

[19] Neasmith & Beaulieu (1998) IEEE transactions on communications, May 1998.

[20] Rasmussen L K, Lim T j & Aulin T M (1997) Breadth-First Maximum Likelihood Detection in Multiuser CDMA. IEEE Transactions on Communications 45(10): p 1176-1178.

[21] Lupas R & Verdu S (1990) Near-far Resistance of Multi-user Detectors in Asynchronous Channels. IEEE Transactions on Communications 38(4): p 496-508.

[22] Lupas R & Verdu S (1989) Linear Multi-user Detectors for Synchronous Code-Division Multiple-Access Channels. IEEE Transactions on Information Theory 35(1): p123-136.

[23] Schneider K S (1979) Optimum Detection of Code Division Multiplexed Signals. IEEE Trans. Aerospace Elect. Sys [AES-15], p181-185.

[24] Verdu S (1993) Multi-User Detection. Advances in Statistical Signal Processing. vol. 2, JAI Press 1993, p 369-409.

[25] Lupas R, Golaszewski & Verdu S (1986) Asymptotic efficiency of Linear Multi-user Detectors. Proc. 25th Conf. on Decision and Control, Athens, Greece, Dec. 1986, p2094-2100.

[26] Duel-Hallen A, Holtzman J and Zvonar Z (1995) Multi-User detection for CDMA systems. IEEE Pers. Commun., vol.2, no. 2, Apr. 1995, p 46-58.

[27] Xie Z, Short R T & Rushforth C K (1990) A family of suboptimum detectors for coherent multi-user communications. IEEE JSAC, vol. 8, no. 4, May 1990, p683-690.

[28] Wijayasuriya S S H, Norton G H & McGeehan J P (1992) A near-far resistant sliding window decorrelating algorithm for multi-user detectors in DS-CDMA Systems. Proc. IEEE Globecom '92, Dec. 1992, p 1331-1338.

[29] Kajiwara A & Nakagawa M (1994) Microcellular CDMA system with a linear multi-user interference canceller. IEEE JSAC, vol. 12, no. 4, May 1994, p 605-611.

[30] Zheng F & Barton S K (1995) Near far resistant detection of CDMA signals via isolation bit insertion. IEEE Trans. Commun., vol. 43, no. 2/3/4, Feb/Mar/Apr. 1995, p1313-1317.

[31] Duel-Hallen A (1995) A family of multi-user decision-feedback detectors for asynchronous code-division multiple access channels. IEEE Trans. Commun., vol. 43, no. 2/3/4, Feb/Mar/Apr. 1995, p421-434.

[32] Jung P & Blanz J (1995) Joint detection with coherent receiver antenna diversity in CDMA mobile radio systems. IEEE Trans. Vehic. Tech., vol. 44, no. 1, Feb 1995, p76-88.

[33] Varanasi M K & Aazhang B (1991) Optimally near-far resistant multiuser detection in differentially coherent synchronous channels, IEEE Trans. Information Theory, vol. IT-37, p. 1006-1018.

[34] Iltis R A & Mailaender L (1996) Multiuser Detection of Quasisynchronous CDMA Signals Using Linear Decorrelators. IEEE Trans. Commun. vol. 44, no. 11, Nov. 1996, p 1561-1571.

[35] Paris BP (1996) Finite Precision Decorrelating receivers for multiuser CDMA communication systems. IEEE Trans. Commun. vol. 44, no. 4, April 1996, p 496-507.

[36] Juntti M J & Aazhang B (1998) Iterative implementation of Linear multiuser detection for dynamic asynchronous CDMA systems. IEEE Trans. Commun., vol. 46, no. 4, April 1998, p 503-508.

[37] Juntti M J & Aazhang B (1997) Finite memory-length linear multiuser detection for asynchronous CDMA communications. IEEE Trans. Commun., vol. 45, no. 5, May 1997, p 611-622.

[38] Madhow U & Honig M L (1994) MMSE interference suppression for direct-sequence spread-spectrum CDMA. IEEE Trans. Commun., vol. 43, no. 12, Dec. 1994, p 3178-3187.

[39] Miller S L (1995) An adaptive direct-sequence code-division multiple-access receiver for multiuser interference rejection, IEEE Trans. Commun., vol. 43, no. 2/3/4, Feb/Mar/April 1995, p 1746-1755.

[40] Mitra U & Poor H V (1995) Adaptive receiver algorithms for near-far resistant CDMA. IEEE Trans. Commun., vol. 43, no. 2/3/4, Feb/Mar/April 1995, p 1713-1724.

[41] Madhow U, Honig M L & Verdu S (1995) Blind adaptive multiuser detection. IEEE Trans. Info. Theory, vol. 41, no. 4, July 1995, p 944-960.

[42] Wie L & Rasmussen L K (1996) A near ideal noise whitening filter for an asynchronous time-varying CDMA system. IEEE Trans. Commun., vol. 44, no. 10, Oct. 1996, p 1355-1361.

[43] Moshavi S, Kanterakis EG & Schilling DL (1996) Multistage Linear Receivers for DS-CDMA systems. Int'l. J. Wireless Info. Networks, vol. 3, no. 1, Jan. 1996.

[44] Wu H Y & Duel-Hallen A (1996) Performance comparison of multi-user detectors with channel estimation for flat Rayleigh Fading CDMA channels, Wireless Pers. Commun., July/Aug. 1996.

[45] Gray S D, Kocic M & Brady D (1995) Multi-user detection in mismatched multiple-access channels, IEEE Trans. Commun., vol. 43, no. 12, Dec. 1995, p. 3080-3089.

[46] Viterbi A J (1990) Very low rate convolutional codes for maximum theoretical performance of spread-spectrum multiple-access channels, IEEE JSAC, vol. 8, no. 4, May 1990, p. 641-649.

[47] Kohno R, Imai H, Hatori M & Pasupathy S (1990) Combination of an adaptive array antenna and a canceller of interference for direct-sequence spread-spectrum multiple access systems, IEEE JSAC, vol. 8, no. 4, May 1990, p. 675-682.

[48] Patel P & Holtzman J (1994) Analysis of a simple successive interference cancellation scheme in a DS/CDMA system, IEEE JSAC, vol. 12, no. 5, June 1994, p. 796-807.

[49] Varanasi M K & Aazhang B (1990) Multistage detection in asynchronous code-division multiple-access communications, IEEE Trans. Commun., vol. 38, no. 4, Apr. 1990, p. 509-519.

[50] Kohno R, et al (1990) An adaptive canceller of cochannel interference for spread-spectrum multiple-access communications networks in a power line, IEEE JSAC, vol. 8, no. 4, May 1990, p. 691-699.

[51] Varanasi M K & Aazhang B (1991) Near-Optimum detection in Synchronous Code-division multiple-access systems, IEEE Trans. Commun., vol. 39, no. 5, May 1991, p. 725-736.

[52] Rusch L A & Poor H V (1995) Multi-user detection techniques for narrowband interference suppression in spread spectrum communications, IEEE Trans. Commun., vol. 43, no. 2/3/4, Feb/Mar/Apr. 1995, p. 1725-1737.

[53] Patel P & Holtzman J (1994) Performance comparison of a DS/CDMA system using a successive interference cancellation (IC) scheme and a parallel IC scheme under fading, Proc. ICC '94, New Orleans, LA, May 1994, p. 510-514.

[54] Divsalar D & Simon M (1995) Improved CDMA performance using parallel interference cancellation, JPL pub. 95-21, Oct. 1995.

[55] Buehrer R M & Woerner B D (1995) Analysis of adaptive multistage interference cancellation for CDMA using an improved Gaussian Approximation, Proc. IEEE MILCOM '95, San Diego, CA, Nov. 1995, p. 1195-1199.

[56] Giallorenzi T R & Wilson S G (1993) Decision feedback multi-user receivers for asynchronous CDMA systems, Proc. IEEE Globecom '93, Houston, TX, Dec. 1993, p. 1677-1682.

[57] Duel-Hallen A (1993) Decorrelating decision-feedback multi-user detector for synchronous code-division multiple access channel, IEEE Trans. Commun., vol. 41, no. 2, Feb. 1993, p285-290.

[58] Klein A, Kaleh G K & Baier P W (1996) Zero-forcing and minimum mean-square-error equalization for multi-user detection in code-division multiple-access channels, IEEE Trans. Vehic. Tech., vol. 45, no. 2, May 1996, p. 276-287.

[59] Stewart G W (1973) Introduction to Matrix computations, New York:academic, 1973.

[60] Aazhang B & Paris B P (1992) Neural networks for multiuser detection in code-division multiple-access communications, IEEE Trans. Commun., vol. 40, no. 7, July 1992, p. 1212-1222.

[61] Mitra U & Poor H V (1995) Adaptive Receiver algorithms for near-far resistant CDMA, IEEE Trans. Commun., vol. 43, no. 2/3/4, Feb/Mar/Apr. 1995, p. 1713-1724.

[62] Nelson L B & Poor H V (1996) Iterative multiuser receivers for CDMA channels: An EM-based approach, IEEE Trans. Commun., vol. 44, no. 12, December 1996, p. 1700-1710.

[63] Xie Z, Rushforth C K, Short R T & Moon T K (1993) Joint Signal Detection and parameter estimation in multiuser communications, IEEE Trans. Commun., vol. 41, no. 7, August 1993, p. 1208-1215.

[64] Moon T K, Xie Z, Rushforth C K & Short R T (1994) Parameter estimation in a multi-user communication system, IEEE Trans. Commun., vol. 42, no. 8, August 1994, p. 2553-2559.

[65] Steinberg Y & Poor H V (1994) Sequential amplitude estimation in multiuser communications, IEEE Trans. Inform. Theory, Jan. 1994, vol. 40, p. 11-20.

[66] Iltis R A & Mailaender L (1994) An adaptive multiuser detector with joint amplitude and delay estimation, IEEE JSAC., June 1994, vol. 12, no. 5, p. 774-785.

[67] Iltis R A & Mailaender L (1994) Multiuser code acquisition using parallel decorrelators, Proc. CISS '94, Princeton, NJ, Mar. 1994.

[68] Bensley S E & Aazhang B (1996) Subspace-based channel estimation for code division multiple access communication systems, IEEE Trans. Commun., vol. 44, no. 8, August 1996, p. 1009-1019.

[69] Bensley S E & Aazhang B (1998) Maximum-likelihood synchronization of a single user for code-division multiple-access communication systems, IEEE Trans. Commun., vol. 46, no. 3, March 1998, p. 392-399.

[70] Iltis R A (1990) Joint estimation of PN code delay and multipath using the extended Kalman filter, IEEE Trans. Commun., vol. 38, no. 10, October 1990, p. 1677-1685.

[71] Iltis R A (1994) An EKF-based joint estimator for interference, multipath and code delay in a DS spread-spectrum receiver, IEEE Trans. Commun., vol. 43, no. 2/3/4, Feb/Mar/April 1994, p 1288-1299.

[72] Iltis R A (1991) A Digital DS spread-spectrum receiver with joint channel and doppler shift estimation, IEEE Trans. Commun., vol. 39, no. 8, August 1991, p. 1255-1267.

[73] Lim T J & Rasmussen L K (1997) Adaptive symbol and parameter estimation in asynchronous multiuser CDMA detectors, IEEE Trans. Commun., vol. 45, no. 2, February 1997, p 213-220.

[74] Chen D S & Roy S (1994) An adaptive multi-user receiver for CDMA systems, IEEE JSAC, vol. 12, no. 5, June 1994, p. 808-816.

[75] Forney G D (1972) Maximum-likelihood sequence estimation of digital sequences in the presence of intersymbol interference. IEEE Tran. Inform. Theory, vol. 18, no. 3.

[76] Forney G D (1973) The Viterbi algorithm. Proceedings of the IEEE. vol. 61, no. 3, p. 268-278.

[77] Lu L & Sun W (1997) The minimal eigenvalues of a class of block-tridiagonal matrices. IEEE Trans. Inform. Theory, vol. 43, no. 2, p. 797-791.

[78] Schlegel C & Wei L (1997) A simple way to compute the minimum distance in multiuser CDMA systems. IEEE Trans. Commun., vol. 45, no. 5, p. 532-535.

[79] Fawer U & Aazhang B (1996) Multiuser receivers for code-division multiple-access systems with trellis-based modulation. IEEE JSAC., vol. 14, no. 8, p. 1602-1609.

[80] Giallorenzi T R & Wilson S G (1996) Multiuser ML sequence estimator for convolutionally coded asynchronous DS-CDMA systems. IEEE Trans. Commun., vol. 44, no. 8, p. 997-1007.

[81] Poor H V & Verdu S (1988) Single-user detectors for multiuser channels. IEEE Trans. Commun., vol. 36, no. 1, p. 50-60.

[82] Miller S Y & Schwartz S C (1995) Integrated spatial-temporal detectors for asynchronous Gaussian multiple-access channels. IEEE Trans. Commun., vol. 43, no. 2/3/4, p. 396-411.

[83] Zvonar Z (1996) Combined multiuser detection and diversity reception for wireless CDMA systems. IEEE Trans. Vehic. Tech., vol. 45, no. 1, p. 205-211.

[84] Kandala S, Sousa E S & Pasupathy S (1995) Multi-user multi-sensor detectors for CDMA networks. IEEE Trans. Commun., vol 43, no. 2/3/4, p. 946-957.

[85] Kandala S, Sousa E S & Pasupathy S (1995) Decorrelators for multi-sensor systems in CDMA networks. European transactions. Commun., vol 43, no. 2/3/4, p. 946-957.

[86] Saquib M, Yates R & Mandayam N (1996) Decorrelating detectors for a dual rate synchronous DS/CDMA system. Proc. IEEE Vehic. Tech. Conf., Atlanta, Georgia, USA, 1: p. 377-381.

[87] Juntti M J & Lilleberg J O (1997) Linear FIR multiuser detection for multiple data rate CDMA systems. Proc. IEEE Vehic. Tech. Conf., Phoenix, Arizona, USA, 2: p. 455-459.

[88] Mitra U & Poor H V (1996) Analysis of an adaptive decorrelating detector for synchronous CDMA channels. IEEE Trans. Commun., vol. 44, no. 2, p. 257-268.

[89] Giallorenzi T R & Wilson S G (1996) Suboptimum multiuser receivers for convolutionally coded asynchronous DS-CDMA systems. IEEE Trans. Commun., vol. 44, no. 9, p. 1183-1196.

[90] Van Heeswyk F, Falconer D D & Sheikh A U H (1996) A delay independent decorrelating detector for quasi-synchronous CDMA, IEEE JSAC., vol. 14, no. 8, p. 1619-1626.

[91] Iltis R A (1996) Demodulation and code acquisition using decorrelating detectors for QS-CDMA. IEEE Trans. Commun., vol. 44, no. 11, p. 1553-1560.

[92] Zheng F C & Barton S K (1995) On the performance of near-far resistant CDMA detectors in the presence of synchronization errors. IEEE Trans. Commun., vol. 43, no. 12, p. 3037-3045.

[93] Parkvall S, Strom E & Ottersten B (1996) The impact of timing errors on the performance of linear DS-CDMA receivers. IEEE JSAC., vol. 14, no. 8, p. 1660-1668.

[94] Zvonar Z & Brady D (1994) Multiuser detection in single-path fading channels. IEEE Trans. Commun., vol. 42, no. 2/3/4, p. 1729-1739.

[95] Vasudevan S & Varanasi MK (1996) Achieving near-optimum asymptotic efficiency and fading resistance over the time-varying Rayleigh-faded CDMA channel. IEEE Trans. Commun., vol. 44, no. 9, p. 1130-1143.

[96] Varanasi M K & Vasudevan S (1994) Multiuser detectors for synchronous CDMA communication over non-selective Rician fading CDMA channels. IEEE Trans. Commun., vol. 42, no. 2/3/4, p. 711-722.

[97] Vasudevan S & Varanasi M K (1994) Optimum diversity combiner based multiuser detection for time-dispersive Ricean fading CDMA channels. IEEE JSAC., vol. 12, no. 4, p. 580-592.

[98] Turin G L (1980) Introduction to spread-spectrum antimultipath techniques and their application to urban digital radio. Proceedings of the IEEE, vol. 68, no. 3, p. 328-353.

[99] Stojanovic M, Proakis J G & Catipovic J A (1995) Analysis of the impact of channel estimation errors on the performance of a decision-feedback equalizer in fading multipath channels. IEEE Trans. Commun., vol. 43, no. 2/3/4, p. 877-886.

[100] Kam P Y (1991) Optimal detection of digital data over the nonselective Rayleigh fading channel with diversity reception. IEEE Trans. Commun., vol. 39, no. 2, p. 214-219.

[101]Hagmanns F J & Hespelt V (1994) On the detection of bandlimited direct-sequence spread-spectrum signals transmitted via fading multipath channels. IEEE JSAC., vol. 12, no. 5, p. 891-899.

[102]Sung P A & Chen K C (1996) A linear minimum mean square error multiuser receiver in Rayleigh-fading channels. IEEE JSAC., vol. 14, no. 8, p. 1583-1594.

[103]Lilleberg J, Nieminen E & Latva-aho M (1996) Blind iterative multiuser delay estimator for CDMA. Proc. IEEE International Symposium on Personal, Indoor and Mobile Radio Communications (PIMRC), Taipei, Taiwan, p. 565-568.

[104]Klein A & Baier P W (1993) Linear unbiased data estimation in mobile radio systems applying CDMA. IEEE JSAC, vol. 11, no. 7, p. 1058-1066.

[105]Zvonar Z & Brady D (1995) Suboptimal multiuser detector for frequency-selective Rayleigh fading synchronous CDMA channels. IEEE Trans. Commun., vol. 43, no. 2/3/4, p. 154-157.

[106]Zvonar Z (1996) Multiuser detection in asynchronous CDMA frequency-selective fading channels. Wireless Personal Communications, Kluwer Academic Publishers, vol. 3, no. 3-4, p. 373-392.

[107]Zvonar Z & Brady D (1995) Differentially coherent multiuser detection in asynchronous CDMA flat Rayleigh fading channels. IEEE Trans. Commun., vol. 43, no. 2/3/4, p. 1252-1255.

[108]Stojanovic M & Zvonar Z (1996) Linear multiuser detection in time-varying multipath fading channels. Proc. Conference on Information Sciences and Systems (CISS), Princeton University, Princeton, New Jersey, USA, p. 349-354.

[109]Stojanovic M & Zvonar Z (1996) Performance of linear multiuser detectors in time-varying multipath fading CDMA channels. Proc. Communication Theory Miniconference (CTMC) in conjunction with IEEE Global Telecommunications Conference (GLOBECOM), London, U.K., p. 163-167.

[110]Kawahara T & Matsumoto T (1995) Joint decorrelating multiuser detection and channel estimation in asynchronous CDMA mobile communications channels. IEEE Trans. Vehic. Tech., vol. 44, no. 3, p. 506-515.

[111]Mitra U & Poor H V (1996) Adaptive decorrelating detectors for CDMA systems, Wireless Personal Communications, Kluwer Academic Publishers, vol. 2, no. 4, p. 415-440.

[112]Kay S (1993) Fundamentals of Statistical Signal Processing: Estimation Theory. Prentice-Hall, Englewood Cliffs, New Jersey, USA.

[113]Wu W C & Chen K C (1996) Linear multiuser detectors for synchronous CDMA communication over Rayleigh fading channels. Proc. IEEE International Symposium on Personal, Indoor and Mobile Radio Communications (PIMRC), Taipei, Taiwan, p. 578-582.

[114]Bernstein X & Haimovich A M (1996) Space-time optimum combining for CDMA communications. Wireless Personal

Communications, Kluwer Academic Publishers, vol. 3, no. 2, p. 73-89.

[115]Gray S D, Preisig J C & Brady D (1997) Multiuser detection in a horizontal underwater acoustic channel using array observations. IEEE Trans. Signal Processing, vol. 45, no. 1, p. 148-160.

[116]Rapajic P B & Vucetic B S (1994) Adaptive receiver structures for asynchronous CDMA systems. IEEE JSAC, vol. 12, no. 4, p. 685-697.

[117]Rapajic P B & Vucetic B S (1995) Linear adaptive transmitter-receiver structures for asynchronous CDMA systems. European Trans. Telecommunications, vol. 6, no. 1, p. 21-27.

[118]Miller S L, (1995) An adaptive direct-sequence code-division multiple-access receiver for multiuser interference rejection. IEEE Trans. Communications, vol. 43, no. 2/3/4, p. 1746-1755.

[119]Miller S L (1996) Training analysis of adaptive interference suppression for direct-sequence code-division multiple-access systems. IEEE Trans. Commun., vol. 44, no. 4, p. 488-495.

[120]Lee K B (1996) Orthogonalization based adaptive interference suppression for direct-sequence code-division multiple access systems. IEEE Trans. Commun., vol. 44, no. 9, p. 1082-1085.

[121]Woodward G, Rapajic P & Vucetic B S (1996) Adaptive algorithms for asynchronous DS-CDMA receivers. Proc. IEEE International Symposium on Personal, Indoor, and Mobile Radio Communications (PIMRC), Taipei, Taiwan, p. 583-587.

[122]Latvo-aho M & Juntti M (1997) Modified adaptive LMMSE receiver for DS-CDMA systems in fading channels. Proc. IEEE International Symposium on Personal, Indoor, and Mobile Radio Communications (PIMRC), Helsinki, Finland, p. 554-558.

[123]Yoon Y C, Kohno R & Imai H (1993) Cascaded co-channel interference cancellating and diversity combining for spread-spectrum multi-access system over multipath fading channels. IEICE Trans. Commun., Vol. E76-B(2), p. 163-168.

[124]Yoon Y C, Kohno R & Imai H (1993) A spread-spectrum multiaccess system with cochannel interference cancellation for multipath fading channels. IEEE JSAC, vol. 11, no. 7, p. 1067-1075.

[125]Saifuddin A, Kohno R & Imai H (1995) Integrated receiver structures of staged decoder and CCI canceller for CDMA with multilevel coded modulation. European Trans. Telecommunications, vol. 6, no. 1, p. 9-19.

[126]Saifuddin A & Kohno R (1995) Performance evaluation of near-far resistant receiver DS/CDMA cellular system over fading multipath channel. IEICE Trans. Commun., E78-B(8), p. 1136-1144.

[127]Fawer U & Aazhang B (1995) A multiuser receiver for code division multiple access communications over multipath channels. IEEE Trans. Commun., vol. 43, no. 2/3/4, p. 1556-1565.

[128]Sanada Y & Wang Q (1997) A co-channel interference cancellation technique using orthogonal convolutional codes on multipath Rayleigh fading channel. IEEE Trans. Vehic. Technology, vol. 46, no. 1, p. 114-128.

[129]Hottinen A, Holma H & Toskala A (1995) Performance of multistage multiuser detection in a fading multipath channel. Proc. IEEE International Symposium on Personal, Indoor, and Mobile Radio Communications (PIMRC), Toronto, Ontario, Canada, p. 960-964.

[130]Holma H, Toskala A & Hottinen A (1996) Performance of CDMA multiuser detection with antenna diversity and closed loop power control. Proc. IEEE Vehicular Technology Conference (VTC), Atlanta, Georgia, USA, p. 362-366.

[131]Latva-aho M & Lilleberg J (1996) Parallel interference cancellation in multiuser detection. Proc. IEEE International Symposium on Spread Spectrum Techniques and Applications (ISSSTA), Mainz, Germany, p. 1151-1155.

[132]Latva-aho M & Lilleberg J (1998) Parallel interference cancellation in multiuser CDMA channel estimation. Wireless Personal Communications, Kluwer Academic Publishers.

[133]Latva-aho M & Lilleberg J (1996) Parallel interference cancellation based delay tracker for CDMA receivers. Proc. Conference on Information Sciences and Systems (CISS), Princeton University, Princeton, New Jersey, USA, p. 852-857.

[134]Latva-aho M & Lilleberg J (1996) Delay trackers for multiuser CDMA receivers. Proc. IEEE International Conference on

Universal Personal Communications (ICUPC), Boston, Massachusetts, USA, p. 326-330.

[135]Buehrer R M, Kaul A, Striglis S & Woerner B D (1996) Analysis of DS-CDMA parallel interference cancellation with phase and timing errors. IEEE JSAC, vol. 14, no. 8, p. 1522-1535.

[136]Buehrer R M, Correal N S & Woerner B D (1996) A comparison of multiuser receivers for cellular CDMA. Proc. IEEE Global Telecommunication Conference (GLOBECOM), London, U.K., p. 1571-1577.

[137]Agashe P & Woerner B (1996) Interference cancellation for a multicellular CDMA environment. Wireless Personal Communications, Kluwer Academic Publishers, p. 1-15.

[138]Singh N and Takawira F (1996) A Neural Network and Extended Kalman Filter Based Adaptive Multi-User Receiver for CDMA systems. Africon '96, September 1996, University of Stellenbosch, South Africa, p. 414-418.

[139]Anderson B and Moore J (1979) Optimal filtering. Englewood Cliffs, NJ, Prentice-Hall, 1979.

APPENDICES

APPENDIX 1: PARAMETER ESTIMATION TECHNIQUES

Many suboptimal detectors had been proposed in Chapter 3, but these all assume knowledge at the receiver of all or some of the following parameters - received signal energies, carrier phase or propagation delays. Various algorithms have been proposed for amplitude estimation [63, 64], time-delay estimation [65], and joint parameter tracking [66]. However, these methods are quite complicated and not well suited to practical implementation, except at narrow bandwidths. Of the three system parameters mentioned, time delay appears to be the hardest to estimate accurately because of the nonlinear dependence of the received signal on user delays. This is evident in the work on parameter estimation assuming time delays to be known in [63, 64]. The difficulty with time-delay estimation in an asynchronous CDMA system, is the large uncertainty region involved. With a set of (2M+1)-length codes and K users, the number of possible states to search is at least equal to $(2M+1)^K$.

In [67] , an attempt was made to jointly estimate the arrival times using a modified serial-search correlator strategy. However, the resulting expected acquisition times proved to be quite large. Although the above techniques produce excellent results, they can be computationally intense since they involve solving a multidimensional optimization problem for a large number of parameters. Matters would be simplified if the multidimensional problem could be reduced to a one-dimensional problem while retaining the near-far resistance.

In [66], work was done on joint data detection and parameter estimation, but the resulting algorithm was quite complex. The resulting algorithm of [66] was exponential in the number of users and is hence no better than Verdu's optimal detector [17, 18] in terms of practicality. In [66], an ML algorithm was proposed that involved detecting all K bits transmitted in a given bit interval by the K users at the same time. A number of extended Kalman filters (EKF's) were used to calculate amplitude and delay estimates for all possible bit combinations in a bit interval, and these were then used to update the ML metrics. This very complicated algorithm has a complexity that increases exponentially with the number of users and hence cannot be used in practice.

Sometimes one is only interested in the timing of a single user, or one needs to estimate the delays of several users, but to reduce complexity, this is done sequentially. In [68] the maximum-likelihood estimation of user's delay, amplitude and phase was considered. The multiuser estimation problem was decomposed into a series of single-user problems. In this method, the interfering users were treated as colored non-Gaussian noise. Once acquisition occured, the algorithm was well suited for tracking slowly changing parameters. The estimator required knowledge of the transmitted symbols, but this could be accomplished by feeding back decisions from the detector. The subspace method was also considered in [69], and required no decision feedback. By exploiting the eigenstructure of the received signal's sample correlation matrix, the observation space could be partitioned into a signal subspace and a noise subspace without prior knowledge of the unknown parameters. The channel estimate was formed by projecting a given user's spreading waveform into the estimated noise subspace and then either maximizing the likelihood or minimizing the Euclidean norm of this projection. Both of the approaches in [68, 69] yield algorithms which were near-far resistant and did not require a preamble or decision feedback. This made the algorithm very stable during tracking, since it was able to quickly reacquire the desired user it lost lock. The work of [68] was a significant advancement because the delay estimates were near-far resistant. This implied that changes in the multiple access interference level do not affect the variance of the estimates. However, the need to estimate the interference subspace with each shift of the observation window did place a limit on the ability to track rapidly time-varying delays. The maximum-likelihood algorithm in [69] was able to achieve faster acquisition with lower complexity than the subspace-based algorithm in [68]. This is because the maximum-likelihood method is more optimal and there is less uncertainty in the received signal since the estimator knows the transmitted symbols.

A joint data-sequence and parameter estimator was described in [63]. It combined a suboptimum tree-search algorithm with a recursive least-squares estimator of complex signal amplitude. A joint optimization over the transmitted bits and the complex amplitudes was performed. This receiver had the advantage that the transmitted signal powers and phases were extracted from the received signal in an adaptive fashion without using a test sequence. The assumption made was that the carrier frequency, relative delays τ_k, and the shape of the spreading waveform $a_k(t)$ were known. The

complexity of the tree-search algorithm was $O(K^2)$ computations per decoded bit, and was further dependent on the number of nodes selected. It is most beneficial to use the tree-search algorithm of [63] in circumstances in which the optimum receiver is too complex to be implemented, while at the same time the performance of simpler suboptimum receivers is not acceptable. One of the shortcomings of the work of [63] was that the approach required knowledge of the time delay for each user. The problem of estimating these delays in a multi-user environment had not been fully addressed. It is important to be able to estimate the amplitudes and phases when the delays are not known.

In [64] a method was presented for estimating the amplitudes and phases, both when the time delays were known and when the delays were unknown. The basic assumption was that the transmitted bits were independent and equiprobable. This assumption avoided the need for special training sequences for purposes of acquisition. This was because the sequences transmitted during acquisition had the same statistics as the information-bearing sequences transmitted after acquisition. Each of the estimators considered in [64] was based on the assumption that the parameters were constant. This is a reasonable assumption over an acquisition period, but is restrictive when considering communication among mobile platforms. The estimators described in [64] could be applied equally well with any of the detectors described in Chapter 2, such as the maximum likelihood sequence detector, linear equalization detectors, decision feedback detectors, etc. After convergence of the estimator, the performance of any of these detectors should be nearly as good as if the amplitudes and phases were known a priori [64].

Using either an EKF or a recursive least squares formulation, adaptive algorithms which jointly estimate the transmitted bits of each user and individual amplitudes and time delays may be derived. In [70], the problem of delay estimation in the presence of multipath was considered. An extended Kalman filter was used to estimate both PN code delay and multipath coefficients for a SU system. Analogous to the extension of the single user matched filter or correlating detector to multi user systems using a bank of filters, a simple extension of the delay-tracking single user EKF would be a bank of EKF's, each using its own prediction error in the EKF equations. The EKF can be used to obtain joint estimates of arrival times and multipath coefficients for deterministic signals when the channel can be modeled by a tapped-delay line [70]. In [71], a code tracking algorithm was

developed, and was based on the EKF which provided both code synchronization and joint estimates of interferer and channel parameters. A single EKF-based algorithm was used which provided estimates of the PN code delay, multipath channel coefficients and narrowband interference.

In [73], an adaptive multiuser CDMA detector structure was introduced. A multi-user detector was derived which performed joint data detection and parameter tracking after initial acquisition. The detector structure resembled that of the synchronous detector in [74], but it was more versatile in that it considered the asynchronous, unknown delay case. Two adaptive multiuser asynchronous CDMA detectors were implemented using the EKF and weighted recursive least squares(RLS). It was reasoned that the EKF detector should perform better than the RLS one because it was capable of incorporating prior knowledge about the system, and was therefore more flexible. The multiuser EKF detector was outperformed a bank of single user EKF's in terms of near-far resistance. The proposed detector in [73] operated in a tracking mode, and relied on the availability of accurate initial delay estimates. These delay estimates may perhaps be obtained using one of the subspace-based approaches of [68]. It is less complex to implement than the method in [68], which required the estimation of noise subspaces recursively. The adaptive EKF detector is a viable multiuser CDMA detector for the base station when paired with near-far resistant delay acquisition and phase-lock devices [70-73].

APPENDIX 2: MODEL OF A FREQUENCY SELECTIVE FADING CHANNEL

In order to obtain the same effect of multiple resolvable paths, a wideband signal is employed, covering a bandwidth B. The channel is still assumed to be slowly fading by virtue of the assumption that $T<<(\Delta t)_c$. Suppose that B is the bandwidth occupied by the real bandpass signal. Then the band occupancy of the equivalent lowpass signal $s_{lp}(t)$ is $|f|\leq \frac{1}{2}B$, and application of the sampling theorem results in the signal representation:

$$s_{lp}(t) = \sum_{n=-\infty}^{\infty} s_{lp}(\frac{n}{B}) \frac{\sin[\pi B(t - n/B)]}{\pi B(t - n/B)} \quad \text{.....(A2.1)}$$

The Fourier transform of $s_{lp}(t)$ is

$$S_{lp}(f) = \begin{cases} \frac{1}{B} \sum_{n=-\infty}^{\infty} s_{lp}(n/B) e^{-i2\pi fn/B} & (|f| \leq \frac{1}{2}B) \text{.....(A2.2)} \\ = 0 \text{.....otherwise} \end{cases}$$

The noiseless received signal from a frequency-selective channel was previously expressed in the form

$$r(t) = \int_{-\infty}^{\infty} H(f;t) S_{lp}(f) e^{j2\pi ft} df \quad \text{.....(A2.3)}$$

where H(f;t) is the time-variant transfer function. Substitution for $S_{lp}(f)$ from (A2.2) into (A2.3) yields:

$$r(t) = \frac{1}{B} \sum_{n=-\infty}^{\infty} s_{lp}(t - n/B) h(n/B;t) \quad \text{.....(A2.4)}$$

It is convenient to define a set of time-variable channel coefficients as

$$h_n(t) = \frac{1}{B} h(\frac{n}{B};t) \quad \text{.....(A2.}$$

Then (A2.4) expressed in terms of these channel coefficients becomes

$$r(t) = \sum_{n=-\infty}^{\infty} h^n(t) s_{lp}(t - n/B) \quad \text{.....(A2.6)}$$

(A2.6) implies that the time-variant frequency-selective channel can be modeled as a tapped delay line with tap spacing 1/B and tap weight coefficients {h"(t)}

With an equivalent lowpass signal having a bandwidth ½B, where $B>>(\Delta f)_c$ one achieves a resolution of 1/B in the multipath delay profile. Since the total multipath spread is T_m, the tapped delay line model for the channel can be truncated at $L=[T_m B] + 1$ taps. Then the noiseless received signal can be expressed in the form

$$r(t) = \sum_{n=1}^{L} h^n(t) s_{lp}(t - n/B) \quad \text{.....(A2.7)}$$

APPENDIX 3: THE RAKE DEMODULATOR

The tapped delay line model with statistically independent tap weights provides one with L replicas of the same transmitted signal at the receiver. Hence, a receiver that processes the received signal in an optimum manner will achieve the performance of an equivalent Lth-order diversity communications system.

Consider binary signaling over the channel. Assume there are two equal energy signals $s_{i1}(t)$ and $s_{i2}(t)$, which are orthogonal. Their time duration T is selected to satisfy the condition $T>>T_m$. Thus, the intersymbol interference due to multi-path may be neglected. Since the bandwidth of the signal exceeds the coherence bandwidth of the channel, the received signal is expressed as:

$$r(t) = \sum_{n=1}^{L} h''(t) s_{ln}(t - n/B) + n(t)$$
$$= v_i(t) + n(t), \quad 0 \le t \le T, \quad i = 1,2 \qquad (A3.1)$$

Note that r(t) is the low-pass version of the received signal.

Assume that the channel tap weights are known. Then the optimum receiver consists of two filters matched to $v_1(t)$ and $v_2(t)$, followed by samplers and a decision circuit that selects the signal corresponding to the largest output. An equivalent optimum receiver employs cross correlation instead of matched filtering. The decision variables for coherent detection of the binary signals can be expressed as

$$U_m = \mathrm{Re}[\int_0^T r(t) v_m^*(t) dt]$$
$$= \mathrm{Re}[\sum_{n=1}^{L} \int_0^T r(t) h'' s_{lm}^*(t - \frac{n}{B}) dt]$$

Note the (*) represents the complex conjugate.

An alternative realization of the optimum receiver employs a single delay line through which is passed the received signal r(t). The signal at each tap is correlated with $h''(t)s^*_{lm}(t)$, where n=1,2,...,L and m=1,2. This receiver structure is shown in Figure A3.1.

In effect, the tapped delay line receiver attempts to collect the signal energy from all the received signal paths that fall within the span of the delay line and carry the same information. Its action is somewhat analogous to an ordinary garden rake and, consequently, the name "RAKE receiver" has been given to this receiver structure.

In [6], it was shown that the RAKE receiver with perfect (noiseless) estimates of the channel tap weights is equivalent to a maximal ratio combiner in a system with Lth-order diversity.

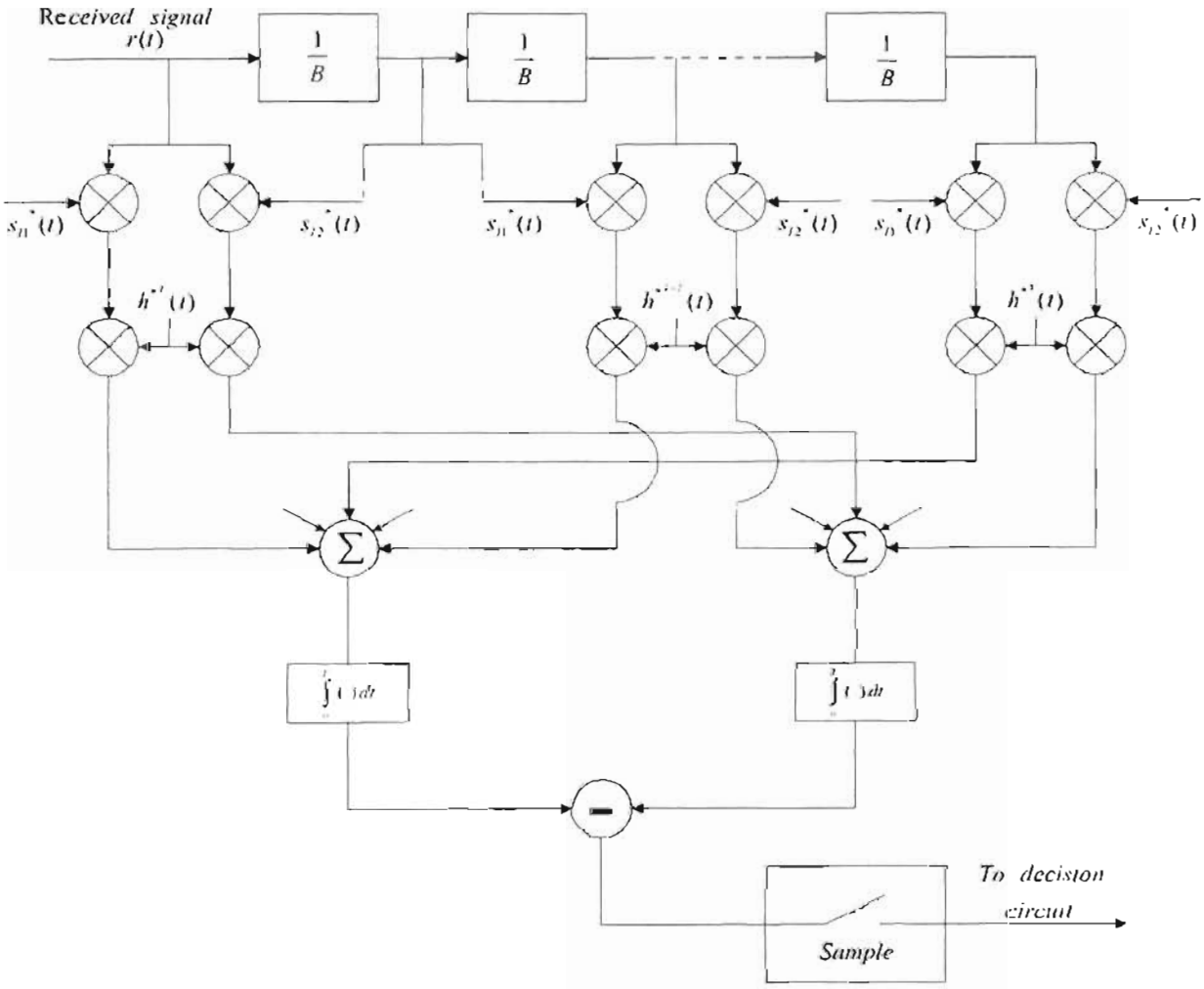

Figure A3.1.
Optimum demodulator for wideband binary signals

APPENDIX 4: SOFTWARE FLOWCHARTS

Figure A4.1
Complete Flowchart for the analytical model

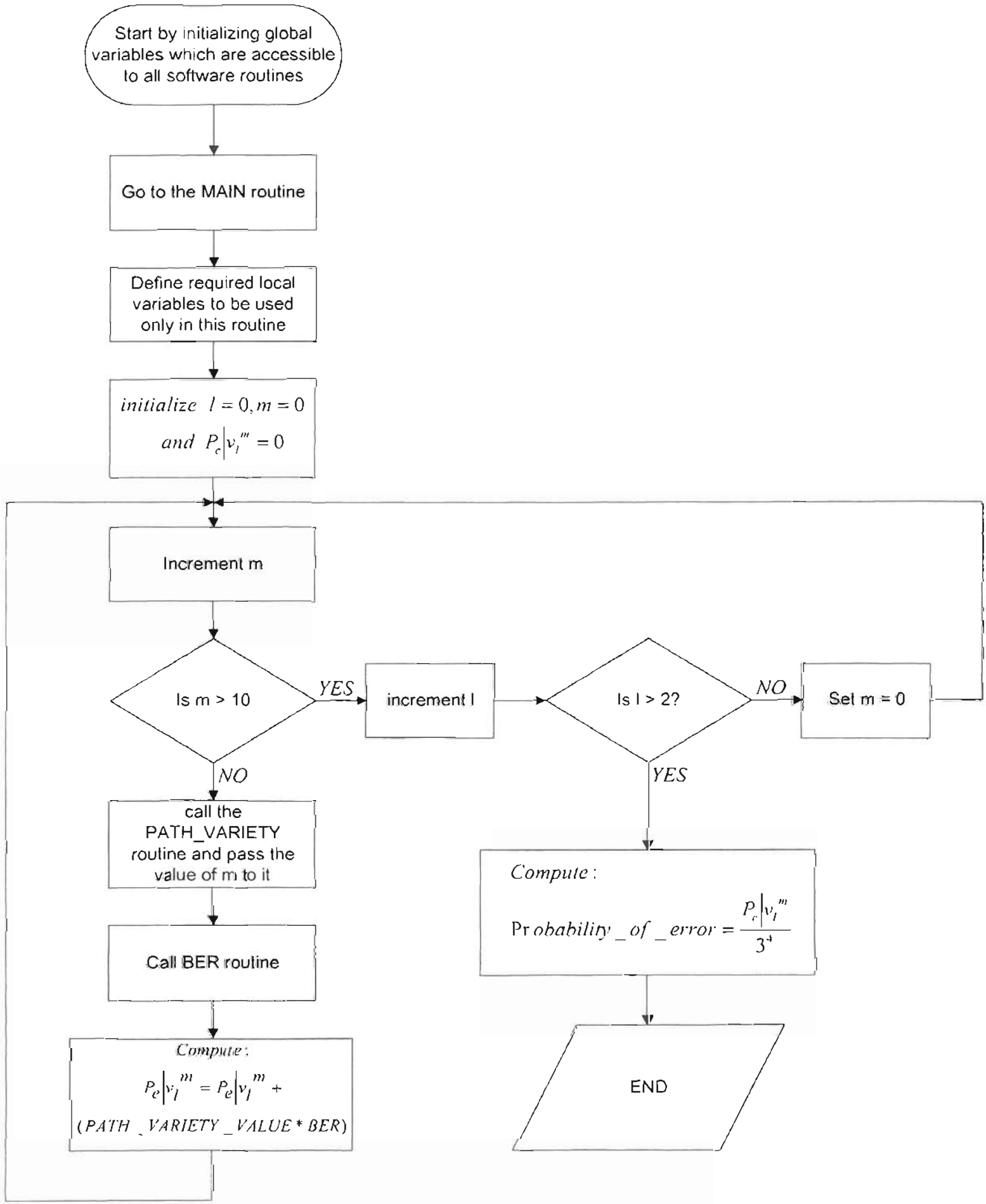

Figure A4.2
Complete Flowchart for the simulation model

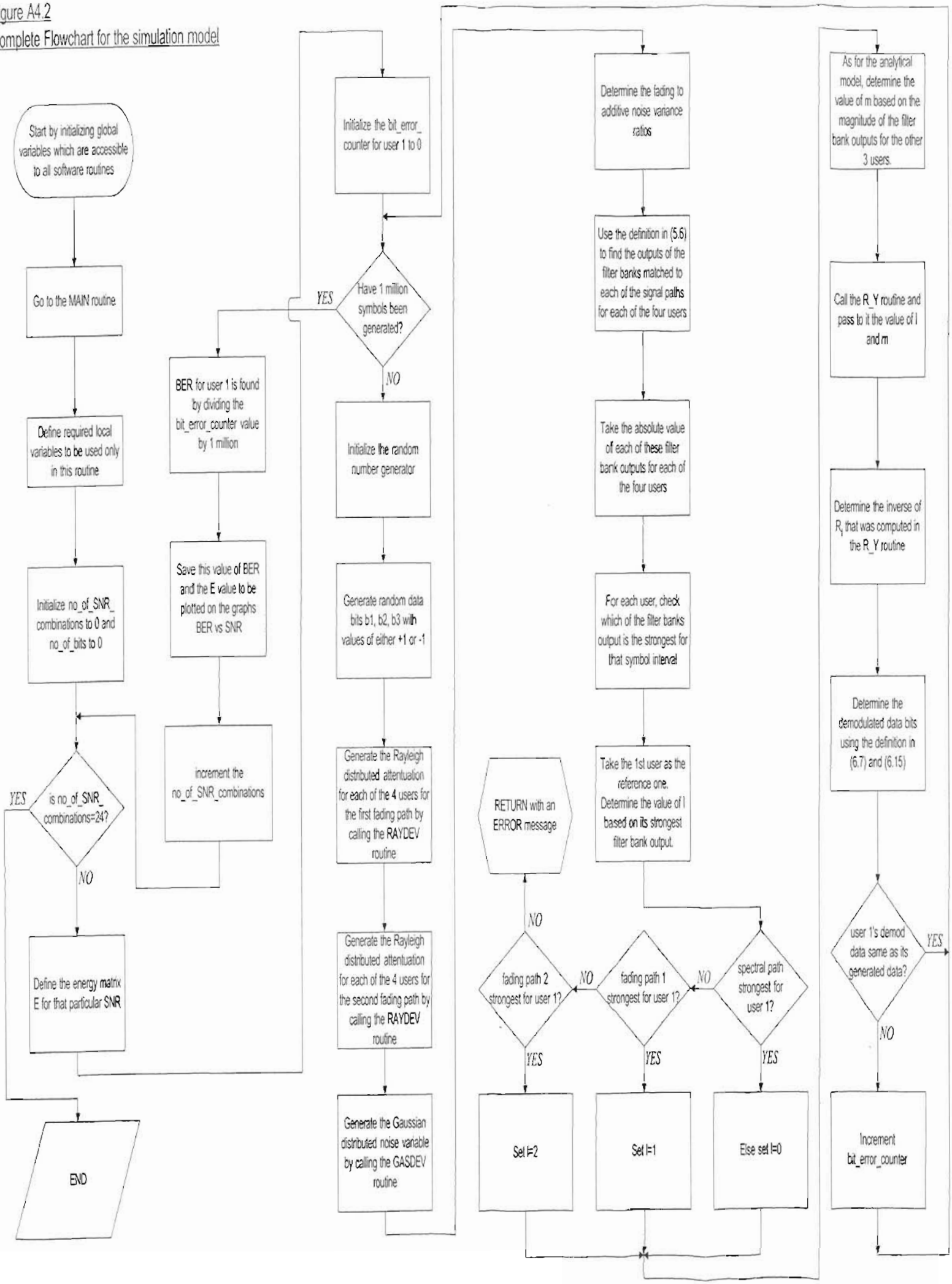

Figure A4.3
The PATH_VARIETY routine

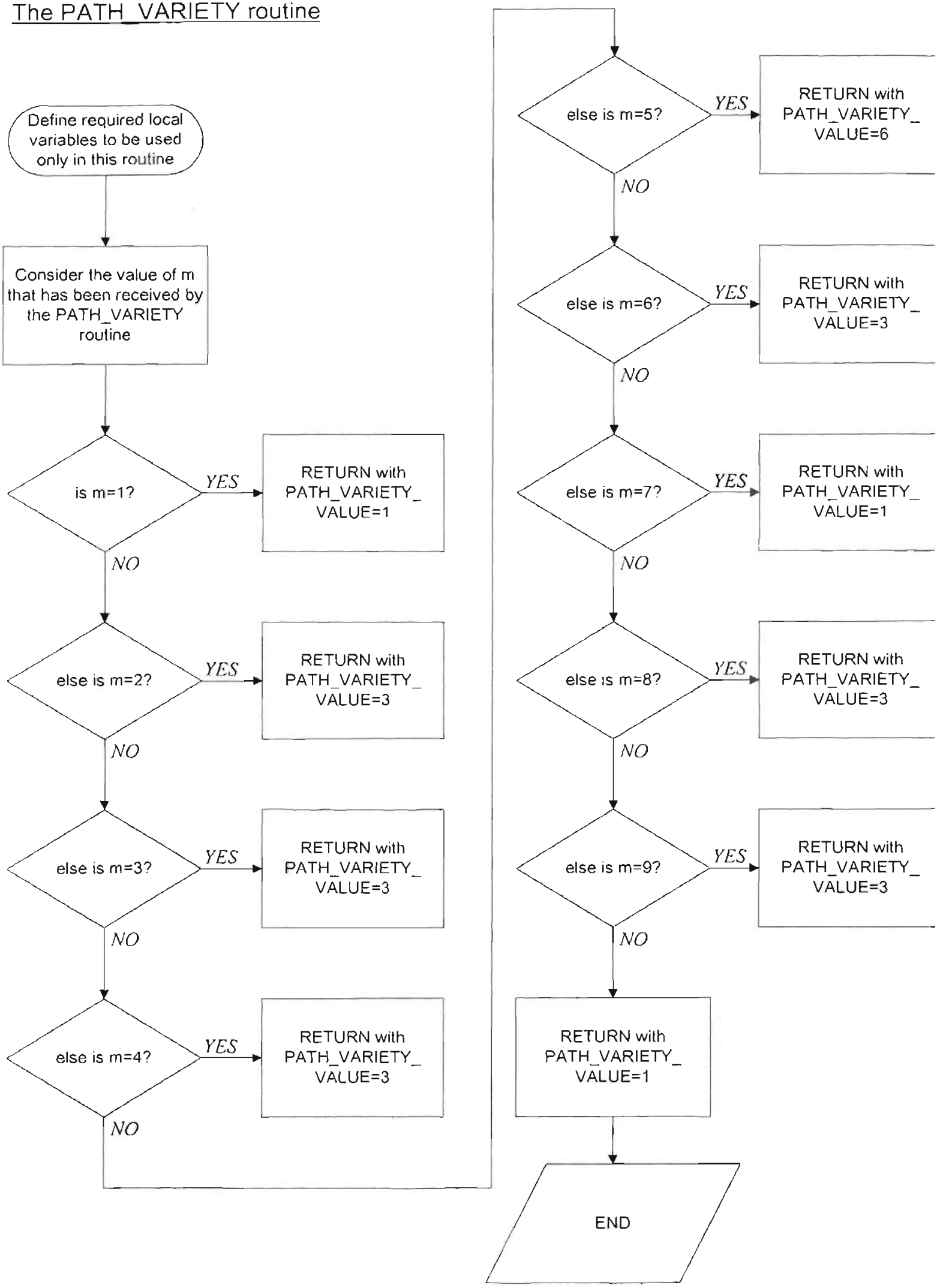

Figure A4.4
The BER and H_I_m routines

BER routine flowchart

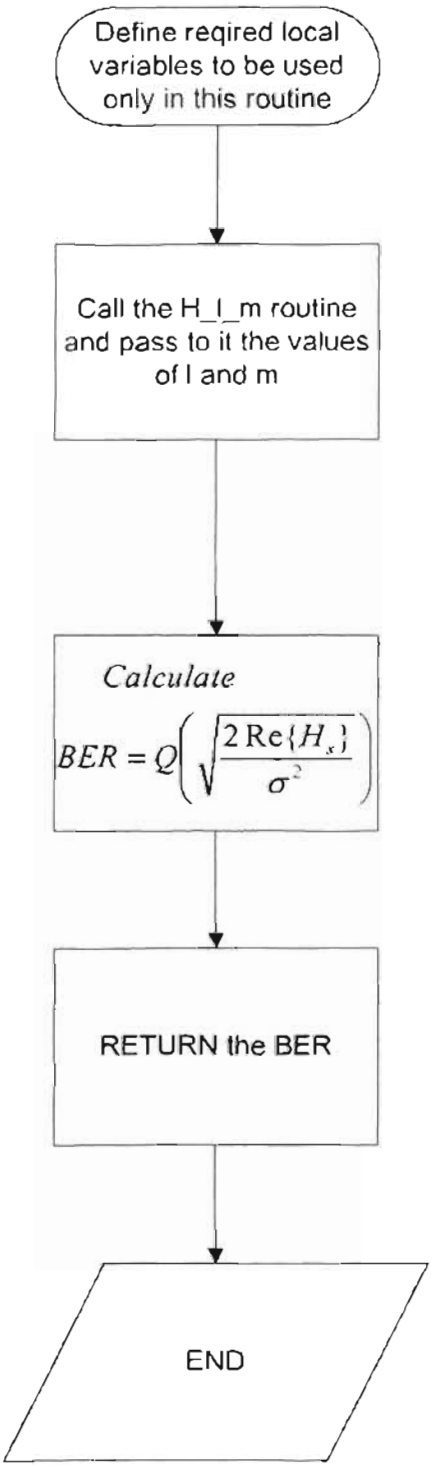

H_I_m routine flowchart

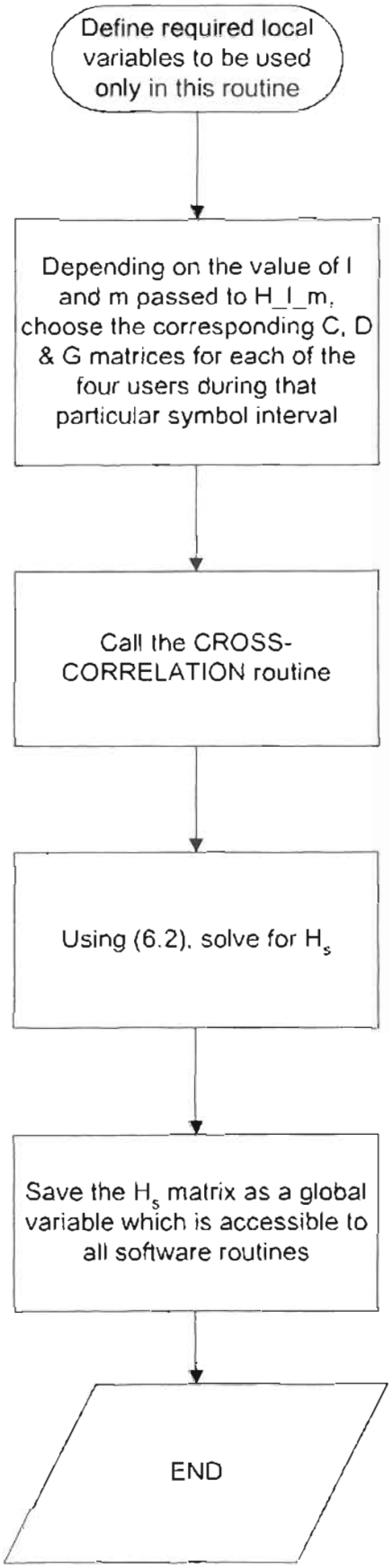

Figure A4.5
The CROSS_CORRELATION and CALCULATION routines